Sameh Adib Abou Rafee

Land Use and Cover or Precipitation?

Changes on Hydrological Response of the Upper Paraná River Basin

Uso e Cobertura da Terra ou Precipitação?

Mudanças na Resposta Hidrológica da Bacia do Alto do Rio Paraná

São Paulo

2020

Land Use and Cover or Precipitation?

Changes on Hydrological Response of the Upper Paraná River Basin

Sameh Adib Abou Rafee

DOCTORAL DISSERTATION

by due permission of the Institute of Astronomy, Geophysics and Atmospheric Sciences, University of São Paulo, Brazil.

Defended at the Institute of Astronomy, Geophysics and Atmospheric Science, Matão Street 1226, São Paulo, room Prof. Dr. Paulo Benevides Soares on April 30, 2020, at 14:00 – 20:00.

Faculty opponent

Prof. Dr. Daniel Gustavo Allasia Piccilli

Federal University of Santa Maria

Sameh Adib Abou Rafee

Land Use and Cover or Precipitation?

Changes on Hydrological Response of the Upper Paraná River Basin

Uso e Cobertura da Terra ou Precipitação?

Mudanças na Resposta Hidrológica da Bacia do Alto do Rio Paraná

Thesis submitted in partial fulfillment of the requirements for the degree of Doctor of Sciences at the Institute of Astronomy, Geophysics and Atmospheric Sciences, University of São Paulo, and degree of Doctor in Technology at the Faculty of Engineering, Lund University.

Major filed: Meteorology and Water Resources Engineering

Advisor: Prof. Dr. Edmilson Dias de Freitas (at University of São Paulo)

Advisor: Profa. Dra. Cintia Bertacchi Uvo (at Lund University)

Co-advisor: Prof. Dr. Jorge Alberto Martins (at Lund University)

Final version. The original copy is available in the library.

São Paulo

2020

Land Use and Cover or Precipitation?

Changes on Hydrological Response of the Upper Paraná River Basin

Sameh Adib Abou Rafee

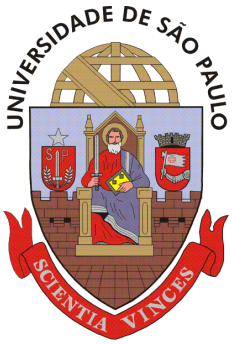

To Abou Rafee family

Everything in life has the same importance until the moment you give value to each of it

Sameh Abou Rafee

Contents

Institutional acknowledgements

I would like to gratefully acknowledge all the institutions for their supports that, together, made this research happen:

- The Department of Atmospheric Sciences at University of São Paulo and the Division of Water Resources Engineering at Lund University for all the support during my PhD studies.

- The "*Coordenação de Aperfeiçoamento de Pessoal de Nível Superior – Brasil*" (CAPES) Finance Code 001 (Process # 88887.115875/2015-01) that supported my PhD studies.

- The PROEX, AFork, and Åke och Greta Lissheds foundations for their financial support giving me the opportunity to participate in conferences and workshops.

- The "*Agência Nacional de Águas - Brasil*" (ANA) and "*Operador Nacional do Sistema Elétrico*" (ONS) by providing discharge and precipitation data for use in this thesis.

Acknowledgements

I would like to express my deepest gratitude and appreciation to my supervisors Cintia Bertacchi Uvo, Edmilson Dias de Freitas, and Jorge Alberto Martins for the opportunity to develop this research. Thank you for all your constant and invaluable support. Thank you for all the suggestions, advices and discussions. Thank you for sharing your knowledge and experiences. Thank you for guiding this study with enthusiasm and fun. Thank you for giving me the freedom to conduct this research. I am very lucky to have you on my side as professors and friends.

I also would like to pay my regards to the professors Pedro Silva Dias, Humberto Ribeiro da Rocha and Ricardo de Camargo for all knowledge and highly insightful suggestions for the research project during my qualification exam. Undoubtedly, it was an important period that contributed to my professional career and development.

I also would like to thank the professors, members, friends, and colleagues at the department of Atmospheric Sciences. Thanks for all the support and special moments that I have spent during my research period.

A lasting thanks to all the people at TVRL for the unforgettable year that I spent there. Thanks for the hospitality and the incredible moments at Fika time.

Special thanks to my officemates Fernando Mendez, Sergio Ibarra, Alberto Afonso Junior, Rafaela Squizzato and Carolyne Machado. It was a pleasure to share the 311 with you. Thanks for all the coffees, conversations, discussions and suggestions for my research project.

I also wish to thank my officemates at the Division of Water Resources Engineering Björn Almström and Clemens Klante. I enjoyed and greatly appreciated all the conversations during my stay.

وأخيراً ، اقدم شكري الخالص لوالدي الغالي أديب يوسف أبو رافع ووالدتي سلامية سيف الدين أبو رافع ، الكلمات تعجزعن التعبير عن امتناني وعرفاني لكم . أنا مدين لكم بكل ما وصلت إليه في حياتي ومسيرتي المهنية. كما أود أن أعرب عن خالص امتناني لإخواني علاء ويوسف وسامر أبو رافع.

عائلة ابو رافع انتم الافضل.

Popular summary

Land use and cover and precipitation changes are the most important factors that affect the hydrological processes. The Upper Paraná River Basin, one of the largest and most socio-economically important river basins in South America has undergone extensive natural vegetation suppression during the latest decades. For example, cerrado (Brazilian savanna) had a reduction of about 173 000 km^2 between 1985 and 2015. Also, precipitation changes after the 1970s were witnessed over basin areas due to a global climatic event known as "climate shift". This work addressed the behavior and effects of these changes on hydrology within the basin.

During the last four decades, between 1977 and 2016, the Upper Parana River has experienced changes in precipitation. For example, the provided results showed that the northern part of the basin mostly presented decreasing in seasonal and annual precipitation totals following the increasing of the consecutive number of days without rain. On the other hand, in the southern areas of the basin, an increase in precipitation totals and rainstorms more pronounced during the summer was observed. Besides, the analyses suggest that most of the areas across the basin are exposed to a longer rainy season.

Furthermore, this study showed that the changes in land use and cover between 1985 and 2015 have a significant effect on basin hydrology. For example, it was observed an increase in discharge at the largest rivers of the basin during the wet season. This followed the decrease in evapotranspiration and both increase in surface runoff and soil moisture. The main reason for these changes was the natural vegetation deforestation that has been replaced by cropland or grassland areas.

In the last part of this work, the cause for the observed increase of about 26% in the annual discharge after the 1970s at the lower Parana River was assessed. For that, both effects on the discharge from land use and cover change since the pristine period (around the Year 1500) until 1985, and precipitation change due the 1970s climate shift were addressed together and separately. The results showed that both changes that happened within the basin have a significant impact on the annual discharge, but the precipitation change after the 1970s being the main driver.

This work suggests the importance of addressing large-scale land use and cover change and global climate shift impacts on hydrology. Hence, these changes should be regarded with much attention by the environmental managers worldwide.

Abstract

The Upper Paraná River Basin (UPRB) has undergone extensive Land Use and Cover Changes (LUCC) in the latest decades, due to rapid population growth and economic development. Furthermore, variation in precipitation patterns was observed across the basin mainly after the 1970s Climate shift. Concurrently, the UPRB has presented significant changes in its hydrology. In this context, this thesis investigates the changes in precipitation and LUCC and their effects on the hydrological processes in the UPRB. The observed trends in the extreme precipitation events from 1977 to 2016 were evaluated using the Mann–Kendall test. Different numerical scenarios were simulated using the Soil and Water Assessment Tool (SWAT) model. The model was calibrated and validated with a satisfactory performance for the main rivers during the period 1984 – 2015 considering the Land Use and Cover (LUC) from 2015. The results revealed that the southern (northern) parts of the basin presented increasing (decreasing) trends in precipitation amounts. In addition, the southern (northern) regions of the UPRB indicated an increase in the number of rainstorms > 50 mm day^{-1} and in the annual greatest 5-day total precipitation (number of dry days < 1 mm). The results also suggest that the basin is exposed to a longer rainy season. By comparing the LUC between 1985 and 2015, the numerical simulations showed that the natural vegetation suppression caused significant changes in basin hydrology. For instance, an increase (decrease) of surface runoff in the wet (dry) season at most UPRB subbasins, was observed. In addition, the simulations revealed a reduction in actual evapotranspiration and an increase in soil moisture in the annual and wet season. Consequently, the major rivers of the basin presented an increase (decrease) in their discharge in the wet (dry) period. This study also addressed the comparison between the LUC from a pristine period (around the year 1500), 1960 and 1985, and changes in precipitation before and after the 1970s Climate shift. In this case, the results showed that the 1970s Climate shift event has a higher effect on the changes in average annual discharge at the river mouth of the UPRB. This research improves the understanding of the effects of LUCC and changes in precipitation patterns on the hydrology across the UPRB. The results from this thesis will hopefully provide insights in improving sustainable management of water resources.

Keywords: discharge, SWAT model, trend analysis, large-scale modelling.

Resumo

A Bacia do Alto do Rio Paraná (BARP) passou por extensas Mudanças no Uso e Cobertura da Terra (MUCT) nas últimas décadas, devido ao rápido crescimento populacional e desenvolvimento econômico. Além disso, foi observada uma variação nos padrões de precipitação na bacia, principalmente após evento de alteração climática observado na década de 1970. Ao mesmo tempo, a BARP apresentou mudanças significativas em sua hidrologia. Nesse contexto, esta tese investigou as mudanças na precipitação e as MUCT, e seus efeitos nos processos hidrológicos na BARP. A tendência dos eventos extremos de precipitação entre 1977 e 2016 foram avaliados utilizando o teste de Mann-Kendall. Diferentes cenários numéricos foram simulados utilizando o modelo *Soil and Water Assessment Tool* (SWAT). O modelo foi calibrado e validado com desempenho satisfatório para os principais rios durante o período 1984 – 2015 considerando o Uso e Cobertura da Terra (UCT) de 2015. Os resultados revelaram que as partes sul (norte) da bacia apresentaram tendências crescentes (decrescentes) nas quantidades de precipitação. Além disso, as regiões sul (norte) da BARP indicaram um aumento no número de tempestades > 50 mm dia^{-1} e na máxima precipitação anual em 5 dias consecutivos (número de dias secos < 1 mm). Simultaneamente, os resultados mostraram que a maior parte da bacia apresenta uma estação chuvosa mais longa. Na comparação entre o UCT de 1985 e 2015, as simulações numéricas mostraram que a supressão natural da vegetação causou mudanças significativas na hidrologia da bacia. Por exemplo, um aumento (diminuição) foi observado no escoamento superficial durante a estação chuvosa (seca) na maioria das subbacias da BARP. Além disso, as simulações revelaram uma redução na evapotranspiração real e aumento na umidade do solo anual e na estação chuvosa. Consequentemente, os principais rios da bacia apresentaram um aumento (diminuição) na vazão no período chuvoso (seco). Este estudo também abordou a comparação entre o UCT de um período primitivo (por volta do ano 1500), 1960 e 1985, e as mudanças na precipitação antes e depois da alteração climática. Nesse caso, os resultados mostraram que a alteração climática de 1970 tem um maior efeito na vazão média anual no exutório da BARP. Esta pesquisa apresenta uma melhor compreensão dos efeitos das MUCT e mudanças nos padrões de precipitação sobre a hidrologia da BARP. Os resultados apresentados oferecem subsídios no sentido de melhorar a gestão sustentável dos recursos hídricos.

Palavras-chave: vazão, modelo SWAT, analise de tendência, modelagem de larga escala.

Sammanfattning

Övre Paranáflodbassängen (UPRB) har genomgått omfattande markanvändnings- och täcknings-ändringar (LUCC) under de senaste decennierna på grund av snabb befolkningstillväxt och ekonomisk utveckling. Dessutom observerades variationer i nederbördsmönstren över bassängen främst efter 1970-talets klimatförändringar. Samtidigt har UPRB presenterat betydande förändringar i sin hydrologi. I detta kontex undersöker denna avhandling förändringarna i nederbörd och LUCC, och deras effekter på de hydrologiska processerna i UPRB. De observerade trenderna i de extrema nederbördshändelserna från 1977 till 2016 utvärderades med hjälp av Mann-Kendall-testet. Olika numeriska scenarier simulerades med hjälp av SWAT-modellen (Soil and Water Assessment Tool). Modellen kalibrerades och validerades med tillfredsställande prestanda för de viktigaste floderna under perioden 1984 - 2015 med tanke på markanvändningen och täckningen (LUC) från 2015. Resultaten visade att de södra (norra) delarna av bassängen presenterade ökande (minskande) trender i nederbördsmängder. Dessutom indikerade de södra (norra) regionerna av UPRB en ökning i antalet regnstormar > 50 mm dag^{-1} och i den årliga största 5-dagars totala nederbörden (antal torra dagar <1 mm). Resultaten visade också att bassängen presenterar en allt längre regnperiod. Genom att jämföra LUC mellan 1985 och 2015 visade de numeriska simuleringarna att det naturliga vegetationsundertrycket orsakade betydande förändringar i bassänghydrologin. Till exempel observerades en ökning (minskning) av ytavströmningen i den våta (torra) säsongen vid de flesta UPRB-underbassänger. Vidare visade simuleringarna en minskning av den faktiska evapotranspirationen och en ökning av markfuktigheten under den årliga våta säsongen. Följaktligen uppvisade de stora floderna i bassängen en ökning (minskning) av deras ansvarsfrihet under den våta (torra) perioden. Denna studie behandlade också jämförelsen mellan LUC från en orörd period (omkring år 1500), 1960 och 1985, och förändringar i nederbörd före och efter 1970-talets klimatförändring. I det här fallet visade resultaten att händelsen av klimatförändring på 1970-talet har en högre effekt på förändringarna i den genomsnittliga årliga ansvarsfrihet vid UPRB-flodmynningen. Denna forskning förbättrar förståelsen för effekterna av LUCC och förändringar i nederbördsmönster på hydrologin över UPRB. Resultaten från undersökningen kan förhoppningsvis användas för att förbättra hållbar förvaltning av vattenresurserna

Nyckelord: ansvarsfrihet, SWAT-modell, trend analys, storskalig modellering.

Resumen

La Cuenca del Alto Río Paraná (CARP) ha sufrido grandes Cambios en el Uso y Cobertura de la Tierra (CUCT) en las últimas décadas, debido al rápido crecimiento de la población y al desarrollo económico. Además, se observó una variación en los patrones de precipitación en la cuenca, principalmente después del evento de alteración climática observado en la década de 1970. Al mismo tiempo, la CARP mostró cambios significativos en su hidrología. Por lo expuesto, esta tesis investigó los cambios en la precipitación y en los CUCT, y sus efectos sobre los procesos hidrológicos en la CARP. La tendencia en los eventos de precipitación extrema fue evaluada durante el periodo 1977 – 2016 a través de la aplicación del test estadístico de Mann-Kendall. Diferentes escenarios numéricos fueron simulados con el modelo *Soil and Water Assessment Tool* (SWAT). El modelo fue calibrado y validado con un desempeño satisfactorio para los ríos principales de la cuenca durante el período 1984 – 2015 considerando el Uso y Cobertura de la Tierra (UCT) de 2015. Los resultados revelaron que partes del sur (norte) de la cuenca presentaron tendencias crecientes (decrecientes) en las cantidades de precipitación. Además, las regiones del sur (norte) de la CARP indicaron un aumento en el número de tormentas > 50 mm día^{-1} y en el máximo anual de la precipitación acumulada en cinco días consecutivos (número de días secos < 1 mm). Simultáneamente, los resultados mostraron que la cuenca presenta una temporada de lluvia más larga. Al comparar el UCT de 1985 y 2015, las simulaciones numéricas mostraron que la supresión de la vegetación natural causó cambios significativos en la hidrología de la cuenca. Por ejemplo, se observó un aumento (disminución) en la escorrentía de la superficie en temporada húmeda (seca) en la mayoría de las subcuencas de la CARP. Además, las simulaciones revelaron una reducción en la evapotranspiración real y un aumento en la humedad del suelo en temporada anual y húmeda. En consecuencia, los principales ríos de la cuenca presentaron un aumento (disminución) en su descarga en periodos de lluvia (secos). Este estudio también abordó la comparación entre el UCT de un período prístino (alrededor del año 1500), 1960 y 1985, y los cambios en la precipitación antes y después de la alteración climática. En este caso, los resultados mostraron que el evento de alteración climática de 1970 presentó un mayor efecto sobre los cambios en la descarga anual promedio en la desembocadura de la CARP. Esta investigación presenta una mejor comprensión de los efectos de los CUCT y los cambios en los patrones de precipitación sobre la hidrología de la CARP. Los resultados presentados proporcionan información para mejorar la gestión sostenible de los recursos hídricos.

Palabras clave: descarga, modelo SWAT, análisis de tendencia, modelación en gran escala.

الملخص

يخضع حوض نهر بارانا العلوي لتغيرات واسعة في استخدام الأراضي وتغطيتها في العقود الأخيرة نتيجة النمو السكاني والتنمية الاقتصادية المتسارعة. علاوة على ذلك ، لقد لوحظ تباين في أنماط هطول الأمطار عبر حوض النهر بشكل رئيسي بعد تغير على المناخ في سبعينيات القرن الخالي. وفي الوقت نفسه ، لقد ساهم حوض النهرفي احداث تغييرات كبيرة في المياه السطحية. وفي هذا السياق ، تأتي هذه الدراسة (رساله الدكتوراه) لتبحث في هذه التغيرات الحاصله في هطول الأمطار واستخدام الأراضي والتغطية وآثارها على العمليات الهيدرولوجية في هذا الحوض. لقد تم تقييم الترددات المشاهدة في هطولات الامطار الغزيره في الفترة بين عام 1977 ولغاية 2016 باستخدام اختبار مان - كيندال. ايضا، لقد تم اجراء دراسة نمذجة رقمية للعديد من السيناريوهات باستخدام نموذج أداة تقييم التربة والمياه (SWAT).

لقد تم معايرة النموذج والتحقق من صحته من خلال الاداء المقبول للانهار الرئيسية خلال الفترة ما بين الاعوام 1984 ولغاية 2015 مع الأخذ بعين الاعتباراستخدامات الاراضي وتغطيتها من عام 2015.

اظهرت النتائج أن الأجزاء الجنوبية (الشمالية) من الحوض شهدت ترادات متزايدة (متناقصة) في كميات هطول الأمطار. بالإضافة إلى ذلك ، اظهرت نتائج المناطق الجنوبية (الشمالية) من حوض النهر إلى زيادة في عدد العواصف المطيرة (> 50 مم) وفي أكبر هطول سنوي إجمالي لمدة 5 أيام (عدد الأيام الجافة <1 مم). كما أظهرت النتائج أن الحوض يشهد موسمًا مطيرًا متزايدًا.من خلال مقارنة الغطاء النباتي واستخدامات الاراضي في الحوض في الفترة ما بين عام 1985 ولغاية 2015 ، أظهرت المحاكاة والنمذجه الرقمية أن غياب الغطاء النباتي الطبيعي تسبب في تغييرات كبيرة في هيدرولوجيا الحوض.على سبيل المثال ، لوحظ زيادة (نقصان) الجريان السطحي في الموسم الرطب (الجاف) في معظم انهار ألحواض الفرعية. بالإضافة إلى ذلك ، كشفت عمليات المحاكاة والنمذجه عن انخفاض في التبخر الفعلي وزيادة في رطوبة التربة في الموسم السنوي الرطب. ونتيجة لذلك ، شهدت معظم الأنهار الرئيسية للحوض زيادة (نقصان) في تصريفها في الفترة الرطبة (الجافة).

لقد تناولت هذه الدراسة أيضا المقارنة بين الغطاء النباتي واستخدامات الاراضي في الفترات السابقة (حوالي عام 1500) ، وفترة الدراسة الحالية ما بين عام 1960 ولغاية 1985 ، والتغيرات في هطول الأمطار قبل وبعد بدء تغير المناخ. وفي هذه الحالة ، أظهرت النتائج أن حدث تحول المناخ كان له تأثير أعلى على التغيرات في متوسط التصريف السنوي في أكبر أنهارالحوض.

يقدم هذا العمل فهمًا أفضل لتأثيرات الغطاء النباتي واستخدامات الاراضي والتغيرات في أنماط هطول الأمطار على الجريان في الحوض. وعلية ، النتائج المقدمه في هذه الرسالة يمكن اعتبارها جزء من عملية تحسين الإدارة المستدامة لموارد المياه في المنطقة.

الكلمات المفتاحية: الجريان. SWAT؛ النمذجة الموسعه.

Papers

Appended papers

I. **Abou Rafee, S.A.,** Freitas, E.D., Martins, J.A., Martins,L.D., Domingues, L.M., Nascimento, J.M., Machado,C.B., Santos, E.B., Rudke, A.P., Fujita, T., Souza, R.A., Hallak, R., Uvo, C.B., 2020: Spatial Trends of Extreme Precipitation Events in the Paraná River Basin. *Journal of Applied Meteorology and Climatology*, v. 59, n. 3, p. 443 – 454. https:// doi.org/10.1175/JAMC-D-19-0181.1

II. **Abou Rafee, S.A.,** Uvo, C.B., Martins, J.A., Domingues, L.M., Rudke, A.P., Fujita, T., Freitas, E.D., 2019. Large-scale hydrological modelling of the Upper Paraná River Basin. *Water (Switzerland*), v. 11, n. 5, p. 882. https:// doi.org/10.3390/w11050882

III. **Abou Rafee, S.A.,** Freitas, E.D., Martins, J.A., Machado, C.B., Uvo, C.B., 2020. Hydrologic Response to Large-Scale Land Use and Cover Changes in the Upper Paraná River Basin between 1985 and 2015. *Journal of Hydrology: Regional Studies* (Submitted 2020-05-22, Under review).

IV. **Abou Rafee, S.A.,** Uvo, C.B., Martins, J.A., Machado, C.B., Freitas, E.D., 2020. Land Use and Cover Changes versus Climate Shift: Who is the main player in river discharge? - A case study in the Upper Paraná River Basin. *Science of the Total Environment* (Submitted 2020-06-06, Under review).

Author's contribution to the appended papers

I. The author collected all the data, did all the statistical analysis and wrote the major part of the manuscript. The co-authors contributed to the analysis and discussions of the results, and wrote minor parts of the manuscript.

II. The author collected the major part of the data, performed all the numerical simulation and statistical analysis, and wrote the major part of the manuscript. The co-authors collected minor parts of the data, contributed in discussion and wrote minor parts of the manuscript.

III. The author collected the major part of the data, performed all the numerical simulation and wrote all the sections of the manuscript. The co-authors participated in discussion of the results.

IV. The author collected the major part of the data, performed all the numerical simulations and worte all the sections of the manuscript. The co-authors participated in the construction of the scenarios and discussion of the reuslts.

Related Publications not included

Journal Papers

I. Rudke, A.P., Fujita, T., Almeida, D.S. de, Eiras, M.M., Xavier, A.C.F., **Abou Rafee, S.A.,** Santos, E.B., Morais, M.V.B. de, Martins, L.D., Souza, R.V.A. de, Souza, R.A.F., Hallak, R., Freitas, E.D. de, Uvo, C.B., Martins, J.A., 2019. Land cover data of Upper Parana River Basin, South America, at high spatial resolution. Int. *International Journal of Applied Earth Observation and Geoinformation*, v. 83, p. 101926. https:// doi.org/10.1016/j.jag.2019.101926

II. Xavier, A.C.F., Rudke, A.P., Fujita, T., Blain, G.C., de Morais, M.V.B., de Almeida, D.S., **Abou Rafee, S.A.,** Martins, L.D., de Souza, R.A.F., de Freitas, E.D., Martins, J.A., 2020. Stationary and non-stationary detection of extreme precipitation events and trends of average precipitation from 1980 to 2010 in the Paraná River basin, Brazil. *International Journal of Climatology*, v. 40, n. 2, p. 1197 – 1212 .https:// doi.org/10.1002/joc.6265

Conferences and workshops

I. **Abou Rafee**, **S. A.,** Xavier, A. C. F., Rudke A. P., Fujita, T., Brand, V. S., Morais, M. V. B., Basso, J. L. M., Santos, E. B., Martins, L. D., Souza, R. A. F., Hallak, R., Martins, J. A., Freitas, E. D., 2016. Análise de tendência de vazão e precipitação da bacia do rio Tietê. *XIX Congresso Brasileiro de Meteorologia, João Pessoa – PB, Brazil.*

II. Rudke, A. P., Fujita, T., Xavier, A. C. F., Morais, M. V. B., Brand, V. S., **Abou**

Rafee, S. A., Martins, L. D., Souza, R. A. F., Freitas, E. D., Martins, J. A., 2016. Avaliação de produtos globais de uso e ocupação do solo para a bacia do Rio Paraná. *XIX Congresso Brasileiro de Meteorologia, João Pessoa – PB, Brazil.*

III. Santos, E. B., **Abou Rafe, S. A.,** Morais, M. V. B., Martins, L. D., Souza, R. A. F., Hallak, R., Martins, J. A., Freitas, E. D., 2016. Análise de eventos extremos de precipitação na bacia do Rio Iguaçu- Paraná. *XIX Congresso Brasileiro de Meteorologia, João Pessoa – PB, Brazil.*

IV. Fujita, T., Rudke, A. P., Xavier, A. C. F., Morias, M. V. B., Brand, V. S., **Abou Rafee, S. A.,** Freitas, E. D., Souza, R. A. F., Martins, J. A., 2016. Aplicação de técnicas de Krigagem e IDW na espacialização de dados de precipitação na bacia do rio Paraná *XIX Congresso Brasileiro de Meteorologia, João Pessoa – PB, Brazil.*

V. Santos, E. B., **Abou Rafee, S. A.,** Martins, L. D., Souza, R. A. F., Hallak, R., Martins, J. A., Freitas, E. D., 2017 . Influência do El Niño Oscilação Sul sobre o Regime de Chuvas na Bacia do Rio Paraná. *Simpósio Internacional de Climatologia, Petrópolis - Rio de Janeiro, Brazil.*

VI. **Abou Rafee, S.A.,** Rudke, A. P., Fujita, T., Morais, M. V. B., Santos, E. B., Hallak, R., Souza, R. A. F., Martins, L. D., Martins, J. A., Freitas, E. D., 2017. Analysis of spatial distribution of observed ground-based data and large scale modelling of the Parana River Basin. *2017 International SWAT Conference, Warsaw, Poland.*

VII. Fujita, T., Rudke, A. P., Morais, M. V. B., **Abou Rafee, S.A.,** Souza, R. A. F., Souza, R. V. A., Freitas, E. D., Martins, L. D., Martins, J. A., 2017. Response of Randomized Subsets of Rainfall Gauges Over a Paraná River Sub-basin. *2017 International SWAT Conference, Warsaw, Poland.*

VIII. Rudke, A. P., Fujita, T., Morias, M. V. B., **Abou Rafee, S.A.,** Souza, R. A. F., Souza, R. V. A., Freitas, E. D., Martins, L. D., Martins, J. A., 2017. Hydrological Response of a Brazilian Catchment to Different Land Use and Land Cover Products. *2017 International SWAT Conference, Warsaw, Poland.*

IX. Santos, E. B., Freitas, E. D., **Abou Rafee, S.A.,** Fujita, T., Rudke, A. P., Martins, J. A., Martins, L. D., Hallak, R.; Souza, R. A. F., 2018. The Relationships Between El Niño Southern Oscillation and Climate Extremes in Paraná River Basin, Brazil. *American Meteorology Society, Austin, TX, United States.*

X. **Abou Rafee, S.A.,** Freitas, E.D., Martins, J. A., Machado, C., Rudke, A. P., Fujita, T., Uvo, C. B., 2019. Hydrologic response to land use changes in the Upper Paraná River Basin. *The Inaugural International Symposium on Water Modelling (iSymWater2019), Beijing, China.*

XI. Freitas, E. D., **Abou Rafee, S.A.,** Fujita, T., Xavier, A. C. F., Machado, C., Campos, T. L. O. B. , Martins, L. D. , Uvo, C. B., Souza, R. A. F., Santos, E. B., Hallak, R., Morais, M. V. B., Martins, J. A., 2019 . Effects of climate change and land use on the hydrology of the Paraná River Basin - Brazil. *Sixth International Soil and Water Assessment Tool, South East and East Asia Conference, Seam Reap, Cambodia*.

XII. Martins, J. A., Rudke, A. P., **Abou Rafee, S.A.,** Fujita, T., Xaveir, A. C. F., Machado, C., Martins, L. D., Campos, T. L. O. B., UVO, C. B., Freitas, E. D., 2019. Land cover dynamics by agricultural activities over the Upper Paraná River Basin. *Sixth International Soil and Water Assessment Tool, South East and East Asia Conference, Seam Reap, Cambodia.*

XIII. **Abou Rafee, S.A.,** Uvo, C. B., Martins, J. A., Freitas, E.D., 2019. Assessing the hydrologic impacts of land use change in the Upper Paraná River Basin between 1985 and 2015. *Sixth International Soil and Water Assessment Tool, South East and East Asia Conference, Seam Reap, Cambodia.*

XIV. Machado, C., **Abou Rafee, S. A.,** Freitas, E. D., 2019. Future land use and land cover simulation and analysis of extreme rainfall events in an important Brazilian hydrographic basin: a support to regional atmospheric modeling. *2019 AGU Fall Meeting, São Francisco, United States.*

XV. Machado, C.; Campos, T. L. O. B.; **Abou Rafee, S.A.;** Martins, J. A.; Freitas, E. D., 2019. Bacia Hidrográfica do Paraná: Uma análise do regime pluviométrico, eventos extremos e ocupação do solo. *XXIII Simpósio Brasileiro de Recursos*

Hídricos, Foz do Iguaçu – PR, Brazil.

Co-supervised Master thesis

I. Nsabimana, B. and Estallo, Utande., 2019. Sustainable Drainage Systems Assessment and Optimisation-A case study for Lussebäcken Catchment, Helsingborg. Master Thesis TVVR-19/5009, Lund University.

List of Figures

List of Tables

List of Abbreviations

ANA	Brazilian National Water Agency
ANEEL	Brazilian Electricity Regulatory Agency
ARS-USDA	Agricultural Research Service of the United States Department of Agriculture
CFSR	Climate Forecast System Reanalysis
CN	Curve Number
DEM	Digital Elevation Model
ECMWF	European Centre for Medium-Range Weather Forecasts
EMBRAPA	Brazilian Agriculture Research Corporation
ENSO	El Niño–Southern Oscillation
HRU	Hydrologic Response Unit
HWSD	Harmonized World Soil Database
IDW	Inverse Distance Weighted
KGE	Kling-Gupta efficiency
LAI	Leaf Area Index
LUC	Land Use and Cover
LUCC	Land Use and Cover Changes
MCS	Mesoscale Convective Systems
MK	Mann–Kendall
NSE	Nash-Sutcliffe efficiency
ONS	Brazilian National Electrical System Operator
PBIAS	Percent Bias
PDO	Pacific Decadal Oscillation

pint	Annual mean precipitation per rain days ($\geq 1\ mm\ day^{-1}$)
pn50	Annual number of days with precipitation $>\ 50\ mm\ day^{-1}$
px5d	Annual greatest 5-day total precipitation
pxcdd	Annual maximum number of consecutive dry days ($< 1\ mm\ day^{-1}$)
R^2	Coefficient of Determination
RSR	Root mean Square Error
SACZ	South Atlantic Convergence Zone
SALLJ	South American Low-Level Jet
SAMS	South American Monsoon System
SNHT	Standard Normal Homogeneity Test
SRTM	Shuttle Radar Topography Mission
SUFI-2	Sequential Uncertainty Fitting
SWAT	Soil and Water Assessment Tool
SWAT-CUP	Soil and Water Assessment Tool Calibration and Uncertainty Program
UPRB	Upper Paraná River Basin

1. Introduction

1.1. Motivation

The Upper Paraná River Basin (UPRB) is part of the second largest and most socio-economically important river basins in South America, the La Plata River Basin. The UPRB plays a significant role in the economic activity and development of Brazil, being a home of more than 65 million inhabitants, of whom 93% live in urban areas (IBGE, 2019). The basin is being responsible for the most extensive livestock, agricultural and biofuel production, transportation of products, and hydroelectricity generation. According to the Brazilian National Water Agency (ANA), the UPRB has the largest water consumption mostly used for agriculture and industrial activities. Besides, the basin has the highest hydroelectric power generation capacity in South America. As reported by the Brazilian Electricity Regulatory Agency (ANEEL, 2020), more than 62% of electricity in Brazil is generated by hydropower plants, which almost 30% are provided from the basin. Currently, the UPRB houses 156 large hydropower plants (with a capacity of more than 30 MW) that provide about 52,000 MW (Figure 1). Also, the basin houses 595 small hydropower plants (capacity between 1.1 MW and 30 MW) and 214 micro hydropower plants (capacity up to 1 MW) which provide 7,074 MW and 193 MW, respectively.

Land Use and Cover Changes (LUCC) is one of the main factors that affect the hydrological processes within watersheds (DeFries & Eshleman, 2004, Francesconi *et al.*, 2016). In the latest decades, the UPRB has undergone extensive LUCC due to rapid population growth and economic development. Rudke (2018) observed significant natural vegetation suppression over the basin between 1985 and 2015. For instance, cerrado (Brazilian savanna) had a reduction of about 173×10^3 km^2 that were mostly concentrated in the central-western and northern parts of the basin. Also, the Brazilian Ministry of the Environment reported deforestation of 76% of the Atlantic forest biome and 49% of the cerrado (MMA, 2011, 2012). Particularly, Paraná and São Paulo states, located in the east of the basin, have lost more than 70% of their primitive forests, while the original vegetation in the western part of the basin, was maintained until the 1970s when the development of agri-business increased. Deforestation occurred for different objectives, but in most cases, natural vegetation was replaced by cropland and grassland areas (Tucci,

2002). Concurrently, significant changes in hydrology have been presented over the UPRB (Antico *et al.*, 2016, Bayer, 2014, Camilloni & Barros, 2003, Lee *et al.*, 2018, Tucci, 2002).

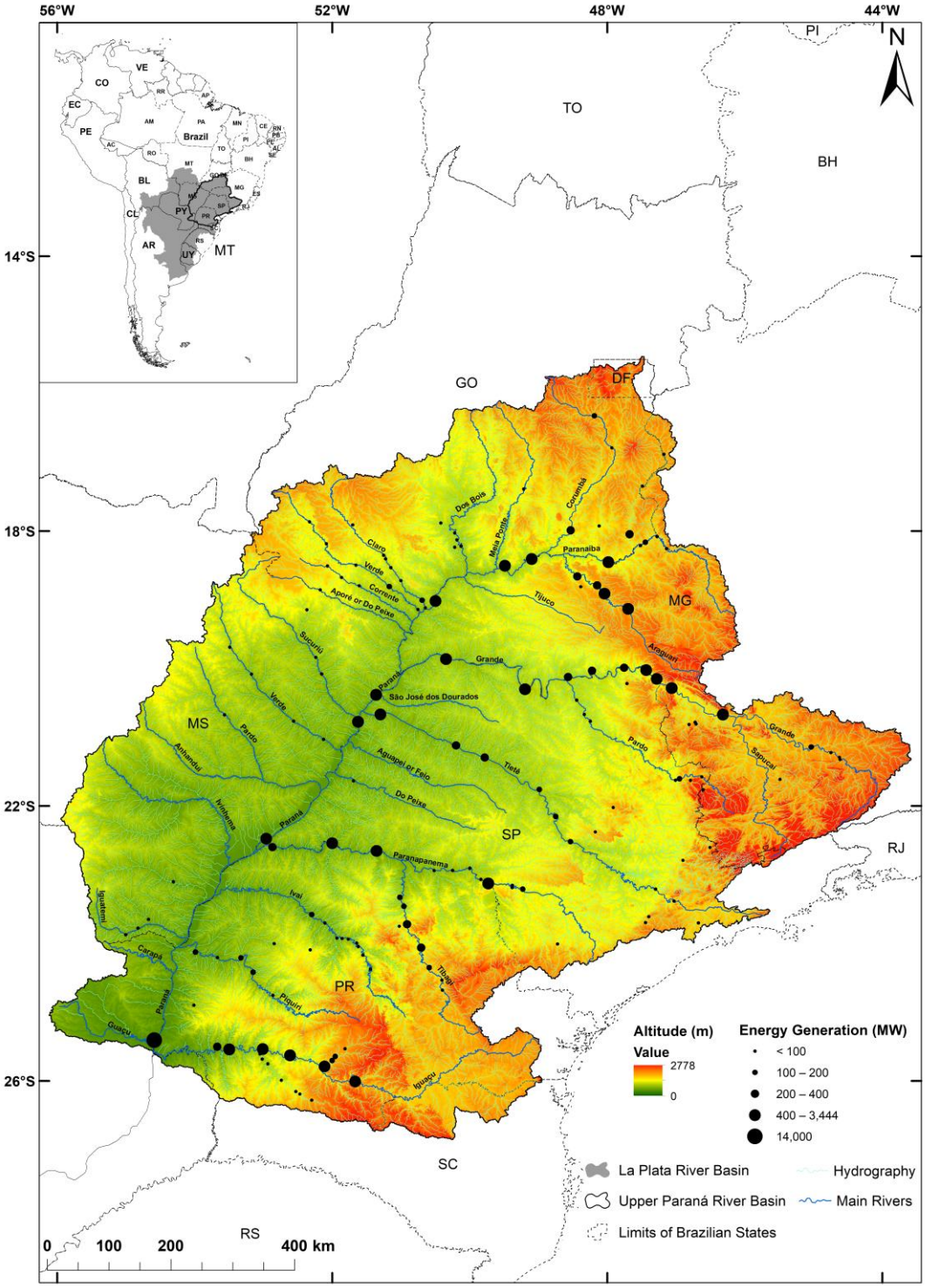

Figure 1. Location of the UPRB showing the topographic patterns, hydrography, and the spatial distribution of the largest hydropower plants (installed or planned with a capacity of more than 30 MW).

In addition to the LUCC, the 1970s climate shift (Jacques-Coper & Garreaud, 2015) is pointed out as one of the main events that led to a variation in precipitation patterns over the URPB that consequently could have affected the basin hydrology. The impacts of the climate shift on precipitation has been investigated over North American (Hartmann & Wendler, 2005, Litzow, 2006) and South American (Agosta & Compagnucci, 2008; Jacques-Coper & Garreaud, 2015) regions, and considered by the researchers as an unprecedented event. Climate shift is defined as the short period when several climate oscillations such as Pacific Decadal Oscillation (PDO) and El Niño–Southern Oscillation (ENSO) changed phases, out of which could lead the climate system to a new state (Jacques-Coper & Garreaud, 2015, Meehl *et al.*, 2009, Tsonis *et al.*, 2007, Wang *et al.*, 2009, Yuan Zhang *et al.*, 1997). During the 1970s climate shift, a cold to warm sea surface temperature shift in the tropical pacific was observed. Thereby, it induced an increase in annual mean precipitation in southernmost areas of South America (Jacques-Coper & Garreaud, 2015).

1.2. Research objective

Under such a perspective of the issues discussed in the previous section, this research aims to investigate the changes in precipitation and LUCC and their effects on the hydrological processes in the UPRB. Hence, the thesis intended to fill the gaps by answering the following questions:

- *Are there any trends of seasonal, annual, and extreme precipitation events in the UPRB?*
- *What are the hydrologic responses to land use and cover changes occurred in the latest decades in the UPRB?*
- *To which extent are changes associated with observed land use and cover, and climate shift responsible for the increase in the discharge of the Paraná River?*

To achieve these questions, the specific objectives were:

I. To investigate the behavior of the precipitation trend and climate shift in the UPRB;

II. To set up the SWAT model with the most appropriate dataset available;

III. To calibrate and validate the SWAT model for the main rivers of the UPRB;

IV. To prepare the Land Use and Cover (LUC) and climate shift scenarios;

V. To identify the changes in LUC and precipitation patterns over the basin;

VI. To simulate the scenarios constructed;

VII. To quantify the potential impacts of LUCC and climate shift scenarios.

1.3. Thesis Structure

This thesis is based on a summary that is connected to the research presented and discussed in the four appended papers, out of which two are published, and two are under review. Paper I, **Spatial trends of extreme precipitation events in the Paraná River Basin**, analyses the spatial trends performed on annual and seasonal precipitation totals as well as for the extreme precipitation indicators at 853 stations from 1977 to 2016. Paper II, **Large-Scale Hydrological Modelling of the Upper Paraná River Basin,** presents the hydrological modelling and the performance of the main rivers of the UPRB using the Soil and Water Assessment Tool (SWAT) model during the period 1984 – 2015. Paper III, **Hydrologic Response to Large-Scale Land Use and Cover Changes in the Upper Paraná River Basin between 1985 and 2015,** estimates the impacts of LUCC between 1985 and 2015 on soil moisture, actual evapotranspiration, surface runoff, and discharge in the UPRB examined for annual, wet, and dry season. Paper IV, **Land Use and Cover Changes versus Climate Shift: Who is the main player in river discharge? A case study in the Upper Paraná River Basin**, addresses the main reasons for the increased annual discharge of the Lower Paraná river by simulating three different LUC from the pristine period (around the Year 1500), 1960 and 1985, during the precipitation period 1961 – 1990.

The remainder of this summary is structured as follows. First, an introduction presents the motivation and research objective of this thesis. Then, chapter two starts with a brief description of the study area. The data preparation and the methods used for trend analysis and hydrological modelling are also described in this chapter. Furthermore, the strategies of the construction of the scenarios are presented. In chapter three, the main results from the appended papers are summarized and discussed. Finally, the main conclusions and future work are presented in chapter four.

2. Material and Methods

Different methods and data were used in this thesis. This chapter provides a brief description of the data prepared and the numerical scenarios constructed, which were used for the statistical analysis and hydrological modelling. For further details, the reader is referred to the appended papers.

2.1. Study area

The study area of this thesis covers the Upper Paraná River Basin (UPRB) located in the central-southern region of Brazil (Figure 1). It is situated between the coordinates 26° 51′ 23.35″ and 15° 27′ 25.54″ S latitude, and 56° 7′ 4.61″ and 43° 34′ 50.61″ W longitude. The basin has a drainage area of 900,480 km^2 and altitude varying from 78 up to 2778 meters above sea level. It covers six Brazilian states: São Paulo (23.5%), Paraná (20.4%), Mato Grosso do Sul (18.9%), Minas Gerais (17.6%), Goiás (15.7%), Santa Catarina (1.2%), and the Federal District (0.4%), and also includes a small portion of Paraguay (2.3%).

Several synoptic systems affect the UPRB which causes a different amount of precipitation across the basin. In the northern part of the basin under the influence of the South American Monsoon System (SAMS) (Carvalho *et al.*, 2011, Grimm *et al.*, 2007, Marengo *et al.*, 2012) has dry winters (< 30 mm), and wet summers (> 800 mm) (Abou Rafee *et al.*, 2020). On the other hand, the precipitation over the southern part of the UPRB is spread over seasons ranging from 240 (winter) to 500 mm (summer) (Abou Rafee *et al.*, 2020). The precipitation in the southern parts of UPRB is associated with different systems such as Mesoscale Convective Systems (MCS), South American Low-Level Jet (SALLJ), the passage of cold fronts, and the South Atlantic Convergence Zone (SACZ) (Carvalho *et al.*, 2004, Morales Rodriguez *et al.*, 2010, Velasco & Fritsch, 1987).

2.2. Precipitation trends

2.2.1. Data quality control and precipitation indices

Daily precipitation data were collected from the Brazilian National Water Agency (ANA). The trend analysis was applied for the dataset from 1977 to 2016. The stations

were selected when the following conditions are met: 1) First, double records and typo errors were verified. Consecutive repeated values above 1mm day^{-1} and precipitation above 250 mm day^{-1} were considered as missing data, 2) Then, stations series with less than 10% of missing data were selected, and finally 3) Data series that presented nonhomogeneity were disregarded. The homogeneity was checked by the Standard Normal Homogeneity Test (SNHT) (Alexandersson, 1986). As a result, a total of 853-gauge stations were selected (Figure 2). After this step, series were created according to the precipitation indices presented in Table 1.

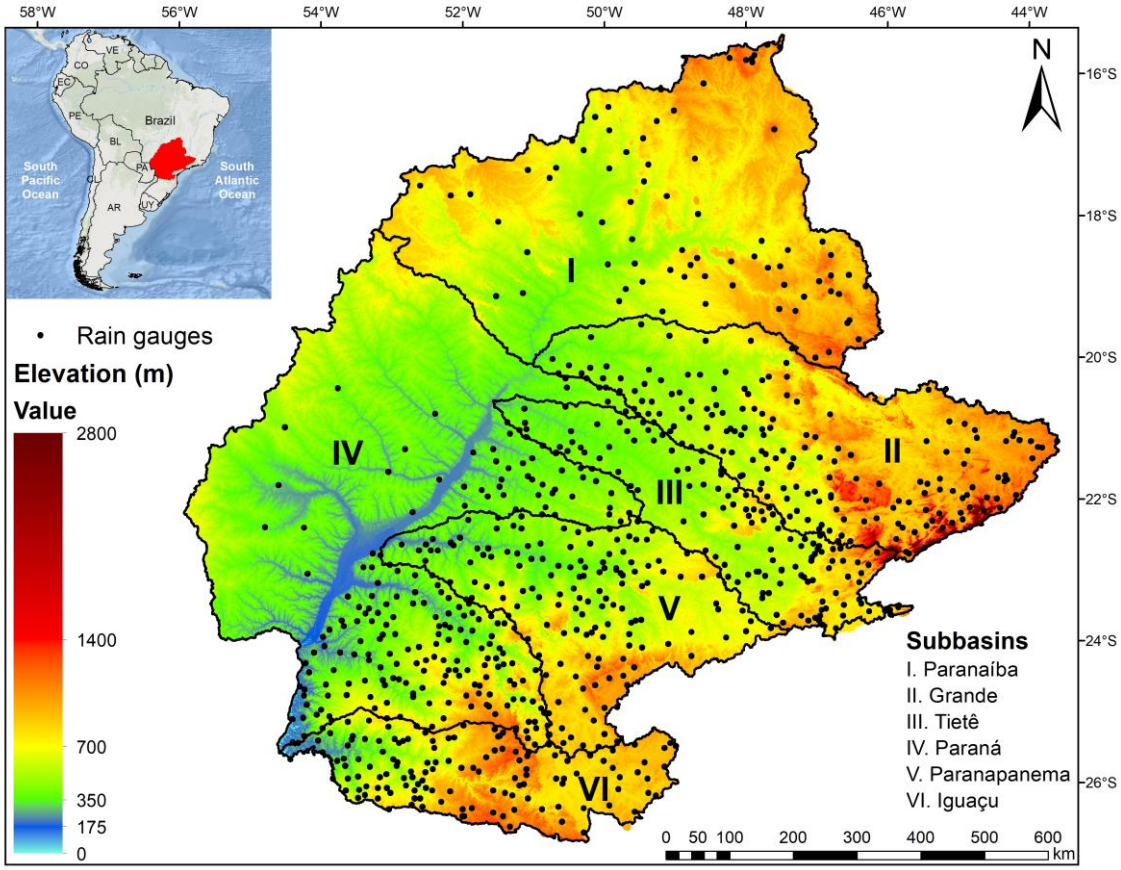

Figure 2. Geographic location and topographic map of the UPRB with its subbasins showing the spatial distribution of the 853 rain gauges.
From Abou Rafee *et al.* (2020).

Table 1. List of precipitation indices selected.
Based on Abou Rafee *et al.* (2020).

Indices	Definition	Unit
Accumulated precipitation totals	Annual Summer (December, January, and February) Autumn (March, April, and May) Winter (June, July, and August) Spring (September, October, and November)	mm
5-day maximum precipitation (px5d)	Annual greatest 5-day total precipitation	mm
Simple daily intensity (pint)	Annual mean precipitation per rain day ($\geq 1\ mm\ day^{-1}$)	$mm\ day^{-1}$
Longest dry period (pxcdd)	Annual maximum number of consecutive dry days ($< 1\ mm\ day^{-1}$)	$days$
Rainstorm days (pn50)	Annual number of days with precipitation $> 50\ mm\ day^{-1}$	$days$

2.2.2. Trend analysis

Trends were investigated by using the nonparametric statistical Mann-Kendall (MK) test (Kendall, 1975, Mann, 1945). To avoid misleading trend detection by missing data, the following criteria were not considered in the trend analysis: i) years with more than 14 missing data, and ii) seasonal totals (3 months) with more than 3 missing data. The statistical evidence against the null hypothesis was evaluated through the bootstrap method (Efron, 1979) by using 500 random samples. It was considered statistically significant if the resampled series trend falls into the upper or lower 5% of the bootstrapped distribution.

To assess the spatial distribution of the values of trends, the climatological mean of the precipitation indices (Table 1) were interpolated using the Inverse Distance Weighted (IDW) method.

2.3. Hydrological modelling of the UPRB

2.3.1. SWAT model

The hydrological simulations of the UPRB were estimated using the 2012 version of the Soil and Water Assessment Tool (SWAT) model with an ArcGIS interface (Arnold *et al.*, 1998, https://swat.tamu.edu). SWAT is an open source, semi-distributed, and physically based model developed by the Agricultural Research Service of the United States Department of Agriculture (ARS-USDA). The model can be used to design analyses related to physical processes, both small (Ferrant *et al.*, 2011) and large-scale (Abou Rafee *et al.*, 2019, Rajib & Merwade, 2017), and can be executed in a continuous simulation in monthly or daily time steps. It has been extensively applied for different approaches such as climate change (Ficklin *et al.*, 2009), LUCC (Chotpantarat & Boonkaewwan, 2018), and climate variability scenarios (Wu & Johnston, 2007). Based on the topography, a basin is discretized into subbasins, which are connected by a stream network. To assess the differences in LUC and the heterogeneous soil in a watershed, each subbasin is further discretized into Hydrologic Response Units (HRUs), according to unique combinations of LUC, soil type, and slopes. For each HRU, simulated hydrological processes, such as surface runoff and evapotranspiration, are generated separately, and then routed through the river network to the outlet of the basin. For a further detailed description of the SWAT model, the reader is referred to Neitsch *et al.* (2011).

The hydrological behavior of a river basin in the SWAT model is based on the water balance equation (1):

$$\boldsymbol{SW_t = SW_o} + \sum_{\boldsymbol{i=1}}^{\boldsymbol{n}} (\boldsymbol{P_{T_i} - E_{sup_i} - ET_i - E_{Lat_i} - E_{sub_i}}) \qquad \textbf{(1)}$$

where SW_t e SW_o are the final and initial water content on day i (mm), and P_{T_i}, E_{sup_i}, E_{Lat_i}, ET_i and E_{sub_i} are the amount of precipitation, surface runoff, subsurface lateral flow, actual evapotranspiration, and base flow, respectively, on day i (mm).

2.3.1.1. Data description

Different input data are required to build a hydrological project with SWAT, which includes climatic, hydrologic, and physical variables. This section intends to describe the processes used to manipulate and organize the data, which was one of the important steps of this research project. An overview of the data used is given in Table 2 and Figure 3.

2.3.1.1.1. Climatic

The daily climatic data were prepared for the period simulation from 1979 to 2015, with the first five years used for the warming up of the model (1979 – 1983), the following 21 years for its calibration (1984 – 2004), and the last 11 years for its validation (2005 – 2015). Due to the low spatial-temporal resolution of observed data pertaining to temperature, solar radiation, relative humidity, and wind speed, the gridded daily meteorological data obtained from the National Center for Environmental Prediction—Climate Forecast System Reanalysis (CFSR) at 38-km grid spacing were used. The data for total daily precipitation was provided by the ANA, which made available a collection of data from 149 institutions (Figure 3a).

The study area has a good spatial density of stations, with 2,494 rain gauges within the basin. The precipitation data were thoroughly controlled before use. First, quality checks, such as double records, typographical errors, and the location of stations were evaluated. Then, the data were interpolated to a spatial resolution of 0.1 degrees using the IDW method.

2.3.1.1.2. Topography

For topographic data, a Digital Elevation Model (DEM) at a 90-meter resolution obtained from the Shuttle Radar Topography Mission (SRTM) (available at http://srtm.csi.cgiar.org/srtmdata/) was used (Figure 3b). Based on this data, the digital river network, as well as the subbasins, were generated.

2.3.1.1.3. Soil

The soil map was elaborated from the information provided by the Brazilian Agriculture Research Corporation (EMBRAPA) at a scale of 1:5,000,000. For the Paraguayan portion of the basin, the Harmonized World Soil Database (HWSD) with a

spatial resolution of $1\,km \times 1\,km$ was used. In this study, the characteristics of oligotropic, mesotropic, eutropic, and dystropic soils were grouped in a single class, resulting in 15 classes (Figure 3c). The properties of each soil class were collected from a diverse set of documents that used the SWAT model in Brazilian basins (Fauconnier, 2017, Mercuri *et al.*, 2009, Pereira, 2013).

2.3.1.1.4. Land Use and Cover

LUC data were obtained from Rudke (2018) and Rudke *et al.* (2019). The map was generated using pixel-based image classifiers, with the Support Vector Machine (SVM) algorithm. Overall, most of the basin regions presented agreement between the classified LUC and observed data, ranging from satisfactory (0.6 – 0.8) to good (0.8 – 1.0) of Kappa coefficient and global accuracy. The original classification of 10 different categories was reclassified into six major classes: forest, cropland, grassland, water, cerrado (Brazilian savanna), and urban areas (Figure 3d).

2.3.1.1.5. River discharge

To evaluate the performance of the model, monthly river discharge data were organized based on the calibration period (1984 – 2004) and validation the period (2005 – 2015). The data comprise both natural streamflow data, derived from ANA, and naturalized discharges, obtained from the National Electrical System Operator (ONS).

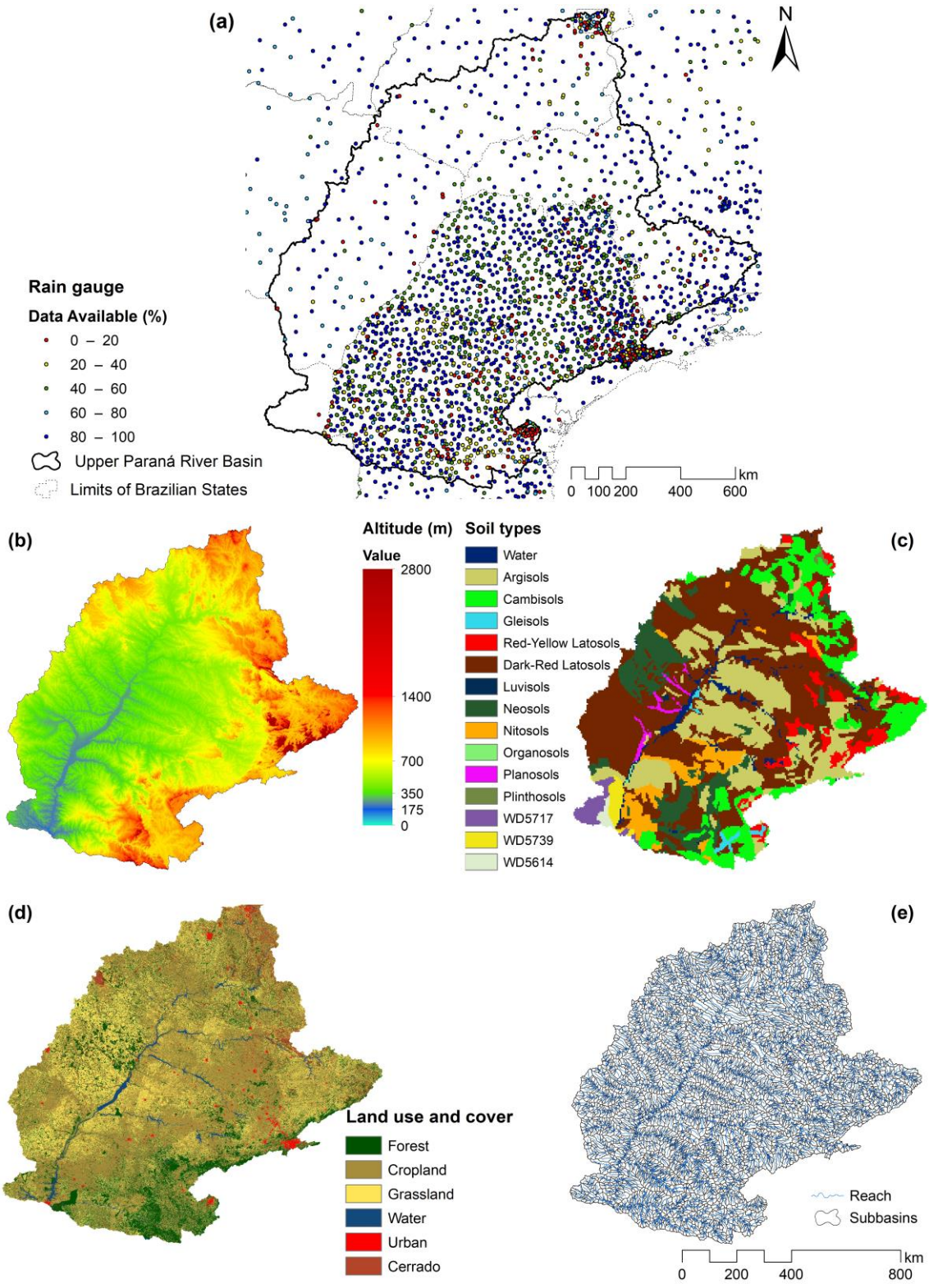

Figure 3. Maps of the (a) spatial distribution of precipitation stations, (b) topography, (c) soil types, (d) Land use and cover, and (e) discretization and reaches of the UPRB.
Based on Abou Rafee *et al.* (2019).

Table 2. Overview of the model input data.

Data	Description	Source
Topography	90-meter resolution Digital Elevation Model (DEM)	Shuttle Radar Topography Mission (SRTM) (http://srtm.csi.cgiar.org/srtmdata/)
Land use and cover	30-meter resolution classification	(Rudke, 2018, Rudke *et al.*, 2019)
Soil	Derived from 1:500000 scale digital map	Brazilian Agriculture Research Corporation (EMBRAPA) (https://www.embrapa.br/solos/sibcs/solos-do-brasil) Harmonized World Soil Database (HWSD) (http://www.fao.org/nr/land/soils/)
Precipitation	Daily (1979 – 2015)	Brazilian National Water Agency (ANA) (http://www.snirh.gov.br/hidroweb)
Maximum and minimum temperature; relative humidity; wind speed; and solar radiation	Daily (1979 – 2015)	Climate Forecast System Reanalysis (CFSR) (https://globalweather.tamu.edu)
River Discharge	Monthly (1984 – 2015)	Brazilian National Water Agency (ANA) (http://www.snirh.gov.br/hidroweb) Brazilian National Electrical System Operator (ONS) (http://www.ons.org.br)

2.3.1.2. Model set up

SWAT model project for the UPRB was built with the highest possible spatial discretization. The slopes were divided into five classes ranging between 0 – 3%, 3 – 8%, 8 – 20%, 20 – 45%, and > 45%. The basin was discretized into 5,187 sub-watersheds, using a threshold drainage area of 100 km^2, with an average size of about 173 km^2 (see Figure 3e). To represent the spatial heterogeneity across the UPRB, these subbasins were further divided into 44,635 HRUs using a defined threshold of 5% for LUC, 10% for soil, and 20% for slope. The Soil Conservation Service curve number (CN) (USDA Soil Conservation Service, 1972) and the Penman-Monteith (Monteith J. L., 1965) methods were used to compute the surface runoff and potential evapotranspiration, respectively. For groundwater flow, SWAT simulates two types of aquifers: shallow (unconfined)

aquifers, which contribute to return flow to streams within the catchment, and deep (confined) aquifers, which are responsible for the flow outside the basin (amount of water used, for example, for irrigation and water supply) and are considered water sinks in the system (Neitsch *et al.*, 2011).

2.3.1.3. Calibration and validation process

2.3.1.3.1. SUFI2 and parameter calibration

The calibration was performed by the Sequential Uncertainty Fitting (SUFI-2) algorithm proposed by Abbaspour *et al.* (2004), using SWAT-CUP version 5.1.6.2 (Soil and Water Assessment Tool Calibration and Uncertainty Program, Abbaspour, 2015). Moreover, to optimize the model execution, the parallel processing module (Rouholahnejad *et al.*, 2012) was used. SUFI-2 was developed by considering the uncertainties of parameter ranges, which are sampled through Latin hypercube sampling. Table 3 shows the list of parameters as well as their ranges used in the calibration process of the discharge series.

In addition, manual calibration to adjust the Leaf Area Index (LAI) curve for forest, cerrado, and pasture using the modified plant growth module provided by Strauch and Volk, (2013) was used. Although SWAT has been applied for tropical basins, previous studies reported that its plant growth module is not suitable in a system that has perennial tropical vegetation since the model was originally designed for temperate areas (Alemayehu *et al.*, 2017, Van Griensven *et al.*, 2012, Strauch & Volk, 2013, Wagner *et al.*, 2011).

2.3.1.3.2. Performance evaluation

To assess the performance of the model, it is recommended that the simulation should be evaluated by several statistical indices (Arnold *et al.*, 1998). Five indices were chosen so that they, together, can provide a general overview of the quality of the simulations. The percent bias (PBIAS) (Yapo *et al.*, 1996), coefficient of determination (R^2), Nash-Sutcliffe efficiency (NSE) (Nash & Sutcliffe, 1970), The Kling-Gupta efficiency (KGE) (Gupta *et al.*, 2009), and the root mean square error (RSR) (Moriasi et al., 2007) were selected.

Table 3. List of sensitive parameters selected for calibration

Based on Abou Rafee *et al.* (2019).

Parameter *	Description	Initial Range	
		Min	Max
From Soil			
r_CN2.mgt	SCS runoff curve number	−0.4	0.4
r_SOL_AWC.sol	Soil available water storage Capacity (mm H_2O mm $soil^{-1}$)	−0.4	0.4
r_SOL_K.sol	Saturated hydraulic conductivity (mm h^{-1})	−0.8	0.8
r_ESCO.hru	Soil evaporation compensation factor	−0.4	0.4
r_OV_N.hru	Manning´s n value for overland flow	−0.4	0.4
Groundwater			
r_GWQMIN.gw	Threshold depth of water in the shallow aquifer for return flow (mm)	−0.8	0.8
r_GW_DELAY.gw	Groundwater delay (days)	−0.8	0.8
r_REVAPMN.gw	Threshold depth of water in the shallow aquifer for "revap" (mm)	−0.5	0.5
r_RCHRG_DP.gw	Deep aquifer percolation fraction	−0.5	0.5
r_GW_REVAP.gw	Groundwater "revap" coefficient	−0.4	0.4
r_ALPHA_BF.gw	Base flow alpha factor (days)	−0.8	0.8
r_ALPHA_BNK.rte	Base flow alpha factor for bank storage	−0.5	0.5
Channel			
r_CH_K2.rte	Effective hydraulic conductivity in channel (mm h^{-1})	−0.8	0.8
r_CH_N2.rte	Manning´s value for main channel	−0.8	0.8
Land use and Cover			
r_EPCO.bsn	Plant uptake compensation factor	−0.5	0.5
r_CANMX.hru	Maximum canopy storage (mm H_2O)	−0.4	0.4
Subbasin			
r_SURLAG.bsn	Surface runoff lag time	−0.5	0.5
r_SLSUBBSN.hru	Average slope length (m)	−0.4	0.5
r_ LAT_TTIME.hru	Lateral flow travel time (days)	−0.5	0.5
r_HRU_SLP.hru	Average slope steepness (m m^{-1})	−0.4	0.4

*****"r_" refers to a relative change in the parameters where the current value is multiplied by 1 plus a factor from the given parameter range.

2.3.1.3.3. Modelling protocol

The criteria and the procedures used for the calibration processes are summarized as follows:

I. In order to run the simulation with parallel processing, due to memory limitations as a result of the project size, the basin area was divided into 9 watersheds for

calibration and the fitted values in each subbasin were used for the initial project (see Figure 4).

II. To avoid the incorrect location of the calibration outlets, its geographic position was verified.

III. A multi-site calibration from upstream to downstream outlets calibration, recommended by Leta *et al.* (2017) for heterogeneous basins was applied.

IV. The discharge outlets which performed satisfactory or better in all statistical indices (listed in Performance evaluation section) were not considered in the calibration process. The subbasins that were not considered in the calibration process are illustrated in black in Figure 4.

V. The initial parameter ranges followed the calibration protocol presented by Abbaspour *et al.* (2015) for large-scale basins. For example, if the simulation presented base flow too low (high), the GWQMN, GW_REVAP, and REVAMPM parameters should increase (decrease). Therefore, before each calibration, the temporal evolution of the discharge simulation was evaluated as to whether it underestimated or overestimated the observation.

VI. The objective function selected in the calibration process was NSE index.

VII. Once the sub-project was built for the subbasin, and the ranges of parameters were defined, the model simulations were run between 150 and 500 times, with a maximum of 3 iterations. The numbers of simulations, as well as of iterations, were based on the size of the sub-project and performance of the initial simulation.

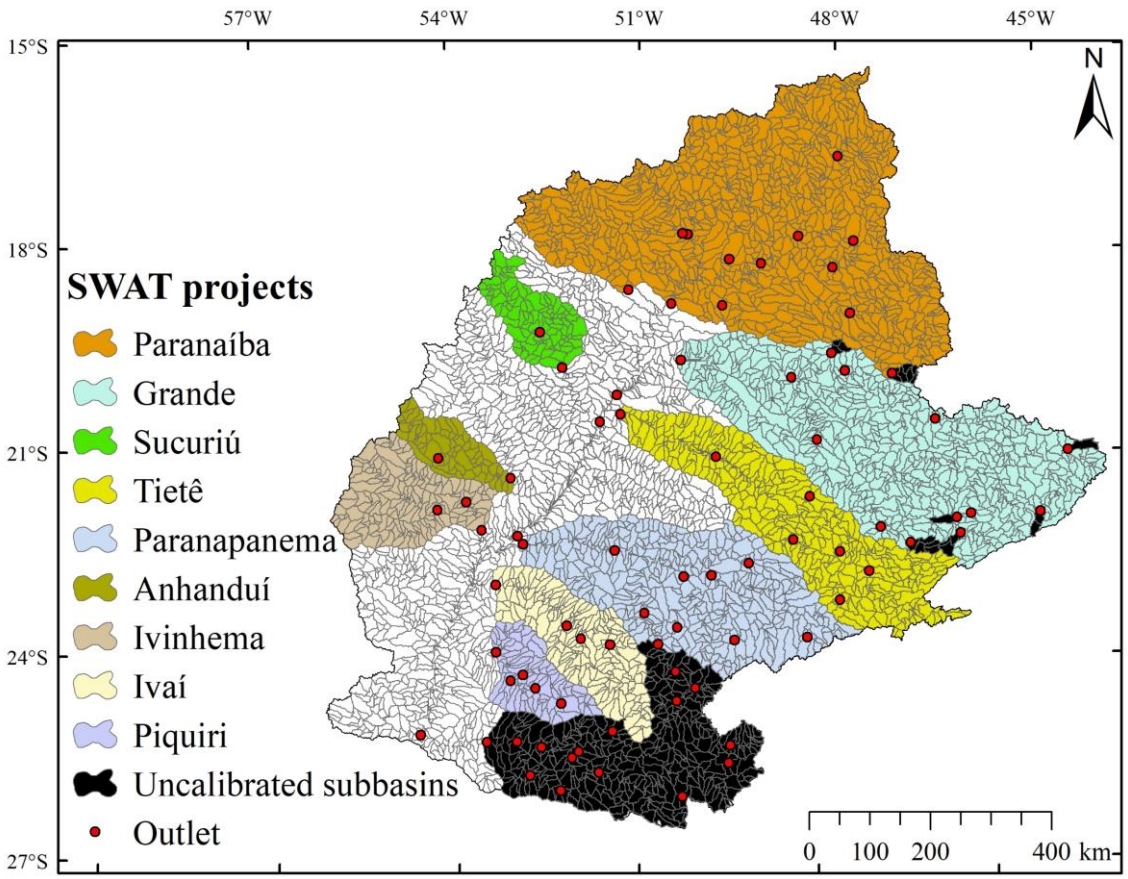

Figure 4. Division of SWAT projects for calibration.

2.4. Numerical scenarios

2.4.1. LUC 1985 versus LUC 2015

2.4.1.1. Data

Two LUC under unchanged climatic conditions were simulated. The LUC correspond to the years 1985 and 2015 (Figure 5) classified by Rudke (2018) and Rudke *et al.* (2019). The simulations were based on the data and model set up aforementioned (section 2.3). In this case, following the configuration criteria, 44,635 (LUC 2015) and 50,272 (LUC 1985) HRUs were created.

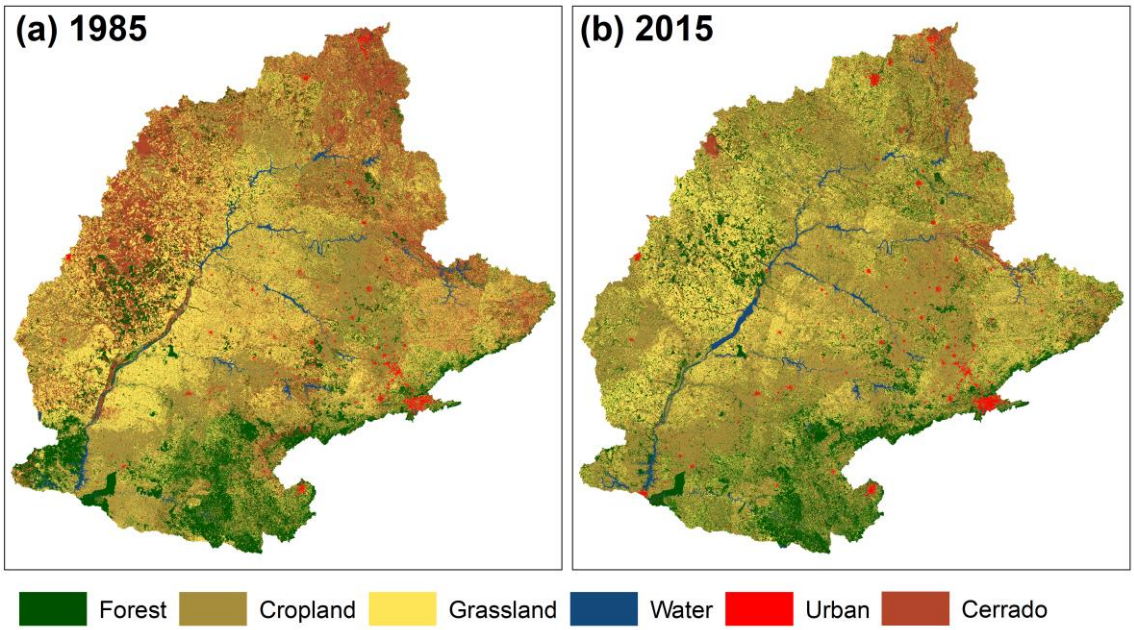

Figure 5. Land use and cover (LUC) classes for 1985 (a) and 2015 (b).

2.4.1.2. Analysis of the effects of LUCC

The effects of LUCC between 1985 and 2015 on the hydrologic components of the UPRB were evaluated as follows:

I. To address the main LUCC between 1985 and 2015 in the basin, 9 major transitions of four LUC classes were calculated: Cerrado to forest; Grassland to forest; Cropland to forest; Forest to grassland; Cerrado to grassland; Cropland to grassland; Forest to cropland; Cerrado to cropland; and Grassland to cropland.

II. To identify the effects of LUCC on hydrology within the UPRB, the surface runoff, actual evapotranspiration, soil moisture, and discharge were analyzed.

III. The aforementioned hydrologic components were calculated by the relative change for the simulation with the LUC from 2015 relative to the simulation with LUC from 1985. Changes were examined for annual (hydrological year, from October to September), wet (October – March), and dry (April – August) seasons considering the calibrated and validated period from 1984 to 2015.

IV. The hydrological variables were calculated using the 5,187 watersheds discretization of the UPRB, however, the results were illustrated and interpreted for the 34 major subbasins as shown in Figure 6.

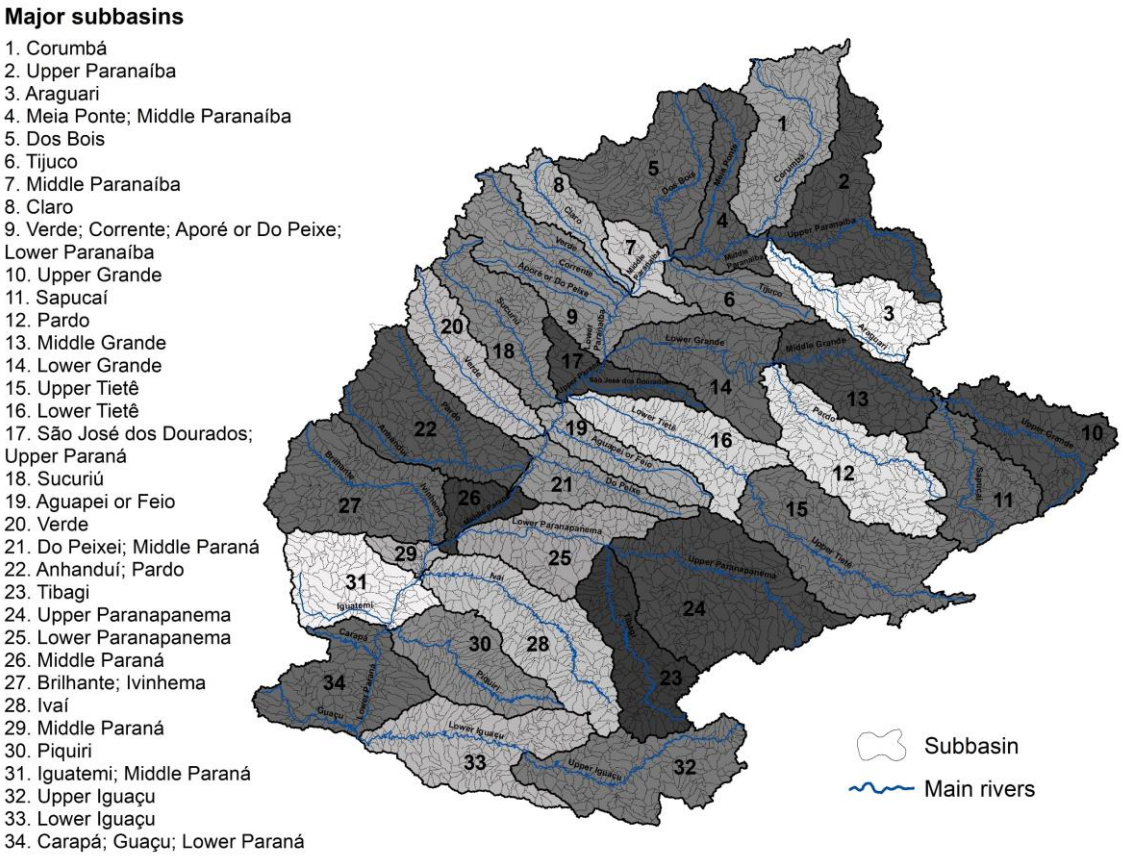

Figure 6. Subbasin discretization, major subbasins and main rivers of the UPRB.

2.4.2. LUCC versus Climate shift

2.4.2.1. Data preparation

2.4.2.1.1. Climatic data

The climatic data were prepared for the simulation period from January 1956 to December 1990, being the first five years used to the warming up of the model (1956 – 1960). Daily maximum and minimum temperature, solar radiation, wind speed, and relative humidity were obtained from the European Centre for Medium-Range Weather Forecasts (ECMWF) reanalysis ERA-20C at the grid resolution of 0.25 degrees. Daily precipitation data from the ANA were used. It was provided 2,739 rain gauge stations (2,292 within basin), out of which 38% have less than 20% of missing data. These data were interpolated to a spatial resolution of 0.1 degrees using the IDW method.

2.4.2.1.2. Physical data

Three simulations of discharge were made and scenarios created. Similar to all simulations are the input data of climatic, soil, and topography. A different LUC was used in each simulation. They are a pristine LUC of around 1500, a LUC for 1960 and one for 1985. The description of each LUC is presented as follows:

LUC – 1985

The LUC for 1985 was based on the classification made by Rudke (2018). The map was generated from pixel-based classifications, using 50 Landsat-8 scenes. Based on his classification, the UPRB were divided into six major categories: forest, cerrado (Brazilian savanna), cropland, grassland, water, and urban areas.

LUC – T0

A map of the original vegetation, representing the unchanged landscape from a pristine period (around the Year 1500) named in this work as T0 was constructed. The original vegetation vectors were based on the classification performed by the RADAMBRASIL project. This project generated mappings of the 70's and 80's decades, being the first national effort to know the physical and biotic conditions of the national territory using a large amount of material and human resources (IBGE, 2017). The categories of natural vegetation and savanna phytophysonomies from the T0 map were merged into forest and cerrado, respectively. In addition, the water and natural vegetation categories (cerrado or forest) from the 1985 map were maintained. Hence, three classes were defined as forest, cerrado, and water areas.

LUC – 1960

The LUC for 1960 was created based on the previous described maps (T0 and 1985) and the mapping products of Dias *et al.* (2016) (available at www.biosfera.dea.ufv.br/en-US/bancos). Dias *et al.* (2016) made the first effort of a spatialized database of agriculture areas in Brazil between 1940 and 2012 that includes the percentage, per pixel, of croplands and grasslands. The reconstruction was based on satellite images and census of agriculture data obtained by municipality. Dias *et al.* (2016) provide the cropland and grassland areas estimates with an annual temporal resolution

and 1 km of spatial resolution. This work reconstructed LUC 1960 reconstruction by following the steps described below:

I. The methodology consisted in considering the estimates from Dias *et al.* (2016) to define areas of cropland and grassland, and the LUC from T0 to define areas of cerrado and forest. Urban areas of 1985 map were added to the 1960 map. It was assumed that urban categories maintained their areas between 1960 and 1985 since they represent less than 1% of the UPRB. The map from 1960 describing urban areas are not available on a large-scale, on just a few municipal topographic maps, that are not feasible to use in this study. Therefore, the conversion from cerrado and forest to urban areas were not evaluated from 1960 to 1985.

II. The map from Dias *et al.* (2016) with a spatial resolution of 1 km was resampled to match the 90 meters from the maps of T0 and 1985. In this case, the bilinear interpolation technique (Hilker *et al.*, 2014) was applied.

III. Pixels with estimates of cropland and grassland lower than 15% were defined as natural vegetation areas. These areas followed the forest or cerrado categories from the T0 map.

IV. Pixels with estimates of cropland and grassland higher than 15% were divided into these two categories (cropland or grassland) according to the highest percentage.

V. Pixels classifieds as urban areas, water, forest and cerrado from the 1985 LUC map were maintained in the 1960 LUC map. Areas of natural vegetation in the 1985 are assumed to have been always natural and not a regeneration.

VI. To evaluate the level of agreement of the reconstruction, the aforementioned steps of estimation of cropland and grassland areas were applied to the LUC from 1985. The reconstruction of the 1985 map performed satisfactorily with 72% of similarity based on Global Accuracy test.

2.4.2.2. Model set up

The simulations for the three LUC were built with the same configuration described in section 2.3 (Hydrological modelling of the UPRB) that includes the

parameterization and best-fit calibration parameters. As a result, the model generated 24,839 (LUC T0), 34,029 (LUC 1960) and 50,272 (LUC 1985) HRUs.

2.4.2.3. Construction of scenarios

The construction of specific scenarios to assess the impacts due to LUCC between 1960 and 1985 and due to climate shift on river discharge were defined based on the series of discharge as shown in Table 4.

Five scenarios were created, A to E as shown in Table 4. Scenario A was defined by the relative change in the average annual median discharge under the values of D3 relative to the values of D1 was calculated. Scenario B, the same but with the values of D4 relative to D2. Scenario C, with the values of D2 relative to D1. Scenario D with the values of D4 relative to D3. Scenario E with the values of D4 relative to D1. Scenario A and B indicate the impact of LUCC between 1960 and 1985 for two periods of precipitation patterns (1961 – 1973 and 1978 – 1990). Scenarios C and D show the effect of the changes in precipitation before (1961 – 1973) and after (1978 – 1990) climate shift over the annual discharge values. In these cases, the comparison is performed for the same simulation (i.e., same LUC). Finally, Scenario E estimates the effect of both LUCC and climate shift as the comparison is performed for different precipitation periods and LUC.

In addition, five scenarios were constructed with the simulation T0 as shown in Table 5. The same criteria of the aforementioned scenarios were used but the simulation with LUC 1960 was replaced by the simulation T0. On these conditions, the maximum impact of LUCC until the year 1985 on annual discharge was achieved. In this case, in order to distinguish from the previous ones, the scenarios are referred by Roman Numerals from I to V.

Table 4. Overview of the defined discharge series for the construction of the scenarios A to E.

Discharge	Description
D1	Discharge values between 1961 and 1973 from simulation with LUC 1960
D2	Discharge values between 1978 and 1990 from simulation with LUC 1960
D3	Discharge values between 1961 and 1973 from simulation with LUC 1985
D4	Discharge values between 1978 and 1990 from simulation with LUC 1985
Scenarios	**Description**
Scenario A	D3 minus D1
Scenario B	D4 minus D2
Scenario C	D2 minus D1
Scenario D	D4 minus D3
Scenario E	D4 minus D1

Table 5. Overview of the defined discharge series for the construction of the scenarios I to V.

Discharge	Description
D1’	Discharge values between 1961 and 1973 from simulation with LUC T0
D2’	Discharge values between 1978 and 1990 from simulation with LUC T0
D3’	Discharge values between 1961 and 1973 from simulation with LUC 1985
D4’	Discharge values between 1978 and 1990 from simulation with LUC 1985
Scenarios	**Description**
Scenario I	D3’ minus D1’
Scenario II	D4’ minus D2’
Scenario III	D2’ minus D1’
Scenario IV	D4’ minus D3’
Scenario V	D4’ minus D1’

2.4.2.4. Analysis of the effects of LUCC and Climate shift

For the analysis of the scenarios, ten outlets were selected. The selection was based on the largest rivers of the UPRB or those that had their upstream subbasins with expressive suppression of natural vegetation (forest or cerrado) replaced mainly by cropland or grassland areas. The location of the selected outlets is shown in Figure 7.

Four outlets of Paraná river were evaluated: Upper Paraná (4) after the confluence of Lower Tietê (3); Middle Paraná (6), before the confluence of Ivinhema (7), Lower Paraná (8), and Lower Paraná (10), the river mouth of the UPRB.

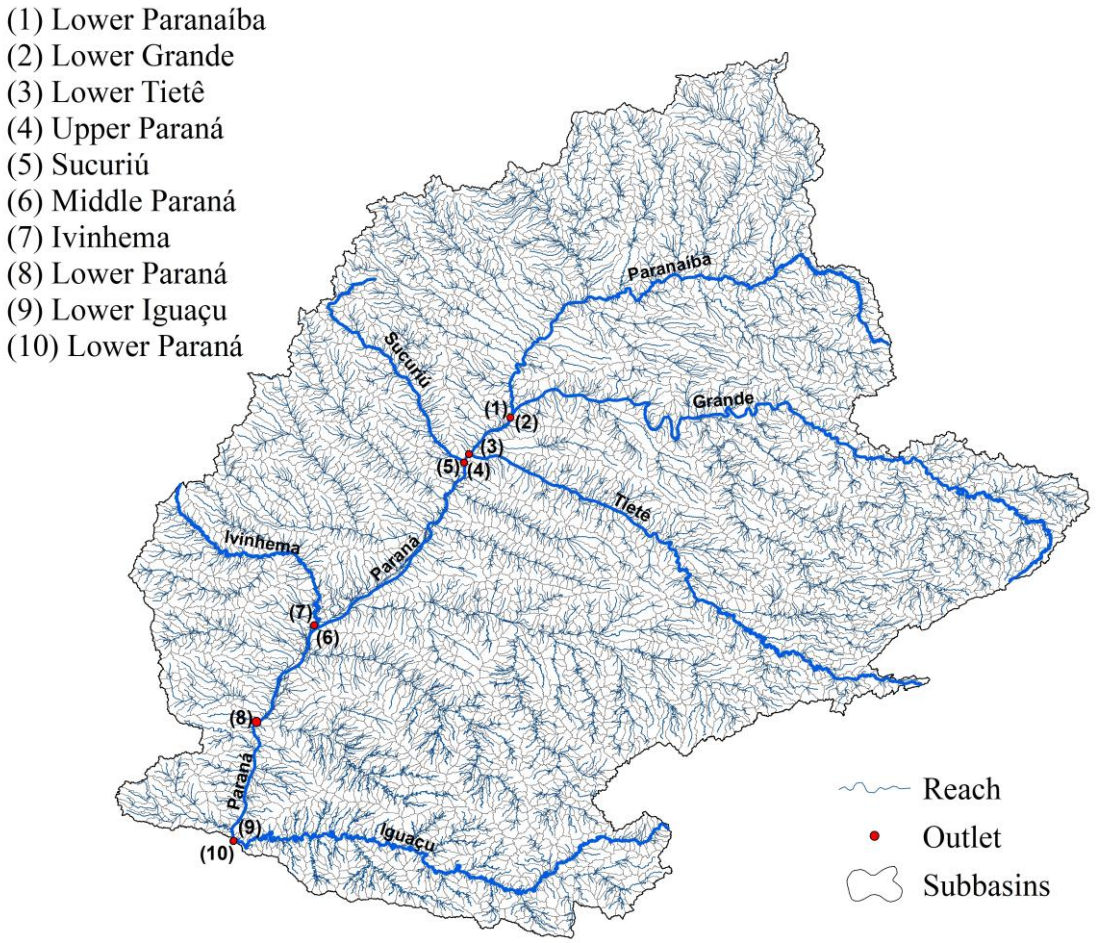

Figure 7. Location of the outlets selected with their respective number, and subbasins discretization.

3. Results and Discussion

This chapter combines the results obtained from the statistical analysis used to detect the trends of precipitation, hydrological modelling of the UPRB, and the results from the numerical scenarios. The main findings are presented. For further details, the reader is referred to the appended papers I to IV.

3.1. Analysis of the precipitation trends

In the following sections, the results of the trends detected by MK test are discussed as the division shown in Figure 2 into six subbasins: I – Paranaíba, II – Grande, III – Tietê, IV – Paraná, V – Paranapanema and VI – Iguaçu.

3.1.1. Annual and seasonal precipitation

Figure 8 shows the spatial distribution of trends of annual and seasonal precipitation totals between 1977 and 2016. The following significant trends (at the 95% confidence level) were found:

- **Annual:** 36 stations presented significant negative trends, being mostly located at Grande (20) and Paranaíba (8) subbasins. 34 presented significant positive trends, concentrated in parts of the Paranapanema (12), Iguaçu (11) and Paraná (9) subbasins.
- **Summer:** negative trends are observed mostly in the Paranaíba (9) and Grande (4) subbasins. Positive trends are concentrated in the southeast of the Paraná (12), Iguaçu (5) and Paranapanema (4) subbasins.
- **Autumn:** all the significant trends were negative, and they were mainly located in the central portion and northeastern region of the UPRB.
- **Winter:** few stations presented significant trends, with a clear north-south separation. Negative trends predominated in the north (9) and positive in the south (4) of the basin.
- **Spring:** Statistically significant negative trends predominated in the northeastern region of the UPRB, with 16 stations in the Grande subbasin.

The spatial distribution of trends of annual and seasonal total precipitation shows that significant negative trends are mostly located in the northern part at Paranaíba and Grande subbasins. A decreasing amount of precipitation in those regions may have a significant impact on energy generation as these basins house 70 hydropower plants that, together, provide more than 17,000 MW of electricity (ANEEL, 2020). In contrast, the significant positive trends are concentrated in the southern part particularly in the Paranapanema and Iguaçu subbasins, notably in the summer season.

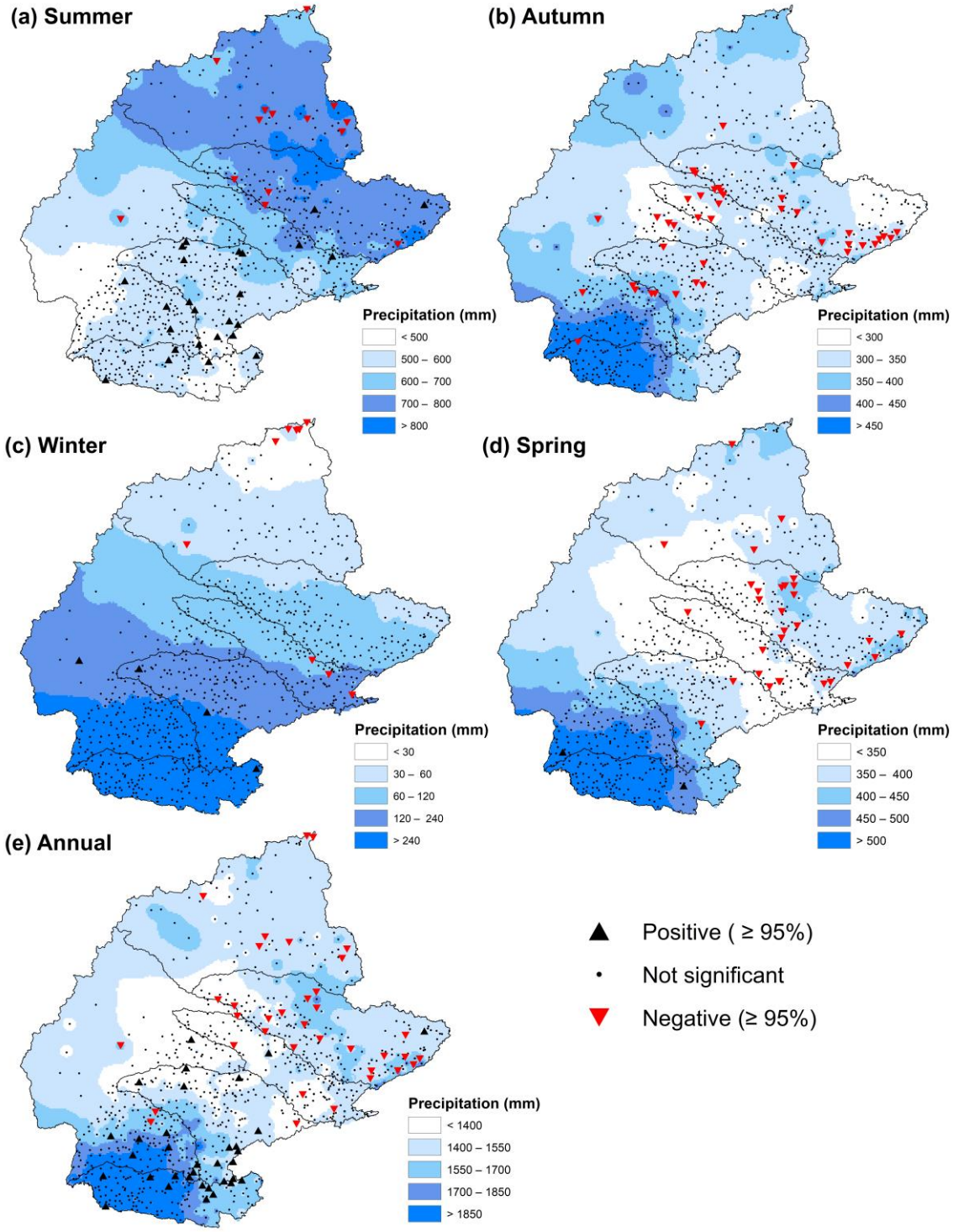

Figure 8. Spatial distribution of trends and interpolated values of annual and seasonal average precipitation totals in the UPRB over the period of 1977–2016 for (a) summer, (b) autumn, (c) winter, (d) spring, and (e) annual. The blue-shaded patterns are the annual and seasonal values, triangles show the significant trend (red is negative, and black is positive), and black circles indicate no significant trend.

From Abou Rafee *et al.* (2020).

3.1.2. Extreme precipitation events

Figure 9 illustrates the spatial distribution of trends of four extreme precipitation indices detected between 1977 and 2016. The following significant trends (at the 95% confidence level) were found:

- **Annual greatest 5-day total precipitation (px5d):** 20 stations presented positive significant trends observed mostly on the central portion of the basin. 9 of these stations are located at the Lower Paranapanema subbasin, where extreme precipitation events were witnessed and caused considerable damages (e.g. Camilloni and Barros 2000). On the other hand, 14 stations with negative trends were detected mostly located in the northern and northeastern regions of the UPRB.

- **Annual mean precipitation per rainy day** ($\geq \mathbf{1}\ \boldsymbol{mm\ day^{-1}}$) **(pint):** 263 stations were identified with a significant trend. 87% of these stations presented positive trends and are mostly located at the Paraná subbasin, with 70 stations, followed by the Paranapanema (54) and Iguaçu (48) subbasins. This result is in accordance with previous studies (Zandonadi *et al.*, 2016) and indicates that most of the areas of the basin are lengthening the wet season.

- **Annual maximum number of consecutive dry days** ($< \mathbf{1}\ \boldsymbol{mm\ day^{-1}}$) **(pxcdd):** 41 stations showed a significant trend, of which 36 are positive and 5, negative. Most of these (15) located in the northern region of the UPRB, particularly in the northern Paranaíba subbasin, which is the region that presents a high number of dry days (> 90). This might have a significant impact as the subbasin is home of the Corumbá IV reservoir, which is responsible for the water supply of 1.3 million inhabitants.

- **Annual number of days with precipitation** ($> \mathbf{50}\ \boldsymbol{mm\ day^{-1}}$) **(pn50):** 85 stations showed a significant trend, of which 60 are positive and 25, negative. Positive trends are mostly located on the south and negative ones on the northeast of UPRB. The positive trends could be associated with the increasing trends in strength and frequency of SALLJ over southern Brazil as reported by Montini *et al.* (2019).

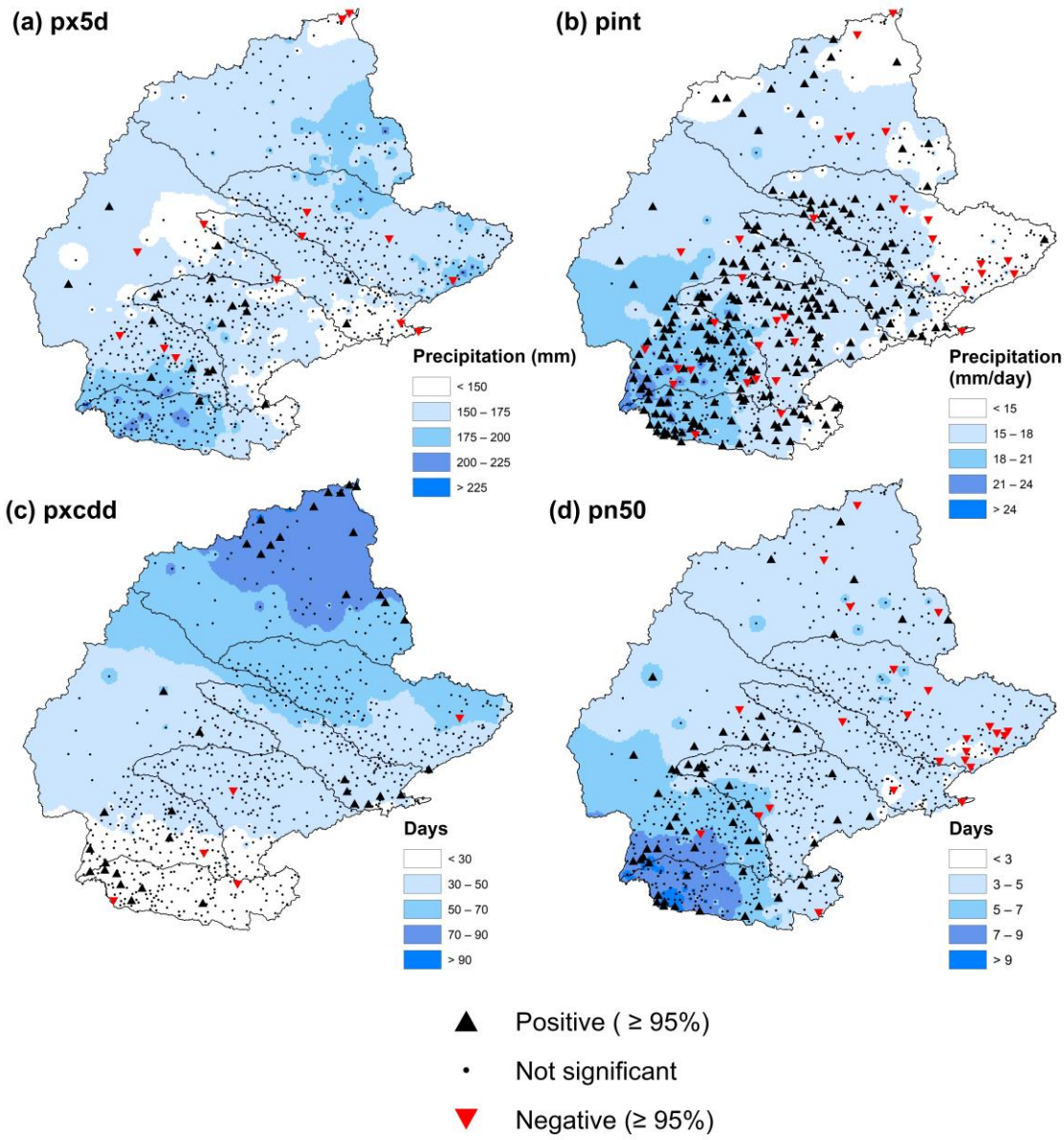

Figure 9. Spatial distribution of trends and interpolated values of annual average extreme precipitation indices in the UPRB over the period of 1977–2016 for (a) px5d, (b) pint, (c) pxcdd, and (d) pn50. The blue-shaded patterns are average extreme precipitation indices values, triangles show the significant trend (red is negative, and black is positive), and black circles indicate no significant trend.

From Abou Rafee *et al.* (2020).

3.2. SWAT model performance

In this section, the main results of calibration and validation for the main discharge rivers of the UPRB are presented. Furthermore, the values of LAI considering all the HRUs are illustrated. For more details, the reader is encouraged to refer the Papers II and III as well as their supplementary materials.

3.2.1. River discharge

As shown in Figure 10, the simulated results were consistent with the observed monthly discharge at the main rivers of the UPRB. According to the performance rating proposed by Moriasi *et al.* (2007) and Thiemig *et al.* (2013), the simulations ranged from satisfactory to very good in the statistical indices presented in Table 6. During the calibration period (1984 – 2004), PBIAS ranged from -0.2 to 6.4, R^2 from 0.71 to 0.88, NSE from 0.7 to 0.8, KGE from 0.7 to 0.9, and RSR from 0.44 to 0.55. For the validation period (2005 – 2015), the simulations reached index values up to 0.7 for PBIAS and 0.92 for R^2 (at Grande river), and, 0.84 for NSE, 0.88 for KGE, and 0.4 for RSR (at Paranaíba river).

3.2.2. Leaf Area Index

The average monthly simulated LAI values considering all the HRUs for the whole basin are presented in Figure 11. SWAT vegetation parameters were manually calibrated to adjust the magnitude and shape of LAI in accordance with the observations (Bucci *et al.*, 2008, Hoffmann *et al.*, 2005, Negrón Juárez *et al.*, 2009). The estimated values of LAI ranged between 2.5 and 5.5 $m^2\ m^{-2}$ for forest, 0.7 and 2.5 $m^2\ m^{-2}$ for cerrado, and 0.5 and 2.0 $m^2\ m^{-2}$ for grassland. As shown in Figure 11 LAI varies seasonally with the highest values within the wet season (October – March), and the lowest values in the dry season (April – September) due to the dormancy period. LAI values from the current study are comparable to those simulated by Santos *et al.* (2018), who used SWAT to evaluate the impacts of LUCC on hydrology in the Iriri River basin in the Brazilian Amazon. Their results showed LAIs with annual averages of 4.02, 1.25, and 1.09 $m^2\ m^{-2}$ (versus 3.53, 1.49, and 1.23 $m^2\ m^{-2}$ in this study) for the forest, cerrado, and grassland, respectively.

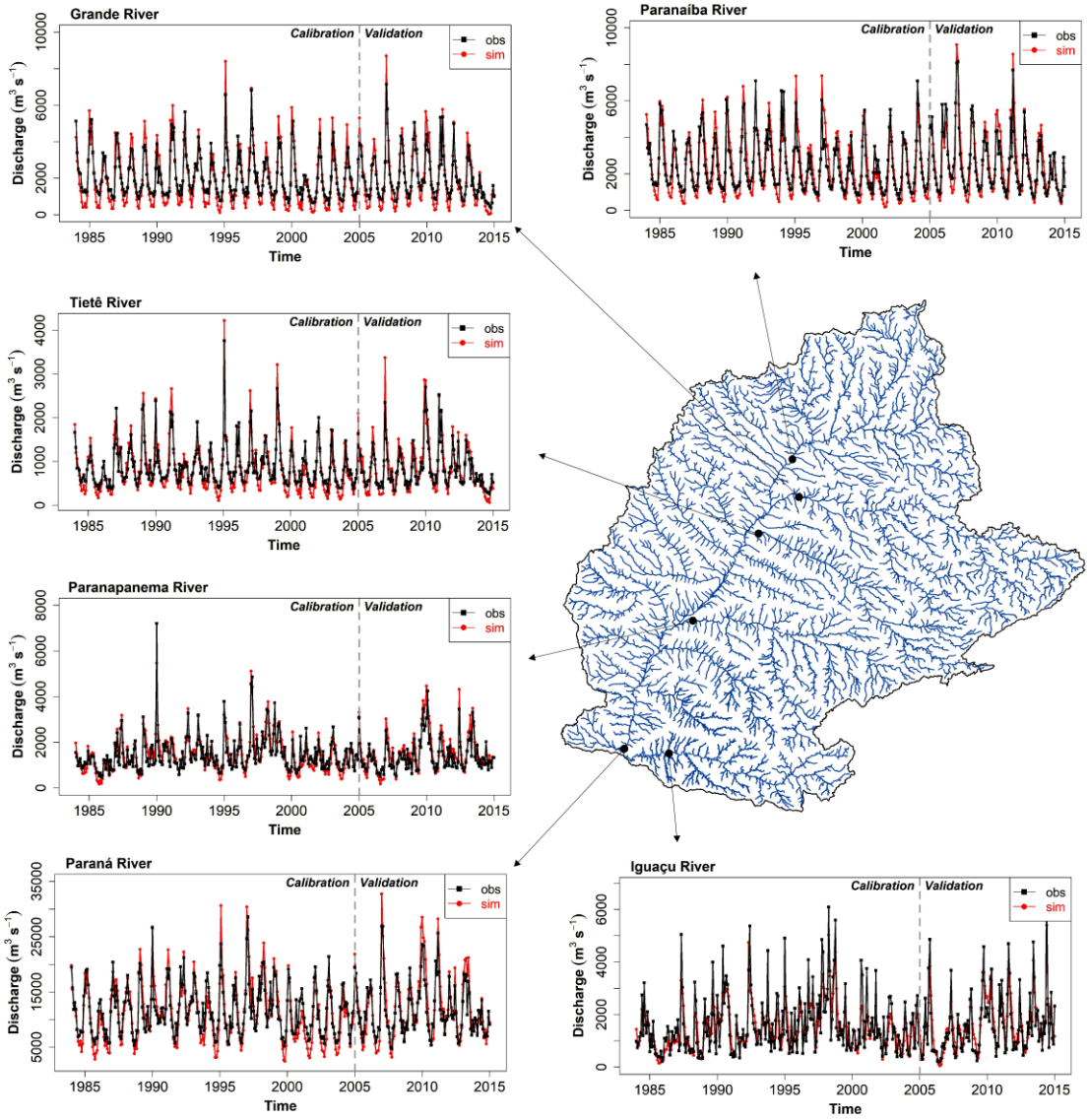

Figure 10. Comparison between the observed and simulated monthly discharge at the main rivers of the UPRB.

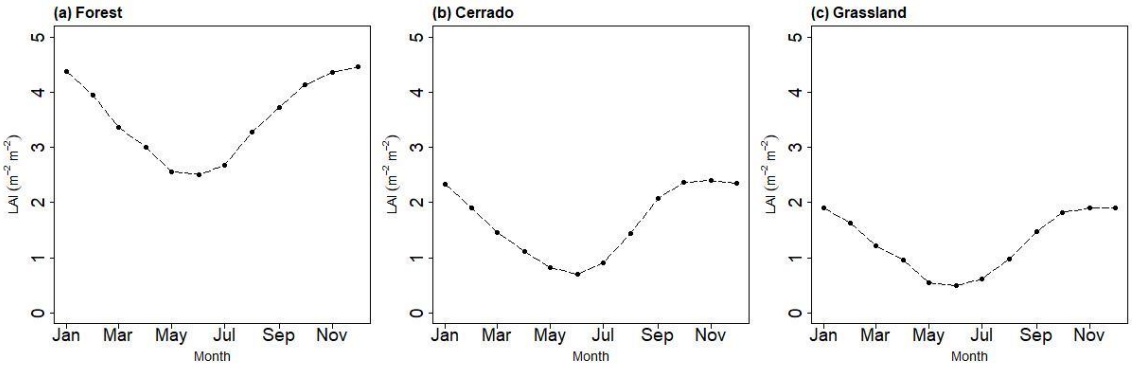

Figure 11. Average monthly simulated LAI values considering all HRUs from LUC 2015 scenario for Forest (a), Cerrado (b), and Grassland (c).

Table 6. SWAT model performance for the main rivers of the UPRB.

Outlet	Index	Calibration (1984 - 2004)	Validation (2005 - 2015)	Whole Period
Paranaíba	PBIAS	0.1	-4.5	-1.5
	R^2	0.82	0.87	0.84
	NSE	0.76	0.84	0.79
	KGE	0.81	0.88	0.84
	RSR	0.49	0.40	0.45
Grande	PBIAS	6.4	0.7	4.5
	R^2	0.88	0.92	0.89
	NSE	0.75	0.82	0.78
	KGE	0.71	0.73	0.72
	RSR	0.5	0.42	0.47
Tietê	PBIAS	5.7	-3.9	2.6
	R^2	0.87	0.86	0.86
	NSE	0.78	0.74	0.77
	KGE	0.78	0.72	0.76
	RSR	0.47	0.51	0.48
Paranapanema	PBIAS	-0.2	-12.9	-4.6
	R^2	0.82	0.88	0.83
	NSE	0.80	0.74	0.78
	KGE	0.90	0.75	0.85
	RSR	0.44	0.51	0.46
Iguaçu	PBIAS	5.5	-0.8	3.3
	R^2	0.71	0.78	0.74
	NSE	0.70	0.77	0.72
	KGE	0.70	0.75	0.72
	RSR	0.55	0.48	0.52
Paraná	PBIAS	3.6	-6.2	0.2
	R^2	0.84	0.87	0.84
	NSE	0.75	0.75	0.75
	KGE	0.78	0.75	0.76
	RSR	0.50	0.50	0.50

3.3. Analysis of LUC 1985 versus LUC 2015

3.3.1. Detection of LUCC transitions

The total area of the main transitions of LUCC between 1985 and 2015 at the major subbasin level are shown in Figure 12. The largest areas of LUCC were the conversion from grassland to cropland occurred within the Brilhante/Invinheima (27) and Lower Tietê (16) subbasins, which reached up to 8,490 and 9,250 km^2, respectively. Besides, in the Carapá/Guaçu/Lower Paraná (34) subbasin, 6,640 km^2 of forests were replaced by cropland areas. Most of these areas were replaced mainly by sugarcane cultivation due to the high demand for bioenergy in the form of ethanol and raw material

for the thermoelectric power plants (Adami *et al.*, 2012, Rudorff *et al.*, 2010). Also, this growth is largely caused by the development of agricultural mechanization, climate conditions, population growth, and economic factors (Mueller & Mueller, 2016). Particularly, in the southern part of the basin, the main reason for the expansion of cropland was the construction of the Itaipu hydroelectric power plant (1974 – 1985) at the border between Brazil, Argentina, and Paraguay. This construction made an important contribution to rapid population growth in the region (Baer & Birch, 1984). It is also worth mentioning that the increase of areas of cropland in the basin happens over areas that were previously covered with cerrado. Deforestation of cerrado contributed to an increase of up to 6,550 km^2 in cropland areas in the Corumbá (1) and Upper Paranaíba (2) subbasins. Still, cerrado reductions also had a significant contribution to the grassland expansion. For example, about 6,670 km^2 of cerrado were deforested replaced by grassland in the Anhanduí/Pardo (22) subbasin.

The central-western and northern parts of the basin were the ones that most witnessed afforestation or reforestation in the last recent decades. For example, the transition from cerrado to forest in the Corumbá (1) and Anhanduí/Pardo (22) subbasins contributed to a forest cover increase of up to 3,070 and 3,040 km^2, respectively. The increase in forests is mainly related to the transitions of the LUC classes of cerrado, grassland, and cropland to Eucalyptus plantations. According to the Brazilian Association of Forest Plantation Producers, the growth of Eucalyptus in Brazil has been mainly driven by the profit growth generated that is up to six times greater than the one of livestock production. Besides economic issues, Gonçalves *et al.* (2008) pointed out that the increase of Eucalyptus plantation is due to the investments in research and technology in the last decades, which improved seed or clonal plantations.

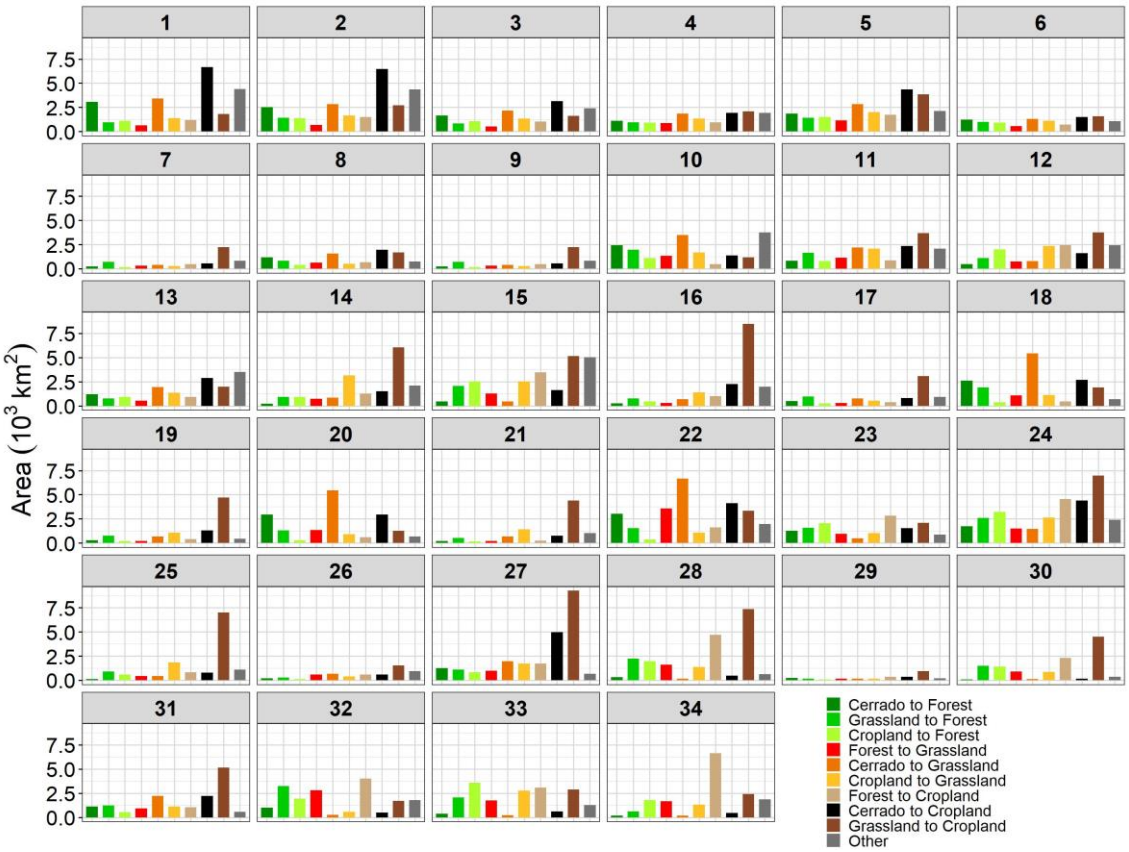

Figure 12. Area (10^3 km^2) of the main transitions of LUCC between 1985 and 2015 at the major subbasins of UPRB. **1.** Corumbá; **2.** Upper Paranaíba; **3.** Araguari; **4.** Meia Ponte-Middle Paranaíba; **5.** Dos Bois; **6.** Tijuco; **7.** Middle Paranaíba; **8.** Claro; **9.** Verde-Corrente-Aporé or Do Peixe-Lower Paranaíba; **10.** Upper Grande; **11.** Sapucaí; **12.** Pardo; **13.** Middle Grande; **14.** Lower Grande; **15.** Upper Tietê; **16.** Lower Tietê; **17.** São José dos Dourados-Upper Paraná; **18.** Sucuriú; **19.** Aguapei or Feio; **20.** Verde; **21.** Do Peixei-Middle Paraná; **22.** Anhanduí-Pardo; **23.** Tibagi; **24.** Upper Paranapanema; **25.** Lower Paranapanema; **26.** Middle Paraná; **27.** Brilhante-Ivinhema; **28.** Ivaí; **29.** Middle Paraná; **30.** Piquiri; **31.** Iguatemi-Middle Paraná; **32.** Upper Iguaçu; **33.** Lower Iguaçu; **34.** Carapá-Guaçu-Lower Paraná.

3.3.2. Effects of LUCC on hydrology

The two simulated scenarios for the LUC from 1985 and 2015 with unchanged climatic conductions were compared. The effects of LUCC on hydrologic components within the basin are illustrated in the spatial distribution of changes in surface runoff, actual evapotranspiration, and soil moisture (Figure 13). These changes were calculated considering the long-term means (1984 – 2015) from the difference between LUC2015 and LUC1985 simulated hydrologic variables for annual (October – September), wet (October – March), and dry (April – September) season values. Also, to address the

LUCC impacts for interannual variation of climate, box plots of annual and seasonal from 32 years (1984 – 2015) for hydrological variables were calculated (see Figure 14), considering the means values of simulated hydrological variables at the major subbasin level (as shown in Figure 6).

3.3.2.1. Surface runoff, actual evapotranspiration, and soil moisture

Overall, the LUC caused an increase in the annual and wet season surface runoff, while a decrease in the dry period (Figure 13 and Figure 14). The interannual values show that the increases at the major subbasins level reach up to 31.8 and 25.3 mm in the annual and wet season runoff, respectively. In contrast, the decrease overtakes 5.6 mm in the dry season. The effects are remarkable at the Corumbá (1), Upper Paranaíba (2), Corrente, Aporé or do Peixe (9), and Carapá-Guaçu-Lower Paraná (34) subbasins. In these regions, a major cause for the increase in surface runoff is the substantial removal of the cerrado and forest vegetation, replaced mainly to cropland and grassland (see Figure 12). In addition, it was observed a significant increase in the Lower Tietê (16), Brilhante-Invinheima (27), Piquiri (30) watersheds. However, in these regions, an expressive reduction of cerrado and grassland areas replaced by cropland was observed.

In addition, it should be noted in the spatial distribution (Figure 13) that small catchments presented a decrease in surface runoff during the wet season. This could be attributed to the increase in forest areas due to the afforestation (e.g. cerrado to forest) and reforestation (e.g. grassland to forest).

In SWAT, the surface runoff is estimated by the Curve Number (CN) method (USDA Soil Conservation Service, 1972). CN varies spatially according to LUC, soil type, and slope. It can be easily interpreted by the order of higher values: Urban>Cropland>Grassland>Cerrado>Forest. Consequently, the increase or decrease in the generated runoff during the period could be explained by the major conversions of LUC in the basin such as from cerrado to cropland, or from grassland to cropland. Also, CN has temporal variation due to changes in soil moisture. During the dry season, a possible explanation for the decreasing amounts of surface runoff is due to the reduction in the water content storage. Li *et al.* (2015) who applied the SWAT model also observed runoff decrease due reduction in soil water storage during dry season over deforestation areas in the south-eastern Fujian Province of China.

In contrast to surface runoff, a decrease in the actual evapotranspiration mainly in the annual and wet season was observed. A decrease greater than 200 mm mostly in

central-western (e.g. Anhanduí-Pardo (22)) and southern parts (e.g. Carapá-Guaçu-Lower Paraná (34)) of the basin (Figure 13). For instance, in these watersheds it was observed a median decrease considering the mean values discretization up to 110, 87, and 21 mm in the annual, wet and dry season, respectively (Figure 14). Similar to surface runoff, this is likely because of the natural vegetation suppression that were replaced by cropland areas. The reduction in the actual evapotranspiration values is explained by the shallower roots of cropland or grassland compared to natural vegetation (forest or cerrado), which leads to less access to deep soil moisture (Nepstad *et al.*, 1994, Oliveira *et al.*, 2005). Also, the mean LAI values are smaller which consequently decreases the transpiration.

It is important to highlight that even in the dry season, the spatial distribution (Figure 13) shows that in the Carapá-Guaçu-Lower Paraná (34) and Lower Iguaçu (33) subbasins there is a significant increase in the amounts of surface runoff and decrease in the actual evapotranspiration. Besides the influence of LUCC, the precipitation in this region in the dry period is much higher compared to the other parts of the basin (Abou Rafee *et al.*, 2020).

As shown in Figure 13, the impacts of LUCC on soil moisture storage ranged from an increase up to 400 mm to a decrease up to 100 mm within the major subbasin level. Similar to surface runoff, it was observed mainly an increase in the wet and annual values, and a decrease in the dry season. The higher values of soil moisture during the wet season are explained by the reduction of actual evapotranspiration. As mentioned previously, it occurred as a result of the removal of cerrado areas and the expansion of cropland in the basin.

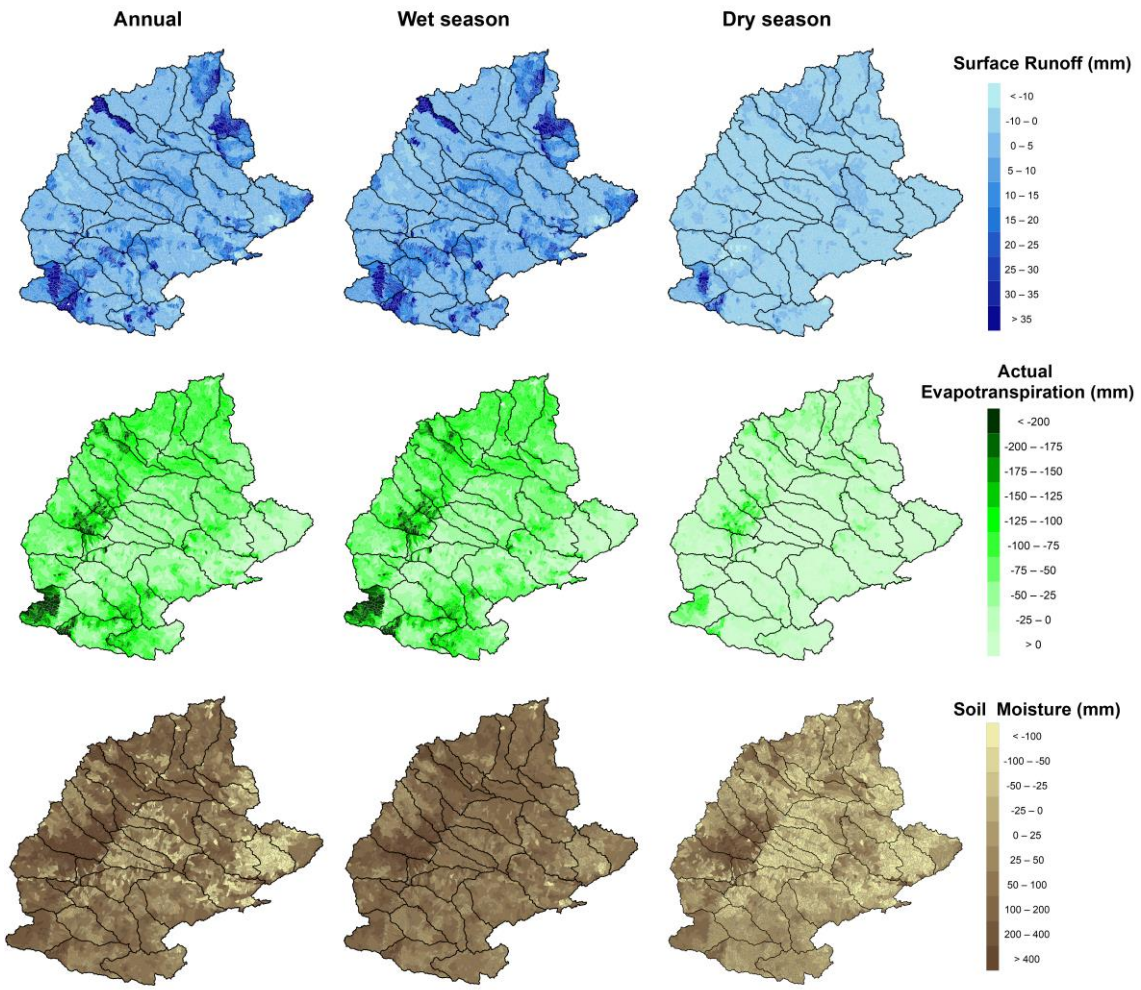

Figure 13. Spatial distribution of changes (mm) in surface runoff, actual evapotranspiration, and soil moisture considering the long-term means (1984 – 2015) for the annual, wet, and dry season values calculated from the difference between the simulated scenarios (LUC2015 minus LUC1985).

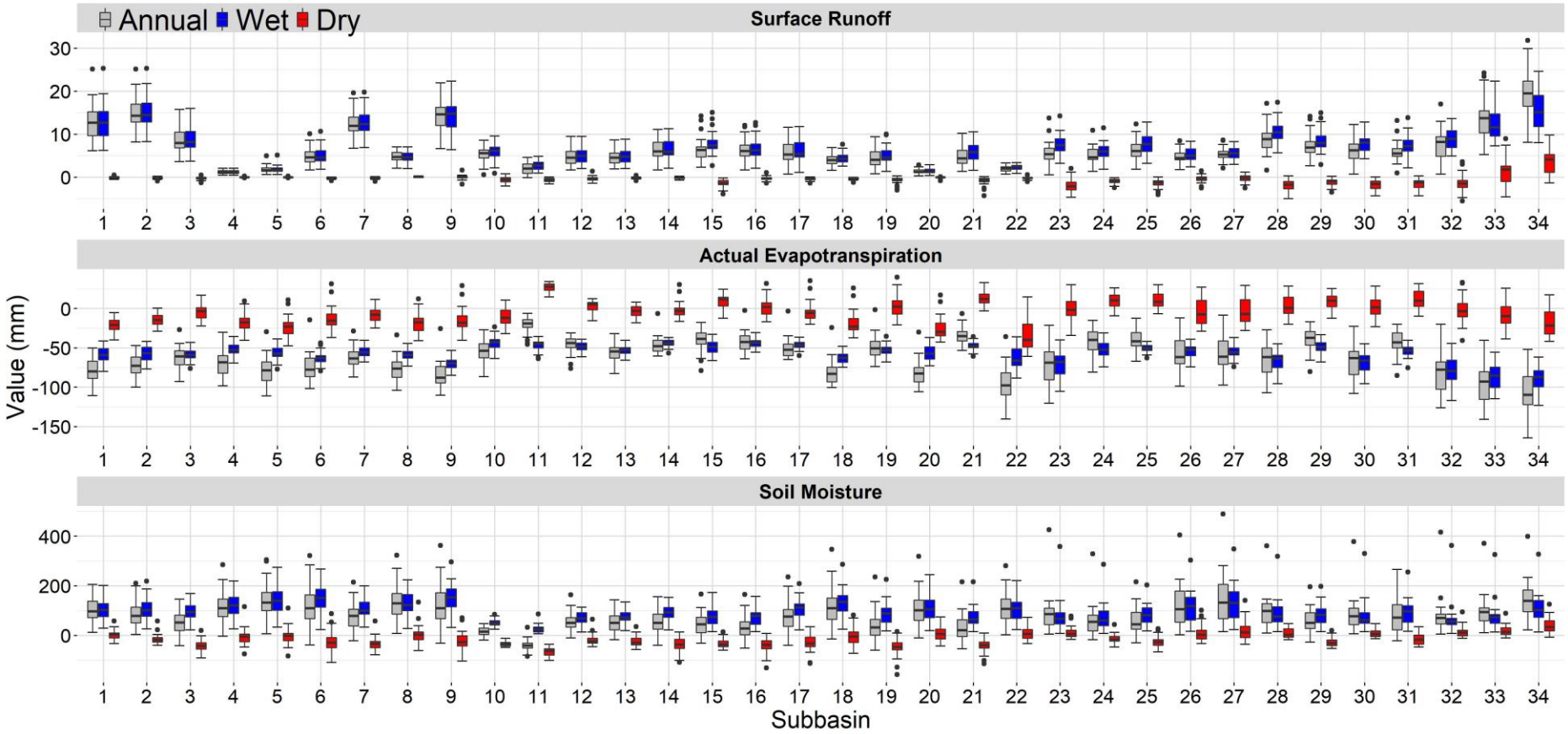

Figure 14. Box plots of surface runoff, actual evapotranspiration, and soil moisture for annual and seasonal (wet and dry) values from 32 years (1984 – 2015). There were calculated from the difference between the simulated scenarios (LUC2015 minus LUC1985) at major subbasin level. **1.** Corumbá; **2.** Upper Paranaíba; **3.** Araguari; **4.** Meia Ponte-Middle Paranaíba; **5.** Dos Bois; **6.** Tijuco; **7.** Middle Paranaíba; **8.** Claro; **9.** Verde-Corrente-Aporé or Do Peixe-Lower Paranaíba; **10.** Upper Grande; **11.** Sapucaí; **12.** Pardo; **13.** Middle Grande; **14.** Lower Grande; **15.** Upper Tietê; **16.** Lower Tietê; **17.** São José dos Dourados-Upper Paraná; **18.** Sucuriú; **19.** Aguapei or Feio; **20.** Verde; **21.** Do Peixei-Middle Paraná; **22.** Anhanduí-Pardo; **23.** Tibagi; **24.** Upper Paranapanema; **25.** Lower Paranapanema; **26.** Middle Paraná; **27.** Brilhante-Ivinhema; **28.** Ivaí; **29.** Middle Paraná; **30.** Piquiri; **31.** Iguatemi-Middle Paraná; **32.** Upper Iguaçu; **33.** Lower Iguaçu; **34.** Carapá-Guaçu-Lower Paraná.

3.3.2.2. River discharge

Figure 15 shows the temporal evolution of relative changes (%) in discharge under the scenario for the year 2015 relative to 1985. Values for annual, dry, and wet seasons were calculated considering the river mouth of the main rivers from the major subbasin level of the UPRB.

The simulation results revealed that the LUCC between 1985 and 2015 had an expressive impact on discharge values. Overall, the LUCC implied an increase in the annual's and wet season's discharges at the main rivers of the UPRB. The major relative changes in discharge were observed at the Lower Tietê, Anhanduí, Ivinheima, and Guaçu rivers. For instance, an increase of more than 29% in annual mean values was found at the Guaçu river. All of these subbasins have in common a significant reduction in natural vegetation (forest or cerrado). On the other hand, a decrease was observed during the dry period, except for Anhandui and Guaçu rivers. A mean decrease of more than 4% was observed at the Lower Tietê, Lower Paranapanema, and Sucuriú rivers. This behavior decreases the effect of annual increased discharge in many rivers of the basin. For example, at the river mouth of the UPRB, over the Lower Paraná River, it was observed an increase in the annual discharge of only 1.13%, an increase of 4.25% in the wet, and a decrease of only 2.24% in the dry season.

Surface runoff is one of the major contributors to discharge. Thereby, the changes in annual and wet season discharge values are likely associated with the increase of generated runoff in the subbasins. The results presented here are consistent with other large-scale simulations. For instance, Costa *et al.* (2003) analyzed the effects of large-scale changes on the discharge of the Tocantins Rivers, southeastern Amazonia. The authors observed an increase in the average annual long-term discharge due to the conversion of the natural vegetation to cropland and grassland.

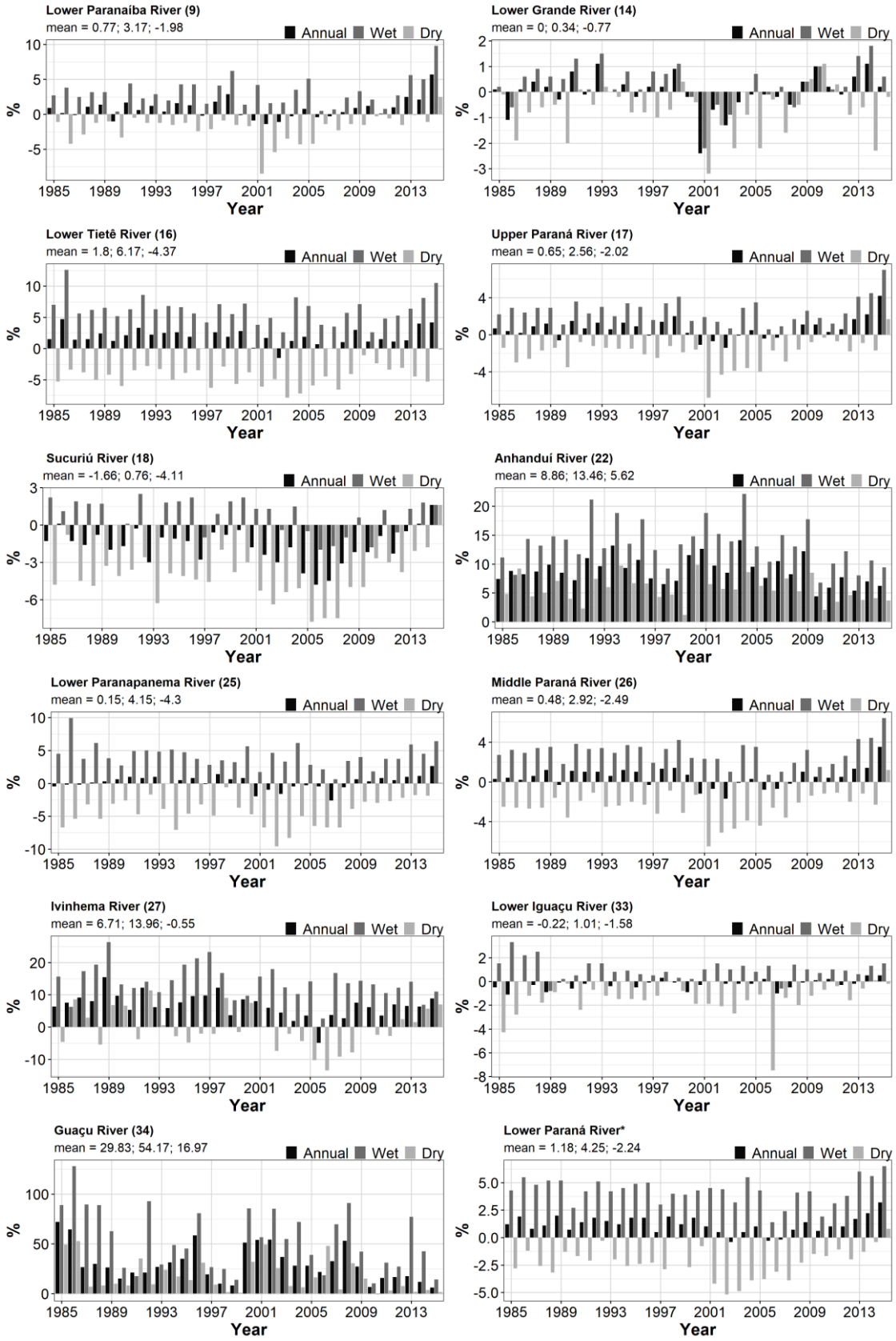

Figure 15. Temporal evolution of relative changes (%) in discharge for annual, wet and dry seasons under the scenarios for the year 2015 relative to 1985 at the main rivers of the UPRB. At the top left of the plots are shown the mean values and the name of the rivers with the respective number of the subbasin. *The last graph represents the river mouth of the UPRB.

3.4. Analysis of LUCC versus Climate shift

3.4.1. LUC T0, 1960 and 1985

Figure 16 shows the generated LUC map from T0, 1960 and 1985. Overall, the east part of the basin had the greatest natural vegetation suppression. Forested areas decreased from 57% in T0 to 35.9% in 1960, and to 17.6% in 1985. The area of cerrado decreased only 1.4% from T0 to the reconstruction for 1960, but it experienced an expressive reduction from 1960 to 1985 to almost half of the original area. The expressive natural vegetation suppression could be associated with the development of agri-business in Brazil since the early 1960s (Mueller & Mueller, 2016).

The original vegetation areas were replaced mainly by grassland and cropland, which represents, respectively, 9% and 12%, in 1960, and 27.7% and 31.1%, in 1985. Grassland and cropland areas are mostly located in the central-eastern part of the UPRB, close to the main socio-economically city of the basin, São Paulo. As stated in the methodology section, the water areas classified at the 1985 map were maintained in all LUC that represent 1.7% of the basin. Urban areas cover 0.9% of the UPRB in both 1985 and 1960 LUC. No urban areas are present at T0.

As noted in Figure 16a-c, the rate of LUCC from T0 to 1960 is much lower than from 1960 to 1985. This is due to the agricultural expansion at the beginning of the twentieth century, which resulted on an extensive transformation of the ecosystems (Salazar *et al.*, 2015). The population growth of UPRB followed a similar development, presenting an exponential increase in the early 1960s (IBGE, 2010).

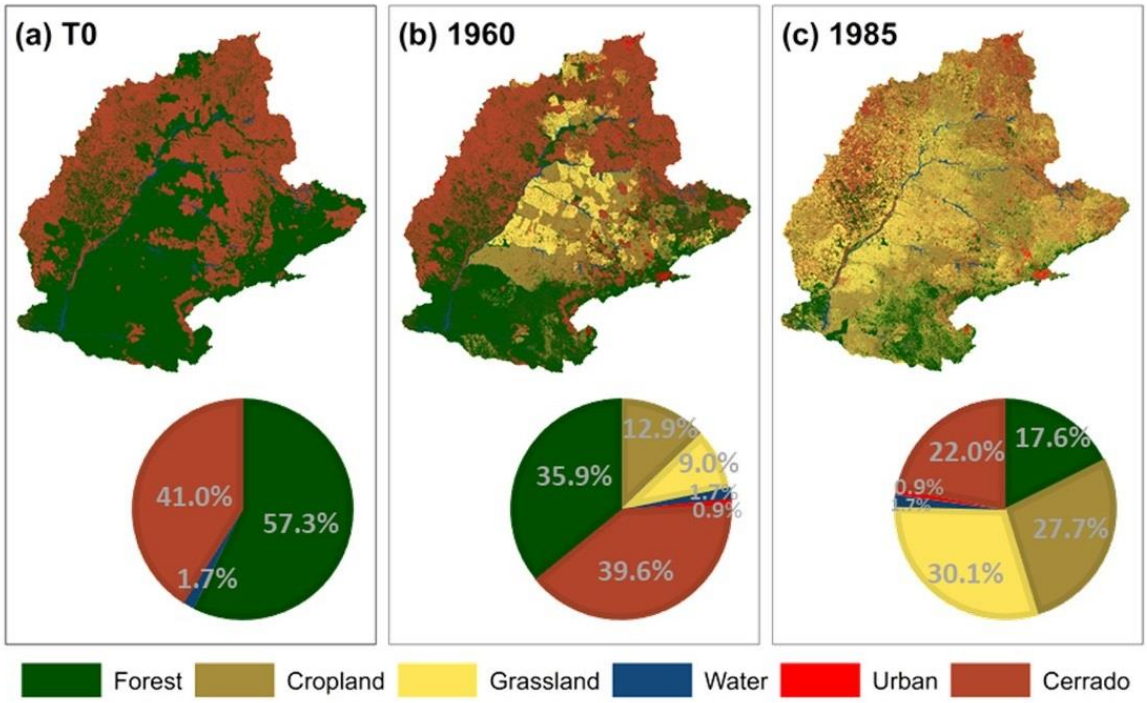

Figure 16. Land use and Cover (LUC) for (a) T0; 1960 (b) and 1985 (c).

3.4.2. Precipitation change

Figure 17 shows the relative changes in the average annual median precipitation under the period 1978 – 1990 relative to 1961 – 1973. The data were interpolated using the IDW method at the grid resolution of 0.05 degrees. Overall, the changes in precipitation were mostly positive and occurred mainly in the southern parts of the basin. Only specific areas in the northern-eastern part of the UPRB showed decreased precipitation.

In the northern part of the basin, the increased precipitation values are mostly ranging between 0 – 10% and some areas up to 15%. This increase could be associated with the significant changes in the SAMS in early the 1970s as reported by Carvalho *et al.* (2011). According to the authors, the mean duration of SAMS increased from 170 days (1948–1972) to 195 days (1972–1982).

In the southern region of the UPRB, the annual median precipitation increased more than 20%. Our results are supported by the ones from Liebmann *et al.* (2004) that observed increase of precipitation in this region after the observed climate shift, observing increasing when comparing the 1948 – 1975 period to 1976 – 1999, i.e., before and after the climate shift. The precipitation increase in this southern region is related to the fact

that this area is more affected by the low frequency oscillations such as ENSO and PDO if compared to other parts of the basin (e.g. Cavalcanti *et al.*, 2015, Grimm *et al.*, 2000, da Silva *et al.*, 2011). Grimm *et al.* (1998) connects ENSO and PDO to the strengthened of the upper-tropospheric subtropical jet, that intensifies the MCS inducing more precipitation over the region.

It is important to recognize that many rain gauge stations have a high percentage of missing data, especially before the climate shift period, which may affect the results of the interpolation method. However, the basin has 629 stations with less than 5% missing data that are mainly located in the central-east and south-east of the basin, areas where the increase in precipitation before and after the climate shift can be seen (Figure 17).

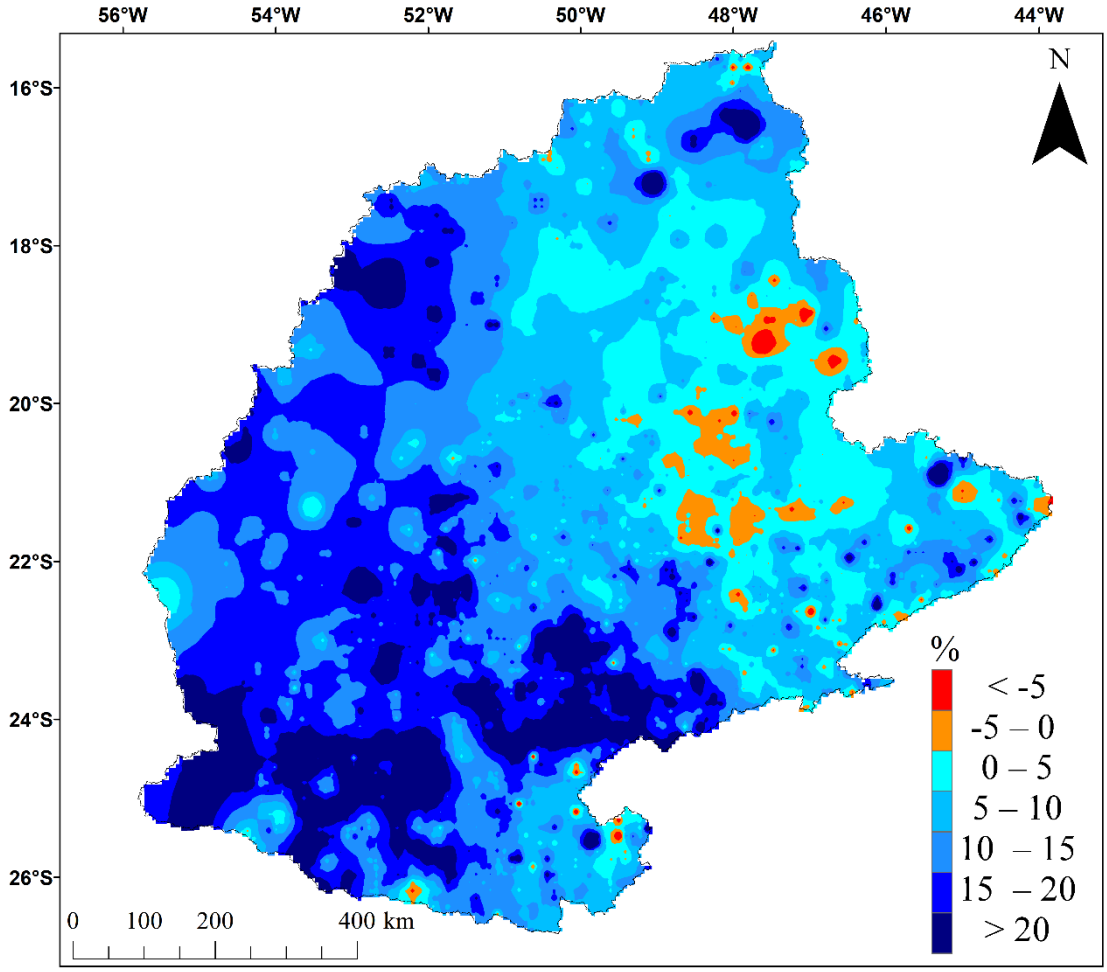

Figure 17. Spatial distribution of the relative change (%) in the average annual median precipitation under the period 1978 – 1990 relative to 1961 – 1973.

3.4.3. LUCC 1960 – 1985 versus Climate shift

Figure 18 illustrates the relative changes (%) in the average annual median discharge in the scenarios A to E. Overall, all scenarios and runs generated increased discharge. Also, the scenarios related to the climate shift (C and D) had higher increases compared to only LUCC scenarios (A and B).

Considering the precipitation from 1961 – 1973, scenario A showed that the LUCC between 1960 and 1985 lead to an increase in the discharge from 4% to 16.7% (at Ivinhema river) in all displayed rivers, except for the Lower Grande river where the changes were 1.8%. In scenario B, which considered the precipitation during the period 1978 – 1990, the LUCC lead an increased discharge of about 11% and 18% at the Lower Iguaçu and Ivinhema rivers, respectively. Both rivers had significant LUCC in their upstream subbasins as shown in Figure 16. Note that 1960 already registered enough changes in LUC to impact the discharge within the basin. For example, at the upstream to the Lower Tietê river has only a few fragments of its original LUC in 1960.

Scenarios C and D show the impacts in discharge due to the changes in precipitation (between 1961 – 1973 and 1978 – 1990) considering the LUC from 1960 and 1985, respectively. It was observed that the higher changes at discharge are located in the southern part of the basin. For instance, both scenarios showed that the Lower Iguaçu and Lower Paraná rivers had an increase of more than 30% in the average annual median discharge when comparing the precipitation for 1961 – 1973 and 1978 – 1990 periods. This increase is likely associated with the increase of precipitation amounts mainly concentrated close to rivers mouth (Figure 17).

Scenario E assesses the joint effect of LUCC and climate shift on discharge. The highest increases in discharge are observed at the Lower Ivinhema and Lower Iguaçu rivers outlets with about 67% and 52%, respectively. This scenario clarify that the Paraná river increased presents a discharge that amplifies from upstream to downstream with the confluence of the largest rivers of the basin that also presented a significant increase. The Upper, Middle and Lower Paraná (river mouth of the UPRB) rivers presented a discharge increase of about 14%, 15%, and 38%, respectively.

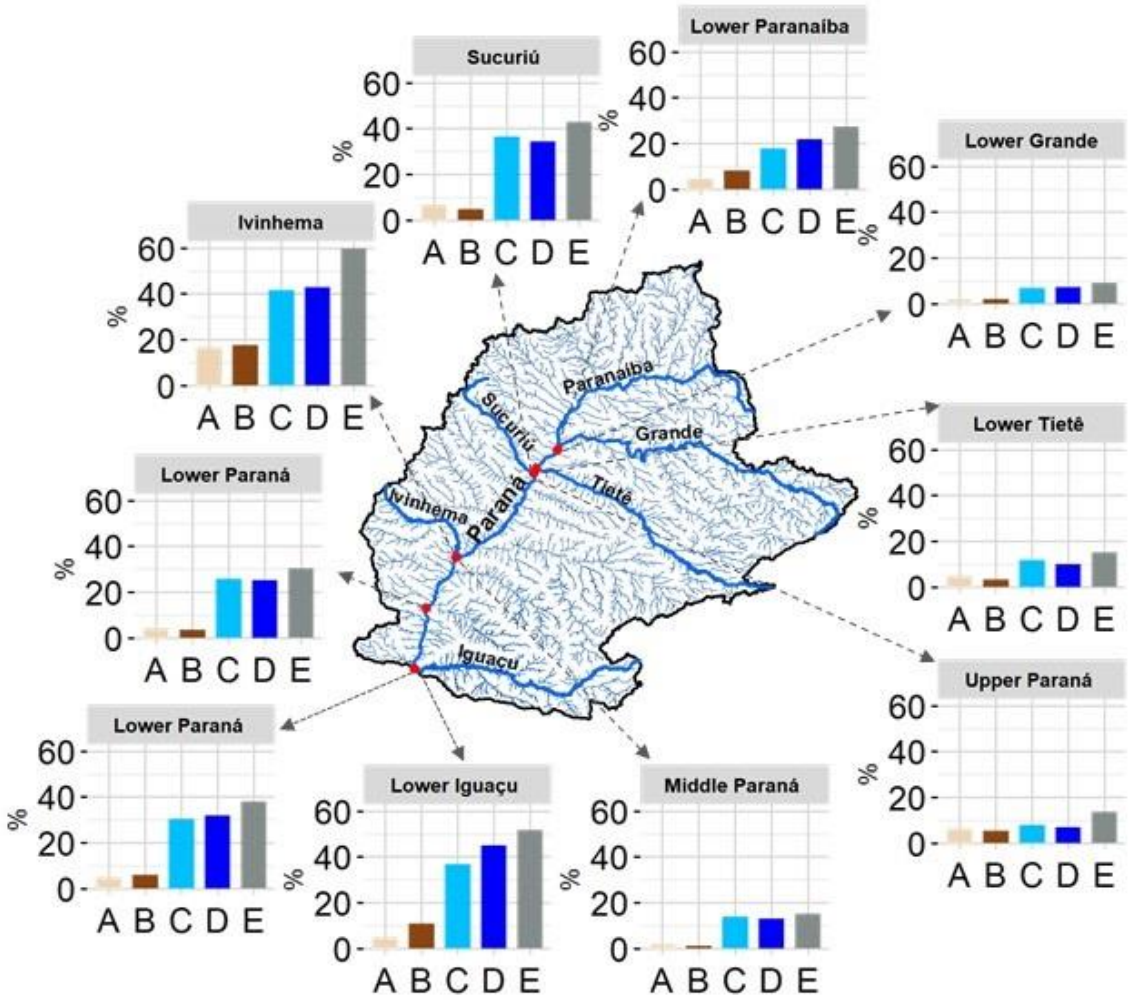

Figure 18. Relative changes (%) in the average annual median discharge at the largest river of the UPRB in scenario A to E. The scenarios are defined in Table 4.

3.4.4. LUCC T0 – 1985 versus Climate shift

The maximum impact of LUCC until 1985 on the discharge was assessed by the comparison between the simulation with the LUC from T0 (around the Year 1500) and from 1985. The scenarios that covered this issue are presented in Figure 19. Similar to the previously described scenarios A to E, it was observed increased discharge in scenarios I to IV.

The scenarios I and II related to the LUCC between T0 and 1985 had the increased discharge much higher compared to the scenarios A and B. The highest values are observed at the Lower Tietê river outlet as a consequence of the large LUCC in the upstream subbasins. In these subbasins, the natural vegetation areas, composed mostly by forests were replaced mainly by grassland and cropland (see Figure 16). This caused an increase in the average annual median discharge more than 55% under the scenarios.

Scenario III assess the effect of the precipitation change between 1961 – 1973 and 1978 – 1990 considering the T0 LUC. Similar relative changes discharges to scenario C (with LUC 1960) were achieved. The scenario IV has the same characteristics as scenario D.

Finally, scenario V assesses the consequence of changes in LUC up to 1985 and in precipitation due to the climate shift. Again, the highest changes in discharge were observed at the Lower Tietê that presented an increase of about 85% in the average annual median. The river mouth of the UPRB (Lower Paraná), the discharge increased more than 50%.

In all the rivers outlet analyzed, the scenarios I to IV revealed that the changes in precipitation had a higher impact in the annual discharge than the LUCC, except for the Lower Tietê and the Upper Paraná rivers. In these cases, changes in precipitation over the Tietê subbasin were not as high as in the southern part of the basin which were exceeded 20% (Figure 17). In the southern part of the basin, despite the important observed LUCC, the changes in precipitation had a greater impact on discharge. This becomes clear when analyzing the changes in discharge at the Lower Paraná (river mouth of the UPRB), Scenario I and II, related to LUCC, indicate a discharge increase of about 15%, while the climate shift scenarios (III and IV) of about 30%.

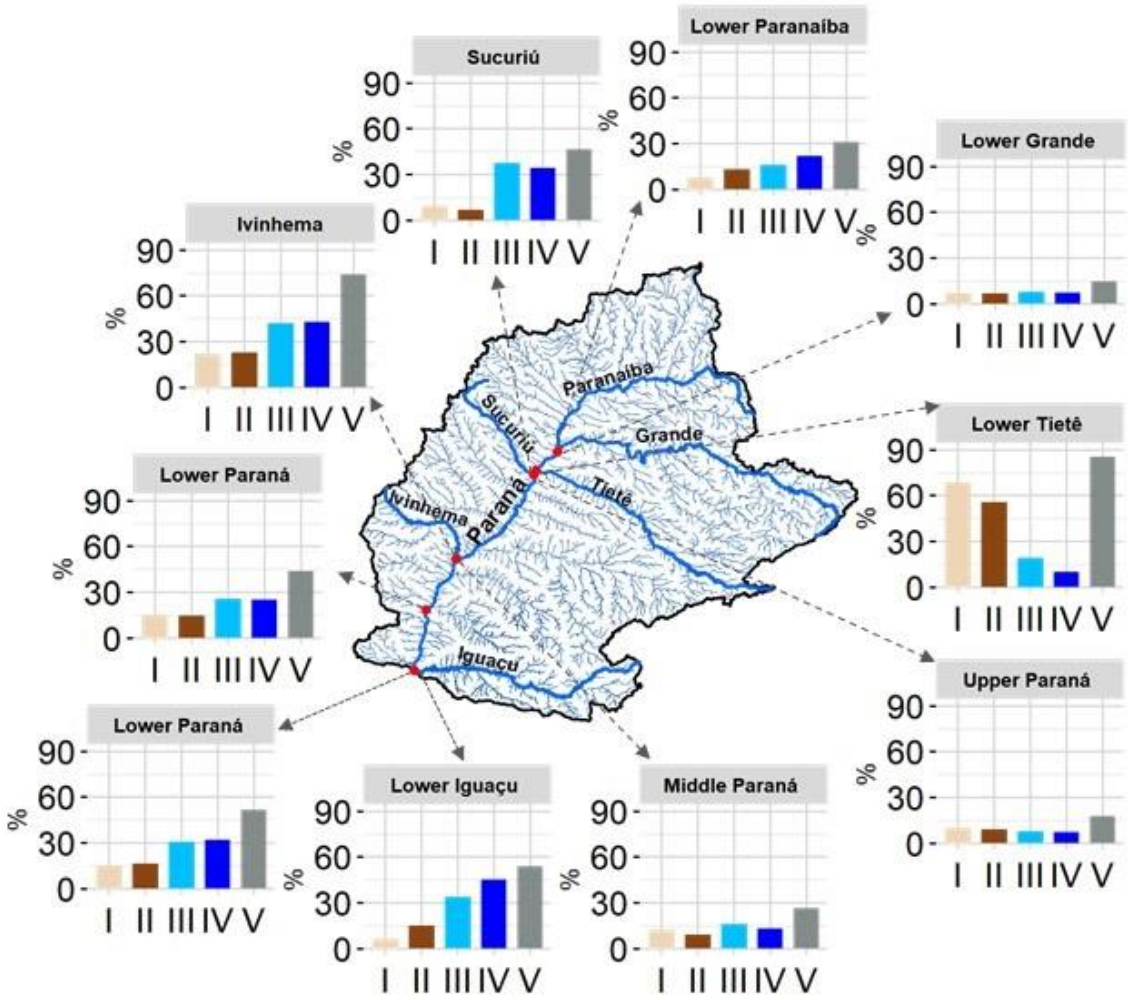

Figure 19. Relative changes (%) in the average annual median discharge at the largest river of the UPRB in scenarios I to V. The scenarios are defined in Table 5.

4. Main conclusions

This thesis aimed to investigate the changes in precipitation and LUCC and their effects on the hydrological processes in the UPRB. To fulfill the major goal, the research was organized into four parts.

The trends of annual and seasonal precipitation, as well as extreme precipitation events over the UPRB using the MK test, were investigated. The significant trends were analyzed at the 95% confidence level using the data from 853 rain gauge stations during the period 1977 – 2016. The main conclusions are presented as follows:

1. The northern and southern regions of the basin presented decreasing and increasing trends in precipitation amounts, respectively.

2. In the southern part of the UPRB, an increase of extreme precipitation events with annual maximum 5-day precipitation and in the number of rainstorms (> 50 mm/day) was observed.

3. The northern part of the basin presented an increase in the number of consecutive dry days (< 1 mm).

4. Most of the areas across the UPRB presented an increasingly long rainy season.

The UPRB was built with the highest possible spatial discretization using the SWAT model for a long-term period between 1984 and 2015. The model was calibrated and validated for the main rivers of the basin. The main contributions of the work can be drawn:

1. Satisfactory SWAT calibration and validation of the monthly discharge from main rivers and LAI values were achieved. Thereby, the proposed project could be used for other studies not addressed in this thesis such as climate change scenarios.

2. The methodology used in this work regarding data preparation, model setup, and strategies for calibration and validation, as well as evaluation, can be used for other large-scale basins, especially in South America.

It was estimated the hydrologic response to LUCC between 1985 and 2015 in the UPRB. The effects of LUCC were addressed for the annual, wet and dry season during

the period 1984 – 2015. The main conclusions from the simulated scenarios are presented as follows:

1. Most of the major subbasins presented an increase in the surface runoff and soil moisture amounts in the annual and wet season values, while a decrease was observed in the dry season.
2. A significant decrease in actual evapotranspiration in the annual and wet season values was observed.
3. LUCC induced an increase in discharge in the wet, while a decrease in the dry season.
4. Several rivers had little changes in their discharge due to the compensation of discharge in the wet and dry season.

The effects of LUCC and climate shift on the changes in the average annual discharge at the largest rivers of the UPRB were estimated. The numerical simulations were performed using three LUC from a pristine period (around the Year 1500), 1960 and 1985. The scenarios were conducted through the SWAT model during the precipitation period from 1961 to 1990. The following conclusions from the simulated scenarios can be drawn:

1. It was observed that more than half of natural vegetation (forest or cerrado) until the LUC 1985 was suppressed.
2. A significant increase in average median precipitation in most of the areas across the basin after the 1970s climate shift event was observed.
3. Both LUCC and climate shift have a significant impact on the annual discharge at the largest rivers of the UPRB, but with the climate shift being the main driver.
4. The greatest impacts in the annual discharge were observed mainly at rivers located in the southern parts of the basin following the highest increase in precipitation rates observed.

This research is the first to analyze precipitation trends using a large number of rain gauges (853) over the UPRB during a long-term period 1977 – 2016. Furthermore, it is the first to address the integration of both LUCC and climate shift effects on hydrology

in the UPRB using a model at a high spatial resolution. The trends analyses revealed that special attention should be paid to the northern and southern regions of the basin, which presented decreasing and increasing trends in precipitation amounts and in extreme precipitation events, respectively. Both regions have an important role in various sectors of the economy and development of Brazil. The LUCC scenarios from 1985 and 2015 indicated that the natural vegetation suppression increased the discharge in the wet season, and decrease in the dry season. In addition, the simulations indicated that both LUCC (from T0, 1960, and 1985) and climate shift have a significant impact on the annual discharge at the largest rivers of the UPRB. However, the main driver is the climate shift, which affected mainly the southern region of the basin.

The provided results describing what happened in hydrology over the past decades under the effects of climate shift and anthropization, investigated here at large-scale basin should be regarded with much attention by the environmental managers worldwide. Hence, future conservation and sustainable use of water resources could be achieved.

4.1. Future work

In spite of the valuable results presented in this thesis, more research is needed within the UPRB. The following future work intended to be developed:

- To extend the evaluation to climate change scenarios.
- To investigate the effect of projection of future LUC.
- To simulate the effect of the observed agricultural expansion with different types of crops.
- To use the SWAT project performed for the UPRB to investigate concerns related to water quality within the basin.
- To quantify the economic valuation from the anthropogenic impacts on hydrology across the basin.

References

Abbaspour, K. C., Johnson, C. A. & Genuchten, M. T. van. (2004) Estimating Uncertain Flow and Transport Parameters Using a Sequential Uncertainty Fitting Procedure. *Vadose Zo. J.* **3**(4), 1340–1352. doi:10.2136/vzj2004.1340

Abbaspour, K. C., Rouholahnejad, E., Vaghefi, S., Srinivasan, R., Yang, H. & Kløve, B. (2015) A continental-scale hydrology and water quality model for Europe: Calibration and uncertainty of a high-resolution large-scale SWAT model. *J. Hydrol.* **524**, 733–752. doi:10.1016/j.jhydrol.2015.03.027

Abbaspour, Karim C. (2015) SWAT-CUP: SWAT Calibration and Uncertainty Programs - A User Manual. *Sci. Technol.* doi:10.1007/s00402-009-1032-4

Abou Rafee, S. A., Freitas, E. D., Martins, J. A., Martins, L. D., Domingues, L. M., Nascimento, J. M. P., Machado, C. B., et al. (2020) Spatial Trends of Extreme Precipitation Events in the Paraná River Basin. *J. Appl. Meteorol. Climatol.* **59**(3), 443–454. American Meteorological Society. doi:10.1175/JAMC-D-19-0181.1

Abou Rafee, S. A., Uvo, C. B., Martins, J. A., Domingues, L. M., Rudke, A. P., Fujita, T. & Freitas, E. D. (2019) Large-scale hydrological modelling of the Upper Paraná River Basin. *Water (Switzerland)*. doi:10.3390/w11050882

Adami, M., Rudorff, B. F. T., Freitas, R. M., Aguiar, D. A., Sugawara, L. M. & Mello, M. P. (2012) Remote sensing time series to evaluate direct land use change of recent expanded sugarcane crop in Brazil. *Sustainability*. doi:10.3390/su4040574

Agosta, E. A. & Compagnucci, R. H. (2008) The 1976/77 austral summer climate transition effects on the atmospheric circulation and climate in Southern South America. *J. Clim.* **21**(17), 4365–4383. doi:10.1175/2008JCLI2137.1

Alemayehu, T., Griensven, A. Van, Woldegiorgis, B. T. & Bauwens, W. (2017) An improved SWAT vegetation growth module and its evaluation for four tropical ecosystems. *Hydrol. Earth Syst. Sci.* doi:10.5194/hess-21-4449-2017

Alexandersson, H. (1986) A homogeneity test applied to precipitation data. *J. Climatol.* doi:10.1002/joc.3370060607

ANEEL, (2020). BIG - Banco de Informações de Geração - Capacidade de Geração do Brasil - Usinas hidrelétricas, BIG. Available online: https://www2.aneel.gov.br/aplicacoes/capacidadebrasil/Combustivel.cfm (accessed March 2020).

Antico, A., Torres, M. E. & Diaz, H. F. (2016) Contributions of different time scales to extreme Paraná floods. *Clim. Dyn.* **46**(11–12), 3785–3792. doi:10.1007/s00382-015-2804-x

Arnold, J. G., Srinivasan, R., Muttiah, R. S. & Williams, J. R. (1998) Large Area Hydrologic Modelling and Assessment Part I : Model Development. *Am. Water Resour. Assoc.* doi:10.1111/j.1752-1688.1998.tb05961.x

Baer, W. & Birch, M. H. (1984) Expansion of the economic frontier: Paraguayan growth in the 1970s. *World Dev.* doi:10.1016/0305-750X(84)90074-3

Bayer, D. M. (2014) *Efeitos das mudanças de uso da terra no regime hidrológico de bacias de grande escala*. Universidade Federal do Rio Grande do Sul, Porto Alegre, Brazil, p. 172.

Bucci, S. J., Scholz, F. G., Goldstein, G., Hoffmann, W. A., Meinzer, F. C., Franco, A. C., Giambelluca, T., et al. (2008) Controls on stand transpiration and soil water utilization along a tree density gradient in a Neotropical savanna. *Agric. For. Meteorol.* doi:10.1016/j.agrformet.2007.11.013

Camilloni, I. A. & Barros, V. R. (2003) Extreme discharge events in the Paraná River and their climate forcing. *J. Hydrol.* doi:10.1016/S0022-1694(03)00133-1

Camilloni, I. & Barros, V. (2000) The Parana River Response to El Nino 1982 – 83 and 1997 – 98 Events. *J. Hydrometeorol.* **1**(1998), 412–430. doi:https://doi.org/10.1175/1525-7541(2000)001

Carvalho, L. M. V., Jones, C. & Liebmann, B. (2004) The South Atlantic convergence zone: Intensity, form, persistence, and relationships with intraseasonal to interannual activity and extreme rainfall. *J. Clim.* doi:10.1175/1520-0442(2004)017<0088:TSACZI>2.0.CO;2

Carvalho, L. M. V., Jones, C., Silva, A. E., Liebmann, B. & Silva Dias, P. L. (2011) The South American Monsoon System and the 1970s climate transition. *Int. J. Climatol.* **31**(8), 1248–1256. doi:10.1002/joc.2147

Cavalcanti, I. F. A., Carril, A. F., Penalba, O. C., Grimm, A. M., Menéndez, C. G., Sanchez, E., Cherchi, A., et al. (2015) Precipitation extremes over La Plata Basin - Review and new results from observations and climate simulations. *J. Hydrol.* doi:10.1016/j.jhydrol.2015.01.028

Chotpantarat, S. & Boonkaewwan, S. (2018) Impacts of land-use changes on watershed discharge and water quality in a large intensive agricultural area in Thailand. *Hydrol. Sci. J.* doi:10.1080/02626667.2018.1506128

Costa, M. H., Botta, A. & Cardille, J. A. (2003) Effects of large-scale changes in land cover on the discharge of the Tocantins River, Southeastern Amazonia. *J. Hydrol.* doi:10.1016/S0022-1694(03)00267-1

DeFries, R. & Eshleman, K. N. (2004) Land-use change and hydrologic processes: a major focus for the future. *Hydrol. Process.* doi:10.1002/hyp.5584

Dias, L. C. P., Pimenta, F. M., Santos, A. B., Costa, M. H. & Ladle, R. J. (2016) Patterns of land use, extensification, and intensification of Brazilian agriculture. *Glob. Chang. Biol.* doi:10.1111/gcb.13314

Efron, B. (1979) the 1977 Rietz Lecture - bootstrap methods: another look at the jackknife. *Ann. Stat.* 7,1-26.

Fauconnier, Y. (2017) Evaluation de La Ressource Dans Le Bassin Versant de l'Ibicuí Grâce à La Modélisation Hydrologique: Application de l'outil SWAT.

Ferrant, S., Oehler, F., Durand, P., Ruiz, L., Salmon-Monviola, J., Justes, E., Dugast, P., et al. (2011) Understanding nitrogen transfer dynamics in a small agricultural catchment: Comparison of a distributed (TNT2) and a semi distributed (SWAT) modeling approaches. *J. Hydrol.* doi:10.1016/j.jhydrol.2011.05.026

Ficklin, D. L., Luo, Y., Luedeling, E. & Zhang, M. (2009) Climate change sensitivity assessment of a highly agricultural watershed using SWAT. *J. Hydrol.*

doi:10.1016/j.jhydrol.2009.05.016

Francesconi, W., Srinivasan, R., Pérez-Miñana, E., Willcock, S. P. & Quintero, M. (2016) Using the Soil and Water Assessment Tool (SWAT) to model ecosystem services: A systematic review. *J. Hydrol.* doi:10.1016/j.jhydrol.2016.01.034

Gonçalves, J. L. M., Stape, J. L., Laclau, J. P., Bouillet, J. P. & Ranger, J. (2008) Assessing the effects of early silvicultural management on long-term site productivity of fast-growing eucalypt plantations: The Brazilian experience. *South. For.* doi:10.2989/SOUTH.FOR.2008.70.2.6.534

Griensven, A. Van, Ndomba, P., Yalew, S. & Kilonzo, F. (2012) Critical review of SWAT applications in the upper Nile basin countries. *Hydrol. Earth Syst. Sci.* doi:10.5194/hess-16-3371-2012

Grimm, A. M., Barros, V. R. & Doyle, M. E. (2000) Climate variability in southern South America associated with El Nino and La Nina events. *J. Clim.* doi:10.1175/1520-0442(2000)013<0035:CVISSA>2.0.CO;2

Grimm, A. M., Ferraz, S. E. T. & Gomes, J. (1998) Precipitation anomalies in southern Brazil associated with El Nino and La Nina events. *J. Clim.* doi:10.1175/1520-0442(1998)011<2863:PAISBA>2.0.CO;2

Grimm, A. M., Pal, J. S. & Giorgi, F. (2007) Connection between spring conditions and peak summer monsoon rainfall in South America: Role of soil moisture, surface temperature, and topography in eastern Brazil. *J. Clim.* **20**(24), 5929–5945. doi:10.1175/2007JCLI1684.1

Gupta, H. V., Kling, H., Yilmaz, K. K. & Martinez, G. F. (2009) Decomposition of the mean squared error and NSE performance criteria: Implications for improving hydrological modelling. *J. Hydrol.* **377**(1–2), 80–91. Elsevier B.V. doi:10.1016/j.jhydrol.2009.08.003

Hartmann, B. & Wendler, G. (2005) The significance of the 1976 Pacific climate shift in the climatology of Alaska. *J. Clim.* doi:10.1175/JCLI3532.1

Hilker, T., Lyapustin, A. I., Tucker, C. J., Hall, F. G., Myneni, R. B., Wang, Y., Bi, J., et

al. (2014) Vegetation dynamics and rainfall sensitivity of the Amazon. *Proc. Natl. Acad. Sci. U. S. A.* doi:10.1073/pnas.1404870111

Hoffmann, W. A., Silva, E. R. Da, Machado, G. C., Bucci, S. J., Scholz, F. G., Goldstein, G. & Meinzer, F. C. (2005) Seasonal leaf dynamics across a tree density gradient in a Brazilian savanna. *Oecologia*. doi:10.1007/s00442-005-0129-x

IBGE, (2010). Evolução da população total. Available online: https://brasil500anos.ibge.gov.br/estatisticas-do-povoamento/evolucao-da-populacao-brasileira.html (accessed December 2019)

IBGE, (2017). Recuperação e compatibilização do projeto RADAMBRASIL, tema vegetação. Available online: http://www.metadados.geo.ibge.gov.br/geonetwork_ibge/srv/por/metadata.show?id=19626&currTab=simple (accessed January 2020)

IBGE, (2019). População. Available online: http://www.ibge.gov.br/apps/populacao/projecao/ (accessed November 2019).

Jacques-Coper, M. & Garreaud, R. D. (2015) Characterization of the 1970s climate shift in South America. *Int. J. Climatol.* doi:10.1002/joc.4120

Kendall, M. G. (1975) *Rank Correlation Methods*. *Charles Griffin*. Charles Griffin and Company.

Lee, E., Livino, A., Han, S. C., Zhang, K., Briscoe, J., Kelman, J. & Moorcroft, P. (2018) Land cover change explains the increasing discharge of the Paraná River. *Reg. Environ. Chang.* doi:10.1007/s10113-018-1321-y

Leta, O. T., Griensven, A. van & Bauwens, W. (2017) Effect of Single and Multisite Calibration Techniques on the Parameter Estimation, Performance, and Output of a SWAT Model of a Spatially Heterogeneous Catchment. *J. Hydrol. Eng.* doi:10.1061/(ASCE)HE.1943-5584.0001471

Li, Z., Deng, X., Wu, F. & Hasan, S. S. (2015) Scenario analysis for water resources in response to land use change in the middle and upper reaches of the heihe river Basin. *Sustain.* doi:10.3390/su7033086

Liebmann, B., Vera, C. S., Carvalho, L. M. V., Camilloni, I. A., Hoerling, M. P., Allured, D., Barros, V. R., et al. (2004) An observed trend in central South American precipitation. *J. Clim.* doi:10.1175/3205.1

Litzow, M. A. (2006) Climate regime shifts and community reorganization in the Gulf of Alaska: how do recent shifts compare with 1976/1977? *ICES J. Mar. Sci.* doi:10.1016/j.icesjms.2006.06.003

Mann, H. B. (1945) Nonparametric test against trend. *Econometrica* **13**(3), 245–259. doi:10.2307/1907187

Marengo, J. A., Liebmann, B., Grimm, A. M., Misra, V., Silva Dias, P. L., Cavalcanti, I. F. A., Carvalho, L. M. V., et al. (2012) Recent developments on the South American monsoon system. *Int. J. Climatol.* doi:10.1002/joc.2254

Meehl, G. A., Hu, A. & Santer, B. D. (2009) The mid-1970s climate shift in the pacific and the relative roles of forced versus inherent decadal variability. *J. Clim.* doi:10.1175/2008JCLI2552.1

Mercuri, E. G. F., Deppe, F., Lohmann, M. & Simões, K. (2009) Metodologia da geração de dados de entrada e aplicação do modelo SWAT para bacias hidrográficas brasileiras. *An. XIV Simpósio Bras. Sensoriamento Remoto*.

MMA. (2011) Monitoramento do desmatamento nos biomas brasileiros por satélite: monitoramento do bioma Cerrado - 2009 a 2010.

MMA. (2012) Monitoramento do desmatamento nos biomas brasileiros por satélite: monitoramento do bioma Mata Atlântica - 2008 a 2009. *Ministério do Meio Ambient. Brasília, DF* 101.

Monteith J. L. (1965) Evaporation and envrionment. *Symp. Soc. Exp. Biol.*

Montini, T. L., Jones, C. & Carvalho, L. M. V. (2019) The South American Low-Level Jet: A New Climatology, Variability, and Changes. *J. Geophys. Res. Atmos.* doi:10.1029/2018JD029634

Morales Rodriguez, C. A., Rocha, R. P. da & Bombardi, R. (2010) On the development of summer thunderstorms in the city of São Paulo: Mean meteorological

characteristics and pollution effect. *Atmos. Res.* doi:10.1016/j.atmosres.2010.02.007

Moriasi, D. N., Arnold, J. G., Liew, M. W. Van, Bingne, R. L., Harmel, R. D. & Veith, T. L. (2007) Model Evaluation Guidelines for Systematic Quantification of Accuracy in Watershed Simulations. *Trans. ASABE*. doi:10.13031/2013.23153

Mueller, C. & Mueller, B. (2016) The evolution of agriculture and land reform in Brazil, 1960-2006. In: *Economic Development in Latin America: Essay in Honor of Werner Baer*. doi:10.1057/9780230297388_10

Nash, J. E. & Sutcliffe, J. V. (1970) River flow forecasting through conceptual models part I - A discussion of principles. *J. Hydrol.* doi:10.1016/0022-1694(70)90255-6

Negrón Juárez, R. I., Rocha, H. R. da, e Figueira, A. M. S., Goulden, M. L. & Miller, S. D. (2009) An improved estimate of leaf area index based on the histogram analysis of hemispherical photographs. *Agric. For. Meteorol.* doi:10.1016/j.agrformet.2008.11.012

Neitsch, S. ., Arnold, J. ., Kiniry, J. . & Williams, J. . (2011) Soil & Water Assessment Tool: Theoretical Documentation Version 2009. *Texas Water Resour. Institute, TR-406*. doi:10.1016/j.scitotenv.2015.11.063

Nepstad, D. C., Carvalho, C. R. De, Davidson, E. A., Jipp, P. H., Lefebvre, P. A., Negreiros, G. H., Silva, E. D. Da, et al. (1994) The role of deep roots in the hydrological and carbon cycles of Amazonian forests and pastures. *Nature*. doi:10.1038/372666a0

Oliveira, R. S., Bezerra, L., Davidson, E. A., Pinto, F., Klink, C. A., Nepstad, D. C. & Moreira, A. (2005) Deep root function in soil water dynamics in cerrado savannas of central Brazil. *Funct. Ecol.* doi:10.1111/j.1365-2435.2005.01003.x

Pereira, D. R. (2013) Simulação hidrológica na bacia hidrográfica do rio Pomba usando o modelo SWAT. *Tese* 126.

Rajib, A. & Merwade, V. (2017) Hydrologic response to future land use change in the Upper Mississippi River Basin by the end of 21st century. *Hydrol. Process.* doi:10.1002/hyp.11282

Rouholahnejad, E., Abbaspour, K. C., Vejdani, M., Srinivasan, R., Schulin, R. & Lehmann, A. (2012) A parallelization framework for calibration of hydrological models. *Environ. Model. Softw.* doi:10.1016/j.envsoft.2011.12.001

Rudke, A. P. (2018) *Dinâmica da cobertura do solo para a bacia hidrográfica do alto rio Paraná*. Master´s Thesis, Federal University of Tecnology Parana, Londrina, Brazil.

Rudke, A. P., Fujita, T., Almeida, D. S. de, Eiras, M. M., Xavier, A. C. F., Rafee, S. A. A., Santos, E. B., et al. (2019) Land cover data of Upper Parana River Basin, South America, at high spatial resolution. *Int. J. Appl. Earth Obs. Geoinf.* doi:10.1016/j.jag.2019.101926

Rudorff, B. F. T., Aguiar, D. A. de, Silva, W. F. da, Sugawara, L. M., Adami, M. & Moreira, M. A. (2010) Studies on the rapid expansion of sugarcane for ethanol production in São Paulo state (Brazil) using Landsat data. *Remote Sens.* doi:10.3390/rs2041057

Salazar, A., Baldi, G., Hirota, M., Syktus, J. & McAlpine, C. (2015) Land use and land cover change impacts on the regional climate of non-Amazonian South America: A review. *Glob. Planet. Change*. doi:10.1016/j.gloplacha.2015.02.009

Santos, V. Dos, Laurent, F., Abe, C. & Messner, F. (2018) Hydrologic response to land use change in a large basin in eastern Amazon. *Water (Switzerland)*. doi:10.3390/w10040429

Silva, G. A. M. da, Drumond, A. & Ambrizzi, T. (2011) The impact of El Niño on South American summer climate during different phases of the Pacific Decadal Oscillation. *Theor. Appl. Climatol.* doi:10.1007/s00704-011-0427-7

Soil Conservation Service Engineering Division. (1972) Section 4: Hydrology. In: *National Engineering Handbook*.

Strauch, M. & Volk, M. (2013) SWAT plant growth modification for improved modeling of perennial vegetation in the tropics. *Ecol. Modell.* doi:10.1016/j.ecolmodel.2013.08.013

Thiemig, V., Rojas, R., Zambrano-Bigiarini, M. & Roo, A. De. (2013) Hydrological evaluation of satellite-based rainfall estimates over the Volta and Baro-Akobo Basin. *J. Hydrol.* doi:10.1016/j.jhydrol.2013.07.012

Tsonis, A. A., Swanson, K. & Kravtsov, S. (2007) A new dynamical mechanism for major climate shifts. *Geophys. Res. Lett.* doi:10.1029/2007GL030288

Tucci, C. E. . (2002) Impactos da variabilidade climática e do uso do solo nos recursos hídricos. *Câmara Temática sobre Recur. Hídricos* 150.

Velasco, I. & Fritsch, J. M. (1987) Mesoscale convective complexes in the Americas. *J. Geophys. Res.* **92**(D8), 9591–9613. doi:10.1029/JD092iD08p09591

Wagner, P. D., Kumar, S., Fiener, P. & Schneider, K. (2011) Technical Note: Hydrological Modeling with SWAT in a Monsoon-Driven Environment: Experience from the Western Ghats, India. *Trans. ASABE*. doi:10.13031/2013.39846

Wang, G., Swanson, K. L. & Tsonis, A. A. (2009) The pacemaker of major climate shifts. *Geophys. Res. Lett.* doi:10.1029/2008GL036874

Wu, K. & Johnston, C. A. (2007) Hydrologic response to climatic variability in a Great Lakes Watershed: A case study with the SWAT model. *J. Hydrol.* doi:10.1016/j.jhydrol.2007.01.030

Yapo, P. O., Gupta, H. V. & Sorooshian, S. (1996) Automatic calibration of conceptual rainfall-runoff models: Sensitivity to calibration data. *J. Hydrol.* doi:10.1016/0022-1694(95)02918-4

Yuan Zhang, Wallace, J. M. & Battisti, D. S. (1997) ENSO-like interdecadal variability: 1900-93. *J. Clim.* doi:10.1175/1520-0442(1997)010<1004:eliv>2.0.co;2

Zandonadi, L., Acquaotta, F., Fratianni, S. & Zavattini, J. A. (2016) Changes in precipitation extremes in Brazil (Paraná River Basin). *Theor. Appl. Climatol.* **123**(3–4), 741–756. doi:10.1007/s00704-015-1391-4

Paper I

I. **Abou Rafee, S.A.,** Freitas, E.D., Martins, J.A., Martins,L.D., Domingues, L.M., Nascimento, J.M., Machado,C.B., Santos, E.B., Rudke, A.P., Fujita, T., Souza, R.A., Hallak, R., Uvo, C.B., 2020: Spatial Trends of Extreme Precipitation Events in the Paraná River Basin. *Journal of Applied Meteorology and Climatology*., 59, 443–454, https://doi.org/10.1175/JAMC-D-19-0181.1

Spatial Trends of Extreme Precipitation Events in the Paraná River Basin

SAMEH A. ABOU RAFEE,[a,b] EDMILSON D. FREITAS,[b] JORGE A. MARTINS,[c] LEILA D. MARTINS,[c] LEONARDO M. DOMINGUES,[b] JANAÍNA M. P. NASCIMENTO,[d] CAROLYNE B. MACHADO,[b] ELIANE B. SANTOS,[e] ANDERSON P. RUDKE,[c] THAIS FUJITA,[c] RODRIGO A. F. SOUZA,[d] RICARDO HALLAK,[b] AND CINTIA B. UVO[a]

[a] *Division of Water Resources Engineering, Lund University, Lund, Sweden*
[b] *Departamento de Ciências Atmosféricas, Instituto de Astronomia, Geofísica e Ciências Atmosféricas, Universidade de São Paulo, São Paulo, Brazil*
[c] *Federal University of Technology–Paraná, Londrina, Brazil*
[d] *Amazonas State University–Amazonas, Manaus, Brazil*
[e] *Darcy Ribeiro State University of Northern Rio de Janeiro, Campos dos Goytacazes, Rio de Janeiro, Brazil*

(Manuscript received 23 July 2019, in final form 3 February 2020)

ABSTRACT

This work presents an analysis of the observed trends in extreme precipitation events in the Paraná River basin (PRB) from 1977 to 2016 (40 yr) based on daily records from 853 stations. The Mann–Kendall test and inverse-distance-weighted interpolation were applied to annual and seasonal precipitation and also for four extreme precipitation indices. The results show that the negative trends (significance at 95% confidence level) in annual and seasonal series are mainly located in the northern and northeastern parts of the basin. In contrast, except in the autumn season, positive trends were concentrated in the southern and southeastern regions of the basin, most notably for annual and summer precipitation. The spatial distributions of the indices of annual maximum 5-day precipitation and number of rainstorms indicate that significant positive trends are mostly located in the south-southeast part of the basin and that significant negative trends are mostly located in the north-northeast part. The index of the annual number of dry days shows that 88% of significant trends are positive and that most of these are located in the northern region of the PRB, which is a region with a high number of consecutive dry days (>90). The simple daily intensity index showed the highest number of stations (263) with mostly positive significant trends.

1. Introduction

Precipitation is considered to be one of the most important variables in the fields of hydrology, meteorology, and climate. Its variation patterns may affect agriculture and livestock development, the public and industrial water supply, hydropower generation, or even the risk of floods in urban areas. Therefore, understanding and identifying the spatial behavior of precipitation during both extremely dry and wet spells is relevant for offering subsidies for policy makers to improve the planning and sustainable management of water resources as well as to warn regions about further increases or decreases rainfall rates. In addition, attributing the increases or decreases in the frequency of precipitation events to global warming has been the focus of many investigations (Huntington 2006; Min et al. 2011; Trenberth 2011; Armal et al. 2018). Both understanding the behavior of precipitation extremes and improving the performance of global models in predicting future scenarios are issues of great importance in modern environmental sciences.

The Paraná River basin (PRB) plays an important role in the economic activity and development of Brazil. The watershed plays a major role in food production and has the largest installed capacity and energy generation in Brazil, with 156 hydropower plants that provide more than 45 000 MW of electricity (National Agency of Electric Energy 2019). Previous studies have reported that this region has presented changes in precipitation. By studying 59 stations during the period between 1950 and 1999, Dufek and Ambrizzi (2008) investigated trends using the Mann–Kendall (MK) test for six annual precipitation indicators in São Paulo state, which is

Corresponding author: S. A. Abou Rafee, sameh.adib@iag.usp.br

DOI: 10.1175/JAMC-D-19-0181.1

located in the central-eastern region of the PRB. Their results showed that the region presents positive significant trends in annual total precipitation, maximum 5-day precipitation, and consecutive wet days, representing 59.3%, 20.3%, and 32.2% of stations, respectively. In accordance with these results, they observed a significant negative trend in consecutive dry days in 23.7% of stations. In the southern part of the basin, Luiz Silva et al. (2015) observed significant positive trends for the annual maximum number of consecutive dry days and for the annual number of days with more than 30 mm of precipitation.

Some studies such as Silva Dias et al. (2013) and Pedron et al. (2017) identified a significant increase in extreme events of rainfall that may be related to the urbanization of the metropolitan regions of São Paulo and Curitiba cities, respectively. These authors used local daily rainfall from individual stations. Teixeira and Satyamurty (2011) also observed significant trends in annual heavy and extreme rainfall occurrence in southern Brazil within a 45-yr period (1960–2004), using cluster analysis and area-mean time series. However, the trends in southeastern Brazil were not significant in their study, which may be a result of the restrictive methodology of extreme events identification (Teixeira and Satyamurty 2011). Nevertheless, Zilli et al. (2017) observed an increase of rainy days and extreme events over the state of São Paulo, contributing to positive trends in total seasonal precipitation. These authors used more than 70 years of data with individual stations and gridded data, and their results suggests that the spatial patterns of trends are influenced by the proximity of large urban centers.

Although some studies have investigated the precipitation trends in the PRB over the past decades, most of these studies have been local (Silva Dias et al. 1995; Pedron et al. 2017) or regional (Dufek and Ambrizzi 2008; Luiz Silva et al. 2015) or used limited numbers of precipitation stations or cluster analysis (Zandonadi et al. 2016; Teixeira and Satyamurty 2011; Liebmann et al. 2004). The main goal of this work is to analyze the spatial trends in the Paraná River basin that have not been covered by previous research and extend the trend analysis period. Besides that, the current study describes the method of the quality control assessment for the precipitation data. The analysis of the spatial trends was performed on annual and seasonal precipitation totals as well as for the extreme precipitation indicators at 853 stations from 1977 to 2016.

2. Materials and methods

a. Study area

The study area comprises the Brazilian Paraná River basin, which extends from 26°50.02′ to 15°25.01′S latitude and from 55°55.05′ to 43°34.06′W longitude, with a drainage area of 879 873 km^2. The PRB is one of the most important and largest watersheds in Brazil; it is located in the central-southern region of Brazil, which covers six Brazilian states (São Paulo, Paraná, Mato Grosso do Sul, Minas Gerais, Goiás, and Santa Catarina) and the Federal District (Fig. 1). Currently, the PRB has an estimated population of more than 65 million inhabitants, with 93% of its population living in urban areas (Brazilian Institute of Geography and Statistics 2019). According to the Brazilian National Water Agency (ANA), this region has the highest demand for water resources in Brazil, equivalent to 736 m^3 s^{-1}, most of which are used for agricultural (42%) and industrial (27%) activities.

The PRB extends over an area large enough to cross different climatic zones as described by Reboita et al. (2017). Precipitation over the basin is generated by several meteorological and climatic phenomena crossing diverse temporal and spatial scales. Due to its location in a subtropical region of the South American continent, the PRB is susceptible to a series of convective systems that range from small-scale, isolated convective cells to frontal systems with hundreds of kilometers in their longest axis. The northern part of the basin is located north of the Tropic of Capricorn line and characterized by wet summers and dry winters, a regime of precipitation strongly associated with the South American monsoon system (SAMS) (Grimm et al. 2007; Carvalho et al. 2011; Marengo et al. 2012).

During the summer, the South Atlantic convergence zone, a system associated with strong and continuous precipitation that expands from the central parts of the Amazon region to the subtropical eastern coastal of Brazil, strongly influences precipitation in the central and northernmost parts of the PRB (Carvalho et al. 2004). Furthermore, the Bolivian high, the upper-level anticyclonic system associated with surface heating (Rao et al. 1996), frequently induces strong convection in the central and western parts of the PRB.

In the southern parts of the PRB, the precipitation is strongly influenced by baroclinic systems (Morales Rodriguez et al. 2010), with rainfall equally spread throughout the year. Moreover, it is also influenced by mesoscale convective systems (MCS), mainly during spring and summer. The formation of such MCS, in turn, is strongly connected to the South American low-level jet (SALLJ), which brings heat and moisture from the tropical areas of South America to this region (Marengo et al. 2002; Salio et al. 2007). Recent studies showed that the spatiotemporal intensity distribution and frequency of SALLJ is modulated and influenced by the low-frequency events such as the Atlantic multidecadal

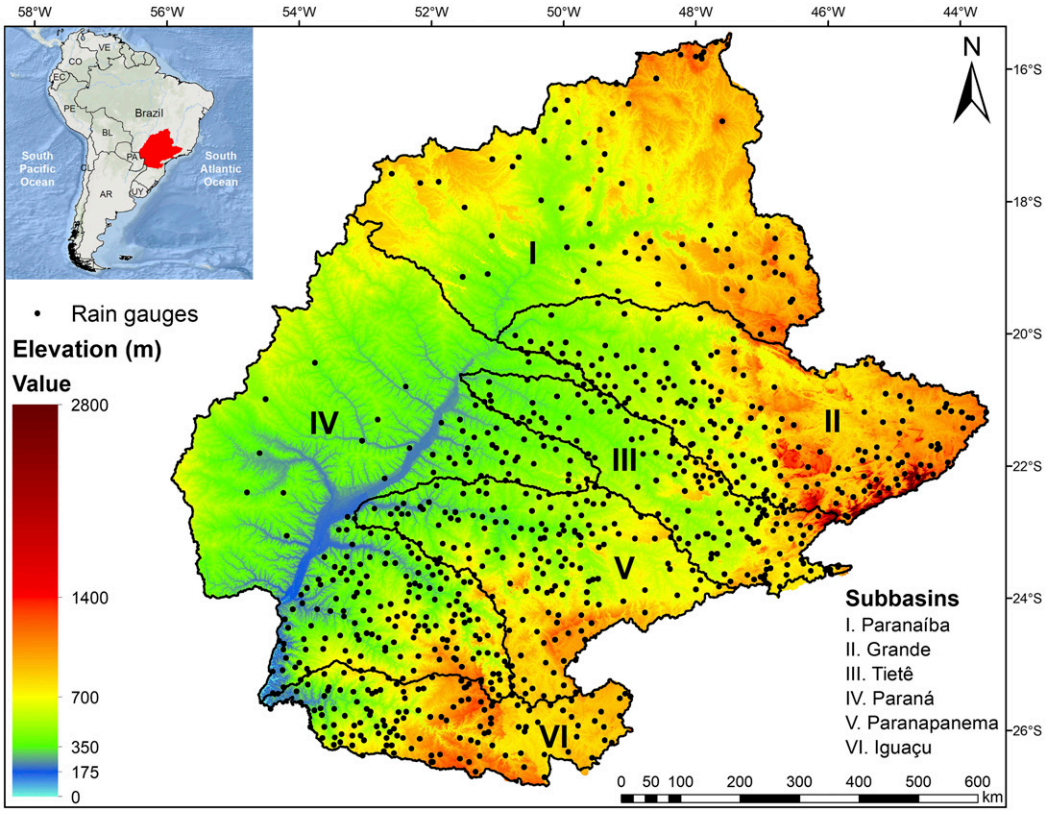

FIG. 1. Geographic location and topographic map of the PRB with its subbasins, showing the spatial distribution of the 853 weather stations used in this paper.

oscillation and El Niño–Southern Oscillation (ENSO) (Jones and Carvalho 2018; Montini et al. 2019). Locally, MCS includes squall lines and mesoscale convective complexes, as described by Velasco and Fritsch (1987).

Baroclinic instabilities influence precipitation in most of the PRB. They are associated with transient systems such as cold fronts and frontogenetic effects (Satyamurty and De Mattos 1989) connected to the presence of the upper-level subtropical jet. Squall lines can be seen year-round and are associated with sea breeze in the east of the PRB.

To facilitate understanding of the results and discussion, the study area was divided into six subbasins: Paranaíba (I), Grande (II), Tietê (III), Paraná (IV), Paranapanema (V), and Iguaçu (VI) (see Fig. 1).

b. Dataset description, quality control, and preprocessing

The dataset of 40 years of daily precipitation totals, from 1 January 1977 to 31 December 2016, from gauges distributed over the PRB was provided by ANA. The set comprises 5107 rain gauge stations from 149 different institutions. Before use, these data were thoroughly controlled via the following steps:

(i) Double records and typographical errors were verified. Several consecutive repeated values above 1 mm day^{-1} and precipitation above 250 mm day^{-1} were considered as missing data. Stations with values above 250 mm day^{-1} were verified if possible before considering them as missing data. The values were analyzed by comparing the amounts of rainfall among nearby stations.

(ii) Stations missing more than 10% of their data during the period from 1 January 1977 to 31 December 2016 were disregarded.

(iii) Missing data were not filled, and, to avoid misleading detection of a trend as a result of missing data, years with more than 14 missing data were not considered in the trend analysis. For the analysis of seasonal totals (3 months), seasons with more than three missing data were disregarded.

(iv) A test of homogeneity was performed on the annual precipitation time series by using the standard normal homogeneity test (SNHT) (Alexandersson 1986). SNHT has been previously used in several studies for the homogeneity analysis of precipitation time series (e.g., Jónsdóttir et al. 2006; Javari 2016). Data series that presented nonhomogeneity were disregarded.

(v) Autocorrelation was tested on both annual and seasonal precipitation as a quality check, because no autocorrelation is expected in precipitation data, and to assure that no serially correlated time series will be tested for trends (e.g., Yue et al. 2002).

After data quality control, 853 gauge stations were selected. Most gauge stations are located in the Paraná (IV) subbasin, mainly in the southeastern part of the PRB, followed by the Grande (II) and Paranapanema (V) ones, which have 209 (24.5%), 171 (20%), and 146 (17%) stations, respectively. The highest number of rain gauges in the east side of the basin is due to the majority of the stations being located on large rivers, where most of the hydropower plants are located, and surrounding densely populated areas. The spatial distribution of the rain gauges is illustrated in Fig. 1.

These daily precipitation series were the basis for creating series of accumulated annual and seasonal precipitation. Seasons follow the austral ones: summer (December, January, and February), autumn (March, April, and May), winter (June, July, and August), and spring (September, October, and November). In addition, four indices used in the Statistical and Regional Dynamical Downscaling of Extremes for European Regions (STARDEX; Goodess et al. 2005) were selected to analyze extreme precipitation. To evaluate the intensity of extreme precipitation events, series of annual 5-day maximum precipitation (px5d) and simple daily intensity (pint) were generated. To assess the persistence of precipitation, the indices of longest dry period (pxcdd) and rainstorm days (pn50) were generated. An overview of these indices is given in Table 1.

c. Methods

Annual and seasonal precipitation were interpolated over the PRB using inverse-distance-weighted (IDW) interpolation. Trends were tested by the MK test, and their statistical significance was tested by bootstrap. This section presents the description of these methods.

1) MK TEST

The nonparametric statistical MK test (Mann 1945; Kendall 1975) was used to analyze the trends in the annual, seasonal, and daily precipitation amounts at all 853 stations (1977–2016). The MK test is widely used to investigate trends in series of meteorological variables (e.g., Marengo et al. 1998; Dufek and Ambrizzi 2008; Li et al. 2011, 2010; Shifteh Some'e et al. 2012; Sayemuzzaman and Jha 2014; Shi et al. 2016). We applied the MK test on the indices of the accumulated annual and seasonal rainfall as well as on the indices calculated and described in Table 1.

The MK test is calculated using Eqs. (1)–(4):

$$S = \sum_{j=1}^{n-1} \sum_{i=j+1}^{n} \operatorname{sgn}(x_i - x_j), \tag{1}$$

$$\operatorname{sgn}(x) = \begin{cases} +1, & \text{if} \quad (x_i - x_j) > 0 \\ 0, & \text{if} \quad (x_i - x_j) = 0 \\ -1, & \text{if} \quad (x_i - x_j) < 0 \end{cases}, \tag{2}$$

$$\operatorname{VAR}(S) = \frac{\left[n(n-1)(2n+5) - \sum_{j=1}^{m} t_j (t_j - 1)(2t_j + 5) \right]}{18}, \tag{3}$$

and

$$Z_{\mathrm{MK}} = \begin{cases} \dfrac{S-1}{[\operatorname{VAR}(S)]^{1/2}} & \text{if} \quad S > 0 \\ 0 & \text{if} \quad S = 0 \\ \dfrac{S+1}{[\operatorname{VAR}(S)]^{1/2}} & \text{if} \quad S < 0 \end{cases}, \tag{4}$$

where n represents the length of the dataset; x_i and x_j are the data values in i and j, respectively; t_j represents the number of observations for the jth group; m is the number of groups; and Z_{MK} indicates that there is an increasing trend (positive value) or decreasing trend (negative value) with time in the analyzed variable. When $|Z_{\mathrm{MK}}| > Z_1 - (\alpha/2)$, the null hypothesis is rejected and a significant trend is detected in the dataset. The value of $Z_1 - (\alpha/2)$ is available from the standard normal distribution table. In this study, statistical significance at the 95% confidence level ($\alpha = 0.05$) was adopted. Therefore, the null hypothesis of no trend is rejected when $|Z_{\mathrm{MK}}| > 1.96$.

Bootstrap method

According to Clarke (2010), the effect of spatial correlation between stations should be considered when a trend detection is applied. The spatial correlation was evaluated by testing the significance level of the MK test using the bootstrap method (Efron 1979), which is suggested by Douglas et al. (2000). For all the indices (Table 1), 500 random samples from the original time series and their trends were calculated. The original data were considered to be statistically significant if the resampled series trend fell into the upper or lower 5% of the bootstrapped distribution.

2) IDW INTERPOLATION

To analyze the spatial distribution of trends in precipitation, the IDW interpolation method was used. This interpolation technique was applied to the annual and

TABLE 1. List of precipitation indices selected.

Indices	Definition	Unit
Accumulated precipitation	Annual or seasonal precipitation totals	mm
5-day max precipitation (px5d)	Annual greatest 5-day total precipitation	mm
Simple daily intensity (pint)	Annual mean precipitation per rain day ($\geq$1 mm day^{-1})	mm day^{-1}
Longest dry period (pxcdd)	Annual max no. of consecutive dry days ($<$1 mm day^{-1})	days
Rainstorm days (pn50)	Annual no. of days with precipitation $>$50 mm day^{-1}	days

seasonal average precipitation totals as well as to the extreme precipitation indices. IDW has been carried out in several studies for the spatial interpolation of precipitation and has provided satisfactory results (e.g., Cannarozzo et al. 2006; Lu and Wong 2008; Gemmer et al. 2011; Chen et al. 2017). The IDW interpolator essentially depends on the number of observations around the point of interest, with individual contributions diminishing with distance. The local influence of observations is defined using Eqs. (5) and (6):

$$\hat{Z}(S_0) = \sum_{i=1}^{N} \lambda_i Z(S_i) \quad \text{and} \tag{5}$$

$$\lambda_i = \frac{d_{i0}^{-p}}{\sum_{i=1}^{N} d_{i0}^{-p}}, \quad \sum_{i=1}^{N} \lambda_i = 1, \tag{6}$$

where $\hat{Z}(S_0)$ represents the prediction value at point S_0, $Z(S_i)$ is the observed value at point S_i, N is the number of observations surrounding the prediction point, λ_i is the weight assigned to each observed point, p is a power parameter, and d_{i0} is the distance from the target to the observation.

3. Results and discussion

Trends and interpolated values of precipitation

The results of the trends obtained by the MK test and the interpolated values obtained using the IDW method for the annual and seasonal average accumulated precipitation as well as for the precipitation indices from 1977 to 2016 are shown in Figs. 2–4. The results and their discussions are presented in the following sections.

1) ANNUAL AND SEASONAL PRECIPITATION

The interpolated annual average precipitation (Fig. 2e) clarifies that the higher values of accumulated annual precipitation over the PRB, exceeding 1850 mm, are located in the southern PRB (west of the Iguaçu and southeast of the Paraná subbasins). On the other hand, the lower values, lower than 1400 mm, predominate in the center (mostly in the lower Tietê and northeast of the Paraná subbasins). Seventy of the 853 stations (8%) showed trends at the 95% confidence level of significance. Of them, 36 presented significant negative trends, being mostly located in the Grande (20) and Paranaíba (8) subbasins. Thirty-four series (4%) presented significant positive trends, and they are concentrated in parts of the Paranapanema (12), Iguaçu (11), and Paraná (9) subbasins (see Fig. 2e).

In contrast to the accumulated annual precipitation patterns, the north and northeast of the PRB (i.e., the Paranaíba and Grande subbasins) are the regions with the highest summer precipitation values ($>$800 mm), while the southern region (i.e., the Iguaçu subbasin) presents the lowest values ($<$500 mm) (Fig. 2a). The high rates of precipitation in the northern part of the PRB are characterized by the activity of the SAMS during the austral summer (Grimm et al. 2007; Carvalho et al. 2011). Among the series of accumulated summer precipitation, 39 showed significant trends. Negative trends are observed mostly in the Paranaíba and Grande subbasins, with 9 and 4 stations, respectively. Positive trends are concentrated in the southeast of the Paraná, Iguaçu, and Paranapanema subbasins with 12, 5, and 4 stations, respectively (Fig. 2a).

Precipitation totals in autumn show great spatial variability with higher precipitation values of more than 450 mm in the southeastern region (Iguaçu), as seen in Fig. 2b. All the significant trends in autumn were negative, and they were mainly located in the central portion and northeastern region of the PRB (Fig. 2b).

Figure 2c shows that the winter precipitation in the PRB increases from north to south, from less than 30 mm (north of the Paranaíba subbasin) to more than 240 mm (southeast of the Paraná and south of the Paranapanema and Iguaçu subbasins). As mentioned before, this scenario of low rainfall in the northern part of the basin occurs due to the presence of the SAMS, which is responsible for the low precipitation rates in winter and high rates in austral summer (Fig. 2a) (Grimm et al. 2007; Carvalho et al. 2011). For this season, few stations presented significant trends, with a clear north–south separation. Negative trends predominated in the north (9) and positive in the south (4).

The series of spring precipitation showed totals ranging from 350 to 500 mm. Statistically significant

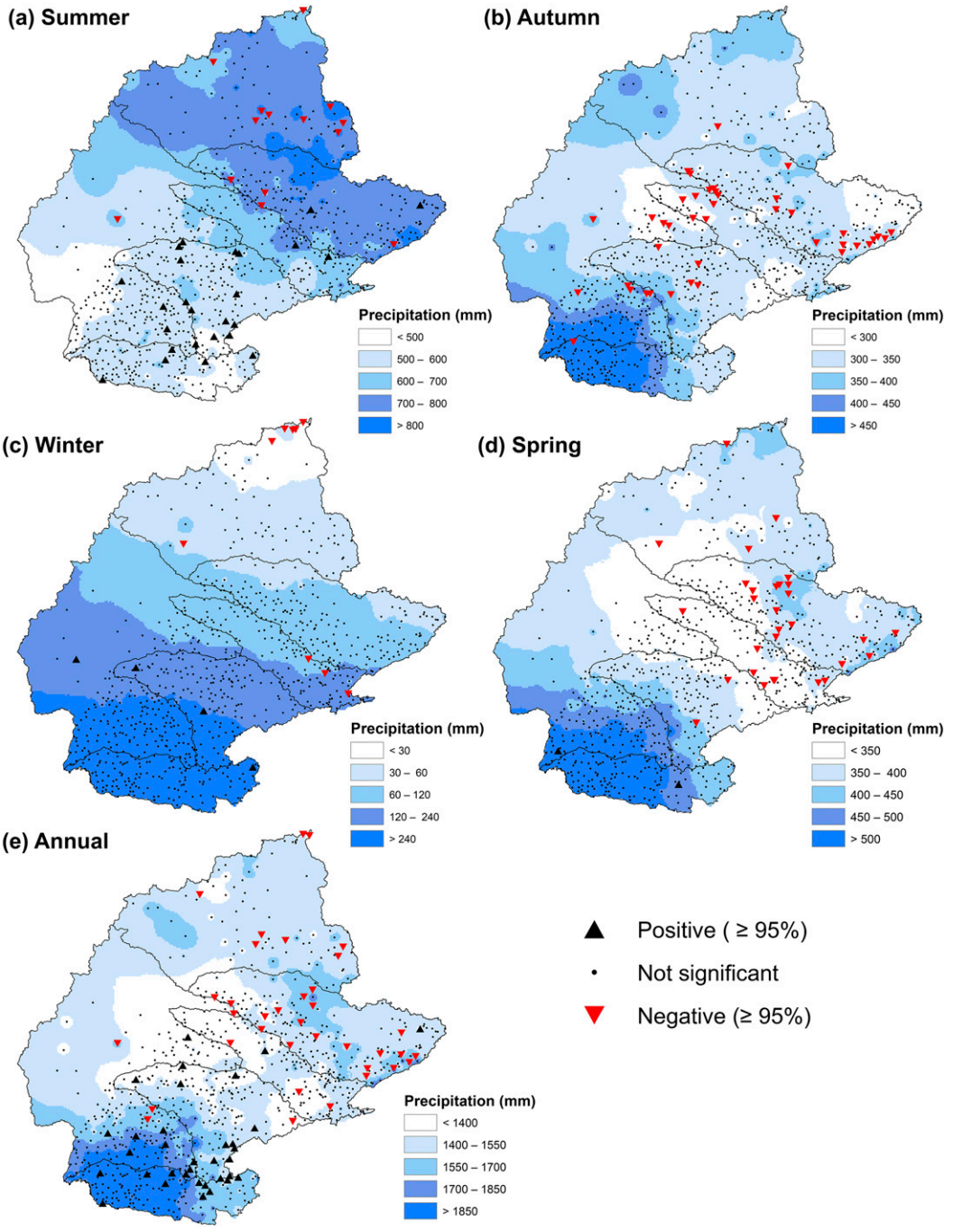

FIG. 2. Spatial distribution of trends and interpolated values of annual and seasonal average precipitation totals in the PRB over the period of 1977–2016 for (a) summer, (b) autumn, (c) winter, (d) spring, and (e) annual. The blue-shaded patterns are the annual and seasonal values, triangles show the significant trend (red is negative, and black is positive), and black circles indicate no significant trend.

negative trends predominated in the northeastern region of the PRB, with 16 stations in the Grande subbasin (Fig. 2d).

The spatial distribution of trends of annual and seasonal total precipitation shows that significant negative trends are mostly located in the Paranaíba and Grande subbasins. A decreasing amount of precipitation in those regions may have a significant impact on energy generation as these basins house 70 hydropower plants that, together, provide more than 17 000 MW of electricity

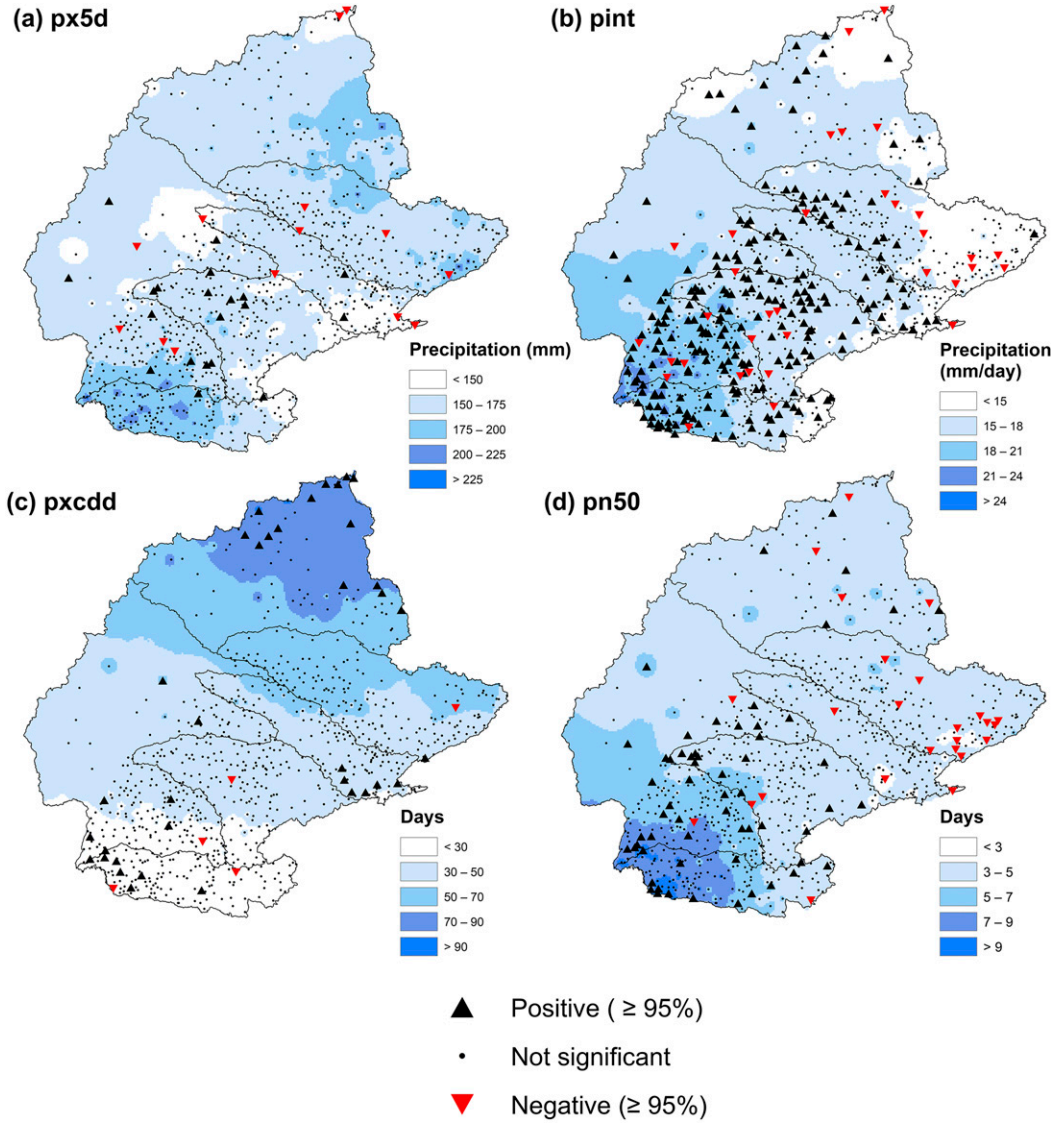

FIG. 3. Spatial distribution of trends and interpolated values of annual average extreme precipitation indices in the PRB over the period of 1977–2016 for (a) px5d, (b) pint, (c) pxcdd, and (d) pn50. The blue-shaded patterns are average extreme precipitation indices values, triangles show the significant trend (red is negative, and black is positive), and black circles indicate no significant trend.

(National Agency of Electric Energy 2019). In contrast, the significant positive trends are concentrated in the Paranapanema and Iguaçu subbasins, notably in the summer season, which explains most of the annual trends.

Figures 4a–e show the spatial distribution of only significant trends (positive or negative) in both indices as a result of the comparison of the indicators from Figs. 2 and 3. Negative significant trends in annual totals in the northern portion of the basin could be associated with the decreasing of precipitation during the summer, spring, or autumn seasons, as shown in Figs. 4a–c. Similarly, the positive significant trends in annual totals in the southern areas of the basin follow the trend in summer rainfall (Fig. 4a). Almeida et al. (2017) found equivalent results for annual and seasonal trends in the Brazilian Legal Amazon region for the 40-yr period 1973–2013. Stations with significant positive annual trends were associated with positive trends during the wet season. On the other hand, significant negative annual trends were associated with the negative trends in the dry season. Liebmann et al. (2004), studying the La Plata basin, observed a positive trend of up to 10.89 mm in the January–March season, during the period of 1976–99, over the southern parts of the PRB. This trend was

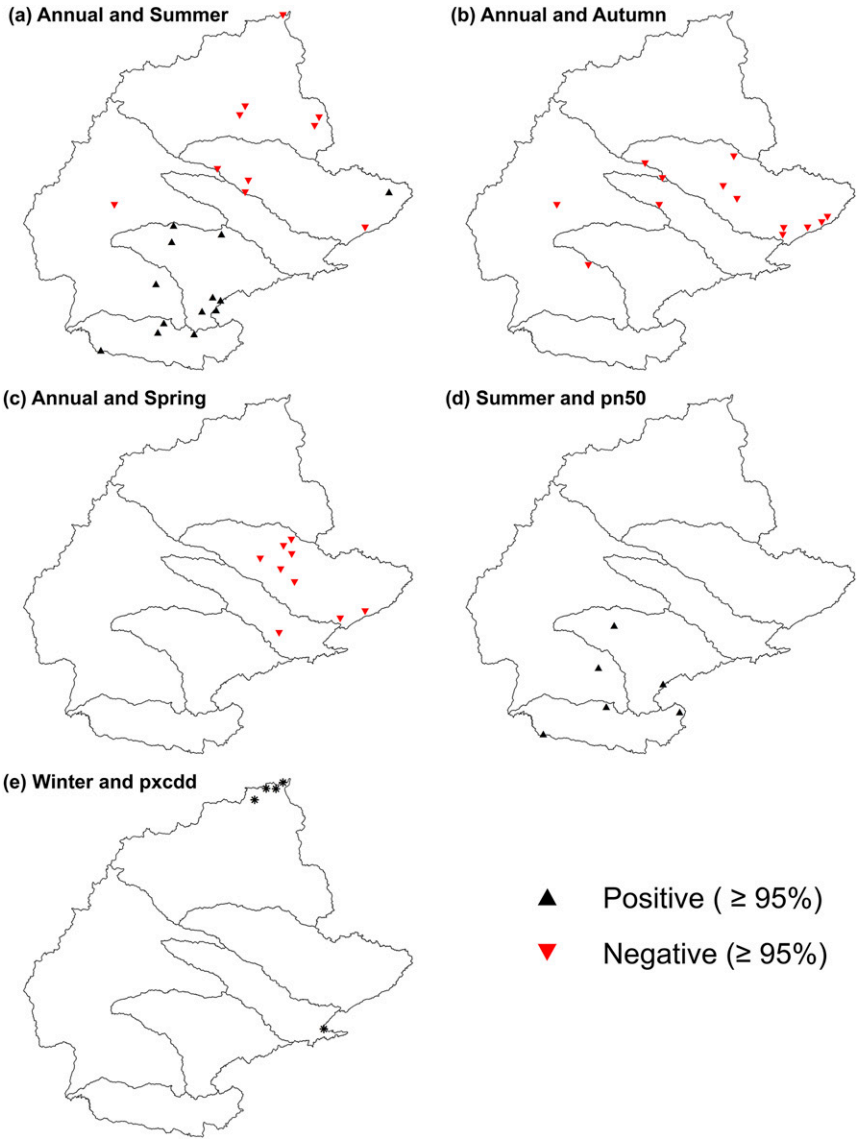

FIG. 4. Spatial distribution of trends at the 95% confidence level for both (a) annual precipitation and summer precipitation, (b) annual precipitation and autumn precipitation, (c) annual precipitation and spring precipitation, (d) summer precipitation and pn50, and (e) winter precipitation (for negative significant trend) and pxcdd (for positive significant trend). The triangles show the significant trend (red is negative, and black is positive) at both indices, and the black asterisks represent the opposite trends of the displayed indices. The indices are defined in Table 1.

correlated with positive trends in the southwestern Atlantic sea surface temperature and streamflow in the area that essentially coincides with the Iguaçu subbasin, but with no obvious causes, according to the authors.

Haylock et al. (2006) analyzed trends using gridded data (2° × 2°) from 1960 to 2000 over South America. Their results indicated a positive trend in annual total precipitation for most of the region related to PRB, except for a small part over the northern region. The present work found negative trends in an area that covers the northeastern part of the PRB (Fig. 2e). The discrepancies between the results presented in this work and Haylock et al. (2006) may be due to the different time span and spatial resolution. The gridded analysis performed by the authors may have influenced the local effects that are associated, for example, with urbanization. A study made by Yu and Liu (2015) using the Weather Research and Forecasting (WRF) Model

coupled with a multilayer urban canopy model shows that urbanization plays a significant role in frontal-type rainfall. They demonstrated through simulations that the urbanization and land-use change of Beijing caused the spatial distribution of precipitation to become more concentrated. The different period of study (1977–2016 vs 1960–2000) may also cause changes in trends. This further suggests that there may not be a steady positive or negative trend for the accumulated precipitation in the region.

A recent drought event in the PRB has been experienced by the eastern part of the basin during the years 2014–15. According to Coelho et al. (2016), during the summer of 2014, the South Atlantic convergence zone, the mechanism responsible for most of the rainfall during summer months, was practically absent in the period. The anomalous dry season was attributed to a global circulation pattern connecting the Pacific and Atlantic Oceans that in turn caused a lasting subsidence over the basin. However, the authors point out the negative anomaly in summer precipitation as the main cause of the long-lasting drought. In our study, as shown in Figs. 4a and 4b, the trend of decrease in annual precipitation is a result of trends evident in the summer, autumn, and spring seasons.

2) EXTREME PRECIPITATION EVENTS

The annual 5-day maximum precipitation index (px5d) presented both significant positive and negative trends during 1977–2016 (Fig. 3a). Positive trends were observed in 20 locations mostly in the central portion of the basin. Some of these stations are located in regions with px5d values greater than 225 mm, which indicates an increase of extreme events during this period. On the other hand, the 14 stations with negative trends were mostly located in the northern and northeastern regions of the PRB (Fig. 3a). An increasing of the rainfall amount increases the probability of flooding and, therefore, special attention should be given to the lower Paranapanema subbasin, where nine of the stations that presented significant positive trends are located. Previous studies have analyzed extreme precipitation events in this area and other parts of the PRB that caused considerable damage to local economies (e.g., Camilloni and Barros 2000). Moreover, a significant positive trend in px5d was detected in other basins in South America such as the Cauca River in southwestern Colombia (Ávila et al. 2019).

Simple daily intensity (pint) is the index with the highest number of stations showing significant trends, with 263 of 853 stations (31%). A total of 87% of these stations exhibit positive trends and are mostly located in the Paraná subbasin, with 70 stations, followed by the Paranapanema (54) and Iguaçu (48) subbasins (Fig. 3b). This result is in accordance with those found by Zandonadi et al. (2016) that presented an increase of the trends in almost all domains of the PRB. According to Peterson et al. (2001), the pint index summarizes the wet part of the year. Therefore, the results indicate that most of the areas in the PRB basin are experiencing a lengthening of the wet season. The opposite was observed by Bezerra et al. (2019) over the São Francisco River basin, north of the PRB, in the Brazilian semiarid region. They found mainly negative trends in pint, indicating the shortening of the rainfall season in that region.

Liebmann et al. (2004) connects the increase of the pint index, in an area covering PRB, to the positive trend observed in precipitation during the January—March season. Although summer in this work comprises December to February, the trends presented here are consistent with their results. On the other hand, the neutral trends found by Liebmann et al. (2004) in an area that corresponds to the northern part of the PRB are not consistent with the findings presented here. The one-decade-longer time span of the data in this work could explain these discrepancies. For instance, with a longer analysis period, the present work may have captured more phase change of climate variability than previous studies. As reported by several studies (e.g., Jacques-Coper and Garreaud 2015; Miller et al. 1994), the large-scale modes of variability have a significant influence on the regional precipitation regime within the basin. Also, the spatial resolution (2.5° × 2.5°) analysis used by the authors may have contributed to the trend differences. In the study by Haylock et al. (2006), the trends identified for pint show a clear pattern of increasing over areas of the PRB, which is consistent with the present study.

Figure 3c shows that the longest dry period (pxcdd) increases from south to north in the PRB. Pxcdd ranged from 30 days in the Iguaçu subbasin to more than 90 days in the northern region of the Paranaíba subbasin. This gradient is connected to the different sources of precipitation from south to north and is clearly connected to the dry winters characteristic of the South American monsoon (Fig. 2c). Positive trends represent the majority (88%) of significant trends of pxcdd. Most of these (15) are located in the northern region of the PRB, particularly in northern Paranaíba, which is the region that presents a high number of dry days (>90). The significant positive trends in pxcdd found at four stations in the upper Paranaíba subbasin can be explained by the negative trends in precipitation during winter (Fig. 4e). Evidence of increasing of consecutive dry days in the Paranaíba subbasin was also found by Zandonadi et al. (2016), but with no stations with a significant trend at the 95% confidence level during the period between 1986

and 2011. An increase in the annual maximum number of consecutive days without rainfall in these areas may have a significant impact in water supply to the largest city of Goiás state, Goiânia, and the federal capital of Brazil, Brasilia, with an estimated population of 1.5 and 3.0 million inhabitants, respectively (Brazilian Institute of Geography and Statistics 2019). According to ANA, the Corumbá IV reservoir, located in the northern part of the PRB (within the location of significant positive trends of the pxcdd index) with an area of 173 km^2, is responsible for the water supply of 1.3 million inhabitants.

The remaining stations with significant positive pxcdd trends are located in the upper Tietê subbasin and the western parts of the Iguaçu subbasin. The results obtained in the Tietê and Iguaçu subbasins are consistent with those found by Dufek and Ambrizzi (2008) and Luiz Silva et al. (2015), respectively.

The interpolated values of the pn50 indicator show regions with climatological mean exceeding 9 days per year with rainfall values greater than 50 mm. The MK test showed significant trends at 85 stations (10%), of which 60 are positive and 25 are negative. Positive trends are mostly located in the south and negative ones in the northeast of the PRB (Fig. 3c). One of the main contributors to extreme precipitation events over the PRB, the SALLJ, has been analyzed recently in terms of its strength and spatiotemporal variability. Montini et al. (2019) reported trends of SALLJ from 1979 to 2016 within the same period of the present study. Their results showed significant increasing trends in strength and frequency of SALLJ over southern Brazil. These may likely contribute to the increase of rainstorm days ($>$50 mm day^{-1}) in the south of the PRB. The significant positive trends in rainstorm days may be a contributor to the positive trend in summer rainfall in the southern areas of the PRB observed here. As shown in Fig. 4d, six stations revealed positive trends at 95% confidence level in both summer and pn50 indices. Such behavior has been previously observed in other parts of the world (Jiang et al. 2007).

4. Conclusions

This paper analyzed the annual and seasonal precipitation, as well as extreme precipitation indices, in the PRB. The spatial distributions of the positive and negative significant trends at the 95% confidence level were analyzed using 40 years of data, ranging from 1977 to 2016. The spatial distribution of these data was obtained using the IDW method, and their trends were obtained using the MK test.

Previous studies have shown that the occurrence of extremes in the PRB undergoes intense spatial and temporal variation (Liebmann et al. 2001; Grimm 2011) and that there are many climate regimes affecting the different subbasins of the PRB (see Salio et al. 2007; Zamboni et al. 2010; Tedeschi et al. 2013). Thus, depending on the time scale involved and the resolution used, these studies may not be conclusive or may not agree with the results found in this work. Hence, the importance of the results presented here lies in the fact that they explore trend analysis of extremes over all PRB as well as an update in terms of the number of stations analyzed. Furthermore, these conclusions are based on longer precipitation series, which increases the probability that a given time scale is properly represented, in contrast with previous works, which focused on the trends in rainfall extremes in the PRB for previous or shorter periods. For instance, Silva Dias et al. (2013) found through long-term analysis of data from one rain gauge located in São Paulo city that the climatic indices such as the Pacific decadal oscillation, ENSO, and the North Atlantic Oscillation explained 85% of the increasing frequency of extremes during the dry season. Also, the study performed by Teixeira and Satyamurty (2011) suggests that longer time series are necessary to ensure the existence of monotonic trends.

The results revealed that the Paraná River basin has many stations located in different subbasins recording precipitation series with monotonic trends. Hence, this information, as well as knowledge about the regions that present trends in precipitation, is of interest for policy makers and managers in the implementation of future conservation and sustainable use of water resources. These results also represent an update relative to previous studies, as this study used a large number of rain gauges and a longer rainfall time series.

Special attention should be paid to the northern and southern regions of the basin, which presented decreasing and increasing trends in precipitation amounts, respectively. In the southern part of the basin, an increase of extreme precipitation events with rainfall greater than 50 mm day^{-1} is shown by these analyses. In the northern region of the PRB, an increasing number of dry days may have an impact on economic activity since it is an important region for agriculture production and energy generation and is the location of one of the largest urban centers of Brazil.

In a forthcoming study, the authors will further evaluate the potential impact of changes in land use and land cover and climate shift in the PRB over the last decades on hydrological processes, and they will link this research with changes in precipitation in the basin.

Acknowledgments. This work was supported by Coordenação de Aperfeiçoamento de Pessoal de Nível Superior (CAPES), PROEX and Process 88887.115875/2015-01. The authors gratefully acknowledge ANA for providing the precipitation data. We also acknowledge Fundação de Amparo à Pesquisa do Estado de São Paulo (FAPESP), Process 2015/03804-9. The authors are also grateful for the highly insightful comments and suggestions of Editor Katherine Klink and the anonymous reviewers that enabled us to improve the quality of this work.

REFERENCES

Alexandersson, H., 1986: A homogeneity test applied to precipitation data. *J. Climatol.*, **6**, 661–675, https://doi.org/10.1002/joc.3370060607.

Almeida, C. T., J. F. Oliveira-Júnior, R. C. Delgado, P. Cubo, and M. C. Ramos, 2017: Spatiotemporal rainfall and temperature trends throughout the Brazilian Legal Amazon, 1973–2013. *Int. J. Climatol.*, **37**, 2013–2026, https://doi.org/10.1002/joc.4831.

Armal, S., N. Devineni, and R. Khanbilvardi, 2018: Trends in extreme rainfall frequency in the contiguous United States: Attribution to climate change and climate variability modes. *J. Climate*, **31**, 369–385, https://doi.org/10.1175/JCLI-D-17-0106.1.

Ávila, Á., F. C. Guerrero, Y. C. Escobar, and F. Justino, 2019: Recent precipitation trends and floods in the Colombian Andes. *Water*, **11**, 379, https://doi.org/10.3390/W11020379.

Bezerra, B. G., L. L. Silva, C. M. Santos e Silva, and G. G. de Carvalho, 2019: Changes of precipitation extremes indices in São Francisco River basin, Brazil from 1947 to 2012. *Theor. Appl. Climatol.*, **135**, 565–576, https://doi.org/10.1007/s00704-018-2396-6.

Brazilian Institute of Geography and Statistics, 2019: População. IBGE, accessed 12 November 2019, http://www.ibge.gov.br/apps/populacao/projecao/.

Camilloni, I., and V. Barros, 2000: The Parana River response to El Niño 1982–83 and 1997–98 events. *J. Hydrometeor.*, **1**, 412–430, https://doi.org/10.1175/1525-7541(2000)001<0412:TPRRTE>2.0.CO;2.

Cannarozzo, M., L. V. Noto, and F. Viola, 2006: Spatial distribution of rainfall trends in Sicily (1921-2000). *Phys. Chem. Earth*, **31**, 1201–1211, https://doi.org/10.1016/j.pce.2006.03.022.

Carvalho, L. M. V., C. Jones, and B. Liebmann, 2004: The South Atlantic convergence zone: Intensity, form, persistence, and relationships with intraseasonal to interannual activity and extreme rainfall. *J. Climate*, **17**, 88–108, https://doi.org/10.1175/1520-0442(2004)017<0088:TSACZI>2.0.CO;2.

——, ——, A. E. Silva, B. Liebmann, and P. L. Silva Dias, 2011: The South American monsoon system and the 1970s climate transition. *Int. J. Climatol.*, **31**, 1248–1256, https://doi.org/10.1002/joc.2147.

Chen, T., and Coauthors, 2017: Comparison of spatial interpolation schemes for rainfall data and application in hydrological modeling. *Water*, **9**, 342, https://doi.org/10.3390/w9050342.

Clarke, R. T., 2010: On the (mis)use of statistical methods in hydro-climatological research. *Hydrol. Sci. J.*, **55**, 139–144, https://doi.org/10.1080/02626661003616819.

Coelho, C. A. S., and Coauthors, 2016: The 2014 southeast Brazil austral summer drought: Regional scale mechanisms and teleconnections. *Climate Dyn.*, **46**, 3737–3752, https://doi.org/10.1007/s00382-015-2800-1.

Douglas, E. M., R. M. Vogel, and C. N. Kroll, 2000: Trends in floods and low flows in the United States: Impact of spatial correlation. *J. Hydrol.*, **240**, 90–105, https://doi.org/10.1016/S0022-1694(00)00336-X.

Dufek, A. S., and T. Ambrizzi, 2008: Precipitation variability in São Paulo State, Brazil. *Theor. Appl. Climatol.*, **93**, 167–178, https://doi.org/10.1007/s00704-007-0348-7.

Efron, B., 1979: Bootstrap methods: Another look at the jackknife. *Ann. Stat.*, **7** (1), 1–26, https://doi.org/10.1214/aos/1176344552.

Gemmer, M., T. Fischer, T. Jiang, B. Su, and L. L. Liu, 2011: Trends in precipitation extremes in the Zhujiang River basin, south China. *J. Climate*, **24**, 750–761, https://doi.org/10.1175/2010JCLI3717.1.

Goodess, C. M. M., and Coauthors, 2005: An intercomparison of statistical downscaling methods for Europe and European regions—Assessing their performance with respect to extreme temperature and precipitation events. Climatic Research Unit Rep., 72 pp., http://www.cru.uea.ac.uk/documents/421974/1301877/CRU_RP11.pdf.

Grimm, A. M., 2011: Interannual climate variability in South America: Impacts on seasonal precipitation, extreme events, and possible effects of climate change. *Stochastic Environ. Res. Risk Assess.*, **25**, 537–554, https://doi.org/10.1007/s00477-010-0420-1.

——, J. S. Pal, and F. Giorgi, 2007: Connection between spring conditions and peak summer monsoon rainfall in South America: Role of soil moisture, surface temperature, and topography in eastern Brazil. *J. Climate*, **20**, 5929–5945, https://doi.org/10.1175/2007JCLI1684.1.

Haylock, M. R., and Coauthors, 2006: Trends in total and extreme South American rainfall in 1960–2000 and links with sea surface temperature. *J. Climate*, **19**, 1490–1512, https://doi.org/10.1175/JCLI3695.1.

Huntington, T. G., 2006: Evidence for intensification of the global water cycle: Review and synthesis. *J. Hydrol.*, **319**, 83–95, https://doi.org/10.1016/j.jhydrol.2005.07.003.

Jacques-Coper, M., and R. D. Garreaud, 2015: Characterization of the 1970s climate shift in South America. *Int. J. Climatol.*, **35**, 2164–2179, https://doi.org/10.1002/joc.4120.

Javari, M., 2016: Trend and homogeneity analysis of precipitation in Iran. *Climate*, **4**, 44, https://doi.org/10.3390/cli4030044.

Jiang, T., B. Su, and H. Hartmann, 2007: Temporal and spatial trends of precipitation and river flow in the Yangtze River basin, 1961–2000. *Geomorphology*, **85**, 143–154, https://doi.org/10.1016/j.geomorph.2006.03.015.

Jones, C., and L. M. V. Carvalho, 2018: The influence of the Atlantic multidecadal oscillation on the eastern Andes low-level jet and precipitation in South America. *npj Climate Atmos. Sci.*, **1**, 40, https://doi.org/10.1038/S41612-018-0050-8.

Jónsdóttir, J. F., P. Jónsson, and C. B. Uvo, 2006: Trend analysis of Icelandic discharge, precipitation and temperature series. *Hydrol. Res.*, **37**, 365–376, https://doi.org/10.2166/nh.2006.020.

Kendall, M. G., 1975: *Rank Correlation Methods*. Charles Griffin and Company, 202 pp.

Li, Q., Y. Chen, Y. Shen, X. Li, and J. Xu, 2011: Spatial and temporal trends of climate change in Xinjiang, China. *J. Geogr. Sci.*, **21**, 1007–1018, https://doi.org/10.1007/s11442-011-0896-8.

Li, Z., F.-l. Zheng, W.-z. Liu, and D. C. Flanagan, 2010: Spatial distribution and temporal trends of extreme temperature and precipitation events on the Loess Plateau of China during

1961–2007. *Quat. Int.*, **226**, 92–100, https://doi.org/10.1016/j.quaint.2010.03.003.

Liebmann, B., C. Jones, and L. M. V. de Carvalho, 2001: Interannual variability of daily extreme precipitation events in the state of Saõ Paulo, Brazil. *J. Climate*, **14**, 208–218, https://doi.org/10.1175/1520-0442(2001)014<0208:IVODEP>2.0.CO;2.

——, and Coauthors, 2004: An observed trend in central South American precipitation. *J. Climate*, **17**, 4357–4367, https://doi.org/10.1175/3205.1.

Lu, G. Y., and D. W. Wong, 2008: An adaptive inverse-distance weighting spatial interpolation technique. *Comput. Geosci.*, **34**, 1044–1055, https://doi.org/10.1016/j.cageo.2007.07.010.

Luiz Silva, W., C. Dereczynski, M. Chang, M. Freitas, B. J. Machado, L. Tristão, and J. Ruggeri, 2015: Tendências observadas em indicadores de extremos climáticos de temperatura e precipitação no estado do Paraná. *Rev. Bras. Meteor.*, **30**, 181–194, https://doi.org/10.1590/0102-778620130622.

Mann, H. B., 1945: Nonparametric test against trend. *Econometrica*, **13**, 245–259, https://doi.org/10.2307/1907187.

Marengo, J. A., J. Tomasella, and C. R. Uvo, 1998: Trends in streamflow and rainfall in tropical South America: Amazonia, eastern Brazil, and northwestern Peru. *J. Geophys. Res.*, **103**, 1775–1783, https://doi.org/10.1029/97JD02551.

——, M. W. Douglas, and P. L. Silva Dias, 2002: The South American low-level jet east of the Andes during the 1999 LBA-TRMM and LBA-WET AMC campaign. *J. Geophys. Res.*, **107**, 8079, https://doi.org/10.1029/2001JD001188.

——, and Coauthors, 2012: Recent developments on the South American monsoon system. *Int. J. Climatol.*, **32**, 1–21, https://doi.org/10.1002/joc.2254.

Miller, A., D. Cayan, T. Barnett, N. Graham, and J. Oberhuber, 1994: The 1976-77 climate shift of the Pacific Ocean. *Oceanography*, **7**, 21–26, https://doi.org/10.5670/oceanog.1994.11.

Min, S. K., X. Zhang, F. W. Zwiers, and G. C. Hegerl, 2011: Human contribution to more-intense precipitation extremes. *Nature*, **470**, 378–381, https://doi.org/10.1038/nature09763.

Montini, T. L., C. Jones, and L. M. V. Carvalho, 2019: The South American low-level jet: A new climatology, variability, and changes. *J. Geophys. Res. Atmos.*, **124**, 1200–1218, https://doi.org/10.1029/2018JD029634.

Morales Rodriguez, C. A., R. P. da Rocha, and R. Bombardi, 2010: On the development of summer thunderstorms in the city of São Paulo: Mean meteorological characteristics and pollution effect. *Atmos. Res.*, **96**, 477–488, https://doi.org/10.1016/j.atmosres.2010.02.007.

National Agency of Electric Energy, 2019: Usinas hidrelétricas. Capacidade de Geração do Brasil, BIG—Banco de Informações de Geração, ANEEL, accessed 25 June 2019, http://www2.aneel.gov.br/aplicacoes/capacidadebrasil/capacidadebrasil.cfm.

Pedron, I. T., M. A. F. Silva Dias, S. de Paula Dias, L. M. V. Carvalho, and E. D. Freitas, 2017: Trends and variability in extremes of precipitation in Curitiba—Southern Brazil. *Int. J. Climatol.*, **37**, 1250–1264, https://doi.org/10.1002/joc.4773.

Peterson, T. C., C. Folland, G. Gruza, W. Hogg, A. Mokssit, and N. Plummer, 2001: Report on the activities of the working group on climate change detection and related rapporteurs 1998–2001. WCDMP-47, WMO/TD-1071, 143 pp.

Rao, V. B., I. F. A. Cavalcanti, and K. Hada, 1996: Annual variation of rainfall over Brazil and water vapor characteristics over South America. *J. Geophys. Res.*, **101**, 26 539–26 551, https://doi.org/10.1029/96JD01936.

Reboita, M. S., N. Krusche, T. Ambrizzi, and R. P. da Rocha, 2017: Entendendo o tempo e o clima na América do Sul (Understanding the weather and climate in South America). *Terrae Didat.*, **8**, 34, https://doi.org/10.20396/TD.V8I1.8637425.

Salio, P., M. Nicolini, and E. J. Zipser, 2007: Mesoscale convective systems over southeastern South America and their relationship with the South American low-level jet. *Mon. Wea. Rev.*, **135**, 1290–1309, https://doi.org/10.1175/MWR3305.1.

Satyamurty, P., and L. F. De Mattos, 1989: Climatological lower tropospheric frontogenesis in the midlatitudes due to horizontal deformation and divergence. *Mon. Wea. Rev.*, **117**, 1355–1364, https://doi.org/10.1175/1520-0493(1989)117<1355:CLTFIT>2.0.CO;2.

Sayemuzzaman, M., and M. K. Jha, 2014: Seasonal and annual precipitation time series trend analysis in North Carolina, United States. *Atmos. Res.*, **137**, 183–194, https://doi.org/10.1016/j.atmosres.2013.10.012.

Shi, H., T. Li, J. Wei, W. Fu, and G. Wang, 2016: Spatial and temporal characteristics of precipitation over the Three-River Headwaters region during 1961–2014. *J. Hydrol. Reg. Stud.*, **6**, 52–65, https://doi.org/10.1016/j.ejrh.2016.03.001.

Shifteh Some'e, B., A. Ezani, and H. Tabari, 2012: Spatiotemporal trends and change point of precipitation in Iran. *Atmos. Res.*, **113**, 1–12, https://doi.org/10.1016/j.atmosres.2012.04.016.

Silva Dias, M. A. F., P. L. Vidale, and C. M. R. Blanco, 1995: Case study and numerical simulation of the summer regional circulation in São Paulo, Brazil. *Bound.-Layer Meteor.*, **74**, 371–388, https://doi.org/10.1007/BF00712378.

——, J. Dias, L. M. V. Carvalho, E. D. Freitas, and P. L. Silva Dias, 2013: Changes in extreme daily rainfall for São Paulo, Brazil. *Climatic Change*, **116**, 705–722, https://doi.org/10.1007/s10584-012-0504-7.

Tedeschi, R. G., I. F. A. Cavalcanti, and A. M. Grimm, 2013: Influences of two types of ENSO on South American precipitation. *Int. J. Climatol.*, **33**, 1382–1400, https://doi.org/10.1002/joc.3519.

Teixeira, M. da S., and P. Satyamurty, 2011: Trends in the frequency of intense precipitation events in southern and southeastern Brazil during 1960–2004. *J. Climate*, **24**, 1913–1921, https://doi.org/10.1175/2011JCLI3511.1.

Trenberth, K. E., 2011: Changes in precipitation with climate change. *Climate Res.*, **47**, 123–138, https://doi.org/10.3354/cr00953.

Velasco, I., and J. M. Fritsch, 1987: Mesoscale convective complexes in the Americas. *J. Geophys. Res.*, **92**, 9591–9613, https://doi.org/10.1029/JD092iD08p09591.

Yu, M., and Y. Liu, 2015: The possible impact of urbanization on a heavy rainfall event in Beijing. *J. Geophys. Res. Atmos.*, **120**, 8132–8143, https://doi.org/10.1002/2015JD023336.

Yue, S., P. Pilon, B. Phinney, and G. Cavadias, 2002: The influence of autocorrelation on the ability to detect trend in hydrological series. *Hydrol. Process.*, **16**, 1807–1829, https://doi.org/10.1002/HYP.1095.

Zamboni, L., C. R. Mechoso, and F. Kucharski, 2010: Relationships between upper-level circulation over South America and rainfall over southeastern South America: A physical base for seasonal predictions. *J. Climate*, **23**, 3300–3315, https://doi.org/10.1175/2009JCLI3129.1.

Zandonadi, L., F. Acquaotta, S. Fratianni, and J. A. Zavattini, 2016: Changes in precipitation extremes in Brazil (Paraná River basin). *Theor. Appl. Climatol.*, **123**, 741–756, https://doi.org/10.1007/s00704-015-1391-4.

Zilli, M. T., L. M. V. Carvalho, B. Liebmann, and M. A. Silva Dias, 2017: A comprehensive analysis of trends in extreme precipitation over southeastern coast of Brazil. *Int. J. Climatol.*, **37**, 2269–2279, https://doi.org/10.1002/joc.4840.

Paper II

II. **Abou Rafee, S.A.,** Uvo, C.B., Martins, J.A., Domingues, L.M., Rudke, A.P., Fujita, T., Freitas, E.D., 2019. Large-scale hydrological modelling of the Upper Paraná River Basin. Water (Switzerland). https://doi.org/10.3390/w11050882

water

MDPI

Article

Large-Scale Hydrological Modelling of the Upper Paraná River Basin

Sameh A. Abou Rafee [1,2,*], Cintia B. Uvo [2], Jorge A. Martins [3], Leonardo M. Domingues [1], Anderson P. Rudke [3], Thais Fujita [3] and Edmilson D. Freitas [1]

1 Department of Atmospheric Sciences, University of São Paulo, São Paulo 01000, Brazil; leomdomingues@gmail.com (L.M.D.); edmilson.freitas@iag.usp.br (E.D.F.)
2 Division of Water Resources Engineering, Lund University, 22100 Lund, Sweden; cintia.uvo@tvrl.lth.se
3 Federal University of Technology, Parana, Londrina 86000, Brazil; jmartins@utfpr.edu.br (J.A.M.); rudke@alunos.utfpr.edu.br (A.P.R.); fujita.thais@gmail.com (T.F.)
* Correspondence: samehabou@gmail.com

Received: 16 March 2019; Accepted: 22 April 2019; Published: 26 April 2019

Abstract: The Upper Paraná River Basin (UPRB) has undergone many rapid land use changes in recent decades, due to accelerating population growth. Thus, the prediction of water resources has crucial importance in improving planning and sustainable management. This paper presents a large-scale hydrological modelling of the UPRB, using the Soil and Water Assessment Tool (SWAT) model. The model was calibrated and validated for 78 outlets, over a 32-year simulation period between 1984 and 2015. The results and the comparison between observed and simulated values showed that after the calibration process, most of the outlets performed to a satisfactory level or better in all objective functions analyzed with 86%, 92%, 76%, 88%, and 74% for Percent bias, Coefficient of determination, Nash-Sutcliffe efficiency, Kling-Gupta efficiency, and the Ratio of Standard deviation of observations to root mean square error, respectively. The model output provided in this work could be used in further simulations, such as the evaluation of the impacts of land use change or climate change on river flows of the Upper Paraná Basin.

Keywords: discharge; SWAT model; SWAT-CUP; SUFI-2

1. Introduction

Hydrological models have been used worldwide as a powerful tool for water resources research and management. Many studies have focused on modelling the hydrology of areas that have experienced an increase in the frequency of drought and flood events. Over recent decades, hydrological modelling has contributed to improving the conservation and sustainable use of natural resources, especially through research activities dedicated to mitigating climate change [1,2], land use changes [3,4], and sources of water pollution [5]. However, most such studies are dedicated to small- to medium-sized basins, which produce some difficulty in generalizing the conclusions to large-scale basins. Notably, collecting and organizing a good set of data that describes the physical properties of a small river basins well, is considerably easier than doing the same for a large river basins. The challenge in preparing input data, with high spatial and temporal resolutions, is another factor that prevents hydrological modelling studies from focusing on large-scale river basins. Therefore, only a few studies have been performed for large-scale basins [6].

The Upper Paraná River Basin (UPRB), located in central-southern Brazil, is one of the largest and most socio-economically important basins in South America. It plays a significant role in the Brazilian economy and development, greatly contributing to economic sectors, such as agriculture, livestock, energy, and urban and industrial water supply. In particular, this watershed houses 87 hydropower

plants (see Figure 1) that provide more than 41,000 megawatts (MW) of electricity [7]. The importance of modelling the hydrology of this basin as a whole is evident, but most of the studies discussing the hydrology of the basin, are local ones that focus on sub-basins and do not represent the whole basin [8,9]. Very few examples of the modelling of UPRB are found [10]. Those are either, not detailed or focused on a specific subject, such as hydro-electricity production.

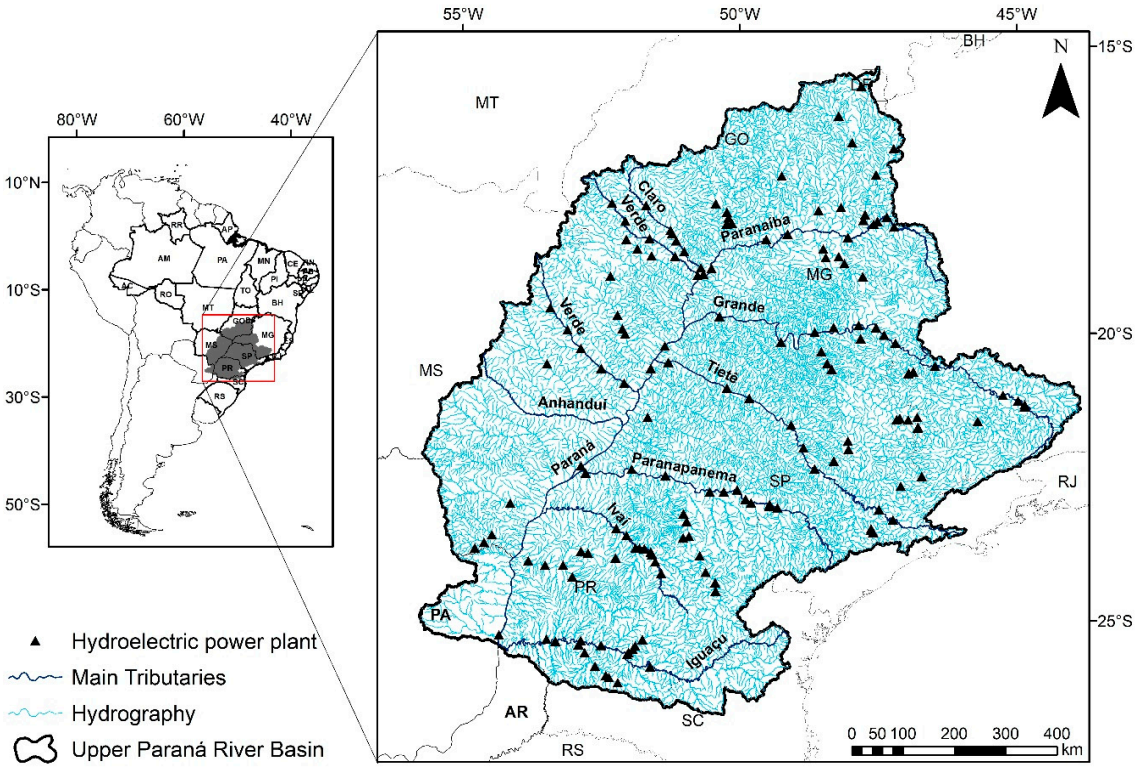

Figure 1. Geographic location of the study area. Blue lines show the hydrography and main tributaries, and black triangles show the hydroelectric power plants (installed or planned) over the Upper Paraná River Basin (UPRB).

During the 20th century, rapid population growth and pronounced urbanization have led to a significant land use change in the UPRB. For instance, Paraná and São Paulo states, located in the east of the basin, have lost more than 70% of their primitive forest, while the original vegetation in the western part of the basin, was maintained until the 1970s, when the development of agro-business increased. Deforestation occurred for different objectives, but in most cases, forests were replaced by agriculture and pasture [11].

The different land covers and the intense internal dynamics of the land uses may have affected the regional hydrology in different ways, since some areas of the basin have increased, while other areas have decreased their stream flows [12,13]. Therefore, studies on the simulation of water resources in the UPRB have great importance in offering subsidies for managers and policy makers. A better understanding of the UPRB hydrology could improve the planning and sustainable management of the wide range of water uses in the basin.

Considering the importance of the UPRB and its significant changes in stream flow, since the mid-1900s, the primary goal of this work was to use the Soil and Water Assessment Tool (SWAT) model to estimate the discharge in monthly time steps at a highest spatial resolution allowed by the simulation system. To achieve this goal, this work pursued the following main objectives: (a) set up the SWAT model with the most appropriate dataset available; (b) calibrate and validate the main outlets of UPRB, including uncertainty assessment; (c) evaluate the performance of the model using several objective functions; and (d) address the spatial and temporal analysis of discharge over the UPRB.

The results of this work address the variability of the discharge at the basin as a whole in the spatial and temporal dimensions. Additionally, the approaches and strategies used for calibration might serve as standards for future simulations of large river basins. Furthermore, this work creates a basis for future studies on the UPRB to assess the potential impacts on hydrological processes and water quality, allowing the simulation of diverse scenarios such as climate and land use changes.

The remainder of this paper is structured as follows. First, it gives a brief description of the study area, the hydrological model used for simulation, the input data, and the setup performed to build a project for UPRB. Then, the strategies for calibration, sensitivity and uncertainty assessment are described in the following three sub-sections: SUFI-2 and parameter calibration, objective function, and modelling protocol. Finally, the results are presented and discussed and are followed by conclusions.

2. Materials and Methods

2.1. Study Area

The UPRB is located in the central-southern region of Brazil (Figure 1), with an area of 900,480 km^2, and drains rivers in six Brazilian states: São Paulo (23.5%), Paraná (20.4%), Mato Grosso do Sul (18.9%), Minas Gerais (17.6%), Goiás (15.7%), Santa Catarina (1.2%), and the Federal District (0.4%), as well as a small portion of Paraguay (2.3%). The Paraná river is the second largest river in South America. From the confluence of the Paranaiba and Grande rivers, the Paraná river flows southward for 738 km until it reaches the border between Brazil, Argentina, and Paraguay.

Before reaching the border between Brazil and Paraguay, the Paraná river receives large and socio-economically important tributaries on the east side of the basin, such as the Tietê and the Paranapanema rivers, in São Paulo state. In addition, the west side of the Paraná river crosses the Maracaju mountain range, in Mato Grosso do Sul, which acts as a natural barrier separating the Pantanal wetlands and leads to the formation of many rivers, shorter than those in the east side of the basin.

The UPRB has a unique geographical profile, with a number of hydropower plants close to the largest urban and industrial areas, which are large consumers of electricity. The basin has an estimated population of over 65 million inhabitants, of whom more than 93% live in urban areas [14]. According to the Brazilian National Water Agency (ANA) [15], this region has the highest demand for water resources in Brazil, equivalent to 736 m^3 s^{-1}, mostly used for agricultural (42%) and industrial (27%) activities.

The UPRB is embedded within the center-east portion of South America, with an approximately oval shape, and with the major axis in the north-south direction. The basin is characterized by different morphologies that range from Atlantic Plateau (elevation higher than 2000 m) to the Paraná River Valley (between 350 and 100 m). It is a sedimentary and igneous basin, with the volcanic rocks of the Serra Geral formation overlaid by sedimentary rocks, mostly located in the central and western region of the basin [16–18]. Sedimentary areas are also found in the contours of the basin, in their higher hills. This type of formation, combined with volcanic rocks, predominates in most of the tributaries and progresses up to near the main course of the UPRB. Most areas of basaltic rocks are formed by high fertility soils. Until a century ago, such areas were covered by a dense forest, predominantly with medium-to-large tree. This forest cover was almost completely removed within the basin and the exposed land was replaced by intensive agricultural exploitation.

The basin has great spatial variability in its precipitation pattern as it covers different climatic areas. Climatologically, the northern part of the UPRB is influenced by the South American Monsoon System [19,20], characterized by wet summers and dry winters. Precipitation during the summer may exceed 800 mm, while during winter it can be as low as 30 mm. In the southern parts of the basin, precipitation is spread out throughout the year and is associated with the Intertropical Convergence Zone (ITCZ), cold fronts, and the Mesoscale Convective Complex (MCC), mainly during the spring and summer [21,22].

2.2. SWAT Model

The hydrological simulations of UPRB were performed using the 2012 version of the Soil and Water Assessment Tool (SWAT) model with an ArcGIS interface. SWAT is an open source, semi-distributed, and physical model developed by the Agricultural Research Service of the United States Department of Agriculture (ARS-USDA). This model can be used to design analyses related to physical processes, both in small and large watersheds, and can be executed in a continuous simulation in monthly or daily time steps. It is widely used to assess impacts on hydrological processes, water quality (e.g., transport of nutrients and pesticides), as well as climate and land use change scenarios [23–25]. Based on the topography, a basin is discretized into sub-basins, which are connected by a stream network. To assess the differences in land cover and the heterogeneous soil in a watershed, each sub-basin is further discretized into hydrologic response units (HRUs), according to unique combinations of land use, soil type, and slopes. For each HRU, simulated hydrological processes, such as surface runoff and evapotranspiration, are generated separately, and then routed through the river network to the outlet of the basin. For further details on the SWAT model, the reader is referred to Neitsch et al. [26].

2.2.1. Data Description and Model Set Up

Different input data are required to build a hydrological project with SWAT, including meteorological, hydrologic, and physical variables. The data used in this work was prepared for the whole simulation period (which includes the warming up, calibration, and validation periods), from January 1979 to December 2015. The first five years (1979–1983) were used for warming up, the following 21 years (1984–2004) constituted the calibration period, and the last 11 years (2005–2015) the validation period.

Figure 2 shows the spatial distribution of the collected data used in this work. A brief description of these data follows, as well as the setup of the SWAT project.

Meteorological Data

Due to the low spatial-temporal resolution of observed data pertaining to temperature, solar radiation, relative humidity, and wind speed, this work uses gridded daily meteorological data obtained from the National Center for Environmental Prediction—Climate Forecast System Reanalysis (CFSR), with global atmosphere spatial resolution of around 38 km. The data for total daily precipitation was provided by the Brazilian National Water Agency (ANA), which made available a collection of data from 149 institutions. As shown in Figure 2a, the study area has a good spatial density of stations, with 2494 rain gauges within the basin, with the majority located in the eastern side of the UPRB. The rain gauges have different data availability during the simulation period, that may range from only a few years of data, up to the total period of simulation with no missing data. About half of the rain gauges (47%) contain less than 20% missing data.

The precipitation data was thoroughly controlled before use. First, quality checks, such as double records, typos, and the location of stations were evaluated. Routines to assess such inconsistencies were developed in R programming language. After that, the inverse distance weighted (IDW) method [27] was used to interpolate the daily precipitation records over the basin to a resolution of 0.1 degree. IDW has been used in several studies for interpolation of precipitation over hydrological basins and provided satisfactory results [28].

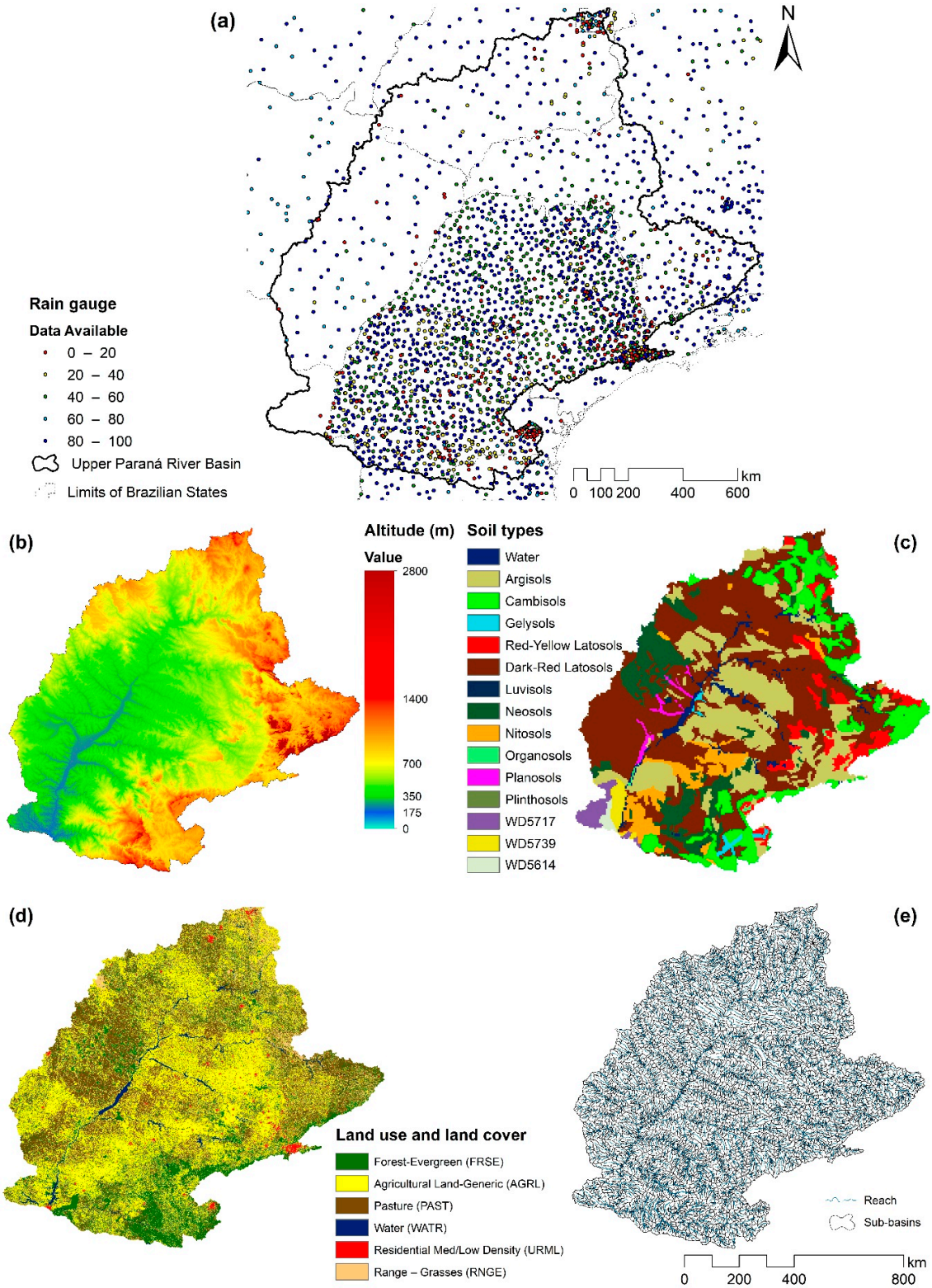

Figure 2. Maps of the (**a**) spatial distribution of precipitation stations, (**b**) topography, (**c**) soil types, (**d**) land use and land cover, and (**e**) discretization and reaches of the UPRB.

Topography

The topographic features (Figure 2b) were characterized according to a Digital Elevation Model (DEM) map at 30-m resolution obtained from the Shuttle Radar Topography Mission, available from

http://srtm.csi.cgiar.org/srtmdata/. Based on this model the digital river network, as well as the sub-basins, were generated.

Soil Data

The soil map was elaborated from the information provided by the Brazilian Agriculture Research Corporation (EMBRAPA, 2011) at a scale of 1:5,000,000. For the Paraguayan portion of the basin, the Harmonized World Soil Database (HWSD, 2011) with spatial resolution of 1 km was used. The initial classification considered 25 classes of soil types. In this study, the characteristics of oligotropic, mesotropic, eutropic, and dystropic soils were grouped in a single class, resulting in 15 classes. The Dark-Red latosols and argisols are predominant in the basin (Figure 2c), representing 43.9% and 20% of the area. The properties of each soil class were collected from a diverse set of documents that used the SWAT model in Brazilian basins [29–31]. The list of soil parameter values adopted in the simulation can be found in the Supplementary Materials (Table S1).

Land Use and Land Cover Data

Land use and land cover data were obtained from the Rudke [32] classification. The original classification of 10 different categories was reclassified into six dominant classes according to the SWAT land use classification (Figure 2d). As a result, the Agriculture Land-Generic (AGRL) and Pasture (PAST) are the main classes and comprise 46.1%, and 25.6% of the total area, respectively. They cover mainly the western portion of the basin. The next two major classes are Forest-Evergreen (FRSE) and Range-Grasses (RNGE), encompassing 20.2%, and 5% of the basin, respectively. The remaining area of the basin is covered by Water (WATR), which covers 2%, and Residential Med/Low Density (URML), 1.1%. Most of the urban areas are concentrated in the headwaters of the main tributaries of the basin, such as in the upper Tietê and Iguaçu rivers.

Model Set Up

Based on the previously described data, the UPRB was discretized into 5,187 sub-watersheds, using a threshold drainage area of 100 km^2, with an average size of about 173 km^2 (see Figure 2e). For most applications, the default threshold values used to define HRU's are 20%, 10%, and 20%, for land use, soil type, and slope, respectively [33]. However, in order to allow the assessment of land use changes in future research, further details are needed. Hence, the resulting sub-watershed was defined by the combinations of land use, soil types, and slope, using a threshold of 5%, 10%, and 20%, respectively. As a result, 44,635 HRU's were generated. In addition, five categories of slope were defined as this is the maximum number of categories possible. They are flat (0–3%), smooth rolling (3–8%), wavy (8–20%), strong wavy (20–40%), and hilly (>45%), according to EMBRAPA [34] classification. The potential evapotranspiration (PET) was calculated using the Penman-Monteith method [35] and the surface runoff within the model with the Soil Conversation Service's Curve Number method [36].

River Discharge Data

Monthly river discharge data were organized based on calibration period (1984–2004) and validation period (2005–2015). The data comprise both natural streamflow data, provided by theNational Water Agency (ANA), and naturalized discharges, obtained from the National Electrical System Operator (ONS). Only discharge series with at least 32 years of daily records and less than 20% of missing data were selected. For the western side of the basin, however, a threshold of 40% of missing data was used due to the low quality of the data available.

In order to facilitate the discussion of the results, the study area was divided into six main sub-basins: I—Paranaíba, II—Grande, III—Tietê, IV—Paraná, V—Paranapanema, and VI—Iguaçu (Figure 3). In addition, all outlets with small affluent rivers or representatives of individual sub-basins

were clustered. Finally, 78 discharge outlets were defined, most of them located in the Paraná (20), Grande (13), Paranapanema (13), and Paranaiba (13) sub-basins (Figure 3).

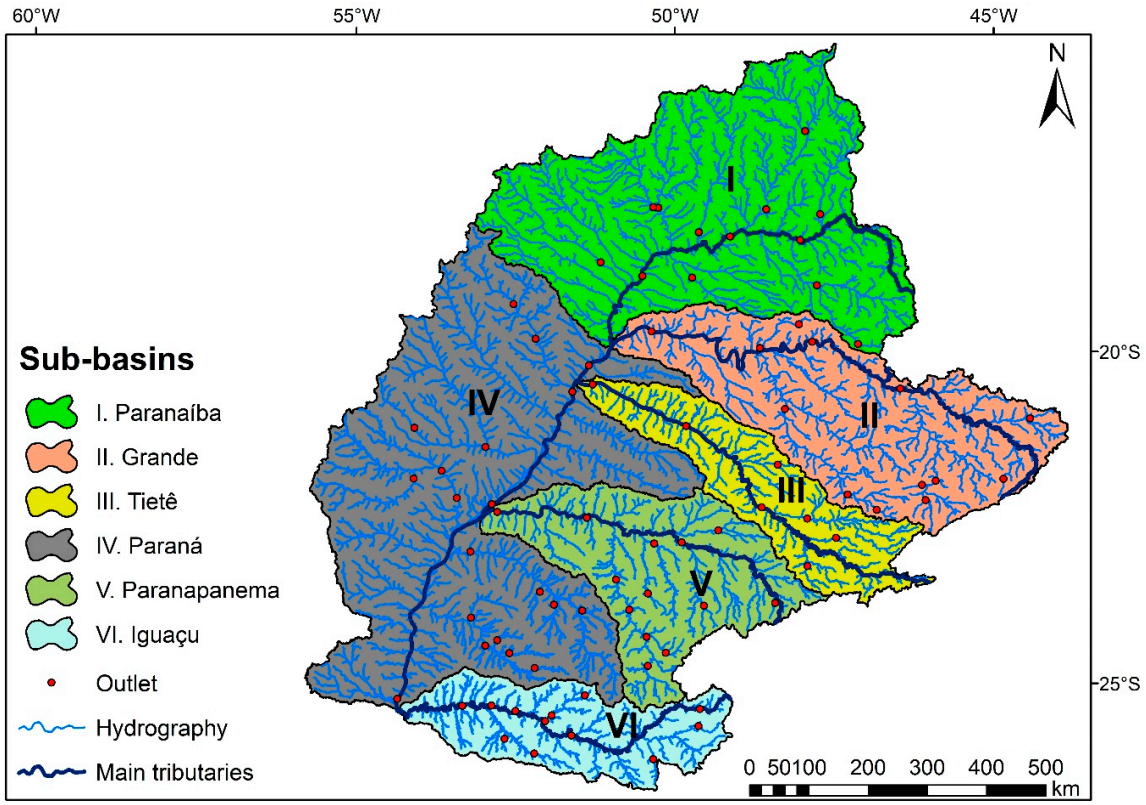

Figure 3. UPRB with its sub-basins showing the spatial distribution of fluviometric stations.

2.3. SUFI-2 and Parameters Calibration

Calibration, sensitivity, and uncertainty analysis were performed by the Sequential Uncertainty Fitting (SUFI-2) algorithm proposed by Abbaspour et al. [37], using SWAT-CUP version 5.1.6.2 [38]. Moreover, to optimize the model execution, the parallel processing module [39] was used. SUFI-2 was developed by considering the uncertainties of parameter ranges, which are sampled through Latin hypercube sampling. The main aim of this algorithm is to estimate the most observed variables within the 95 PPU band, which is quantified at the 2.5% and 97.5% of the cumulative distribution. SUFI-2 considers two indices to evaluate the performance of the calibration: The p-factor, calculated through the percentage of observed variable bracketed by the 95 PPU, which varies (between 0 for useless simulation and 1 for perfect simulation); and the r-factor, calculated through the ratio of the average width of the 95 PPU band (Prediction Uncertainty) and the standard deviation of the observed variable.

SWAT contains a large number of parameters that describe the processes in the soil-plant-atmosphere interface. To calibrate the discharge series, a list of 20 parameters related to stream flow was selected as shown in Table 1. The choice of parameters, as well as their ranges, was based on previous research [6,40–42]. Parameters that govern the soil, SCS runoff curve number, soil available water storage capacity, saturated hydraulic conductivity, and soil evaporation compensation factor were used. The selected parameters that govern groundwater were: Threshold depth of water in the shallow aquifer for return flow, groundwater delay, threshold depth of water in the shallow aquifer for "revap", deep aquifer percolation fraction, groundwater "revap" coefficient, base flow alpha factor, and base flow alpha factor for bank storage. For the channel, effective hydraulic conductivity in channel and Manning´s value for the main channel were chosen. For the parameters governing land use and land cover factor, plant uptake compensation factor and maximum canopy storage were selected.

Finally, for the parameters governing the sub-basin, surface runoff lag time, average slope length, lateral flow travel time, and average slope steepness were used.

Table 1. List of sensitive parameters selected for calibration.

Parameter *	Description	Initial Range	
		Min	Max
From Soil			
r_CN2.mgt	SCS runoff curve number	−0.4	0.4
r_SOL_AWC.sol	Soil available water storage Capacity (mm H_2O mm $soil^{-1}$)	−0.4	0.4
r_SOL_K.sol	Saturated hydraulic conductivity (mm h^{-1})	−0.8	0.8
r_ESCO.hru	Soil evaporation compensation factor	−0.4	0.4
r_OV_N.hru	Manning´s n value for overland flow	−0.4	0.4
Groundwater			
r_GWQMIN.gw	Threshold depth of water in the shallow aquifer for return flow (mm)	−0.8	0.8
r_GW_DELAY.gw	Groundwater delay (days)	−0.8	0.8
r_REVAPMN.gw	Threshold depth of water in the shallow aquifer for "revap" (mm)	−0.5	0.5
r_RCHRG_DP.gw	Deep aquifer percolation fraction	−0.5	0.5
r_GW_REVAP.gw	Groundwater "revap" coefficient	−0.4	0.4
r_ALPHA_BF.gw	Base flow alpha factor (days)	−0.8	0.8
r_ALPHA_BNK.rte	Base flow alpha factor for bank storage	−0.5	0.5
Channel			
r_CH_K2.rte	Effective hydraulic conductivity in channel (mm h^{-1})	−0.8	0.8
r_CH_N2.rte	Manning´s value for main channel	−0.8	0.8
Land use and land cover factor			
r_EPCO.bsn	Plant uptake compensation factor	−0.5	0.5
r_CANMX.hru	Maximum canopy storage (mm H_2O)	−0.4	0.4
Sub-basin			
r_SURLAG.bsn	Surface runoff lag time	−0.5	0.5
r_SLSUBBSN.hru	Average slope length (m)	−0.4	0.5
r_ LAT_TTIME.hru	Lateral flow travel time (days)	−0.5	0.5
r_HRU_SLP.hru	Average slope steepness (m m^{-1})	−0.4	0.4

* "r_" refers to a relative change in the parameters where the current values is multiplied by 1 plus a factor from the given parameter range.

2.4. Objective Function

To assess the performance of the model, it is recommended that the simulation should be evaluated by several statistical indices [23]. Five indices were chosen so that they, together, can provide a general overview of the quality of the simulations (Table 2). The percent bias (PBIAS) [43] provides a measure of how consistently simulated values are higher or lower than observed ones. The coefficient of determination (R^2) provides the proportion of the variance of the original data that is explained by the simulated values. Nash-Sutcliffe efficiency (NSE) [44] measures whether an observed value is better estimated by the model result or by the average of observed values. R^2 generally enhances the fitting of the model to lower values, while NSE tends to emphasize the fitting of high values. The Kling-Gupta efficiency (KGE) [45] intends to be a more general index that compares the variability of the observed and estimated values by including information about the correlation between them and their standard deviations, as well as any bias present, which is expressed by the relation between the mean values. Finally, the ratio between the standard deviation of the observations and the root mean square error (RSR) [46] measures how large the standard error is compared to the variability of the original data.

Table 2 presents the equations of the objective functions used in this work and their model performance rating based on the threshold suggested by Moriasi et al. [46] and Thiemig et al. [47] for monthly discharge. These works classified the simulation into four performance ratings: Uunsatisfactory, satisfactory, good, and very good.

Table 2. Objective functions and their model performance rating used for outlets evaluation.

Objective Function	Equation *	Performance Rating			
		Very Good	**Good**	**Satisfactory**	**Unsatisfactory**
Percent bias (PBIAS)	$\mathrm{PBIAS} = 100 \cdot \left[\frac{\sum_i (Q_{i,o} - Q_{i,s})}{\sum_{i=1}^{n} Q_{i,o}}\right]$	PBIAS < ±10	±10 ≤ PBIAS < ±15	±15 ≤ PBIAS < ±25	PBIAS ≥ ±25
Coefficient of determination (R^2)	$R^2 = \frac{\left[\sum_i \left(Q_{i,o} - \overline{Q_o}\right)\left(Q_{i,s} - \overline{Q_s}\right)\right]^2}{\sum_i \left(Q_{i,o} - \overline{Q_o}\right)^2 \sum_i \left(Q_{i,s} - \overline{Q_s}\right)^2}$	$0.75 < R^2 \leq 1$	$0.65 < R^2 \leq 0.75$	$0.5 < R^2 \leq 0.65$	$R^2 \leq 0.5$
Nash-Sutcliffe efficiency (NSE)	$\mathrm{NSE} = 1 - \left[\frac{\sum_{i=1}^{n} (Q_{i,o} - Q_{i,s})^2}{\sum_{i=1}^{n} \left(Q_{i,o} - \overline{Q_o}\right)^2}\right]$	0.75 < NSE ≤ 1	0.65 < NSE ≤ 0.75	0.5 < NSE ≤ 0.65	NSE ≤ 0.5
Kling-Gupta efficiency (KGE)	$\mathrm{KGE} = 1 - \sqrt{(R-1)^2 + (\alpha - 1)^2 + (\beta - 1)^2}$	0.9 ≤ KGE ≤ 1	0.75 ≤ KGE ≤ 0.9	0.5 ≤ KGE < 0.75	KGE < 0.5
Ratio of standard deviation of observations to root mean square error (RSR)	$\mathrm{RSR} = \frac{\mathrm{RMSE}}{\mathrm{STDEV_o}} = \frac{\left[\sqrt{\sum_{i=1}^{n} (Q_{i,o} - Q_{i,s})^2}\right]}{\left[\sqrt{\sum_{i=1}^{n} \left(Q_{i,o} - \overline{Q_o}\right)^2}\right]}$	0 ≤ RSR ≤ 0.5	0.5 < RSR ≤ 0.6	0.6 < RSR ≤ 0.7	RSR > 0.7

* R: Correlation coefficient between observed and simulated data; $Q_{i,o}$ and $Q_{i,s}$: Observed and simulated values, respectively; $\overline{Q_o}$ and $\overline{Q_s}$: average observed and simulated values, respectively; n: Total number of observations. $\alpha = \frac{\sigma_s}{\sigma_o}$: σ_s and σ_o are the standard deviation of the simulated and observed data, respectively; and $\beta = \frac{\overline{Q_o}}{\overline{Q_s}}$.

2.5. Modelling Protocol

The criteria and the procedures used for the calibration and validation processes are summarized as follows:

I. In order to run the simulation with parallel processing, due to memory limitations as a result of the project size, the basin area was divided into 9 watersheds for calibration and the fitted values in each sub-basin were used for the initial project.
II. The geographic position of each outlet was verified. According to previous modelling studies [6,48], one of the main calibration problems is the incorrect position of the outlets.
III. A multi-objective calibration, which consists of simultaneous multi-site calibration from upstream to downstream outlets, was performed. This technique was recommended by Leta et al. [49] for a heterogeneous basin and presented better results compared to other methods such as single-site calibration (SSC).
IV. The discharge outlets which performed satisfactory or better in all objective functions that are presented in Table 2 were not considered in the calibration process.
V. The initial parameter ranges followed the calibration protocol presented by Abbaspour et al. [48] for large-scale basins. For example, if the simulation presented base flow too low (high), the GWQMN, GW_REVAP, and REVAMPM parameters should increase (decrease). Therefore, before each calibration, the temporal evolution of the discharge simulation was evaluated as to whether it underestimated or overestimated the observation.
VI. SUFI-2 provides several objective functions for calibration. The objective function selected in the calibration process was NSE. This index has been used in several studies and provided satisfactory results [50].
VII. Once the sub-project was built for the sub-basin, and the ranges of parameters were defined, the model simulations were run between 150 and 500 times, with a maximum of 3 iterations. The numbers of simulations, as well as of iterations, were based on the size of the sub-project and performance of the initial simulation.

3. Results and Discussion

3.1. Sub-Basins Selected for Calibration

As stated in the modelling protocol, the criterion for selecting outlets for calibration was that they had an unsatisfactory rating in at least one of the objective functions presented in Table 2 over the simulation period (1984–2015). Figure 4 illustrates the sub-basins used for calibration (top figure), and examples of the temporal evolution of observed and simulated monthly discharge, as well as the values of performance indicators. Considering the 78 outlets selected, 23 performed satisfactory or better in all objective functions following the classification suggested by Moriasi et al. [46] and Thiemig et al. [47]. Hence, these sub-basins outlets were not used for the calibration process. It is clear that most of the outlets that performed well are located in the southern parts of the basin, especially in the Iguaçu sub-basin (VI) and adjacent areas of the Paraná (IV) and Paranapanema (V) sub-basins. This goodness-of-fit between measured and simulated discharge is mainly due to a large number of precipitation stations that are located over the sub-basins, with a low percentage of missing data (see Figure 2). For instance, in the streamflow of the Upper Iguaçu River (Figure 4b), the model has a good representation of the average, minimum and maximum discharge values. Regarding the statistical indices, SWAT has provided more than satisfactory results with 7.8 (very good), 0.77 (very good), 0.74 (good), 0.86 (good), and 0.51 (good) for PBIAS, R^2, NSE, KGE, and RSR, respectively. The remaining figures of the temporal evolution of the outlets that yielded good performance are available in Figure S1 in the Supplementary Materials.

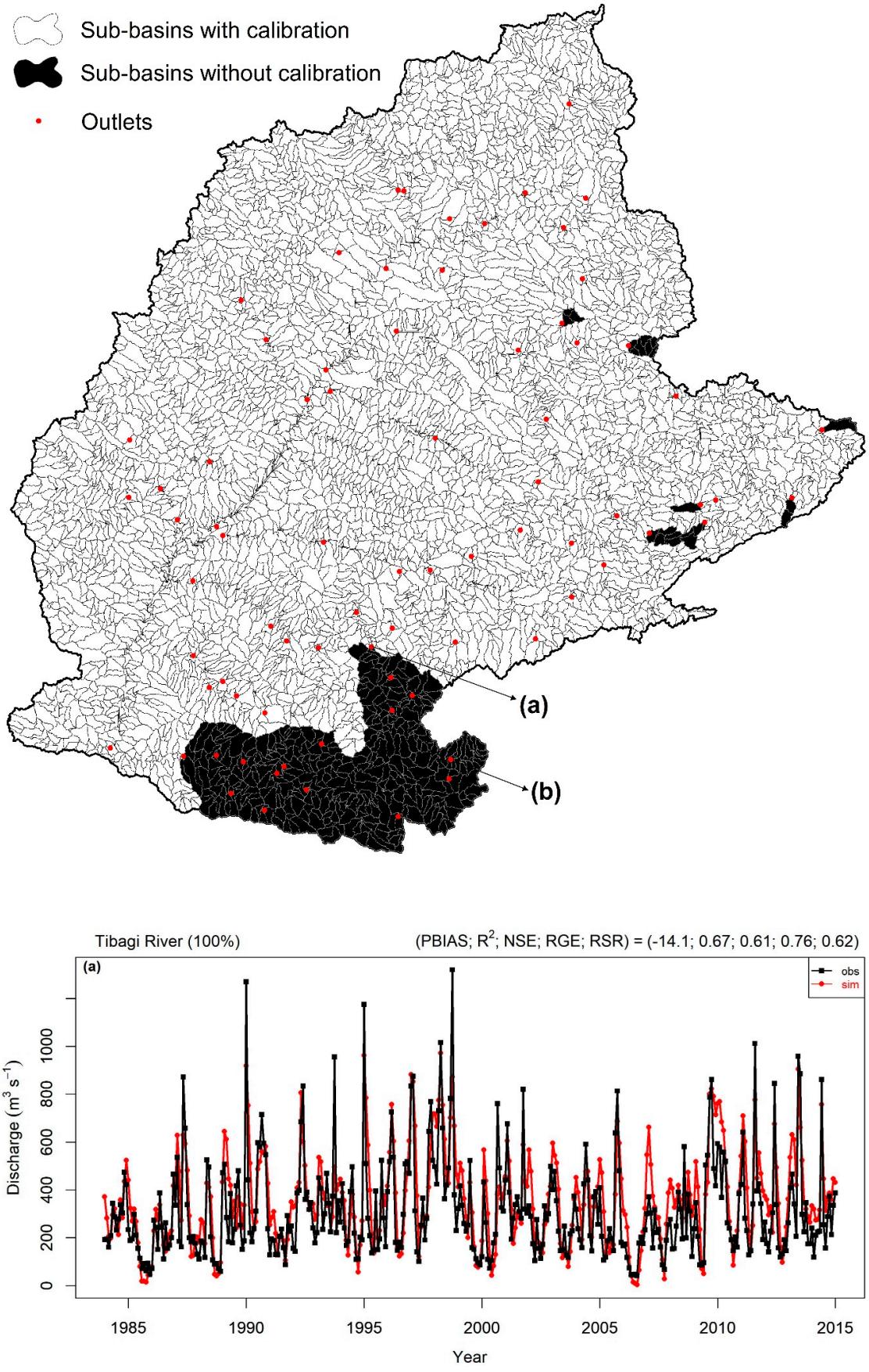

Figure 4. *Cont.*

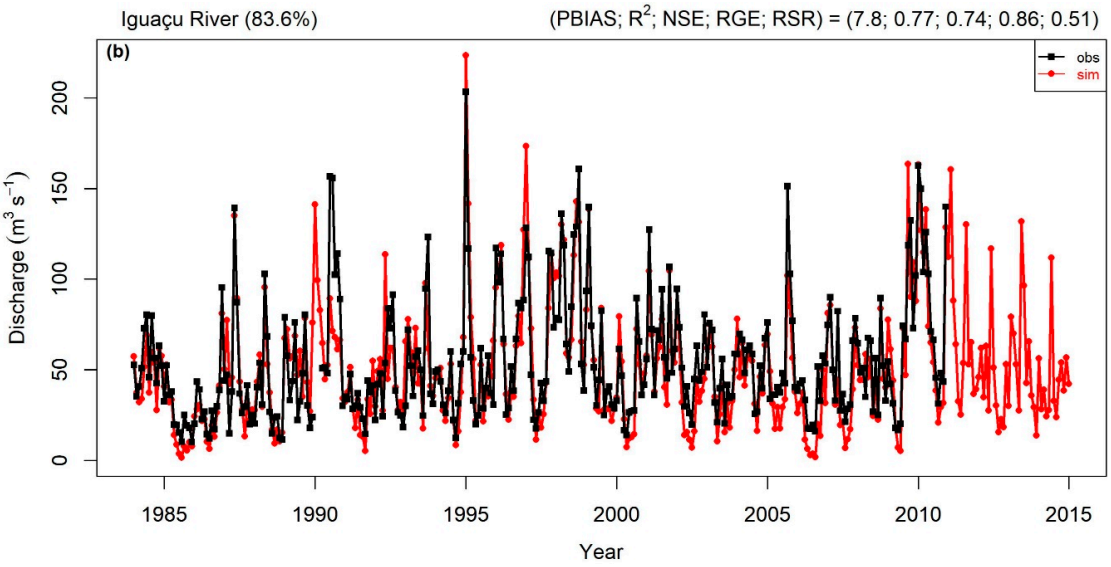

Figure 4. Map showing the sub-basins with and without calibration (on the top), and examples of discharge simulation representing good performance rating.

3.2. Calibration and Validation Performance

Figure 5a–e show the spatial distribution of the values of the objective functions used to evaluate the goodness-of-fit of measured discharge data estimated by SWAT. The performance of the monthly simulations for the calibration (1984–2004) and validation (2005–2015) period ranged from very good to unsatisfactory. It is clear that after the calibration process, the model has a good representation of monthly discharge values for most of the outlets of the UPRB that are located mainly in the Grande (II), Tietê (III), Paranapanema (V), and Iguaçu (VI) sub-basins. On the other hand, Paraná (IV) and Paranaiba (I) were the sub-watersheds that had the highest number of outlets with unsatisfactory simulations. This can be attributed to the low density of rain gauges mainly on the Ivinheima and Sucuriú river basins located on the Paraná sub-basin (IV), on the western side of the basin.

The indices R^2 (Figure 5a) and PBIAS (Figure 5b) present the best hydrological performance for all sub-basins, with 92% and 86% of the outlets showing satisfactory or better performances. For R^2, 61 (78%) of the outlets performed better than satisfactory with values of up to 0.91 over the Paraná and Sapucaí rivers. Similarly, the PBIAS index gave more than half of the outlets (63%) a better than satisfactory rating.

The rating of the KGE index (Figure 5d), which is based on the equal weighting of three different components (correlation, bias, and variability), shows that 88% of the outlets performed better or equally satisfactory. Only 9 outlets produced unsatisfactory simulations. The maximum value obtained for KGE was for the Grande river with 0.87.

Finally, the NSE (Figure 5c) and RSR (Figure 5e) indices were those with the highest number of outlets with unsatisfactory simulation. However, the percentage of satisfactory stations was still high. Considering NSE > 0.5 or RSR < 0.7 for a satisfactory simulation, the model reached this criterion in 76% and 74% of the outlets, respectively. One of the reasons that explain why these indices performed slightly below the others is the low quality of the simulations of the base flow. This limitation is underlined by previous studies that evaluated the hydrological routines of the SWAT model [51]. SWAT simulates two types of aquifers: shallow (unconfined) aquifers, which contribute to return flow to streams within the catchment, and deep (confined) aquifers, which are responsible for the flow outside the basin (amount of water used, for example, for irrigation and water supply) and are considered water sinks in the system [26]. Once the model calculates the groundwater, studies that present difficulties in representing transfers associated with these types of water may present an unsatisfactory performance for the base flow prediction with the SWAT model. For instance, Srivastava et al. [52]

found a NSE value of −0.16 in the predictions of monthly base flows. Similarly to the current study, Wu and Johnston [53] simulating long-term periods found it difficult to simulate dry seasons with the model. In this case study, the SWAT model performed better in simulating wet seasons than dry seasons.

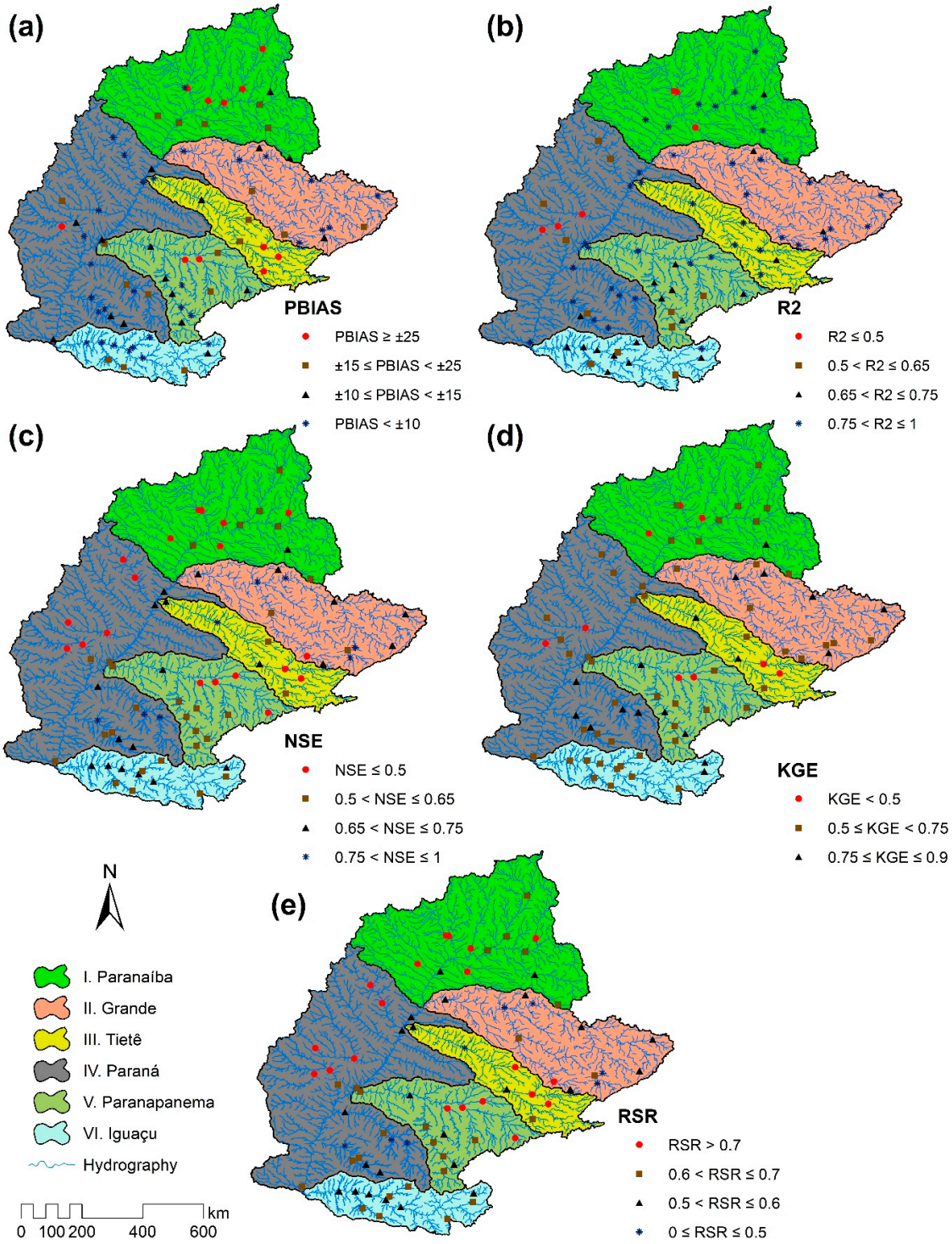

Figure 5. Spatial distribution of the performance rating of the outlets over UPRB. (**a**) PBIAS, (**b**) R^2, (**c**) NSE, (**d**) KGE, and (**e**) RSR.

Figure 6 shows the comparison between the observed data and simulated values for the temporal evolution of the monthly discharge in the calibration and validation (1984–2015) period. The plots show the final outlets of the main rivers of the UPRB. Even though the model did not have a good estimate of the discharge at some outlets in the basin, these did not have a significant effect on the final outlet of the main rivers of the basin, due to their contribution area. This could be explained by the difference among the magnitudes of discharges. For instance, a closer examination of the long-term monthly mean discharge at the final outlets of the rivers shows that the Paranaíba river has a discharge of 2465 m^3 s^{-1}, while the Da Prata river, one of its tributaries has an average discharge about 71 m^3 s^{-1}, which represents 3% of Paranaiba river. The fact that the simulation for the Da Prata river performed an unsatisfactory simulation in R^2, NSE, and RSR indices did not impact the quality of the performance of the Paranaíba. Similar cases occur in other major rivers of the UPRB. Figure S2, in the Supplementary Materials, shows the remaining graphs of the temporal evolution of the discharge on outlets after the calibration process.

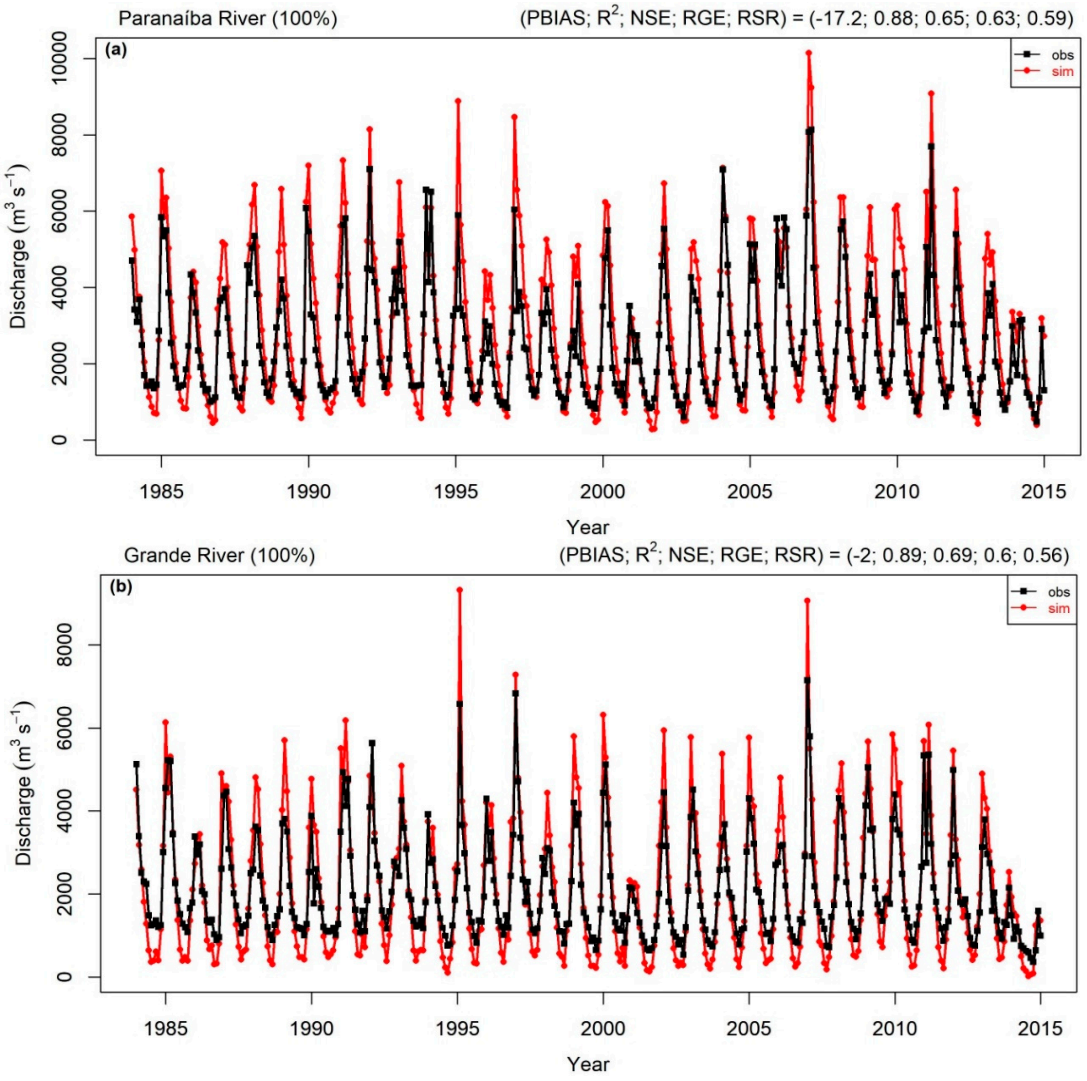

Figure 6. *Cont.*

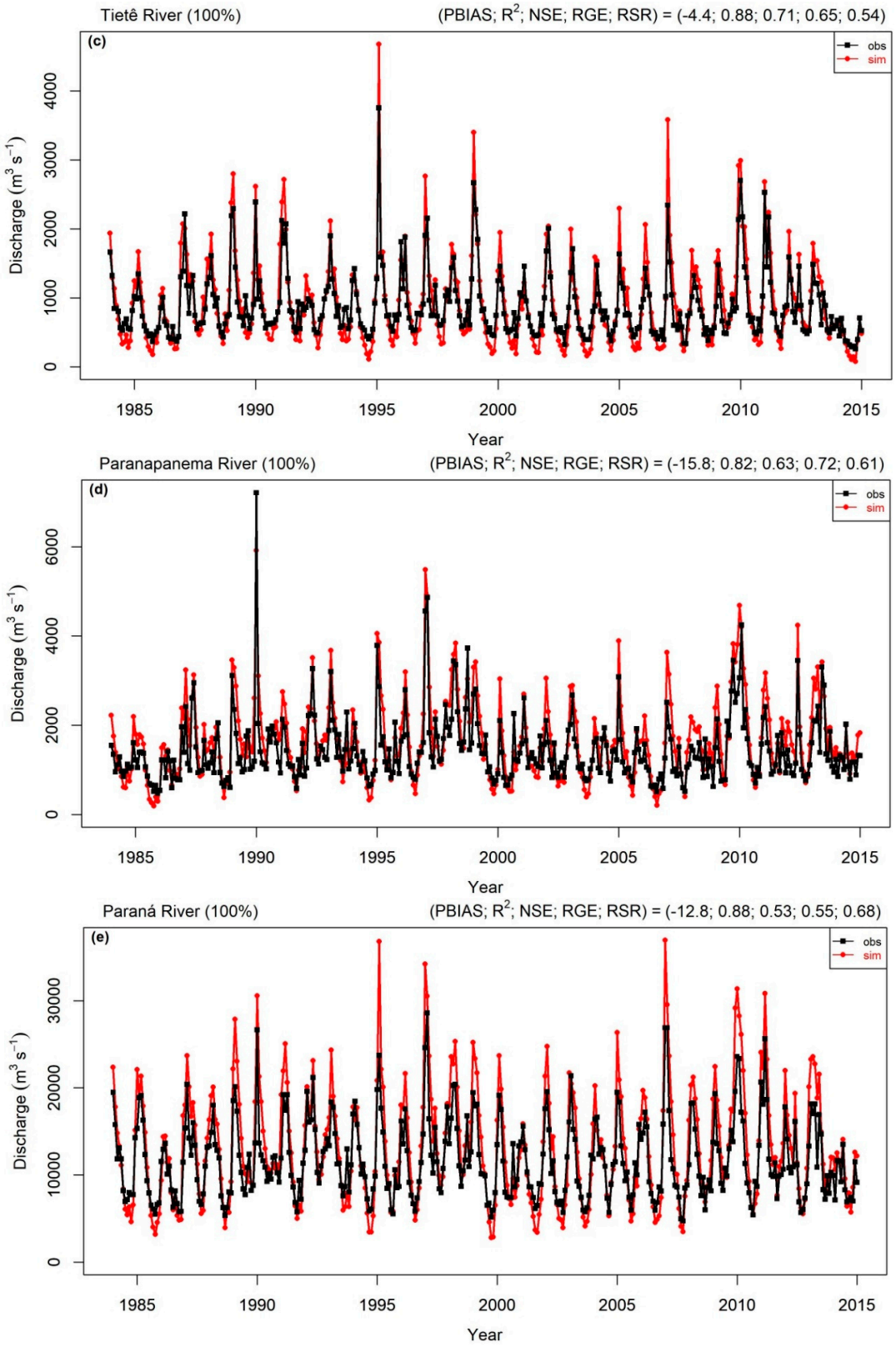

Figure 6. Temporal evolution of the monthly discharge and their statistical indices values from the last outlet of the main rivers of the UPRB. (**a**) Paranaíba; (**b**) Grande; (**c**) Tietê; (**d**) Paraná; and (**e**) Paranapanema.

Table 3 shows the objective function values from the final outlets of the main rivers for the calibration (1984–2004) and validation (2005–2015) periods. PBIAS ranged from satisfactory to very good simulation both for calibration (mean = −7.86) and validation (mean = −15.5) for the five rivers. High values of R^2, greater than 0.80, were found in both calibration and validation results, indicating a very good correlation between the monthly observed and simulated discharges. In the calibration period, the NSE and KGE ranged from 0.56 (satisfactory) to 0.73 (good), and from 0.55 (satisfactory), to 0.77 (good), respectively. In the validation period, the NSE and KGE ranged from to 0.51 (satisfactory) to 0.73 (good), and from 0.55 (satisfactory), to 0.67 (satisfactory), respectively. Regarding the RSR index, values between 0.52 (good) and 0.66 (satisfactory) were found during the calibration process. For the validation process, only the Paraná river represented an unsatisfactory simulation with RSR value of 0.71. The remaining objective functions values of the outlets over the UPRB can be found in the Supplementary Materials (Table S2).

Table 3. Objective function values from the final outlets of the main rivers for the calibration (1984–2004) and validation (2005–2015) periods.

River Name	Calibration	Validation
	PBIAS	
Paranaíba	−16.1	−19.4
Grande	−0.1	−5.8
Tietê	−1.3	−10.7
Paranapanema	−12	−23.1
Paraná	−9.8	−18.5
	R^2	
Paranaíba	0.86	0.9
Grande	0.88	0.92
Tietê	0.88	0.88
Paranapanema	0.81	0.86
Paraná	0.88	0.91
	NSE	
Paranaíba	0.61	0.71
Grande	0.66	0.73
Tietê	0.73	0.66
Paranapanema	0.68	0.53
Paraná	0.56	0.51
	KGE	
Paranaíba	0.6	0.67
Grande	0.59	0.62
Tietê	0.67	0.61
Paranapanema	0.77	0.64
Paraná	0.55	0.55
	RSR	
Paranaíba	0.63	0.53
Grande	0.58	0.52
Tietê	0.52	0.58
Paranapanema	0.56	0.68
Paraná	0.66	0.71

As a whole, the calibration and validation of the outlets of UPRB provided promising results as indicated by acceptable values of statistical indices. The performance is better or comparable to other SWAT applications over Brazilian watersheds. For instance, Creech et al. [54] reported NSE ranging from 0.42 to 0.75 and from 0.42 to 0.77 for monthly discharge calibration and validation periods of the

São Francisco River, the largest basin in the northeast of Brazil. On the other hand, considering small basins, Rocha et al. [55], modelling São Bartolomeu Stream Watershed, showed values of NSE and R^2 indices between −1.19 and 0.91, and 0.22, and 0.96, respectively. In addition, the results presented here agree with the range found in previous works where SWAT was calibrated for large basins worldwide. For example, Pagliero et al. [56] estimated the monthly flow for representative regions of the Danube basin found NSE ranging from 0.22 to 0.75 and R^2 ranging from 0.68 to 0.88. Another study performed by Easton et al. [57] for the Upper Blue Nile Basin showed values of R^2 ranging from 0.73 to 0.92 and NSE from 0.53 to 0.92.

One of the strengths of the current work is that the simulation was performed at a high spatial resolution, with the basin being divided into 5187 sub-basins and further into 44,635 HRUs. In addition, the project was built for a long-term simulation over 37 years (1979–2015). These spatial and temporal resolutions were not found in previous studies of large-scale SWAT applications. For instance, Jha et al. [58] simulated the streamflow of the Upper Mississippi River, which has an area around 447,500 km^2, and discretized the basin into 119 sub-basins. These represent around 3760 km^2 of the average sub-watershed area, compared 179 km^2 for the current study basin. Pagliero et al. [56] defined 4663 HRUs (10% of our HRUs basin) over the Danube Basin, which has a drainage area of about 803,000 km^2.

4. Summary and Conclusions

In this work, the Upper Paraná River Basin was built with the highest possible spatial discretization using the SWAT model for a long-term period between 1979 and 2015. The model was calibrated and validated using the SUFI-2 method for a large number of outlets. In addition, the evaluation of the performance of the model was carried out using several objective functions. The following conclusions can be drawn:

I. The methodology used in this work regarding data preparation, model setup, and strategies for calibration and validation, as well as evaluation can be used for other large scale basins, especially in South America.

II. Due to the high spatial resolution and the good quality of most datasets collected in both meteorological, and physical variables, 23 outlets over the basin performed satisfactory or better in all the objective functions evaluated without the calibration process. Most of these outlets were found in the Iguaçu sub-basin (VI).

III. After the calibration process, most of the outlets analyzed (≥74%) presented better or equally satisfactory in all objective functions, mainly in the southern basin, which is the region with the highest density of stations.

IV. Although there are outlets with some errors in the simulated discharge, most of the evaluated outlets in the basin are in agreement with the observation especially those located at the final outlet of the main rivers of UPRB, which have the most significant contribution for the final discharge of the basin project.

The results provided in this work could be used for evaluating the potential impacts of land use and land cover as well as climate shift scenarios, which is the forthcoming study of the authors.

Supplementary Materials: The following are available online at http://www.mdpi.com/2073-4441/11/5/882/s1, Figure S1: Temporal evolution of the monthly discharge and their statistical indices values without calibration process, Figure S2: Temporal evolution of the discharge rivers and their statistical indices values after the calibration process, Table S1: Soil parameters values used in the model, Table S2: Objective function values from the outlets for the calibration (1984–2004) and validation (2005–2015) periods.

Author Contributions: Conceptualization, S.A.A.R., C.B.U., J.A.M. and E.D.F.; Methodology, S.A.A.R. and L.M.D.; software, S.A.A.R. and L.M.D.; formal analysis, S.A.A.R.; investigation, S.A.A.R.; data curation, S.A.A.R., A.P.R. and T.F.; writing—original draft preparation, S.A.A.R.; writing—review and editing, S.A.A.R., C.B.U., J.A.M. and E.D.F.; visualization, S.A.A.R.; supervision, S.A.A.R., C.B.U., J.A.M. and E.D.F.

Funding: This research was funded by CAPES (Coordenação de Aperfeiçoamento de Pessoal de Nível Superior), PROEX and Process nº 88887.115875/2015-01.

Acknowledgments: The authors would like to gratefully acknowledge the Brazilian National Water Agency (ANA) for providing the precipitation data. We also acknowledge FAPESP (Fundação de Amparo à Pesquisa do Estado de São Paulo), process nº 2015/03804-9.

Conflicts of Interest: The authors declare no conflict of interest.

References

1. Ficklin, D.L.; Luo, Y.; Luedeling, E.; Zhang, M. Climate change sensitivity assessment of a highly agricultural watershed using SWAT. *J. Hydrol.* **2009**, *374*, 16–29. [CrossRef]
2. Narsimlu, B.; Gosain, A.K.; Chahar, B.R. Assessment of Future Climate Change Impacts on Water Resources of Upper Sind River Basin, India Using SWAT Model. *Water Resour. Manag.* **2013**, *27*, 3647–3662. [CrossRef]
3. Ghaffari, G.; Keesstra, S.; Ghodousi, J.; Ahmadi, H. SWAT-simulated hydrological impact of land-use change in the Zanjanrood Basin, Northwest Iran. *Hydrol. Process.* **2010**, *24*, 892–903. [CrossRef]
4. Wang, G.; Yang, H.; Wang, L.; Xu, Z.; Xue, B. Using the SWAT model to assess impacts of land use changes on runoff generation in headwaters. *Hydrol. Process.* **2014**, *28*, 1032–1042. [CrossRef]
5. Yang, S.; Dong, G.; Zheng, D.; Xiao, H.; Gao, Y.; Lang, Y. Coupling Xinanjiang model and SWAT to simulate agricultural non-point source pollution in Songtao watershed of Hainan, China. *Ecol. Modell.* **2011**, *222*, 3701–3717. [CrossRef]
6. Rouholahnejad, E.; Abbaspour, K.C.; Srinivasan, R.; Bacu, V.; Lehmann, A. Water resources of the Black Sea Basin at high spatial and temporal resolution. *Water Resour. Res.* **2014**, *50*, 5866–5885. [CrossRef]
7. ANEEL. *BIG—Banco de Informações de Geração—Capacidade de Geração do Brasil—Usinas hidrelétricas*; 2018. Available online: www2.aneel.gov.br/aplicacoes/capacidadebrasil/GeracaoTipoFase.asp (accessed on 15 January 2019).
8. Martins, J.A.; Brand, V.S.; Capucim, M.N.; Machado, C.B.; Piccilli, D.G.A.; Martins, L.D. The Impact of Rainfall and Land Cover Changes on the Flow of a Medium-sized River in the South of Brazil. *Energy Procedia* **2016**, *95*, 272–278. [CrossRef]
9. Capucim, M.N.; Brand, V.S.; Machado, C.B.; Martins, L.D.; Allasia, D.G.; Homann, C.T.; De Freitas, E.D.; Da Silva Dias, M.A.F.; Andrade, M.F.; Martins, J.A. South America land use and land cover assessment and preliminary analysis of their impacts on regional atmospheric modeling studies. *IEEE J. Sel. Top. Appl. Earth Obs. Remote Sens.* **2015**, *8*, 1185–1198. [CrossRef]
10. Strömbäck, L.; Arheimer, B.; Lindström, G.; Donnelly, C.; Gustafsson, D. The Importance of Open Data and Software for Large Scale Hydrological Modelling. *Open Water J.* **2013**, *2*, 32.
11. Tucci, C.E. *Impactos da Variabilidade Climática e do Uso do Solo Nos Recursos Hídricos*; Câmara Temática de Recursos Hídricos, Agência Nacional de Águas (ANA): Brasilia, Brazil, 2002; p. 150.
12. Antico, A.; Torres, M.E.; Diaz, H.F. Contributions of different time scales to extreme Paraná floods. *Clim. Dyn.* **2016**, *46*, 3785–3792. [CrossRef]
13. Camilloni, I.A.; Barros, V.R. Extreme discharge events in the Paraná River and their climate forcing. *J. Hydrol.* **2003**, *278*, 94–106. [CrossRef]
14. IBGE. Available online: http://www.ibge.gov.br/apps/populacao/projecao/ (accessed on 20 January 2019).
15. ANA—Agência Nacional de Águas. 2018. Available online: http://www3.ana.gov.br/ (accessed on 10 January 2019).
16. Brea, M.; Zucol, A.F. The Paraná-Paraguay Basin: Geology and Paleoenvironments. In *Historical Biogeography of Neotropical Freshwater Fishes*; Albert, J.S., Reis, R., Eds.; University of California Press: Berkeley, CA, USA, 2012; pp. 69–88.
17. Menegazzo, M.C.; Catuneanu, O.; Chang, H.K. The South American retroarc foreland system: The development of the Bauru Basin in the back-bulge province. *Mar. Pet. Geol.* **2016**, *73*, 131–156. [CrossRef]
18. De Paula e Silva, F.; Kiang, C.H.; Caetano-Chang, M.R. Sedimentation of the Cretaceous Bauru Group in São Paulo, Paraná Basin, Brazil. *J. S. Am. Earth Sci.* **2009**, *28*, 25–39. [CrossRef]
19. Carvalho, L.M.V.; Jones, C.; Silva, A.E.; Liebmann, B.; Silva Dias, P.L. The South American Monsoon System and the 1970s climate transition. *Int. J. Climatol.* **2011**, *31*, 1248–1256. [CrossRef]

20. Grimm, A.M. Interannual climate variability in South America: Impacts on seasonal precipitation, extreme events, and possible effects of climate change. *Stoch. Environ. Res. Risk Assess.* **2011**, *25*, 537–554. [CrossRef]
21. Velasco, I.; Fritsch, J.M. Mesoscale convective complexes in the Americas. *J. Geophys. Res.* **1987**, *92*, 9591–9613. [CrossRef]
22. Salio, P.; Nicolini, M.; Zipser, E.J. Mesoscale Convective Systems over Southeastern South America and Their Relationship with the South American Low-Level Jet. *Mon. Weather Rev.* **2007**, *135*, 1290–1309. [CrossRef]
23. Arnold, J.G.; Srinivasan, R.; Muttiah, R.S.; Williams, J.R. Large Area Hydrologic Modelling and Assessment Part I: Model Development. *Am. Water Resour. Assoc.* **1998**, *34*, 73–89. [CrossRef]
24. Gassman, P.W.; Reyes, M.R.; Green, C.H.; Arnold, J.G. The Soil and Water Assessment Tool: Historical Development, Applications, and Future Research Directions. *Trans. ASABE* **2007**, *50*, 1211–1250. [CrossRef]
25. Douglas-Mankin, K.R.; Srinivasan, R.; Arnold, J.G. Soil and Water Assessment Tool (SWAT) Model: Current Developments and Applications. *Trans. ASABE* **2010**, *53*, 1423–1431. [CrossRef]
26. Neitsch, S.; Arnold, J.; Kiniry, J.; Williams, J. *Soil & Water Assessment Tool: Theoretical Documentation Version 2009*; Texas Water Resource Institute: College Station, TX, USA, 2011.
27. Pebesma, E.J. Multivariable geostatistics in S: The gstat package. *Comput. Geosci.* **2004**, *30*, 683–691. [CrossRef]
28. Ruelland, D.; Ardoin-Bardin, S.; Billen, G.; Servat, E. Sensitivity of a lumped and semi-distributed hydrological model to several methods of rainfall interpolation on a large basin in West Africa. *J. Hydrol.* **2008**, *361*, 96–117. [CrossRef]
29. Fauconnier, Y. Evaluation de La Ressource Dans Le Bassin Versant de l'Ibicuí Grâce à La Modélisation Hydrologique: Application de l'outil SWAT. Master´s Thesis, University of Le Mans, Le Mans, France, 2017.
30. Mercuri, E.G.F.; Deppe, F.; Lohmann, M.; Simões, K. Metodologia da geração de dados de entrada e aplicação do modelo SWAT para bacias hidrográficas brasileiras. In Proceedings of the XIV Simpósio Brasileiro de Sensoriamento Remoto, Natal, Brazil, 25–30 April 2009; pp. 4773–4780.
31. Pereira, D.R. Simulação hidrológica na bacia hidrográfica do rio Pomba usando o modelo SWAT. Ph.D. Thesis, Universidade Federal de Viçosa, Viçaso, MG, Brazil, 2013.
32. Rudke, A.P. Dinâmica da cobertura do solo para a bacia hidrográfica do alto rio Paraná. Master´s Thesis, Federal University of Techonology Parana, Londrina, Brazil, 2018.
33. Winchell, M.; Srinivasan, R.; Di Luzio, M.; Arnold, J. *ArcSWAT Interface For SWAT2012: User's Guide*; Blackland Research and Extension Center TEXAS Agrilife Research: Temple, TX, USA, 2013.
34. Embrapa. *Sistema brasileiro de classificação de solos*; Centro Nacional de Pesquisa de Solos: Rio de Janeiro, Brazil, 2006; ISBN 85-85864-19-2.
35. Monteith, J.L. Evaporation and envrionment. *Symp. Soc. Exp. Biol.* **1965**, *19*, 205–235. [PubMed]
36. USDA Soil Conservation Service. *National Engineering Handbook*; Section 4, Hydrology, Chapter 21; USDA Soil Conservation Service: Washington, DC, USA, 1972.
37. Abbaspour, K.C.; Johnson, C.A.; van Genuchten, M.T. Estimating Uncertain Flow and Transport Parameters Using a Sequential Uncertainty Fitting Procedure. *Vadose Zone J.* **2004**, *3*, 1340–1352. [CrossRef]
38. Abbaspour, K.C. *SWAT-CUP: SWAT Calibration and Uncertainty Programs—A User Manual*; Eawag: Duebendorf, Switzerland, 2015.
39. Rouholahnejad, E.; Abbaspour, K.C.; Vejdani, M.; Srinivasan, R.; Schulin, R.; Lehmann, A. A parallelization framework for calibration of hydrological models. *Environ. Modell. Softw.* **2012**, *31*, 28–36. [CrossRef]
40. Piniewski, M.; Szcześniak, M.; Kardel, I.; Berezowski, T.; Okruszko, T.; Srinivasan, R.; Vikhamar Schuler, D.; Kundzewicz, Z.W. Hydrological modelling of the Vistula and Odra river basins using SWAT. *Hydrol. Sci. J.* **2017**, *62*, 1266–1289. [CrossRef]
41. Kouchi, D.H.; Esmaili, K.; Faridhosseini, A.; Sanaeinejad, S.H.; Khalili, D.; Abbaspour, K.C. Sensitivity of calibrated parameters and water resource estimates on different objective functions and optimization algorithms. *Water* **2017**, *9*, 384. [CrossRef]
42. Zhang, X.; Srinivasan, R.; Liew, M. Van Multi-site calibration of the SWAT model for hydrologic modeling. *Trans. ASABE* **2008**, *51*, 2039–2049. [CrossRef]
43. Yapo, P.O.; Gupta, H.V.; Sorooshian, S. Automatic calibration of conceptual rainfall-runoff models: Sensitivity to calibration data. *J. Hydrol.* **1996**, *181*, 23–48. [CrossRef]
44. Nash, J.E.; Sutcliffe, J.V. River flow forecasting through conceptual models part I—A discussion of principles. *J. Hydrol.* **1970**, *10*, 282–290. [CrossRef]

45. Gupta, H.V.; Kling, H.; Yilmaz, K.K.; Martinez, G.F. Decomposition of the mean squared error and NSE performance criteria: Implications for improving hydrological modelling. *J. Hydrol.* **2009**, *377*, 80–91. [CrossRef]
46. Moriasi, D.N.; Arnold, J.G.; Van Liew, M.W.; Bingner, R.L.; Harmel, R.D.; Veith, T.L. Model Evaluation Guidelines for Systematic Quantification of Accuracy in Watershed Simulations. *Trans. ASABE* **2007**, *50*, 885–900. [CrossRef]
47. Thiemig, V.; Rojas, R.; Zambrano-Bigiarini, M.; De Roo, A. Hydrological evaluation of satellite-based rainfall estimates over the Volta and Baro-Akobo Basin. *J. Hydrol.* **2013**, *499*, 324–338. [CrossRef]
48. Abbaspour, K.C.; Rouholahnejad, E.; Vaghefi, S.; Srinivasan, R.; Yang, H.; Kløve, B. A continental-scale hydrology and water quality model for Europe: Calibration and uncertainty of a high-resolution large-scale SWAT model. *J. Hydrol.* **2015**, *524*, 733–752. [CrossRef]
49. Leta, O.T.; van Griensven, A.; Bauwens, W. Effect of Single and Multisite Calibration Techniques on the Parameter Estimation, Performance, and Output of a SWAT Model of a Spatially Heterogeneous Catchment. *J. Hydrol. Eng.* **2016**, *22*, 05016036. [CrossRef]
50. Meng, H.; Sexton, A.M.; Maddox, M.C.; Sood, A.; Brown, C.W.; Ferraro, R.R.; Murtugudde, R. Modeling rappahannock river basin using swat—Pilot for chesapeake bay watershed. *Appl. Eng. Agric.* **2010**, *26*, 795–805. [CrossRef]
51. Peterson, J.R.; Hamlett, J.M. Hydrologic Calibration of the Swat Model in a Watershed Containing Fragipan Soils. *J. Am. Water Resour. Assoc.* **1998**, *34*, 531–544. [CrossRef]
52. Srivastava, P.; McNair, J.N.; Johnson, T.E. Comparison of process-based and artificial neural network approaches for streamflow modeling in an agricultural watershed. *J. Am. Water Resour. Assoc.* **2006**, *42*, 545–563. [CrossRef]
53. Wu, K.; Johnston, C.A. Hydrologic response to climatic variability in a Great Lakes Watershed: A case study with the SWAT model. *J. Hydrol.* **2007**, *337*, 187–199. [CrossRef]
54. Creech, C.T.; Siqueira, R.B.; Selegean, J.P.; Miller, C. Anthropogenic impacts to the sediment budget of São Francisco River navigation channel using SWAT. *Int. J. Agric. Biol. Eng.* **2015**, *8*, 1–20.
55. Rocha, E.O.; Calijuri, M.L.; Santiago, A.F.; de Assis, L.C.; Alves, L.G.S. The Contribution of Conservation Practices in Reducing Runoff, Soil Loss, and Transport of Nutrients at the Watershed Level. *Water Resour. Manag.* **2012**, *26*, 3831–3852. [CrossRef]
56. Pagliero, L.; Bouraoui, F.; Willems, P.; Diels, J. Large-Scale Hydrological Simulations Using the Soil Water Assessment Tool, Protocol Development, and Application in the Danube Basin. *J. Environ. Qual.* **2014**, *43*, 145–154. [CrossRef] [PubMed]
57. Easton, Z.M.; Fuka, D.R.; White, E.D.; Collick, A.S.; Biruk Ashagre, B.; McCartney, M.; Awulachew, S.B.; Ahmed, A.A.; Steenhuis, T.S. A multi basin SWAT model analysis of runoff and sedimentation in the Blue Nile, Ethiopia. *Hydrol. Earth Syst. Sci.* **2010**, *14*, 1827–1841. [CrossRef]
58. Jha, M.; Arnold, J.G.; Gassman, P.W.; Giorgi, F.; Gu, R.R. Climate Chhange Sensitivity Assessment on Upper Mississippi River Basin Streamflows Using Swat. *J. Am. Water Resour. Assoc.* **2006**, *42*, 997–1015. [CrossRef]

water

Large-Scale Hydrological Modelling of the Upper Paraná River Basin

Sameh A. Abou Rafee, Cintia R. B. Uvo, Jorge A. Martins, Leonardo M. Domingues, Anderson P. Rudke, Thais Fujita and Edmilson D. Freitas

Table S1. Soil parameters values used in the model.

Soil type*	Water	Argisols	Cambisols	Geysols	Red-Yellow Latosols	Dark-Red Latosols	Luvisols	Neosols	Nitosols	Organosols	Planosols	Plinthosols	WD5717	WD5739	WD5614
NLAYERS	1	6	5	3	4	5	4	1	6	4	5	6	5	5	5
HYDGRP	D	B	B	D	D	A	D	A	B	B	C	B	B	D	B
SOL_ZMX	25.4	2200	1100	900	1500	3000	900	200	1800	800	1400	2300	1000	1000	1000
ANION_EXCL	0.5	0.5	0.5	0.5	0.38	0.5	0.5	0.5	0.5	0.4	0.5	0.5	0.4	0.4	0.4
SOL_CRK	0.5	0	0	0	0	0	0	0	0	0	0	0	0	0	0
TEXTURE	-	SL	SC	SICL	SCL	SCL	SICL	SIL	SICL	SIL	SICL	SL	SIL	SIL	SIL
SOL_Z1	25.4	250	300	150	360	130	200	200	150	100	200	400	200	200	200
SOL_BD1	1.7	1.4	1.4	1.4	1.5	1.4	1.4	1.35	1.4	1.6	1.4	1.35	1.36	1.24	1.49
SOL_AWC1	0.0	0.165	0.18	0.24	0.3	0.12	0.165	0.255	0.21	0.18	0.24	0.15	0.13	0.1	0.08
SOL_K1	260	4	2	4	12.5	7	8.5	2.5	1.5	12.5	1	1.5	2.55	0.87	7.7
SOL_CBN1	0.0	2	2	2	1.1	2	2	2	2	8.14	2	2	0.5	0.5	0.4
CLAY1	0.0	21	37	41	30.3	21	17	23	49	26	35	18	21	48	16
SILT1	0.0	9	18	52	16	9	31	58	41	31	54	23	20	17	15
SAND1	0.0	70	45	7	53.7	70	52	19	10	43	11	59	59	35	69
ROCK1	0.0	0	0	0	0	0	0	0	0	0	0	0	0	0	0
SOL_ALB1	0.2	0	0	0	0	0	0	0	0	0	0	0	0	0	0
USLE_K1	0.0	0.1	0.16	0.21	0.13	0.1	0.13	0.16	0.16	0.15	0.19	0.13	0.15	0.13	0.15
SOL_EC1	0.0	1	1	1	1	1	1	1	1	1	1	1	1	1	1
SOL_Z2	-	650	600	300	760	350	350	-	400	300	400	800	400	400	400
SOL_BD2	-	1.4	1.4	1.4	1.7	1.4	1.4	-	1.4	1.7	1.4	1.35	1.39	1.26	1.52
SOL_AWC2	-	0.09	0.195	0.195	0.3	0.105	0.5	-	0.18	0.15	0.135	0.195	0.12	0.1	0.08
SOL_K2	-	1.5	0.5	0.4	12.5	5.6	0.9	-	0.3	12.5	0.2	0.1	1.97	0.71	4.3
SOL_CBN2	-	0.5	0.5	0.5	0.2	0.5	0.5	-	0.5	8	0.5	0.5	0.5	0.5	0.5
CLAY2	-	12	34	53	29.8	22	28	-	56	22.36	68	49	28	54	29
SILT2	-	10	36	40	14.3	8	30	-	37	26.42	29	26	19	15	14
SAND2	-	78	30	7	55.9	70	42	-	7	51.22	3	25	49	30	57
ROCK2	-	0	0	0	0	0	0	-	0	0	0	0	0	0	0
SOL_ALB2	-	0	0	0	0	0	0	-	0	0	0	0	0	0	0

Soil type*	Water	Argisols	Cambisols	Geysols	Red-Yellow Latosols	Dark-Red Latosols	Luvisols	Neosols	Nitosols	Organosols	Planosols	Plinthosols	WD5717	WD5739	WD5614
USLE_K2	-	0.13	0.16	0.23	0.14	0.13	0.16	-	0.22	0.12	0.26	0.15	0.15	0.12	0.15
SOL_EC2	-	0	0	0	0	0	0	-	0	0	0	0	0	0	0
SOL_Z3	-	1000	800	900	1210	550	600	-	650	500	550	1500	600	600	600
SOL_BD3	-	1.4	1.4	1.4	1.7	1.4	1.4	-	1.4	1.7	1.4	1.4	1.4	1.27	1.5
SOL_AWC3	-	0.135	0.21	0.18	0.4	0.12	0.18	-	0.165	0.15	0.18	0.195	0.15	0.15	0.15
SOL_K3	-	1	0.7	0.3	12.5	1.6	0.2	-	0.3	12.5	0.2	0.1	1.63	0.6	3.6
SOL_CBN3	-	0.1	0.1	0.1	0.5	0.1	0.1	-	0.1	8	0.1	0.1	0.2	0.2	0.2
CLAY3	-	29	28.4	57	29.5	26	56	-	65	22.38	58	51	33	55	30
SILT3	-	11	37.7	36	13.8	8	24	-	29	21.36	41	26	18	15	13
SAND3	-	60	33.9	7	56.7	66	20	-	6	56.26	1	23	49	30	57
ROCK3	-	0	0	0	0	0	0	-	0	0	0	0	0	0	0
SOL_ALB3	-	0	0	0	0	0	0	-	0	0	0	0	0	0	0
USLE_K3	-	0.13	0.17	0.22	0.14	0.13	0.14	-	0.21	0.12	0.35	0.15	0.14	0.12	0.14
SOL_EC3	-	0	0	0	0	0	0	-	0	0	0	0	0	0	0
SOL_Z4	-	1300	1000	-	1500	1200	900	-	950	800	680	1650	800	800	800
SOL_BD4	-	1.35	1.35	-	1.6	1.35	1.35	-	1.35	1.5	1.35	1.35	1.4	1.25	1.51
SOL_AWC4	-	0.21	0.21	-	0.4	0.21	0.21	-	0.21	0.18	0.14	0.21	0.2	0.2	0.08
SOL_K4	-	0.7	0.7	-	12.5	0.7	0.7	-	0.1	12.5	8	0.7	1.47	0.65	3.1
SOL_CBN4	-	0.1	0.1	-	0.4	0.1	0.1	-	0.7	3.14	0.05	0.1	0.3	0.3	0.3
CLAY4	-	26.8	26.8	-	35.6	26.8	26.8	-	26.8	55.27	27	26.8	36	56	34
SILT4	-	43.7	43.7	-	15.9	43.7	43.7	-	43.7	24.56	39.3	43.7	17	15	13
SAND4	-	29.5	29.5	-	48.5	29.5	29.5	-	29.5	20.16	33.7	29.5	47	29	53
ROCK4	-	0	0	-	0	0	0	-	0	0	0	0	0	0	0
SOL_ALB4	-	0	0	-	0	0	0	-	0	0	0	0	0	0	0
USLE_K4	-	0.18	0.18	-	0.14	0.18	0.18	-	0.18	0.11	0.17	0.18	0.14	0.12	0.13
SOL_EC4	-	0	0	-	0	0	0	-	0	0	0	0	0	0	0
SOL_Z5	-	1600	1100	-	-	3000	-	-	1300	-	1400	2000	1000	1000	1000
SOL_BD5	-	1.35	1.35	-	-	1.35	-	-	1.35	-	1.35	1.35	1.38	1.26	1.5
SOL_AWC5	-	0.14	0.14	-	-	0.14	-	-	0.14	-	0.14	0.14	0.13	0.1	0.1
SOL_K5	-	8	8	-	-	8	-	-	8	-	8	8	1.43	0.66	2.7
SOL_CBN5	-	0.05	0.05	-	-	0.05	-	-	0.05	-	0.05	0.05	0.2	0.2	0.2
CLAY5	-	27	27	-	-	27	-	-	27	-	27	27	36	55	35
SILT5	-	39.3	39.3	-	-	39.3	-	-	39.3	-	39.3	39.3	18	16	14
SAND5	-	33.7	33.7	-	-	33.7	-	-	33.7	-	33.7	33.7	46	29	51
ROCK5	-	0	0	-	-	0	-	-	0	-	0	0	0	0	0
SOL_ALB5	-	0	0	-	-	0	-	-	0	-	0	0	0	0	0

Soil type*	Water	Argisols	Cambisols	Geysols	Red-Yellow Latosols	Dark-Red Latosols	Luvisols	Neosols	Nitosols	Organosols	Planosols	Plinthosols	WD5717	WD5739	WD5614
USLE_K5	-	0.17	0.17	-	-	0.17	-	-	0.17	-	0.17	0.17	0.15	0.15	0.15
SOL_EC5	-	0	0	-	-	0	-	-	0	-	0	0	0	0	0
SOL_Z6	-	2200	-	-	-	-	-	-	1800	-	-	2300	-	-	-
SOL_BD6	-	1.35	-	-	-	-	-	-	1.35	-	-	1.35	-	-	-
SOL_AWC6	-	0.15	-	-	-	-	-	-	0.135	-	-	0.21	-	-	-
SOL_K6	-	0.5	-	-	-	-	-	-	0.06	-	-	0.223	-	-	-
SOL_CBN6	-	0.06	-	-	-	-	-	-	0.3	-	-	0.06	-	-	-
CLAY6	-	35	-	-	-	-	-	-	75	-	-	33	-	-	-
SILT6	-	12	-	-	-	-	-	-	20	-	-	41	-	-	-
SAND6	-	53	-	-	-	-	-	-	5	-	-	26	-	-	-
ROCK6	-	0	-	-	-	-	-	-	0	-	-	0	-	-	-
SOL_ALB6	-	0	-	-	-	-	-	-	0	-	-	0	-	-	-
USLE_K6	-	0.13	-	-	-	-	-	-	0.19	-	-	0.17	-	-	-
SOL_EC6	-	0	-	-	-	-	-	-	0	-	-	0	-	-	-

*** HYDGRP:** Soil hydrologic group (A, B, C, or D); **SOL_ZMX:** Maximum rooting depth of soil profile (mm); **ANION_EXCL:** Fraction of porosity (void space) from which anions are excluded; **SOL_CRK:** Potential or maximum crack volume of the soil profile expressed as a fraction of the total soil volume. **TEXTURE:** Texture of soil layer; **SOL_Z:** Depth from soil surface to bottom of layer (mm); **SOL_BD:** Moist bulk density (Mg/m^3 or g/cm^3); **SOL_AWC:** Available water capacity of the soil layer (mm H_2O/mm soil); **SOL_K:** Saturated hydraulic conductivity (mm/h); **SOL_CBN:** Organic carbon content (% soil weight); **SOL_CLAY:** Clay content (% soil weight); **SOL_SILT:** Silt content (% soil weight); **SOL_SAND:** Sand content (% soil weight); **SOL_ROCK:** Rock fragment content (% total weight); **SOL_ALB:** Moist soil albedo; **USLE_K:** USLE equation soil erodibility (K) factor (units: 0.013 metric ton m^2 h/m^3-metric ton cm).

Table S2. Objective function values from the outlets for the calibration (1984–2004) and validation (2005–2015) periods.

River Name	Latitude	Longitude	PBIAS		R^2		NSE		KGE		RSR	
			Calibration	Validation	Calibration	Validation	Calibration	Validation	Calibration	Validation	Calibration	Validation
Corumbá	−16.79	−47.93	33.30	−16.79	0.83	0.80	0.58	0.51	0.64	0.60	0.65	0.70
Verde/Verdão	−17.97	−50.33	−9.80	−17.97	0.32	0.33	0.10	0.15	0.55	0.56	0.95	0.92
Dos Bois	−17.98	−50.25	−34.40	−17.98	0.37	0.39	0.10	0.01	0.44	0.36	0.95	0.99
Corumbá	−17.99	−48.53	−31.60	−17.99	0.76	0.79	0.50	0.70	0.65	0.71	0.71	0.55
São Marcos	−18.05	−47.67	−14.10	−18.05	0.72	0.74	0.31	0.53	0.49	0.66	0.83	0.68
Meia Ponte	−18.35	−49.60	53.30	−18.35	0.78	0.80	0.01	0.04	0.38	0.30	0.99	0.97
Paranaíba	−18.41	−49.10	−27.00	−18.41	0.80	0.84	0.48	0.69	0.59	0.72	0.72	0.56
Paranaíba	−18.45	−47.98	−17.10	−18.45	0.83	0.88	0.48	0.69	0.50	0.63	0.72	0.56
Verde	−18.81	−51.17	23.40	−18.81	0.77	0.81	−0.41	−0.24	0.26	0.09	1.19	1.11
Da Prata	−19.04	−49.70	−17.60	−19.04	0.42	0.52	0.33	0.15	0.58	0.52	0.82	0.92
Araguari	−19.13	−47.70	−14.10	−19.13	0.77	0.83	0.68	0.61	0.79	0.68	0.56	0.62
Sucuriú	−19.44	−52.57	9.20	−19.44	0.57	0.68	0.42	0.33	0.69	0.70	0.76	0.76
Sucuriú	−19.97	−52.22	7.30	−19.97	0.51	0.93	0.45	0.39	0.61	0.42	0.74	0.72
Grande	−19.99	−47.76	−6.70	−19.99	0.86	0.89	0.82	0.85	0.85	0.84	0.43	0.39
Grande	−20.10	−48.60	10.70	−20.10	0.83	0.88	0.81	0.88	0.85	0.90	0.44	0.35
Paraná	−20.38	−51.36	−10.40	−20.38	0.90	0.92	0.68	0.74	0.61	0.67	0.56	0.50
Grande	−20.67	−46.32	1.90	−20.67	0.84	0.87	0.73	0.78	0.74	0.76	0.52	0.47
Paraná	−20.78	−51.63	−7.60	−20.78	0.91	0.92	0.70	0.75	0.60	0.67	0.55	0.50
Mogi−Guaçu	−21.02	−48.18	24.20	−21.02	0.78	0.88	0.42	0.72	0.61	0.72	0.76	0.53
Anhanduí	−21.30	−54.20	−16.30	−21.30	0.51	0.83	0.28	−0.93	0.59	0.61	0.85	1.29
Tietê	−21.30	−49.78	10.80	−21.30	0.89	0.87	0.82	0.83	0.84	0.87	0.42	0.41
Anhanduí	−21.61	−53.05	−2.70	−21.61	0.39	0.73	0.38	−0.29	0.48	0.40	0.79	1.12
Jacaré−Guaçu	−21.87	−48.28	−15.80	−21.87	0.79	0.86	0.41	0.71	0.67	0.81	0.77	0.53
Ivinheima	−21.96	−53.77	−10.50	−21.96	0.50	0.44	0.44	0.29	0.55	0.58	0.75	0.84
Sapucaí	−22.05	−45.70	−8.20	−22.05	0.90	0.92	0.73	0.82	0.65	0.74	0.52	0.42
Dourados	−22.07	−54.23	−43.30	−22.07	0.41	0.25	−0.90	−1.93	0.43	0.17	1.37	1.69
Mogi−Guaçu	−22.30	−47.13	−11.10	−22.30	0.76	0.77	0.41	0.24	0.53	0.41	0.77	0.87
Ivinheima	−22.38	−53.53	−4.90	−22.38	0.50	0.54	0.49	0.54	0.61	0.61	0.71	0.68
Paraná	−22.48	−52.96	−9.90	−22.48	0.87	0.89	0.61	0.65	0.59	0.64	0.62	0.59
Tietê	−22.52	−48.53	−12.90	−22.52	0.86	0.84	0.79	0.66	0.82	0.72	0.46	0.58
Piracicaba	−22.68	−47.78	−41.50	−22.68	0.83	0.85	0.12	0.62	0.39	0.61	0.94	0.62
Paranapanema	−22.70	−51.40	−11.00	−22.70	0.83	0.85	0.73	0.68	0.79	0.73	0.52	0.56
Pardo	−22.88	−49.24	−11.80	−22.88	0.78	0.79	0.45	0.39	0.57	0.59	0.74	0.78
Capivari	−22.96	−47.30	−32.60	−22.96	0.77	0.75	−0.83	0.38	−0.10	0.51	1.35	0.78
Paranapanema	−23.07	−49.84	−38.90	−23.07	0.78	0.81	0.14	−0.47	0.46	0.26	0.92	1.21

River Name	Latitude	Longitude	PBIAS		R^2		NSE		KGE		RSR	
			Calibration	Validation	Calibration	Validation	Calibration	Validation	Calibration	Validation	Calibration	Validation
Das Cinzas	−23.09	−50.29	−47.50	−23.09	0.71	0.71	0.44	0.23	0.49	0.39	0.74	0.87
Ivaí	−23.20	−53.32	−7.50	−23.20	0.79	0.83	0.76	0.69	0.87	0.74	0.49	0.55
Sarapuí	−23.40	−47.76	−25.90	−23.40	0.80	0.84	0.59	0.45	0.64	0.49	0.64	0.73
Tibagi	−23.64	−50.92	11.60	−23.64	0.68	0.70	0.58	0.66	0.49	0.61	0.65	0.58
Mourão	−23.82	−52.18	−16.50	−23.82	0.75	0.78	0.52	0.62	0.74	0.75	0.69	0.61
Laranjinha	−23.85	−50.39	4.50	−23.85	0.72	0.71	0.68	0.57	0.62	0.45	0.57	0.65
Das Almas	−23.97	−48.28	−10.90	−23.97	0.66	0.70	0.39	0.24	0.64	0.55	0.78	0.87
Corumbatai	−24.02	−51.95	1.30	−24.02	0.88	0.77	0.86	0.72	0.82	0.62	0.37	0.53
Itareré	−24.03	−49.46	−20.60	−24.03	0.63	0.69	0.48	0.63	0.71	0.80	0.72	0.61
Alonso	−24.11	−51.48	−14.50	−24.11	0.83	0.82	0.79	0.76	0.76	0.72	0.45	0.49
Piquiri	−24.20	−53.33	0.90	−24.20	0.85	0.87	0.84	0.86	0.84	0.89	0.40	0.37
Goio Bang/Tricolor	−24.55	−52.90	−6.70	−24.55	0.61	0.73	0.57	0.69	0.76	0.78	0.66	0.55
Sapucaia	−24.63	−53.10	10.50	−24.63	0.62	0.81	0.60	0.80	0.62	0.80	0.63	0.45
Cantu	−24.75	−52.70	11.40	−24.75	0.77	0.76	0.69	0.68	0.59	0.58	0.56	0.56
Piquiri	−24.98	−52.28	13.00	−24.98	0.80	0.81	0.71	0.79	0.61	0.74	0.54	0.45

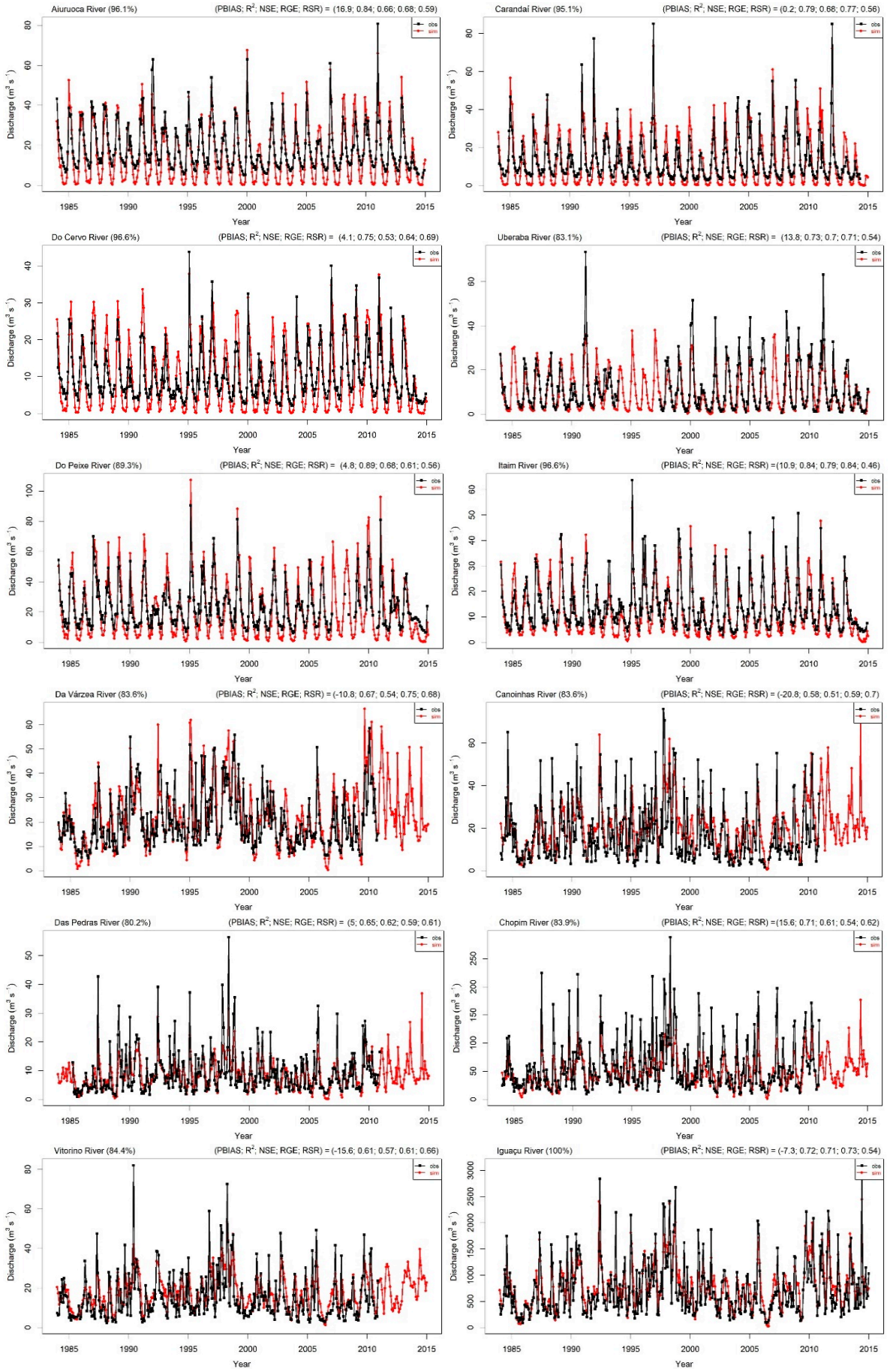
Aiuruoca River (96.1%) (PBIAS; R2; NSE; RGE; RSR) = (16.9; 0.84; 0.66; 0.68; 0.59)
Carandaí River (95.1%) (PBIAS; R2; NSE; RGE; RSR) = (0.2; 0.79; 0.68; 0.77; 0.56)
Do Cervo River (96.6%) (PBIAS; R2; NSE; RGE; RSR) = (4.1; 0.75; 0.53; 0.64; 0.69)
Uberaba River (83.1%) (PBIAS; R2; NSE; RGE; RSR) = (13.8; 0.73; 0.7; 0.71; 0.54)
Do Peixe River (89.3%) (PBIAS; R2; NSE; RGE; RSR) = (4.8; 0.89; 0.68; 0.61; 0.56)
Itaim River (96.6%) (PBIAS; R2; NSE; RGE; RSR) =(10.9; 0.84; 0.79; 0.84; 0.46)
Da Várzea River (83.6%) (PBIAS; R2; NSE; RGE; RSR) = (-10.8; 0.67; 0.54; 0.75; 0.68)
Canoinhas River (83.6%) (PBIAS; R2; NSE; RGE; RSR) = (-20.8; 0.58; 0.51; 0.59; 0.7)
Das Pedras River (80.2%) (PBIAS; R2; NSE; RGE; RSR) = (5; 0.65; 0.62; 0.59; 0.61)
Chopim River (83.9%) (PBIAS; R2; NSE; RGE; RSR) =(15.6; 0.71; 0.61; 0.54; 0.62)
Vitorino River (84.4%) (PBIAS; R2; NSE; RGE; RSR) = (-15.6; 0.61; 0.57; 0.61; 0.66)
Iguaçu River (100%) (PBIAS; R2; NSE; RGE; RSR) = (-7.3; 0.72; 0.71; 0.73; 0.54)
Discharge (m3 s-1)
Year
obs
sim

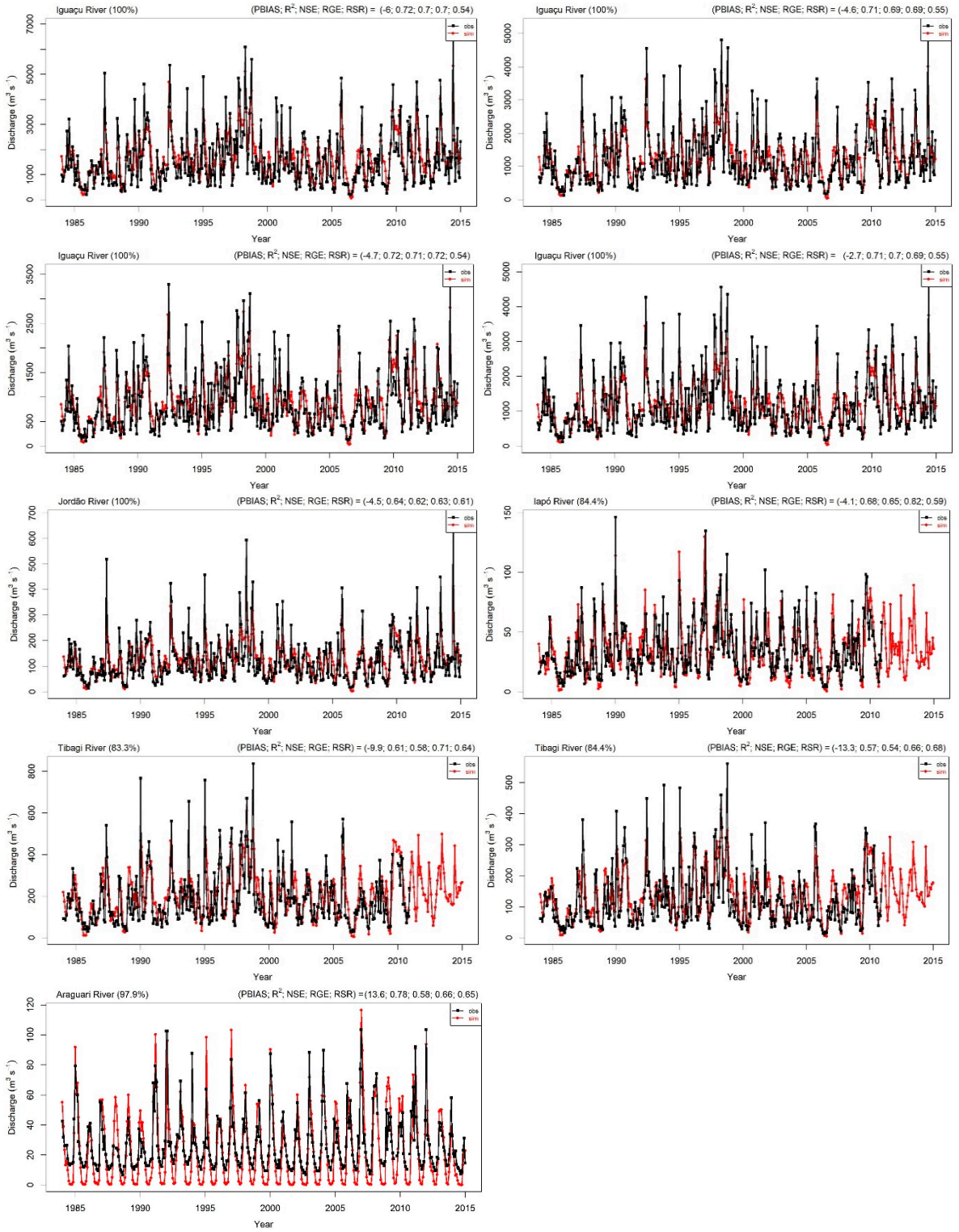

Figure S1. Temporal evolution of the monthly discharge and their statistical indices values without calibration process.

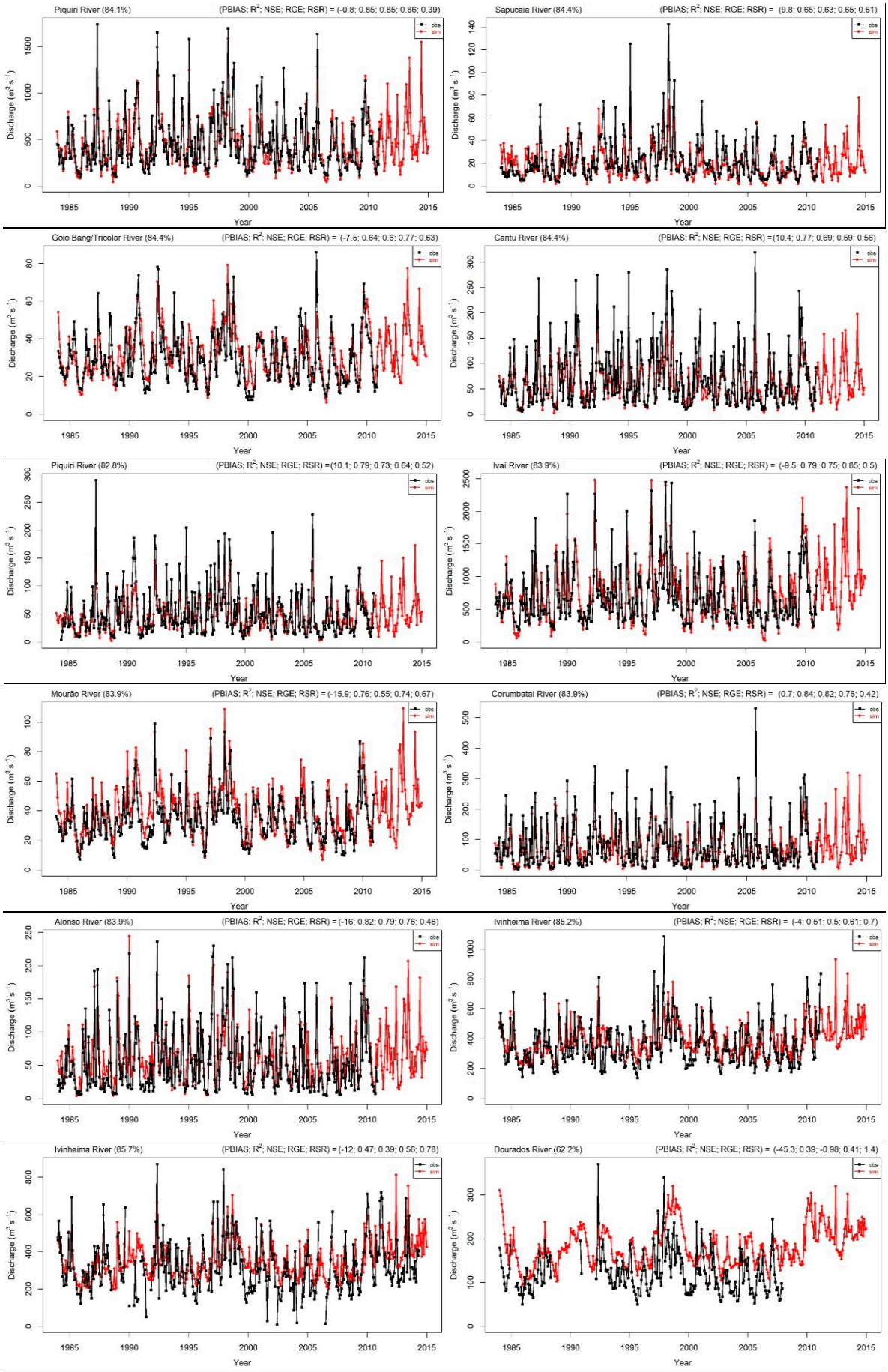
Piquiri River (84.1%) (PBIAS; R2; NSE; RGE; RSR) = (-0.8; 0.85; 0.85; 0.86; 0.39)
Sapucaia River (84.4%) (PBIAS; R2; NSE; RGE; RSR) = (9.8; 0.65; 0.63; 0.65; 0.61)
Goio Bang/Tricolor River (84.4%) (PBIAS; R2; NSE; RGE; RSR) = (-7.5; 0.64; 0.6; 0.77; 0.63)
Cantu River (84.4%) (PBIAS; R2; NSE; RGE; RSR) =(10.4; 0.77; 0.69; 0.59; 0.56)
Piquiri River (82.8%) (PBIAS; R2; NSE; RGE; RSR) =(10.1; 0.79; 0.73; 0.64; 0.52)
Ivaí River (83.9%) (PBIAS; R2; NSE; RGE; RSR) = (-9.5; 0.79; 0.75; 0.85; 0.5)
Mourão River (83.9%) (PBIAS; R2; NSE; RGE; RSR) = (-15.9; 0.76; 0.55; 0.74; 0.67)
Corumbataí River (83.9%) (PBIAS; R2; NSE; RGE; RSR) = (0.7; 0.84; 0.82; 0.76; 0.42)
Alonso River (83.9%) (PBIAS; R2; NSE; RGE; RSR) = (-16; 0.82; 0.79; 0.76; 0.46)
Ivinheima River (85.2%) (PBIAS; R2; NSE; RGE; RSR) = (-4; 0.51; 0.5; 0.61; 0.7)
Ivinheima River (85.7%) (PBIAS; R2; NSE; RGE; RSR) = (-12; 0.47; 0.39; 0.56; 0.78)
Dourados River (62.2%) (PBIAS; R2; NSE; RGE; RSR) = (-45.3; 0.39; -0.98; 0.41; 1.4)
obs
sim
Discharge (m3 s-1)
Year

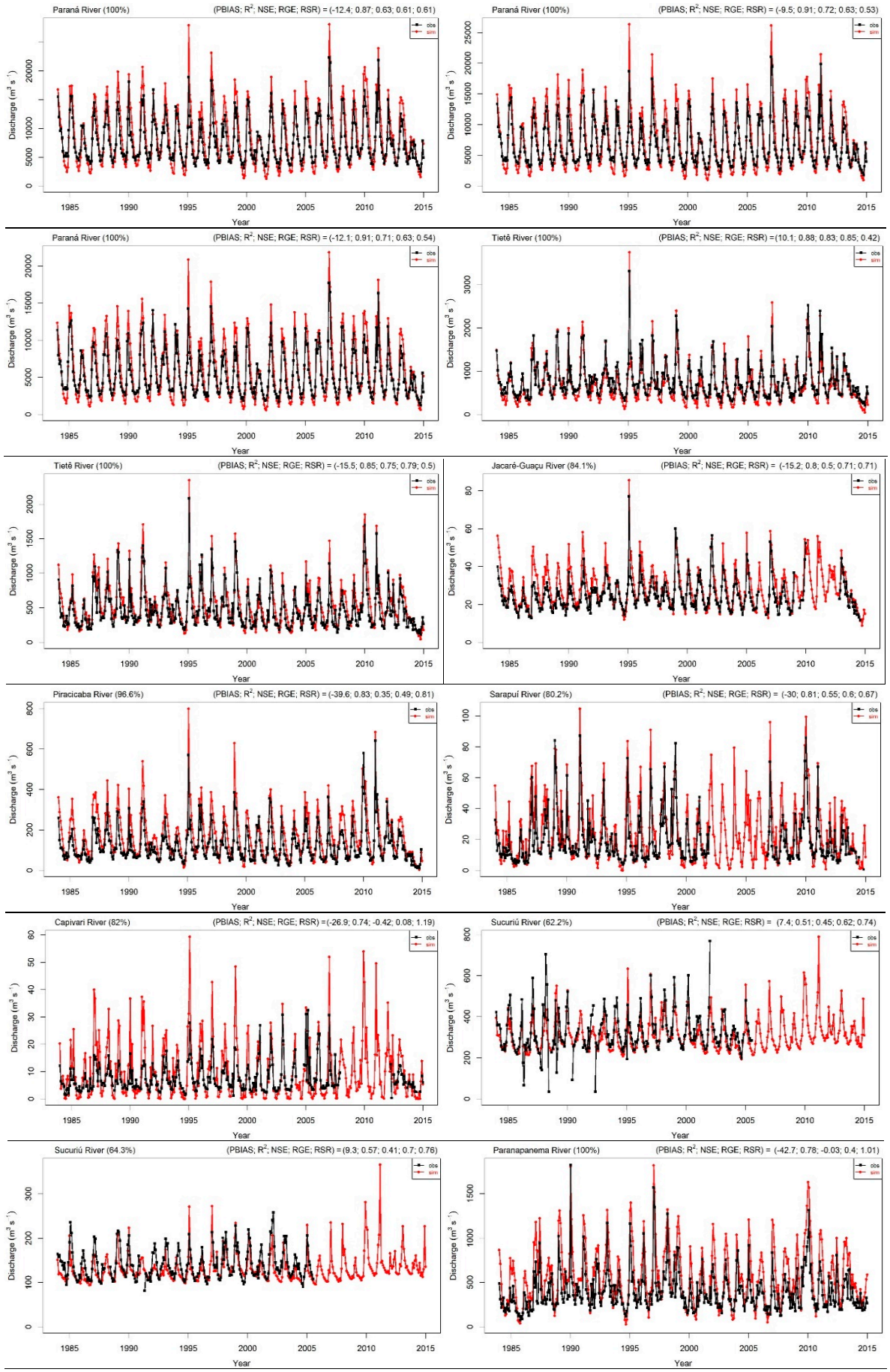
Paraná River (100%) (PBIAS; R²; NSE; RGE; RSR) = (-12.4; 0.87; 0.63; 0.61; 0.61)
Paraná River (100%) (PBIAS; R²; NSE; RGE; RSR) = (-9.5; 0.91; 0.72; 0.63; 0.53)
Paraná River (100%) (PBIAS; R²; NSE; RGE; RSR) = (-12.1; 0.91; 0.71; 0.63; 0.54)
Tietê River (100%) (PBIAS; R²; NSE; RGE; RSR) = (10.1; 0.88; 0.83; 0.85; 0.42)
Tietê River (100%) (PBIAS; R²; NSE; RGE; RSR) = (-15.5; 0.85; 0.75; 0.79; 0.5)
Jacaré-Guaçu River (84.1%) (PBIAS; R²; NSE; RGE; RSR) = (-15.2; 0.8; 0.5; 0.71; 0.71)
Piracicaba River (96.6%) (PBIAS; R²; NSE; RGE; RSR) = (-39.6; 0.83; 0.35; 0.49; 0.81)
Sarapuí River (80.2%) (PBIAS; R²; NSE; RGE; RSR) = (-30; 0.81; 0.55; 0.6; 0.67)
Capivari River (82%) (PBIAS; R²; NSE; RGE; RSR) = (-26.9; 0.74; -0.42; 0.08; 1.19)
Sucuriú River (62.2%) (PBIAS; R²; NSE; RGE; RSR) = (7.4; 0.51; 0.45; 0.62; 0.74)
Sucuriú River (64.3%) (PBIAS; R²; NSE; RGE; RSR) = (9.3; 0.57; 0.41; 0.7; 0.76)
Paranapanema River (100%) (PBIAS; R²; NSE; RGE; RSR) = (-42.7; 0.78; -0.03; 0.4; 1.01)
obs
sim
Discharge (m³ s⁻¹)
Year

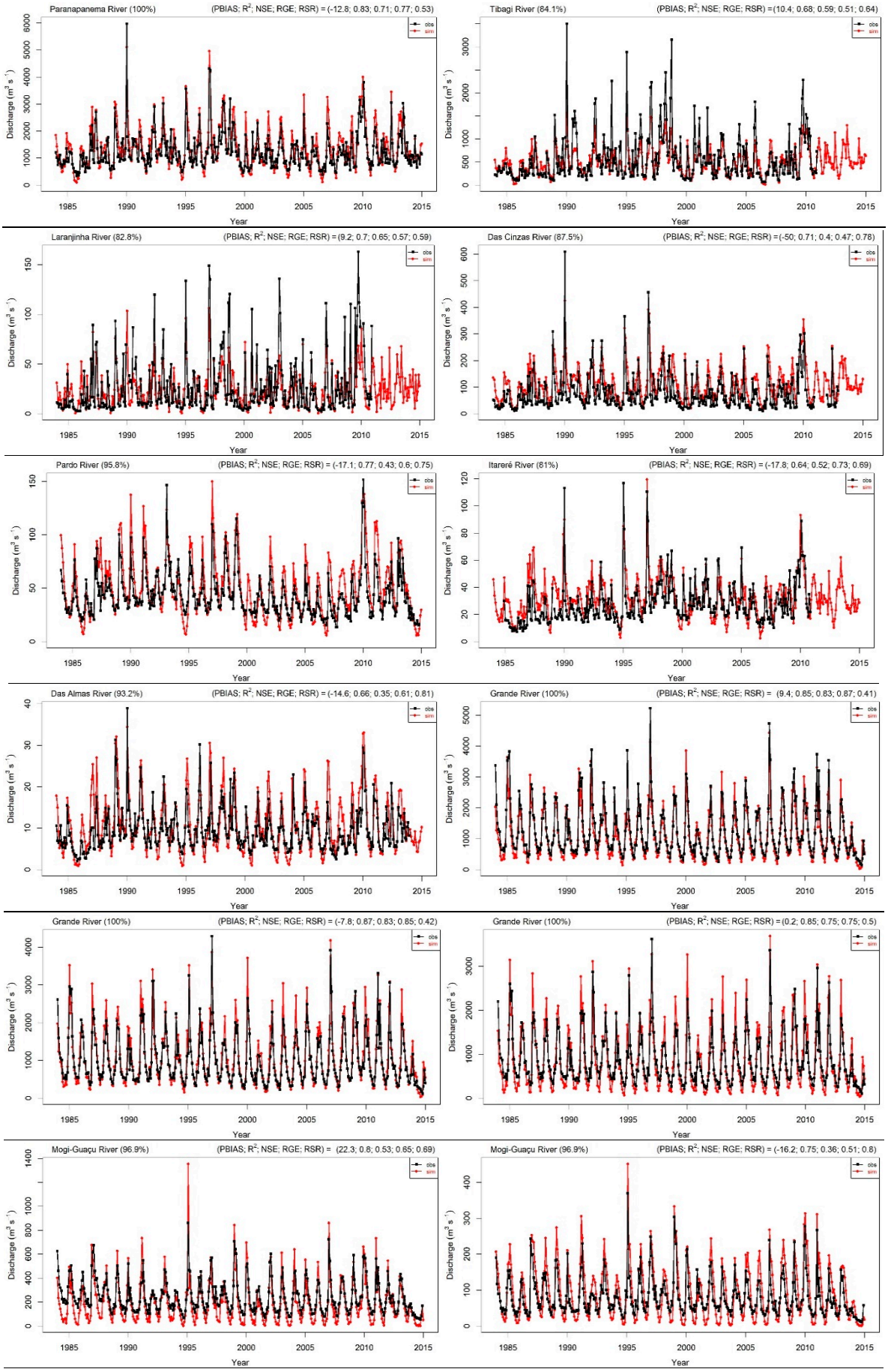
Paranapanema River (100%) (PBIAS; R2; NSE; RGE; RSR) = (-12.8; 0.83; 0.71; 0.77; 0.53)
Tibagi River (84.1%) (PBIAS; R2; NSE; RGE; RSR) = (10.4; 0.68; 0.59; 0.51; 0.64)
Laranjinha River (82.8%) (PBIAS; R2; NSE; RGE; RSR) = (9.2; 0.7; 0.65; 0.57; 0.59)
Das Cinzas River (87.5%) (PBIAS; R2; NSE; RGE; RSR) = (-50; 0.71; 0.4; 0.47; 0.78)
Pardo River (95.8%) (PBIAS; R2; NSE; RGE; RSR) = (-17.1; 0.77; 0.43; 0.6; 0.75)
Itareré River (81%) (PBIAS; R2; NSE; RGE; RSR) = (-17.8; 0.64; 0.52; 0.73; 0.69)
Das Almas River (93.2%) (PBIAS; R2; NSE; RGE; RSR) = (-14.6; 0.66; 0.35; 0.61; 0.81)
Grande River (100%) (PBIAS; R2; NSE; RGE; RSR) = (9.4; 0.85; 0.83; 0.87; 0.41)
Grande River (100%) (PBIAS; R2; NSE; RGE; RSR) = (-7.8; 0.87; 0.83; 0.85; 0.42)
Grande River (100%) (PBIAS; R2; NSE; RGE; RSR) = (0.2; 0.85; 0.75; 0.75; 0.5)
Mogi-Guaçu River (96.9%) (PBIAS; R2; NSE; RGE; RSR) = (22.3; 0.8; 0.53; 0.65; 0.69)
Mogi-Guaçu River (96.9%) (PBIAS; R2; NSE; RGE; RSR) = (-16.2; 0.75; 0.36; 0.51; 0.8)
obs
sim
Discharge (m3 s-1)
Year

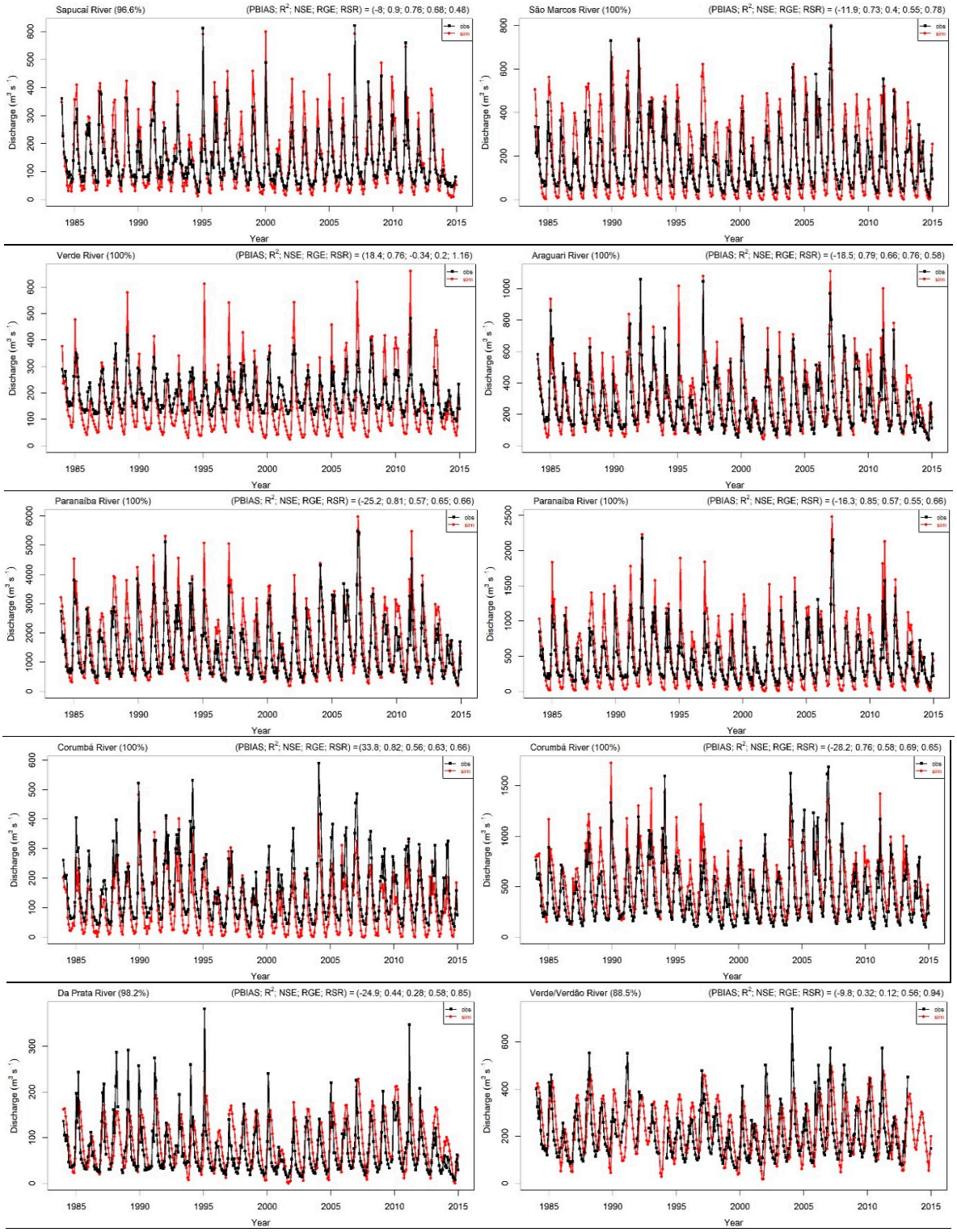
Sapucaí River (96.6%) (PBIAS; R²; NSE; RGE; RSR) = (-8; 0.9; 0.76; 0.68; 0.48)
São Marcos River (100%) (PBIAS; R²; NSE; RGE; RSR) = (-11.9; 0.73; 0.4; 0.55; 0.78)
Verde River (100%) (PBIAS; R²; NSE; RGE; RSR) = (18.4; 0.76; -0.34; 0.2; 1.16)
Araguari River (100%) (PBIAS; R²; NSE; RGE; RSR) = (-18.5; 0.79; 0.66; 0.76; 0.58)
Paranaíba River (100%) (PBIAS; R²; NSE; RGE; RSR) = (-25.2; 0.81; 0.57; 0.65; 0.66)
Paranaíba River (100%) (PBIAS; R²; NSE; RGE; RSR) = (-16.3; 0.85; 0.57; 0.55; 0.66)
Corumbá River (100%) (PBIAS; R²; NSE; RGE; RSR) = (33.8; 0.82; 0.56; 0.63; 0.66)
Corumbá River (100%) (PBIAS; R²; NSE; RGE; RSR) = (-28.2; 0.76; 0.58; 0.69; 0.65)
Da Prata River (98.2%) (PBIAS; R²; NSE; RGE; RSR) = (-24.9; 0.44; 0.28; 0.58; 0.85)
Verde/Verdão River (88.5%) (PBIAS; R²; NSE; RGE; RSR) = (-9.8; 0.32; 0.12; 0.56; 0.94)
Discharge (m³ s⁻¹)
Year
obs
sim

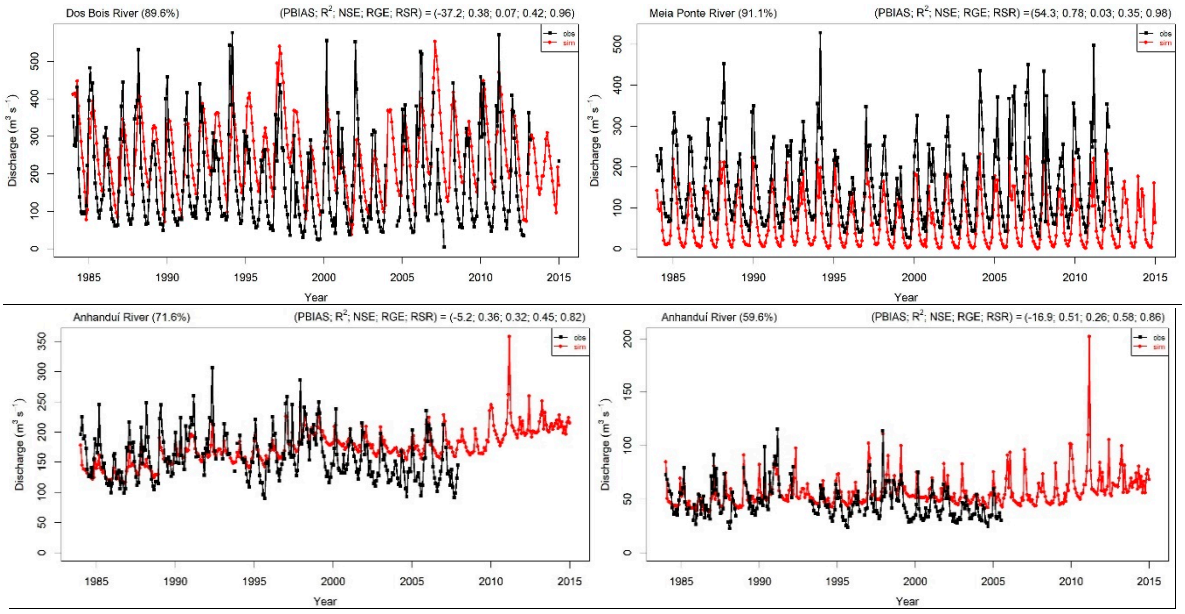

Figure S2. Temporal evolution of the discharge rivers and their statistical indices values after the calibration process.

Paper III

III. **Abou Rafee, S.A.,** Freitas, E.D., Martins, J.A., Machado, C.B., Uvo, C.B., 2020. Hydrologic Response to Large-Scale Land Use and Cover Changes in the Upper Paraná River Basin between 1985 and 2015. *Journal of Hydrology:Regional Studies* (Submitted 2020-05-22, Under review).

Hydrologic Response to Large-Scale Land Use and Cover Changes in the Upper Paraná River Basin between 1985 and 2015

Sameh A. Abou Rafee[1,2], Edmilson D. Freitas[1], Jorge A. Martins[3], Carolyne B. Machado[1], Cintia B. Uvo[2]

[1]Department of Atmospheric Sciences, University of São Paulo, São Paulo, Brazil

[2]Division of Water Resources Engineering, Lund University, Lund, Sweden

[3]Federal University of Technology – Parana, Londrina, Brazil

Correspondence to: S.A. Abou Rafee (sameh.adib@iag.usp.br)

ABSTRACT

The Upper Paraná River Basin (UPRB) has undergone remarkable Land Use and Cover Changes (LUCC) in recent decades. This paper analyses the hydrologic response to LUCC in the UPRB between 1985 and 2015, using the Soil and Water Assessment Tool (SWAT) model. The impacts of LUCC were examined for annual, wet, and dry season (both during calibrated and validated periods) between 1984 and 2015. The most substantial LUCC were the extensive reduction of the cerrado and the expansion of agriculture areas. The simulations demonstrated that the LUCC caused important changes in basin hydrology. For instance, an increase (decrease) of surface runoff in the wet (dry) season at most UPRB subbasins, was observed. In addition, the simulation results revealed a reduction in actual evapotranspiration and an increase in soil moisture in the annual and wet season. Consequently, most of the major rivers of the basin presented an increase (decrease) in their discharge in the wet (dry) period. The major changes in the hydrologic components were observed in the central-western and southern parts of the UPRB. At the river mouth of the UPRB, the LUCC led to an increase in long-term mean discharge values of 4.2% and 1.1% in the annual and wet season and a decrease of about 2.2% in the dry period. This study provides a large-scale modelling and valuable

information that could be used to improve planning and sustainable management of future water resources within the basin.

Keywords: large-scale modeling; surface runoff; actual evapotranspiration; soil moisture; discharge; SWAT model.

Introduction

Rapid population growth and economic development have induced extensive Land Use and Cover Changes (LUCC) in recent decades (Boserup, 2014; Lambin et al., 2001). LUCC is one of the main factors that affect the hydrological processes within watersheds (DeFries and Eshleman, 2004; Francesconi et al., 2016). For instance, in small catchments, the replacement of natural vegetation by cropland or grassland areas could have a significant effect on the surface runoff and actual evapotranspiration processes (De Roo et al., 2001; Kalantari et al., 2014). In a large basin, the impacts could be larger and different due to the greater area and heterogeneity of the LUCC (Costa et al., 2003; Dos Santos et al., 2018; Pokhrel et al., 2018; Rajib and Merwade, 2017). Therefore, understanding the influence of LUCC on hydrology in small- and large-scale basins is vital for planning the sustainable management of water resources. Because of that, LUCC have aroused the interest of scientific researchers worldwide.

The Upper Paraná River Basin (UPRB) belongs to one of the most important and second biggest river basin in South America, the La Plata River Basin. The basin plays a significant role in Brazilian economy, being responsible for the most extensive livestock, agricultural and biofuel production, transportation of products, and hydroelectricity generation. In addition, according to the Brazilian National Water Agency (ANA), the UPRB has the largest water consumption in South America mostly used for agriculture

and industrial activities. In the latest decades, the UPRB has undergone significant LUCC mainly with the deforestation of natural vegetation replaced by cropland and grassland (Rudke, 2018; Tucci, 2002). For instance, 75.9% of the Atlantic forest biome and 48.5% of the cerrado biome had its original vegetation suppressed (MMA, 2012, 2011). At the same time, significant changes in basin hydrology have been presented (Antico et al., 2016; Camilloni and Barros, 2003).

Studies consider LUCC one of the main causes of the hydrologic changes in the UPRB (e.g. Doyle and Barros, 2011). Hernandes et al. (2018) evaluated the impacts of the agriculture expansion within the eastern part of the UPRB, using the Soil and Water Assessment Tool (SWAT) model. Their simulation results showed that the LUCC led to an increase in the stream flow during the dry period. In the northern parts of the basin, the study performed by Viola et al. (2014) showed scenarios of deforestation in areas in the Grande River subbasin (located between Minas Gerais and São Paulo states). The authors demonstrated through the Lavras Simulation of Hydrology (LASH) model that the decreased vegetation area could increase the water yield, with an increase in the maximum stream flows. Relatively few studies have investigated the effects of LUCC on hydrology throughout the basin, and those have been performed for a local or regional watershed. No analysis by subbasins, but with integrated results for the entire UPRB, has yet been developed. Therefore, studies of this nature are needed using large-scale modelling.

This study aims at using the SWAT model to assess the hydrologic response to LUCC between 1985 and 2015 for the entire UPRB. Besides the simulations performed at a high spatial resolution, the evaluation of the impacts of LUCC was addressed over a 32-year long period from January 1984 to December 2015 for annual, wet, and dry seasons values.

2. Material and Methods

2.1. Study Area

The study area is located in the central-southern region of Brazil, comprising the Upper Paraná River Basin (UPRB), between the coordinates 26° 51′ 23.35″ and 15° 27′ 25.54″ S latitude, and 56° 7′ 4.61″ and 43° 34′ 50.61″ W longitude. The basin has a drainage area of 900,480 km^2 and altitude up to 2778 meters above sea level. It covers six Brazilian states: São Paulo (23.5%), Paraná (20.4%), Mato Grosso do Sul (18.9%), Minas Gerais (17.6%), Goiás (15.7%), Santa Catarina (1.2%), and the Federal District (0.4%), and also includes a small portion of Paraguay (2.3%) (Figure 1). Currently, the UPRB has an estimated population of more than 65 million inhabitants, approximately one-third of the Brazilian population, of whom 93% live in urban areas (IBGE, 2019).

The UPRB has different climatic areas, with several different synoptic systems affecting regions across the basin. The northern part of the basin is characterized by wet summers and dry winters, which is strongly associated with the presence of the South American Monsoon System (Carvalho et al., 2011; Grimm et al., 2007). On the other hand, the southern part of the basin, rainfall is spread over all seasons. This occurs due to the influence of baroclinic systems, such as Mesoscale Convective Systems (MCS), South American Low-Level Jet (SALLJ), cold fronts, and South Atlantic Convergence Zone (SACZ) (Carvalho et al., 2004; Velasco and Fritsch, 1987). Annual precipitation over the southern part of the basin reaches 1850 mm, while in the northern part does not exceed 1400 mm (Abou Rafee et al., 2020).

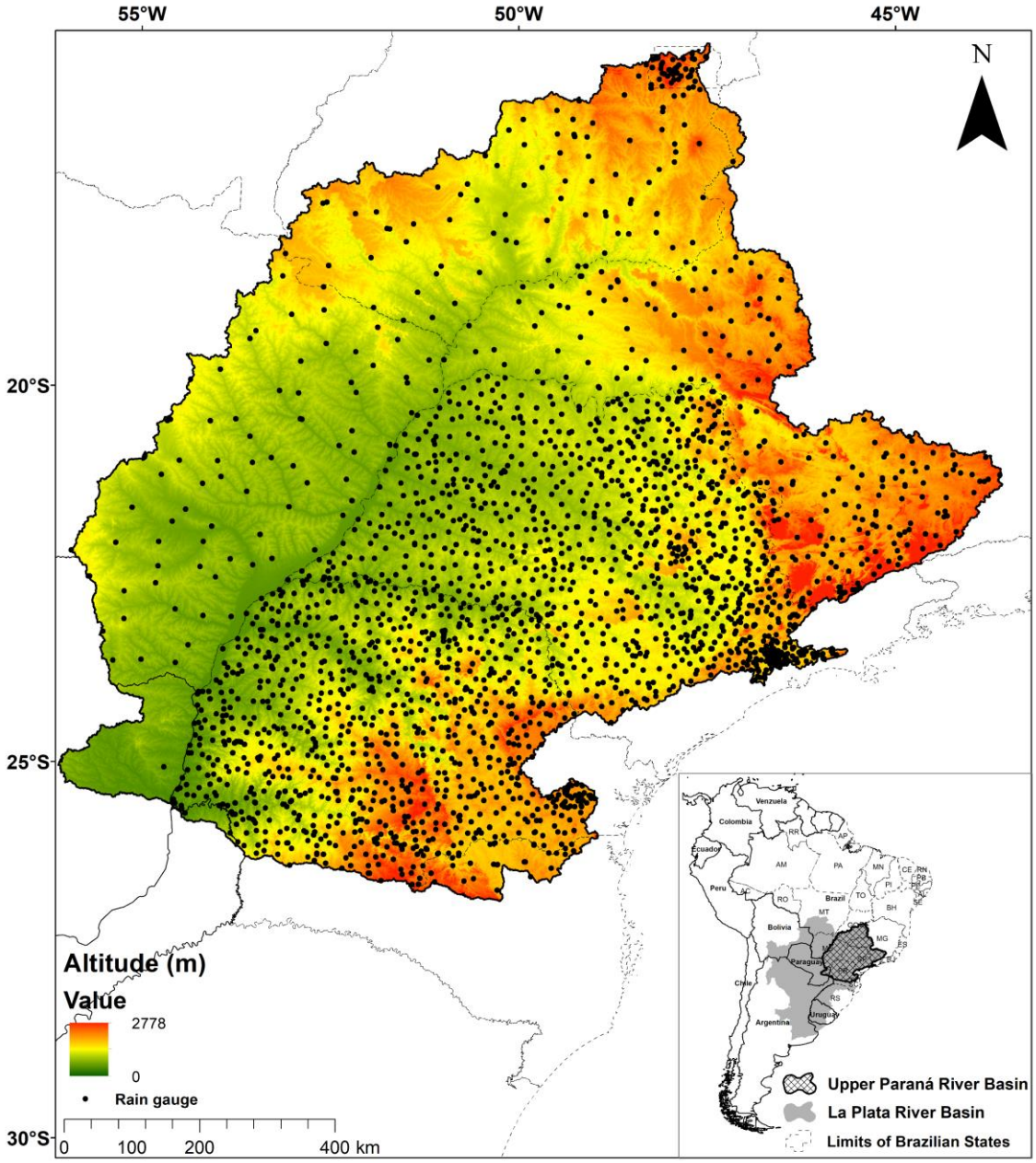

Figure 1. Location of the UPRB Basin showing the topographic patterns and the spatial distribution of rain gauges within the basin.

2.2. SWAT model

Hydrologic response to LUCC was estimated using the SWAT model with an ArcGIS interface (Arnold et al., 1998, https://swat.tamu.edu). SWAT is a semi-distributed and physically based model used both for small (Ferrant et al., 2011) and large-scale (Rajib and Merwade, 2017) river basins applications. The model has been extensively

applied for different approaches such as climate change effects on hydrologic processes (Ficklin et al., 2009), LUCC impacts to streamflow, sediment and water quality (Chotpantarat and Boonkaewwan, 2018), and climate variability effects on snowmelt (Wu and Johnston, 2007). SWAT operates on a daily time step and discretizes the basin into multiple subbasins. Based on user-defined thresholds, each subbasin is further divided into Hydrologic Response Units (HRUs), accounting for the combinations of slope, soil, and land use class. For further detailed description of the SWAT model, the reader is referred to Neitsch et al. (2011).

2.2.1. Data

Table 1 presents an overview of the input data used on the SWAT run experiments that are the basis for this work. The daily climatic data were organized for the simulation period from 1979 to 2015, with the first five years used for warm up the model (1979 – 1983), the following 21 years for calibration (1984 – 2004), and the last 11 years for validation (2005 – 2015). The precipitation database was built using daily rainfall series from 2,494 rain gauge stations within the basin (black dots on Figure 1) provided by the Brazilian National Water Agency (ANA). The data were interpolated to a spatial resolution of 0.1 degree using the Inverse Distance Weighted (IDW) method following previous study (Abou Rafee et al., 2019). Daily minimum and maximum temperature, solar radiation, relative air humidity, and wind speed data were derived from the National Centers for Environmental Prediction— Climate Forecast System Reanalysis (CFSR) at 38-km grid spacing. Topographic data at a 90-meter resolution obtained from the Shuttle Radar Topography Mission (SRTM) were used. The soil data were the same used by Abou Rafee et al. (2019), based on the information provided by the Brazilian Agriculture Research Corporation (EMBRAPA), except for the Paraguayan portion of UPRB, which was derived from the Harmonized World Soil Database (HWSD). To evaluate the

performance of the model, monthly time series of discharge over the period 1984 – 2015 from ANA and the Brazilian National Electrical System Operator (ONS) were used.

Table 1. Overview of the model input data.

Data	Description	Source
Topography	90-meter resolution Digital Elevation Model (DEM)	Shuttle Radar Topography Mission (SRTM) (http://srtm.csi.cgiar.org/srtmdata/)
Land use and cover	30-meter resolution classification (1985 and 2015)	(Rudke, 2018; Rudke et al., 2019)
Soil	Derived from 1:500000 scale digital map	Brazilian Agriculture Research Corporation (EMBRAPA) (https://www.embrapa.br/solos/sibcs/solos-do-brasil) Harmonized World Soil Database (HWSD) (http://www.fao.org/nr/land/soils/)
Precipitation	Daily (1979 – 2015)	Brazilian National Water Agency (ANA) (http://www.snirh.gov.br/hidroweb)
Maximum and minimum temperature; relative humidity; wind speed; and solar radiation	Daily (1979 – 2015)	Climate Forecast System Reanalysis (CFSR) (https://globalweather.tamu.edu)
Discharge	Monthly (1984 – 2015)	Brazilian National Water Agency (ANA) (http://www.snirh.gov.br/hidroweb) Brazilian National Electrical System Operator (ONS) (http://www.ons.org.br)

Two Land Use and Cover (LUC) scenarios under unchanged climatic conditions were simulated. The two scenarios correspond to the validated LUC classifications for the years 1985 and 2015 performed by Rudke, (2018) and Rudke et al. (2019). Both LUC

were generated at a spatial resolution of 30 meters using pixel-based image classifiers, with the Support Vector Machine (SVM) algorithm. Based on the Rudke (2018) and Rudke et al. (2019) generated classifications, the LUCC maps for the UPRB was reclassified into six major classes: forest, cropland, grassland, water, cerrado (Brazilian savanna), and urban areas (Figure 2).

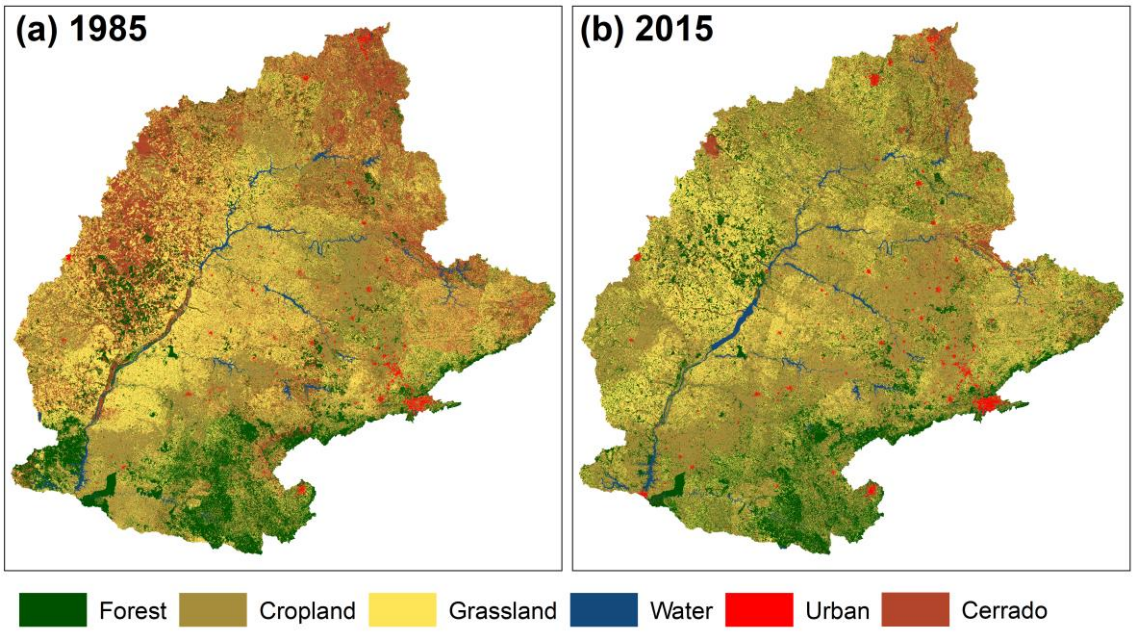

Figure 2. Land use and cover (LUC) classes for 1985 (a) and 2015 (b).

2.2.2 Model set up

The SWAT model project for the UPRB was built with the highest possible spatial discretization. The slopes were divided into five classes ranging between 0 – 3%, 3 – 8%, 8 – 20%, 20 – 45%, and > 45%. The basin was discretized into 5,187 subbasins with an average drainage area of 173 km^2 (Figure 3). To represent the spatial heterogeneity across the UPRB, these subbasins were further divided into HRUs using a defined threshold for both simulations of 5% for LUC, 10% for soil, and 20% for slope classes. As a result, 44,635 (LUC 2015) and 50,272 (LUC 1985) HRUs were generated. The Soil Conservation Service curve number (CN) (USDA Soil Conservation Service, 1972) and

the Penman-Monteith (Monteith J. L., 1965) methods were used to compute the surface runoff and potential evapotranspiration, respectively. For groundwater flow SWAT considers shallow (unconfined) and deep (confined) aquifers, which are responsible for returning flow to the stream and flow outside the basin, respectively (Neitsch et al., 2011).

The best-fit calibration parameters by Abou Rafee et al. (2019) were used. Abou Rafee et al. (2019) applied the SWAT model to estimate discharge values for the UPRB considering LUC from 2015 for the same period as the current study (1984 – 2015). Using the multi-site calibration technique (Leta et al., 2017), Abou Rafee et al. (2019) calibrated and validated the model for 78 outlets using the Sequential Uncertainty Fitting (SUFI-2) algorithm (Abbaspour et al., 2004), available in SWAT-CUP (Soil and Water Assessment Tool Calibration and Uncertainty Program, Abbaspour, 2015). In addition to Abou Rafee et al. (2019), the current study applied manual calibration for parameters related to plant growth to adjust the Leaf Area Index (LAI) curve for forest, cerrado, and grassland using the modified plant growth module provided by Strauch and Volk, (2013). Although SWAT has been applied for tropical basins, previous studies reported that its plant growth module is not suitable in a system that has perennial tropical vegetation since the model was originally designed for temperate areas (Alemayehu et al., 2017; P. D. Wagner et al., 2011; Strauch and Volk, 2013; Van Griensven et al., 2012). The LUC data from 2015 was used in the calibration process and to evaluate the performance of the model.

2.3. Analysis of the effects of LUCC

The effects of LUCC on the hydrologic components under unchanged climatic conditions of the UPRB were evaluated as follows:

I. To address the main LUCC between 1985 and 2015 in the basin, 9 major transitions of four LUC classes were calculated: Cerrado to forest; Grassland to

forest; Cropland to forest; Forest to grassland; Cerrado to grassland; Cropland to grassland; Forest to cropland; Cerrado to cropland; and Grassland to cropland.

II. To identify the effects of LUCC on hydrology within the UPRB, the surface runoff, actual evapotranspiration, soil moisture, and discharge were analyzed.

III. The aforementioned hydrologic components were calculated by the relative change for the simulation with the LUC from 2015 relative to the simulation with LUC from 1985. Changes were examined for annual (hydrological year, from October to September), wet (October – March), and dry (April – August) seasons considering the calibrated and validated period from 1984 to 2015.

IV. The hydrological variables were calculated using the 5,187 watersheds discretization of the UPRB, however, the results were illustrated and interpreted for the 34 major subbasins as shown in Figure 3.

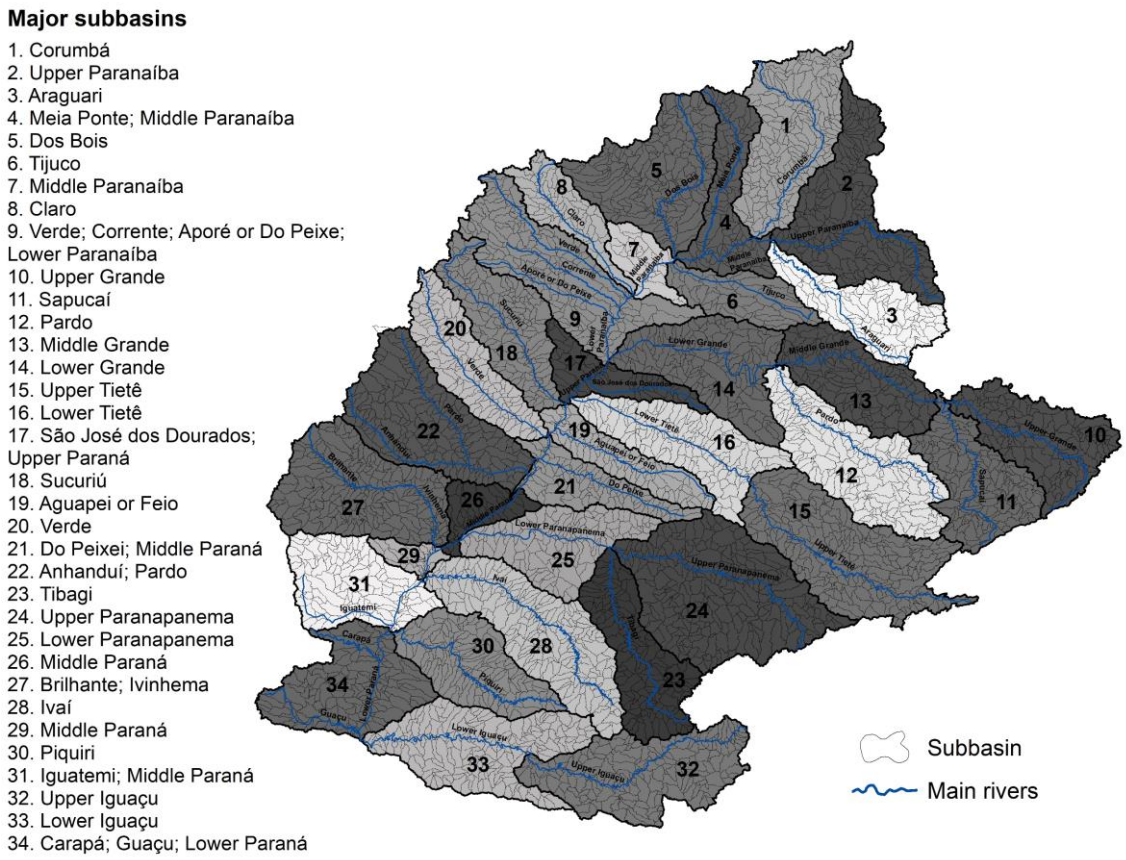

Figure 3. Subbasin discretization, major subbasins and main rivers of the UPRB.

3. Results and Discussion

3.1. SWAT model performance

The average monthly simulated LAI values considering all HRUs for the whole basin are presented in Figure 4. SWAT vegetation parameters were manually calibrated to match the magnitude and shape of LAI following previous studies (Bucci et al., 2008; Hoffmann et al., 2005; Negrón Juárez et al., 2009). The estimated values of LAI ranged between 2.5 and 5.5 $m^2 m^{-2}$ for forest, 0.7 and 2.5 $m^2 m^{-2}$ for cerrado, and 0.5 and 2.0 $m^2 m^{-2}$ for grassland. As shown in Figure 4, LAI varies seasonally with the highest values during the wet season (October – March), and lowest values in the dry season (April – September) due to the dormancy period. Forested areas within the UPRB correspond to

Atlantic Forest, a Brazilian biome that has several forest formations, including deciduous and perennials forests. Therefore, LAI presents great seasonality, reducing the photosynthetic capacity of the forest during the dry season. In perennial forests with a shorter dry season (approximately 3 months) such as the Amazon Rain Forest, values of LAI are higher and the monthly variation is lower, because deep roots and phenology increase the efficiency of photosynthesis during periods of abundant solar radiation but low water availability (Manoli et al., 2018; Morton et al., 2014; Saleska et al., 2016). In turn, the cerrado biome has at least five ecosystem physiognomies with several types of trees and grasses densities, ranging from open shrub to tree savanna and gallery forests (Cruz Ruggiero et al., 2002; Hoffmann et al., 2005). This causes lower values of LAI and greater seasonality, corresponding to a vegetation that decreases its photosynthetic capacity during the dry season (see Figure S1, S2, S3). LAI values from the current study are comparable to the simulated by Dos Santos et al., (2018), who used SWAT to evaluate the impacts of LUCC on hydrology in the Iriri River basin in Brazilian Amazon. Their results showed LAIs with annual averages of 4.02, 1.25, and 1.09 m^{-2} m^{-2} (versus 3.53, 1.49, and 1.23 $m^{-2}m^{-2}$ in this study) for the forest, cerrado, and grassland, respectively. The average monthly simulated LAI values for the forest, cerrado, grassland, and cropland at each subbasin (as divided in Figure 3) are available in the Supplementary Material (Figures S1, S2, S3, and S4).

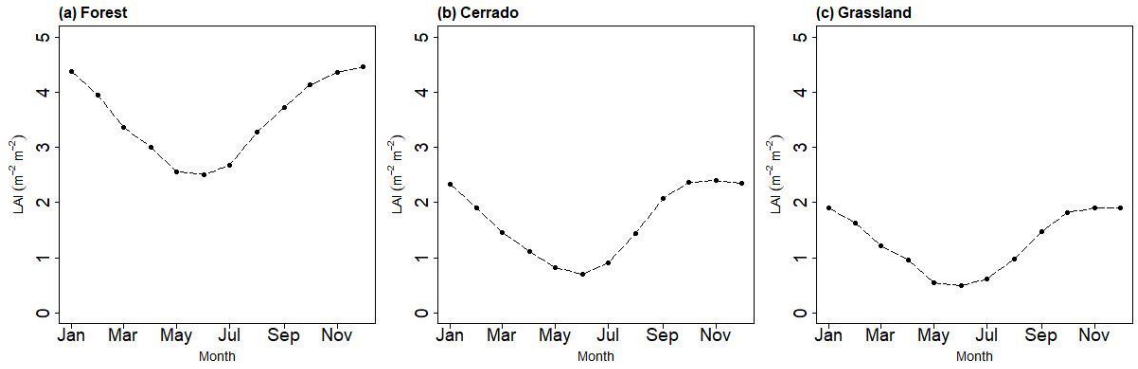

Figure 4. Average monthly simulated LAI values considering all HRUs from LUC 2015 scenario for Forest (a), Cerrado (b), and Grassland (c).

As shown in Figure 5, the simulated monthly discharge was consistent with observed data at the main rivers of the UPRB. However, the model tends to underestimate the low flow as well as the most extreme high flows. According to the performance rating proposed by Moriasi et al. (2007) and Thiemig et al. (2013), the simulations ranged from satisfactory to very good in the statistical indices presented in Table 2. During the calibration period (1984 – 2004), the percent bias (PBIAS) ranged from -0.2 to 6.4, the coefficient of determination (R^2) from 0.71 to 0.88, the Nash-Sutcliffe efficiency (NSE) from 0.7 to 0.8, the Kling-Gupt efficiency (KGE) from 0.7 to 0.9, and the ratio of standard deviation of observations to root mean square error (RSR) from 0.44 to 0.55. For the validation period (2005 – 2015), the simulations reached index values up to 0.7 for PBIAS and 0.92 for R^2 (at Grande river), and, 0.84 for NSE, 0.88 for KGE, and 0.4 for RSR (at Paranaíba river). It is important to mention that the discharge values currently estimated have higher accuracy compared to the results presented by Abou Rafee et al. (2019). The reason for the improved simulation was the better calibration of LAI by using the modified plant growth module (Strauch and Volk, 2013).

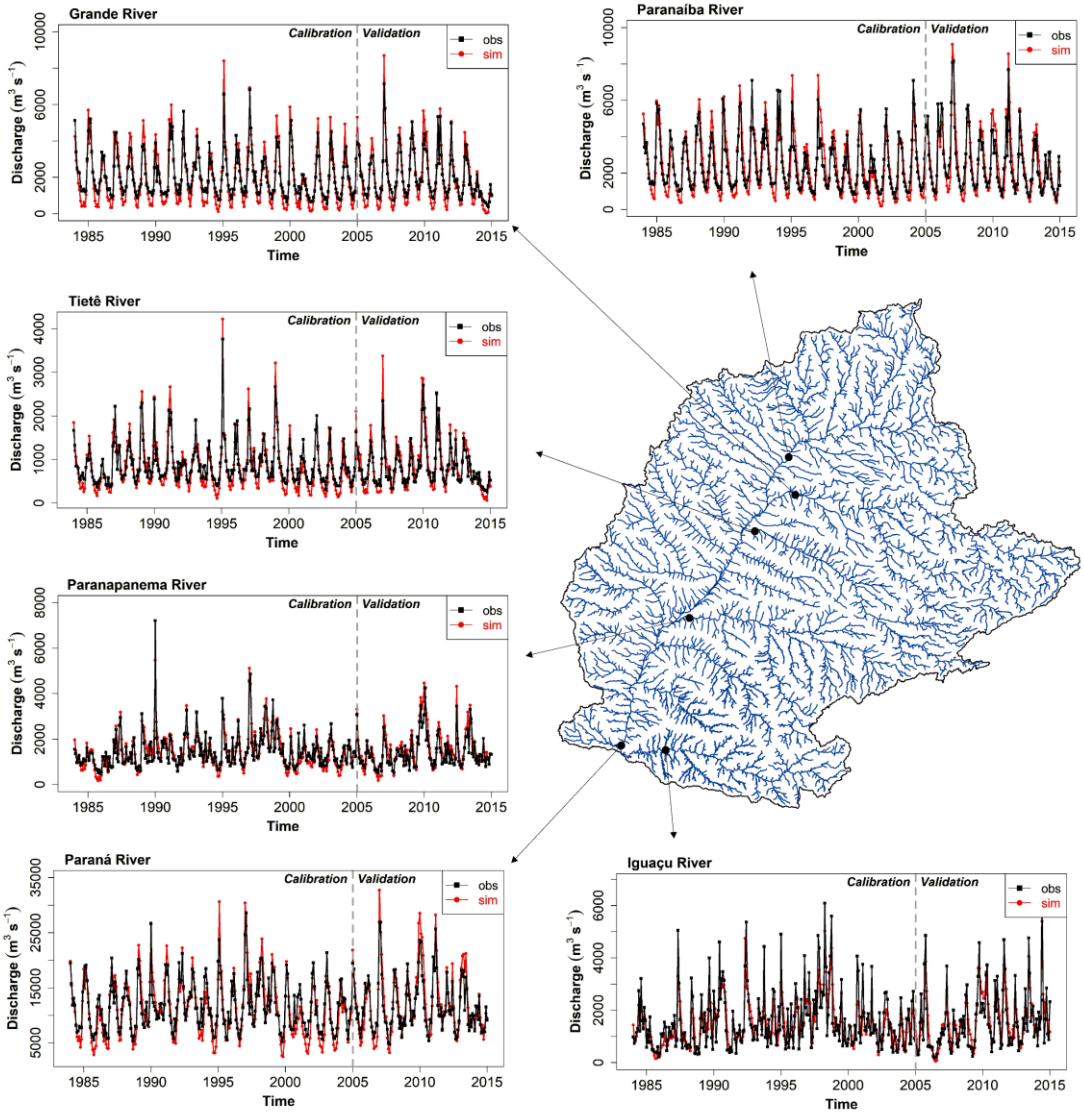

Figure 5. Comparison between the observed and simulated monthly discharge at the main rivers of the UPRB.

Table 2. SWAT model performance for the main rivers of the UPRB.

Outlet	Index*	Calibration (1984 - 2004)	Validation (2005 - 2015)	Whole Period
Paranaíba	PBIAS	0.1	-4.5	-1.5
	R^2	0.82	0.87	0.84
	NSE	0.76	0.84	0.79
	KGE	0.81	0.88	0.84
	RSR	0.49	0.40	0.45
Grande	PBIAS	6.4	0.7	4.5
	R^2	0.88	0.92	0.89
	NSE	0.75	0.82	0.78
	KGE	0.71	0.73	0.72
	RSR	0.5	0.42	0.47
Tietê	PBIAS	5.7	-3.9	2.6
	R^2	0.87	0.86	0.86
	NSE	0.78	0.74	0.77
	KGE	0.78	0.72	0.76
	RSR	0.47	0.51	0.48
Paranapanema	PBIAS	-0.2	-12.9	-4.6
	R^2	0.82	0.88	0.83
	NSE	0.80	0.74	0.78
	KGE	0.90	0.75	0.85
	RSR	0.44	0.51	0.46
Iguaçu	PBIAS	5.5	-0.8	3.3
	R^2	0.71	0.78	0.74
	NSE	0.70	0.77	0.72
	KGE	0.70	0.75	0.72
	RSR	0.55	0.48	0.52
Paraná	PBIAS	3.6	-6.2	0.2
	R^2	0.84	0.87	0.84
	NSE	0.75	0.75	0.75
	KGE	0.78	0.75	0.76
	RSR	0.50	0.50	0.50

Notes: ***PBIAS:** Percent bias (PBIAS); **R^2:** Coefficient of correlation; **NSE:** Nash-Sutcliffe efficiency (Nash and Sutcliffe, 1970); **KGE:** Kling-Gupt efficiency (Gupta et al., 2009); and **RSR:** Ratio of standard deviation of observations to root mean square error (Moriasi et al., 2007).

3.2. Detection of LUC transitions

Figure 6 shows the spatial distribution of the main transitions of LUC between 1985 and 2015 within the UPRB, and their total values are presented in Table 3. There was simultaneously deforestation and afforestation on different areas mainly within the central-western and northern parts of the basin. Cerrado had the greatest reduction of 173×10^3 km^2, which represents deforestation of about 19.2% of the original area in

1985. Cerrado was replaced mainly by cropland (75×10^3 km^2), followed by grassland (59×10^3 km^2), and forest (39×10^3 km^2).

In contrast, cropland class had the greatest gain with more than 250×10^3 km^2. The expansion of agriculture occurred mainly in the central and southern parts of the UPRB. In the central portion of the basin, almost 125×10^3 km^2 of grassland areas were replaced by cropland between 1985 and 2015. Most of these areas were replaced mainly by sugarcane cultivation due to the high demand for bioenergy in the form of ethanol and raw material for the thermoelectric power plants (Adami et al., 2012; Rudorff et al., 2010). Also, this growth is largely caused by the development of agricultural mechanization, climate conditions, population growth, and economic factors (Mueller & Mueller, 2016). Particularly, in the southern part of the basin, the main reason for the expansion of cropland was the construction of the Itaipu hydroelectric power plant (1974 – 1985) at the border between Brazil, Argentina, and Paraguay. This construction made an important contribution to rapid population growth in the region (Baer & Birch, 1984).

It is important to note that the UPRB had a considerable gain in forest cover ($\sim 120 \times 10^3$ km^2), mostly through the plantation of exotic tree species. The reforestation and the afforestation have been concentrated mostly in the central-western and northern parts of the UPRB. The increase in forests is mainly related to the transitions of the LUC classes of cerrado, grassland, and cropland to Eucalyptus plantations. According to the Brazilian Association of Forest Plantation Producers, the growth of Eucalyptus in Brazil has been mainly driven by the profit growth generated that is up to six times greater than the one of livestock production. Besides economic issues, Gonçalves et al. (2008) pointed out that the increase of Eucalyptus plantation is due to the investments in research and technology in the last decades, which improved seed or clonal plantations.

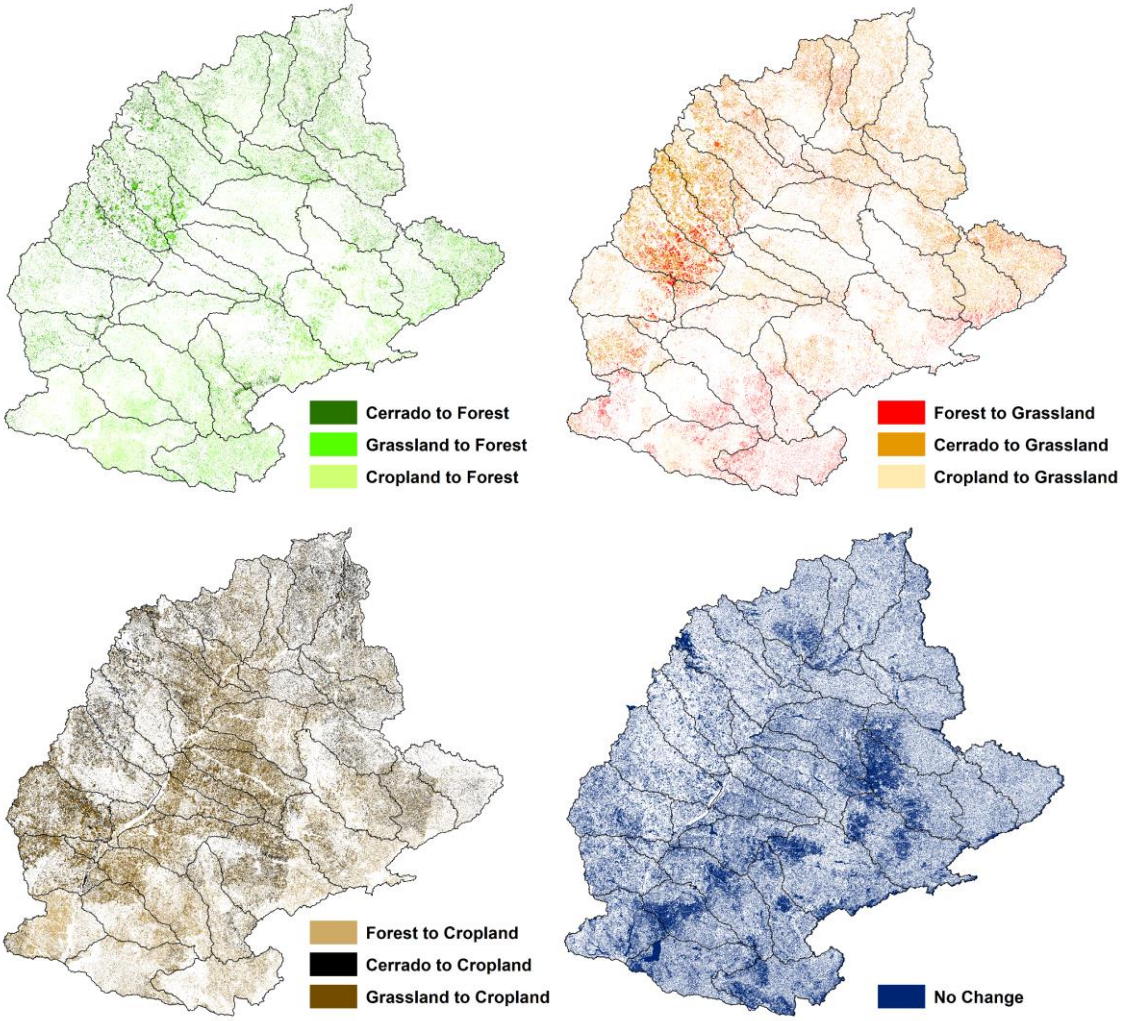

Figure 6. Spatial distribution of the main transitions of LUC between 1985 and 2015.

Table 3. Area (10^3 km^2) and Relative change (%) of the main transitions of LUC between 1985 and 2015 at the UPRB.

Transition	Area (10^3 km^2)	Percentage (%)
Cerrado to Forest	39.11	4.34
Cerrado to Grassaland	59.03	6.56
Cerrado to Cropland	75.01	8.33
Forest to Grassland	33.65	3.74
Forest to Cropland	56.40	6.26
Cropland to Grassland	47.10	5.23
Cropland to Forest	36.33	4.03
Grassland to Cropland	124.78	13.86
Grassland to Forest	43.97	4.88
Other	58.92	6.54
No Change	326.19	36.22

Figure 7 shows the total area of the main transitions of LUC between 1985 and 2015 at the major subbasin level. The largest areas of LUCC were the conversion from grassland to cropland occurred within the Brilhante/Invinheima (27) and Lower Tietê (16) subbasins, which reached up to 8,490 and 9,250 km^2, respectively. Besides, in the Carapá/Guaçu/Lower Paraná (34) subbasin, 6,640 km^2 of forests were replaced by cropland areas. It is also worth mentioning that the increase of cropland happened over areas that were previously covered with cerrado. Deforestation of cerrado contributed to an increase of up to 6,550 km^2 in cropland areas in the Corumbá (1) and Upper Paranaíba (2) subbasins. Still, cerrado reductions also had a significant contribution to the grassland expansion. For example, about 6,670 km^2 of cerrado were deforested replaced by grassland in the Anhanduí/Pardo (22) subbasin. As mentioned before, the central-western and northern parts of the basin were the ones that most had afforestation in the last recent decades. For example, the transition from cerrado to forest in the Corumbá (1) and

Anhanduí/Pardo (22) subbasins contributed to a forest cover increase of up to 3,070 and 3,040 km^2, respectively.

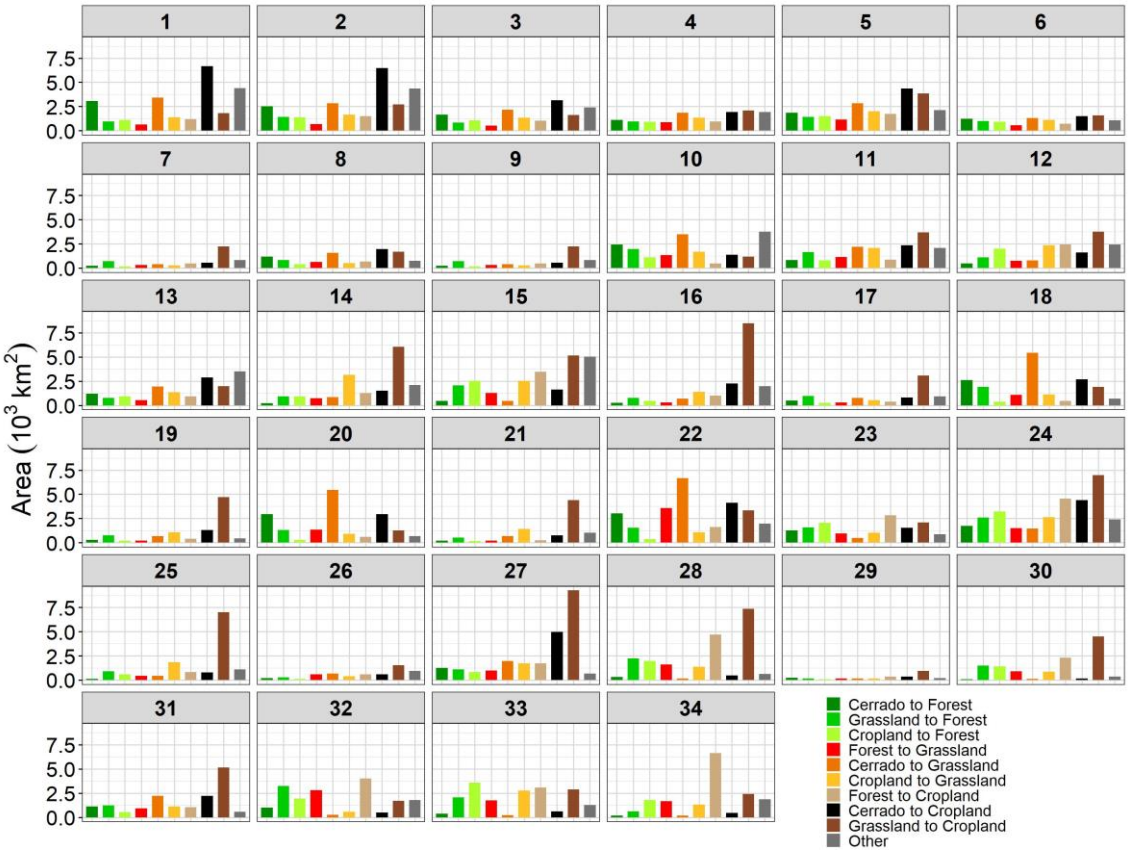

Figure 7. Area (10^3 km^2) of the main transitions of LUC between 1985 and 2015 at the major subbasins of UPRB. **1.** Corumbá; **2.** Upper Paranaíba; **3.** Araguari; **4.** Meia Ponte-Middle Paranaíba; **5.** Dos Bois; **6.** Tijuco; **7.** Middle Paranaíba; **8.** Claro; **9.** Verde-Corrente-Aporé or Do Peixe-Lower Paranaíba; **10.** Upper Grande; **11.** Sapucaí; **12.** Pardo; **13.** Middle Grande; **14.** Lower Grande; **15.** Upper Tietê; **16.** Lower Tietê; **17.** São José dos Dourados-Upper Paraná; **18.** Sucuriú; **19.** Aguapei or Feio; **20.** Verde; **21.** Do Peixei-Middle Paraná; **22.** Anhanduí-Pardo; **23.** Tibagi; **24.** Upper Paranapanema; **25.** Lower Paranapanema; **26.** Middle Paraná; **27.** Brilhante-Invinheima; **28.** Ivaí; **29.** Middle Paraná; **30.** Piquiri; **31.** Iguatemi-Middle Paraná; **32.** Upper Iguaçu; **33.** Lower Iguaçu; **34.** Carapá-Guaçu-Lower Paraná.

3.3. Effects of LUCC on Hydrology

The two simulated scenarios for the LUC from 1985 and 2015 with unchanged climatic conductions were compared. The effects of LUCC on hydrologic components within the basin are illustrated in the spatial distribution of changes in surface runoff, actual evapotranspiration, and soil moisture (Figure 8). These changes were calculated considering the long-term means (1984 – 2015) from the difference between LUC2015 and LUC1985 simulated hydrologic variables for annual (October – September), wet (October – March), and dry (April – September) season values. Also, to address the LUCC impacts for interannual variation of climate, box plots of annual and seasonal from 32 years (1984 – 2015) for hydrological variables were calculated (see Figure 9), considering the means values of simulated hydrological variables at the major subbasin level (as shown in Figure 3).

3.3.1. Surface runoff, actual evapotranspiration, and soil moisture

Overall, the LUC caused an increase in the annual and wet season surface runoff, while a decrease in the dry period (Figures 8 and 9). The interannual values show that the increases at the major subbasins level reach up to 31.8 and 25.3 mm in the annual and wet season runoff, respectively. In contrast, the decrease overtakes 5.6 mm in the dry season. The effects are remarkable at the Corumbá (1), Upper Paranaíba (2), Corrente, Aporé or do Peixe (9), and Carapá-Guaçu-Lower Paraná (34) subbasins. In these regions, a major cause for the increase in surface runoff is the substantial removal of the cerrado and forest vegetation, replaced mainly to cropland and grassland (see Figure 7). In addition, it was observed a significant increase in the Lower Tietê (16), Brilhante-Invinheima (27), Piquiri (30) watersheds. However, in these regions, an expressive reduction of cerrado and grassland areas replaced by cropland was observed. Similar results were reported by

previous studies elsewhere. For instance, Ghaffari et al. (2010) demonstrated that the decrease of grassland areas to other LUC types such as agriculture, led to an increase of 33% in the surface runoff amount in the Zanjanrood Basin, Northwest Iran. Baker and Miller (2013) have used SWAT to assess the LUCC on water resources in an East African Watershed. They also reported increases in the surface runoff related to natural vegetation suppression.

In addition, it should be noted in the spatial distribution (Figure 8) that small catchments presented a decrease in surface runoff during the wet season. This could be attributed to the increase in forest areas due to the afforestation (e.g. cerrado to forest) and reforestation (e.g. grassland to forest). Li et al. (2015) reported similar results investigating the impacts of LUCC on surface runoff and water yield, in the upper and middle reaches of the Heihe River Basin, China. Their results showed that the forest expansion led to a significant decrease in the surface runoff during months with the largest precipitation. Still, in China, Huang et al. (2003) observed a reduction of about 32% in cumulative runoff as a result of afforestation in a watershed of the Loess Plateau.

In SWAT, the surface runoff is estimated by the Curve Number (CN) method (USDA Soil Conservation Service, 1972). CN varies spatially according to land use, soil type, and slope. It can be easily interpreted by the order of higher values: Urban>Cropland>Grassland>Cerrado>Forest. Consequently, the increase or decrease in the generated runoff during the period could be explained by the major conversions of LUC in the basin such as from cerrado to cropland, or from grassland to cropland. Also, CN has temporal variation due to changes in soil moisture. During the dry season, a possible explanation for the decreasing amounts of surface runoff is due to the reduction in the water content storage. Lin et al. (2015) who applied the SWAT model also observed

runoff decrease due reduction in soil water storage during dry season over deforestation areas in the south-eastern Fujian Province of China.

In contrast to surface runoff, a decrease in the actual evapotranspiration mainly in the annual and wet season was observed. A decrease greater than 200 mm mostly in central-western (e.g. Anhanduí-Pardo (22)) and southern parts (e.g. Carapá-Guaçu-Lower Paraná (34)) of the basin (Figure 8) was observed. For instance, in these watersheds it was observed a median decrease up to 110, 87, and 21 mm in the annual, wet and dry season, respectively (Figure 9). Similar to surface runoff, this is likely because of the natural vegetation suppression that were replaced by cropland areas. Besides the area of LUCC, the different magnitude of evapotranspiration reduction within the subbasins could be associated with available soil water and the incidence of solar radiation. Cabral et al. (2012) reported higher evapotranspiration from sugarcane plantation under higher rainfall amounts. Also, Da Rocha et al. (2009) observed that evaporation rates increased under higher precipitation amounts and solar radiation over tropical biome within forest and savanna areas. Wang et al. (2014) also found alterations in hydrology processes due to LUCC, in which the evaporation decreased by 2.13% and 2.41% between 2000 and 2010 with the decrease of natural vegetation areas. The reduction in the actual evapotranspiration values is explained by the shallower roots of cropland or grassland compared to natural vegetation (forest or cerrado), which leads to less access to deep soil moisture (Nepstad et al., 1994; Oliveira et al., 2005). Also, the mean LAI values are smaller which consequently decreases the transpiration.

It is important to highlight that even in the dry season, the spatial distribution (Figure 8) shows that in the Carapá-Guaçu-Lower Paraná (34) and Lower Iguaçu (33) subbasins there is a significant increase in the amounts of surface runoff and decrease in the actual evapotranspiration. Besides the influence of LUCC, the precipitation in this

region in the dry period is different from the other parts of the basin. In these parts of the UPRB, the precipitation is spread out throughout the year and reaches between 700 and 900 mm between April and September (see Supplementary Material, Figure S5). The occurrence of precipitation in this period is associated mainly with cold fronts that are common in winter (June – August).

As shown in Figure 8, the impacts of LUCC on soil moisture storage ranged from an increase up to 400 mm to a decrease up to 100 mm within the major subbasin level. Similar to surface runoff, it was observed mainly an increase in the wet and annual values, and a decrease in the dry season. The higher values of soil moisture during the wet season are explained by the reduction of actual evapotranspiration. As mentioned previously, it occurred as a result of the removal of cerrado areas and the expansion of cropland in the basin. Similar results are reported by previous studies measurements. For instance, Fu et al. (2003) evaluated through soil profile measurements the effects of seven land use types on soil moisture at the Danangou catchment on the Loess Plateau of China. They reported higher mean soil moisture content in cropland and grassland compared to natural vegetation such as Shrubland and woodland. Also, the results presented are in accordance with other hydrological model land use applications. Using the Variable Infiltration Capacity (VIC) model, Costa-Cabral et al. (2008) investigated the influence of LUC on soil moisture in the Mekong River Basin. The authors reported that the highest values of soil moisture occur more in agricultural areas than forest or grassland during the wet season.

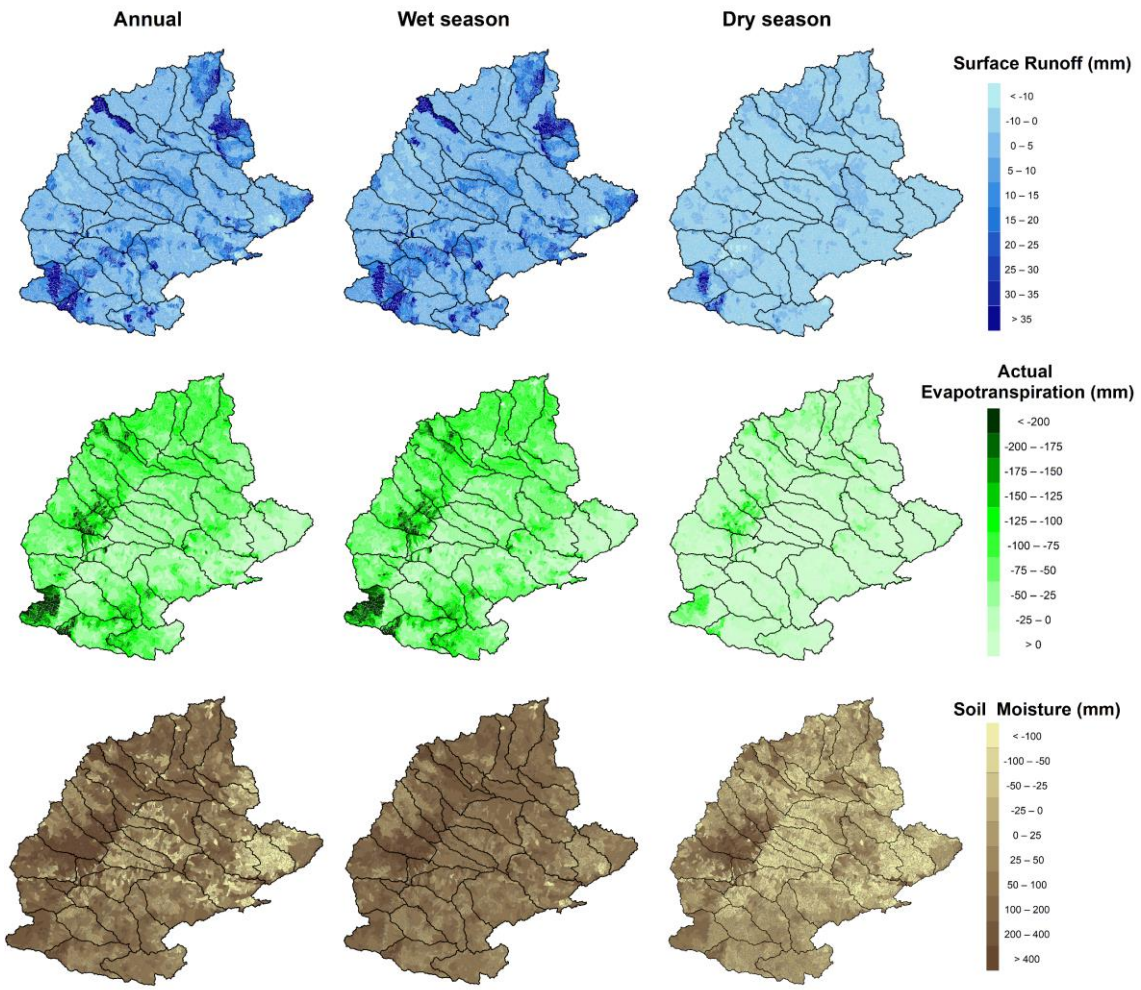

Figure 8. Spatial distribution of changes (mm) in surface runoff, actual evapotranspiration, and soil moisture considering the long-term means (1984 – 2015) for the annual, wet, and dry season values calculated from the difference between the simulated scenarios (LUC2015 minus LUC1985).

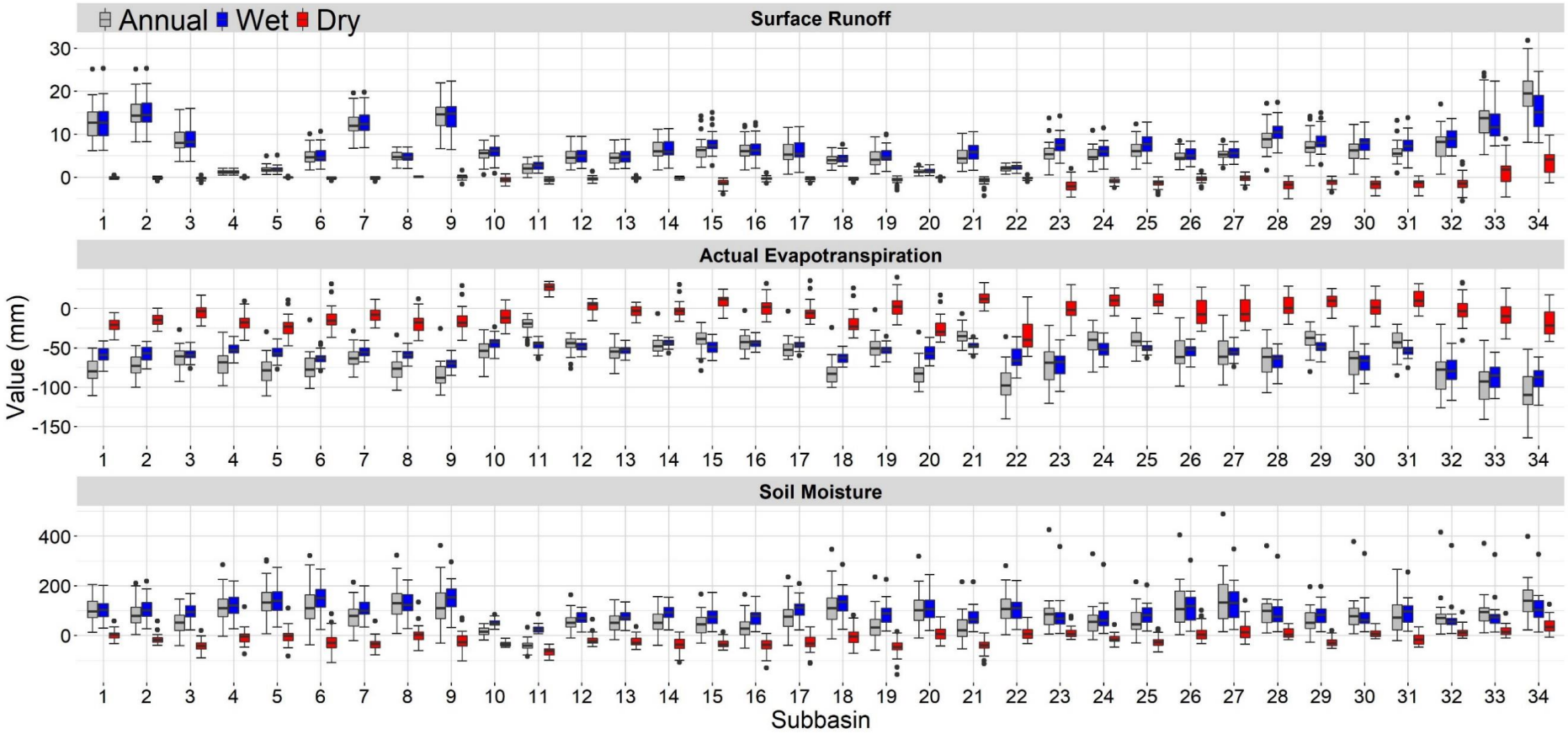

Figure 9. Box plots of surface runoff, actual evapotranspiration, and soil moisture for annual and seasonal (wet and dry) values from 32 years (1984 – 2015). There were calculated from the difference between the simulated scenarios (LUC2015 minus LUC1985) at major subbasin level. **1.** Corumbá; **2.** Upper Paranaíba; **3.** Araguari; **4.** Meia Ponte-Middle Paranaíba; **5.** Dos Bois; **6.** Tijuco; **7.** Middle Paranaíba; **8.** Claro; **9.** Verde-Corrente-Aporé or Do Peixe-Lower Paranaíba; **10.** Upper Grande; **11.** Sapucaí; **12.** Pardo; **13.** Middle Grande; **14.** Lower Grande; **15.** Upper Tietê; **16.** Lower Tietê; **17.** São José dos Dourados-Upper Paraná; **18.** Sucuriú; **19.** Aguapei or Feio; **20.** Verde; **21.** Do Peixei-Middle Paraná; **22.** Anhanduí-Pardo; **23.** Tibagi; **24.** Upper Paranapanema; **25.** Lower Paranapanema; **26.** Middle Paraná; **27.** Brilhante-Invinheima; **28.** Ivaí; **29.** Middle Paraná; **30.** Piquiri; **31.** Iguatemi-Middle Paraná; **32.** Upper Iguaçu; **33.** Lower Iguaçu; **34.** Carapá-Guaçu-Lower Paraná.

3.3.2. River Discharge

Figure 10 shows the temporal evolution of relative changes (%) in discharge under the scenario for the year 2015 relative to 1985. Values for annual, dry, and wet seasons were calculated considering the river mouth of the main rivers from the major subbasin level of the UPRB. Only the rivers with the highest values of discharge and those that had significant LUCC are shown. The remain results are available in Figure S6, in the Supplementary Material.

The simulation results revealed that the LUCC between 1985 and 2015 had an expressive impact on discharge values. Overall, the LUCC implied an increase in the annual's and wet season's discharges at the main rivers of the UPRB. The major relative changes in discharge were observed at the Lower Tietê, Anhanduí, Ivinhema, and Guaçu rivers. For instance, an increase of more than 29% in annual mean values was found at the Guaçu river. All of these subbasins have in common a significant reduction in natural vegetation (forest or cerrado). On the other hand, a decrease was observed during the dry period, except for Anhandui and Guaçu rivers. A mean decrease of more than 4% was observed at the Lower Tietê, Lower Paranapanema, and Sucuriú rivers. This behavior decreases the effect of annual increased discharge in many rivers of the basin. For example, at the river mouth of UPRB, over the lower Paraná River, it was observed an increase in the annual discharge of only 1.13%, an increase of 4.25% in the wet, and a decrease of only 2.24% in the dry season.

Surface runoff is one of the major contributors to discharge. Thereby, the changes in annual and wet season discharge values are likely associated with the increase of generated runoff in the subbasins. The results presented are consistent with other large-scale simulations. For instance, Costa et al. (2003) analyzed the effects of large-scale changes on the discharge of the Tocantins Rivers, Southeastern Amazonia. The authors

observed an increase in the average annual long-term discharge due to the conversion of the natural vegetation to cropland and grassland.

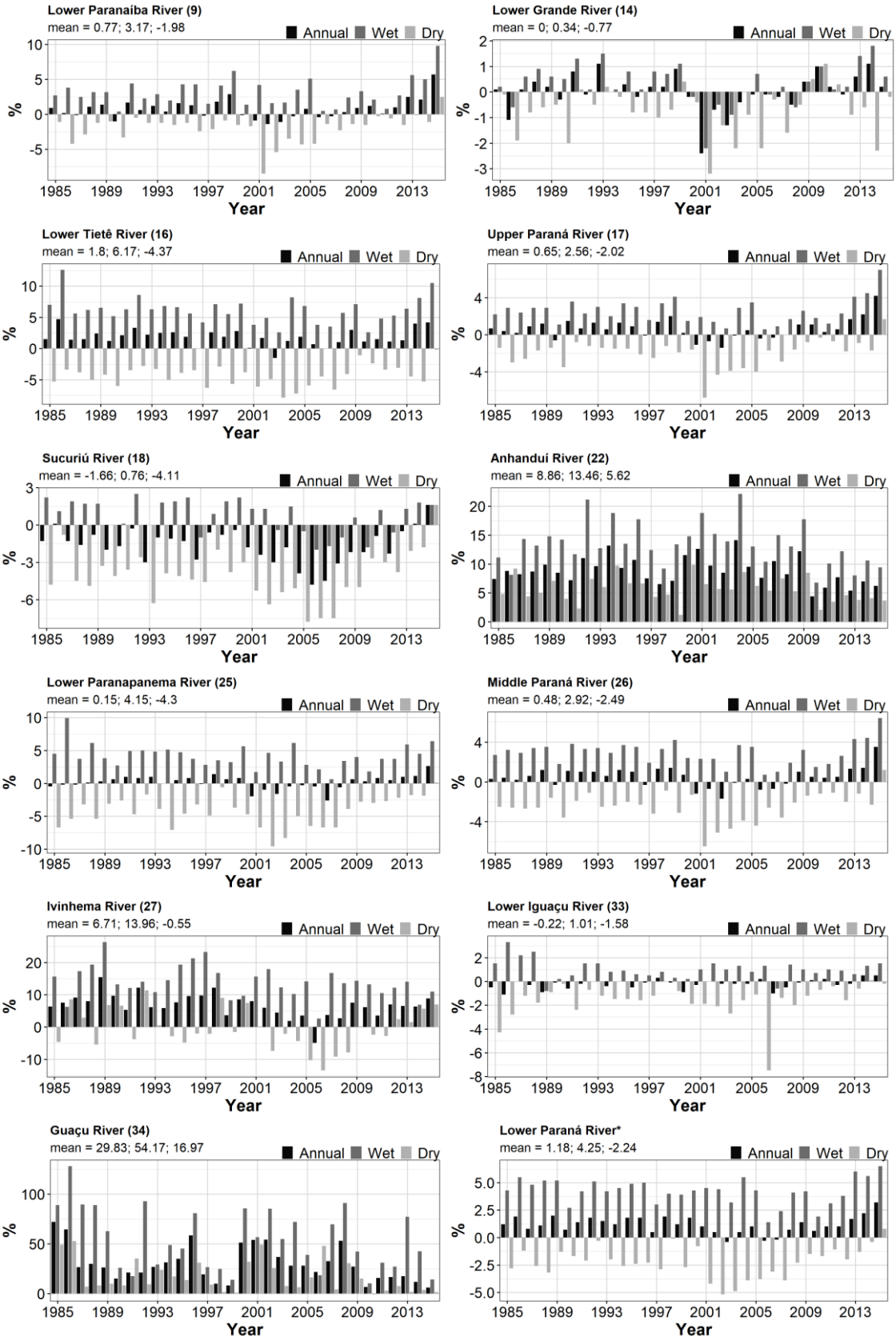

Figure 10. Temporal evolution of relative changes (%) in discharge for annual, wet and dry seasons under the scenarios for the year 2015 relative to 1985 at the main rivers of the UPRB. At the top left of the plots are shown the mean values and the name of the rivers with the respective number of the subbasin. *The last graph represents the river mouth of the UPRB.

4. Summary and conclusions

This paper analyzed the hydrologic response to LUCC between 1985 and 2015 in the UPRB. The effects of LUCC on hydrologic variables were addressed for the hydrological annual (October – September), wet season (October – March) and dry season (April – September) using the calibrated and validated SWAT model from January 1984 to December 2015. The following conclusions can be drawn:

I. Satisfactory SWAT calibration and validation of monthly discharge and LAI values were achieved for the main rivers of the UPRB. Thereby, the proposed project could be used not only for evaluating LUCC but also for climate change and climate variability scenarios.

II. Simulation results revealed that most of the major subbasins presented an increase in the runoff generated and soil moisture amounts in the annual and wet season values, while a decrease in the dry season. In contrast, a significant decrease in actual evapotranspiration in the annual and wet season values was observed.

III. The major changes in the hydrologic components in the UPRB were observed in the central-western and southern parts following the largest areas of LUCC.

IV. Overall, LUCC in the basin caused an increase (decrease) in discharge in the wet (dry) season. For hydrology annual values, several largest rivers had little changes in their discharge due to the compensation of discharge in the wet and dry season. A clear example is the Lower Paraná River, which had a mean increase in annual discharge of 1.13%, while in the wet and dry seasons, an increase and decrease of 4.25 and -2.24%, respectively, were observed.

This work is the first to address the LUCC over the whole UPRB at a high spatial resolution simulation. The provided results were presented and discussed at 34 major

subbasins that have not been covered by previous research. Therefore, the outcomes of this study have valuable information that can be used to improve the planning and sustainable management as well as to support strategies to minimize the impacts of LUCC on water resources in the UPRB.

Acknowledgments. This study was financed in part by the "Coordenação de Aperfeiçoamento de Pessoal de Nível Superior – Brasil" (CAPES) - Finance Code 001 (Process # 88887.115875/2015-01) and "Fundação de Amparo à Pesquisa do Estado de São Paulo" FAPESP (process #2015/03804-9). The authors would like to gratefully acknowledge "Agência Nacional de Águas" (ANA) by providing the precipitation and discharge data.

References

Abbaspour, K.C., 2015. SWAT-CUP: SWAT Calibration and Uncertainty Programs - A User Manual. Sci. Technol. https://doi.org/10.1007/s00402-009-1032-4

Abbaspour, K.C., Johnson, C.A., van Genuchten, M.T., 2004. Estimating Uncertain Flow and Transport Parameters Using a Sequential Uncertainty Fitting Procedure. Vadose Zo. J. 3, 1340–1352. https://doi.org/10.2136/vzj2004.1340

Abou Rafee, S.A., Freitas, E.D., Martins, J.A., Martins, L.D., Domingues, L.M., Nascimento, J.M.P., Machado, C.B., Santos, E.B., Rudke, A.P., Fujita, T., Souza, R.A.F., Hallak, R., Uvo, C.B., 2020. Spatial Trends of Extreme Precipitation Events in the Paraná River Basin. J. Appl. Meteorol. Climatol. 59, 443–454. https://doi.org/10.1175/JAMC-D-19-0181.1

Abou Rafee, S.A., Uvo, C.B., Martins, J.A., Domingues, L.M., Rudke, A.P., Fujita, T., Freitas, E.D., 2019. Large-scale hydrological modelling of the Upper Paraná River Basin. Water (Switzerland). https://doi.org/10.3390/w11050882

Adami, M., Rudorff, B.F.T., Freitas, R.M., Aguiar, D.A., Sugawara, L.M., Mello, M.P., 2012. Remote sensing time series to evaluate direct land use change of recent expanded sugarcane crop in Brazil. Sustainability. https://doi.org/10.3390/su4040574

Alemayehu, T., Van Griensven, A., Woldegiorgis, B.T., Bauwens, W., 2017. An improved SWAT vegetation growth module and its evaluation for four tropical ecosystems. Hydrol. Earth Syst. Sci. https://doi.org/10.5194/hess-21-4449-2017

Antico, A., Torres, M.E., Diaz, H.F., 2016. Contributions of different time scales to extreme Paraná floods. Clim. Dyn. 46, 3785–3792. https://doi.org/10.1007/s00382-015-2804-x

Arnold, J.G., Srinivasan, R., Muttiah, R.S., Williams, J.R., 1998. Large Area Hydrologic Modelling and Assessment Part I : Model Development. Am. Water Resour. Assoc. https://doi.org/10.1111/j.1752-1688.1998.tb05961.x

Baer, W., Birch, M.H., 1984. Expansion of the economic frontier: Paraguayan growth in the 1970s. World Dev. https://doi.org/10.1016/0305-750X(84)90074-3

Baker, T.J., Miller, S.N., 2013. Using the Soil and Water Assessment Tool (SWAT) to assess land use impact on water resources in an East African watershed. J. Hydrol. 486, 100–111. https://doi.org/10.1016/j.jhydrol.2013.01.041

Boserup, E., 2014. The conditions of agricultural growth: The economics of agrarian change under population pressure, The Conditions of Agricultural Growth: The Economics of Agrarian Change Under Population Pressure. https://doi.org/10.4324/9781315070360

Bucci, S.J., Scholz, F.G., Goldstein, G., Hoffmann, W.A., Meinzer, F.C., Franco, A.C., Giambelluca, T., Miralles-Wilhelm, F., 2008. Controls on stand transpiration and soil water utilization along a tree density gradient in a Neotropical savanna. Agric. For. Meteorol. https://doi.org/10.1016/j.agrformet.2007.11.013

Cabral, O.M.R., Rocha, H.R., Gash, J.H., Ligo, M.A.V., Tatsch, J.D., Freitas, H.C., Brasilio, E., 2012. Water use in a sugarcane plantation. GCB Bioenergy. https://doi.org/10.1111/j.1757-1707.2011.01155.x

Camilloni, I.A., Barros, V.R., 2003. Extreme discharge events in the Paraná River and their climate forcing. J. Hydrol. 278, 94–106. https://doi.org/10.1016/S0022-1694(03)00133-1

Carvalho, L.M.V., Jones, C., Liebmann, B., 2004. The South Atlantic convergence zone:

Intensity, form, persistence, and relationships with intraseasonal to interannual activity and extreme rainfall. J. Clim. https://doi.org/10.1175/1520-0442(2004)017<0088:TSACZI>2.0.CO;2

Carvalho, L.M.V., Jones, C., Silva, A.E., Liebmann, B., Silva Dias, P.L., 2011. The South American Monsoon System and the 1970s climate transition. Int. J. Climatol. 31, 1248–1256. https://doi.org/10.1002/joc.2147

Chotpantarat, S., Boonkaewwan, S., 2018. Impacts of land-use changes on watershed discharge and water quality in a large intensive agricultural area in Thailand. Hydrol. Sci. J. https://doi.org/10.1080/02626667.2018.1506128

Costa-Cabral, M.C., Richey, J.E., Goteti, G., Lettenmaier, D.P., Feldkötter, C., Snidvongs, A., 2008. Landscape structure and use, climate, and water movement in the Mekong River basin. Hydrol. Process. https://doi.org/10.1002/hyp.6740

Costa, M.H., Botta, A., Cardille, J.A., 2003. Effects of large-scale changes in land cover on the discharge of the Tocantins River, Southeastern Amazonia. J. Hydrol. https://doi.org/10.1016/S0022-1694(03)00267-1

Cruz Ruggiero, P.G., Batalha, M.A., Pivello, V.R., Meirelles, S.T., 2002. Soil-vegetation relationships in cerrado (Brazilian savanna) and semideciduous forest, Southeastern Brazil. Plant Ecol. https://doi.org/10.1023/A:1015819219386

D. N. Moriasi, J. G. Arnold, M. W. Van Liew, R. L. Bingner, R. D. Harmel, T. L. Veith, 2007. Model Evaluation Guidelines for Systematic Quantification of Accuracy in Watershed Simulations. Trans. ASABE. https://doi.org/10.13031/2013.23153

Da Rocha, H.R., Manzi, A.O., Cabral, O.M., Miller, S.D., Goulden, M.L., Saleska, S.R., Coupe, N.R., Wofsy, S.C., Borma, L.S., Artaxo, R., Vourlitis, G., Nogueira, J.S., Cardoso, F.L., Nobre, A.D., Kruijt, B., Freitas, H.C., Von Randow, C., Aguiar, R.G., Maia, J.F., 2009. Patterns of water and heat flux across a biome gradient from tropical forest to savanna in brazil. J. Geophys. Res. Biogeosciences. https://doi.org/10.1029/2007JG000640

De Roo, A., Odijk, M., Schmuck, G., Koster, E., Lucieer, A., 2001. Assessing the effects of land use changes on floods in the meuse and oder catchment. Phys. Chem. Earth, Part B Hydrol. Ocean. Atmos. 26, 593–599. https://doi.org/10.1016/S1464-1909(01)00054-5

DeFries, R., Eshleman, K.N., 2004. Land-use change and hydrologic processes: a major focus for the future. Hydrol. Process. https://doi.org/10.1002/hyp.5584

Dos Santos, V., Laurent, F., Abe, C., Messner, F., 2018. Hydrologic response to land use change in a large basin in eastern Amazon. Water (Switzerland). https://doi.org/10.3390/w10040429

Doyle, M.E., Barros, V.R., 2011. Attribution of the river flow growth in the Plata Basin. Int. J. Climatol. 31, 2234–2248. https://doi.org/10.1002/joc.2228

Ferrant, S., Oehler, F., Durand, P., Ruiz, L., Salmon-Monviola, J., Justes, E., Dugast, P., Probst, A., Probst, J.L., Sanchez-Perez, J.M., 2011. Understanding nitrogen transfer dynamics in a small agricultural catchment: Comparison of a distributed (TNT2) and a semi distributed (SWAT) modeling approaches. J. Hydrol. https://doi.org/10.1016/j.jhydrol.2011.05.026

Ficklin, D.L., Luo, Y., Luedeling, E., Zhang, M., 2009. Climate change sensitivity assessment of a highly agricultural watershed using SWAT. J. Hydrol. https://doi.org/10.1016/j.jhydrol.2009.05.016

Francesconi, W., Srinivasan, R., Pérez-Miñana, E., Willcock, S.P., Quintero, M., 2016. Using the Soil and Water Assessment Tool (SWAT) to model ecosystem services: A systematic review. J. Hydrol. https://doi.org/10.1016/j.jhydrol.2016.01.034

Fu, B., Wang, J., Chen, L., Qiu, Y., 2003. The effects of land use on soil moisture variation in the Danangou catchment of the Loess Plateau, China. Catena. https://doi.org/10.1016/S0341-8162(03)00065-1

Ghaffari, G., Keesstra, S., Ghodousi, J., Ahmadi, H., 2010. SWAT-simulated hydrological impact of land-use change in the Zanjanrood Basin, Northwest Iran. Hydrol. Process. 24, 892–903. https://doi.org/10.1002/hyp.7530

Gonçalves, J.L.M., Stape, J.L., Laclau, J.P., Bouillet, J.P., Ranger, J., 2008. Assessing the effects of early silvicultural management on long-term site productivity of fast-growing eucalypt plantations: The Brazilian experience, in: Southern Forests. https://doi.org/10.2989/SOUTH.FOR.2008.70.2.6.534

Grimm, A.M., Pal, J.S., Giorgi, F., 2007. Connection between spring conditions and peak summer monsoon rainfall in South America: Role of soil moisture, surface temperature, and topography in eastern Brazil. J. Clim. 20, 5929–5945. https://doi.org/10.1175/2007JCLI1684.1

Gupta, H. V., Kling, H., Yilmaz, K.K., Martinez, G.F., 2009. Decomposition of the mean squared error and NSE performance criteria: Implications for improving hydrological modelling. J. Hydrol. 377, 80–91. https://doi.org/10.1016/j.jhydrol.2009.08.003

Hernandes, T.A.D., Scarpare, F.V., Seabra, J.E.A., 2018. Assessment of the recent land use change dynamics related to sugarcane expansion and the associated effects on water resources availability. J. Clean. Prod. https://doi.org/10.1016/j.jclepro.2018.06.297

Hoffmann, W.A., Da Silva, E.R., Machado, G.C., Bucci, S.J., Scholz, F.G., Goldstein, G., Meinzer, F.C., 2005. Seasonal leaf dynamics across a tree density gradient in a Brazilian savanna. Oecologia. https://doi.org/10.1007/s00442-005-0129-x

Huang, M., Zhang, L., Gallichand, J., 2003. Runoff responses to afforestation in a watershed of the Loess Plateau, China. Hydrol. Process. https://doi.org/10.1002/hyp.1281

IBGE, 2019. Brazilian Institute of Geography and Statistics - Population Available online: http://www.ibge.gov.br/apps/populacao/projecao/ (accessed November 2019).

Kalantari, Z., Lyon, S.W., Folkeson, L., French, H.K., Stolte, J., Jansson, P.E., Sassner, M., 2014. Quantifying the hydrological impact of simulated changes in land use on peak discharge in a small catchment. Sci. Total Environ. https://doi.org/10.1016/j.scitotenv.2013.07.047

Lambin, E.F., Turner, B.L., Geist, H.J., Agbola, S.B., Angelsen, A., Bruce, J.W., Coomes, O.T.,

Dirzo, R., Fischer, G., Folke, C., George, P.S., Homewood, K., Imbernon, J., Leemans, R., Li, X., Moran, E.F., Mortimore, M., Ramakrishnan, P.S., Richards, J.F., Skånes, H., Steffen, W., Stone, G.D., Svedin, U., Veldkamp, T.A., Vogel, C., Xu, J., 2001. The causes of land-use and land-cover change: Moving beyond the myths. Glob. Environ. Chang. https://doi.org/10.1016/S0959-3780(01)00007-3

Leta, O.T., van Griensven, A., Bauwens, W., 2017. Effect of Single and Multisite Calibration Techniques on the Parameter Estimation, Performance, and Output of a SWAT Model of a Spatially Heterogeneous Catchment. J. Hydrol. Eng. https://doi.org/10.1061/(ASCE)HE.1943-5584.0001471

Li, Z., Deng, X., Wu, F., Hasan, S.S., 2015. Scenario analysis for water resources in response to land use change in the middle and upper reaches of the heihe river Basin. Sustain. https://doi.org/10.3390/su7033086

Lin, B., Chen, X., Yao, H., Chen, Y., Liu, M., Gao, L., James, A., 2015. Analyses of landuse change impacts on catchment runoff using different time indicators based on SWAT model. Ecol. Indic. https://doi.org/10.1016/j.ecolind.2015.05.031

Manoli, G., Ivanov, V.Y., Fatichi, S., 2018. Dry-Season Greening and Water Stress in Amazonia: The Role of Modeling Leaf Phenology. J. Geophys. Res. Biogeosciences. https://doi.org/10.1029/2017JG004282

MMA, 2012. Monitoramento do desmatamento nos biomas brasileiros por satélite: monitoramento do bioma Mata Atlântica - 2008 a 2009. Ministério do Meio Ambient. Brasília, DF 101.

MMA, 2011. Monitoramento do desmatamento nos biomas brasileiros por satélite: monitoramento do bioma Cerrado - 2009 a 2010.

Monteith J. L., 1965. Evaporation and envrionment, in: Symp. Soc. Exp. Biol.

Moriasi, D. N., J. G. Arnold, M. W. Van Liew, R. L. Binger, R.D., Harmel, and T.V., 2007. Model Evaluation Guidelines for Systematic Quantification of Accuracy in Watershed

Simulations. Trans. ASABE. https://doi.org/10.13031/2013.23153

Morton, D.C., Nagol, J., Carabajal, C.C., Rosette, J., Palace, M., Cook, B.D., Vermote, E.F., Harding, D.J., North, P.R.J., 2014. Amazon forests maintain consistent canopy structure and greenness during the dry season. Nature. https://doi.org/10.1038/nature13006

Mueller, C., Mueller, B., 2016. The evolution of agriculture and land reform in Brazil, 1960-2006, in: Economic Development in Latin America: Essay in Honor of Werner Baer. https://doi.org/10.1057/9780230297388_10

Nash, J.E., Sutcliffe, J. V., 1970. River flow forecasting through conceptual models part I - A discussion of principles. J. Hydrol. https://doi.org/10.1016/0022-1694(70)90255-6

Negrón Juárez, R.I., da Rocha, H.R., e Figueira, A.M.S., Goulden, M.L., Miller, S.D., 2009. An improved estimate of leaf area index based on the histogram analysis of hemispherical photographs. Agric. For. Meteorol. https://doi.org/10.1016/j.agrformet.2008.11.012

Neitsch, S.., Arnold, J.., Kiniry, J.., Williams, J.., 2011. Soil & Water Assessment Tool: Theoretical Documentation Version 2009, Texas Water Resources Institute, TR-406. https://doi.org/10.1016/j.scitotenv.2015.11.063

Nepstad, D.C., De Carvalho, C.R., Davidson, E.A., Jipp, P.H., Lefebvre, P.A., Negreiros, G.H., Da Silva, E.D., Stone, T.A., Trumbore, S.E., Vieira, S., 1994. The role of deep roots in the hydrological and carbon cycles of Amazonian forests and pastures. Nature. https://doi.org/10.1038/372666a0

Oliveira, R.S., Bezerra, L., Davidson, E.A., Pinto, F., Klink, C.A., Nepstad, D.C., Moreira, A., 2005. Deep root function in soil water dynamics in cerrado savannas of central Brazil. Funct. Ecol. https://doi.org/10.1111/j.1365-2435.2005.01003.x

P. D. Wagner, S. Kumar, P. Fiener, K. Schneider, 2011. Technical Note: Hydrological Modeling with SWAT in a Monsoon-Driven Environment: Experience from the Western Ghats, India. Trans. ASABE. https://doi.org/10.13031/2013.39846

Pokhrel, Y., Burbano, M., Roush, J., Kang, H., Sridhar, V., Hyndman, D.W., 2018. A review of

the integrated effects of changing climate, land use, and dams on Mekong river hydrology. Water (Switzerland). https://doi.org/10.3390/w10030266

Rajib, A., Merwade, V., 2017. Hydrologic response to future land use change in the Upper Mississippi River Basin by the end of 21st century. Hydrol. Process. https://doi.org/10.1002/hyp.11282

Rudke, A.P., 2018. Dinâmica da cobertura do solo para a bacia hidrográfica do alto rio Paraná. Master´s Thesis, Federal University of Tecnology Parana, Londrina, Brazil.

Rudke, A.P., Fujita, T., Almeida, D.S. de, Eiras, M.M., Xavier, A.C.F., Rafee, S.A.A., Santos, E.B., Morais, M.V.B. de, Martins, L.D., Souza, R.V.A. de, Souza, R.A.F., Hallak, R., Freitas, E.D. de, Uvo, C.B., Martins, J.A., 2019. Land cover data of Upper Parana River Basin, South America, at high spatial resolution. Int. J. Appl. Earth Obs. Geoinf. https://doi.org/10.1016/j.jag.2019.101926

Rudorff, B.F.T., de Aguiar, D.A., da Silva, W.F., Sugawara, L.M., Adami, M., Moreira, M.A., 2010. Studies on the rapid expansion of sugarcane for ethanol production in São Paulo state (Brazil) using Landsat data. Remote Sens. https://doi.org/10.3390/rs2041057

Saleska, S.R., Wu, J., Guan, K., Araujo, A.C., Huete, A., Nobre, A.D., Restrepo-Coupe, N., 2016. Dry-season greening of Amazon forests. Nature. https://doi.org/10.1038/nature16457

Soil Conservation Service Engineering Division, 1972. Section 4: Hydrology, in: National Engineering Handbook.

Strauch, M., Volk, M., 2013. SWAT plant growth modification for improved modeling of perennial vegetation in the tropics. Ecol. Modell. https://doi.org/10.1016/j.ecolmodel.2013.08.013

Thiemig, V., Rojas, R., Zambrano-Bigiarini, M., De Roo, A., 2013. Hydrological evaluation of satellite-based rainfall estimates over the Volta and Baro-Akobo Basin. J. Hydrol. 499, 324–338. https://doi.org/10.1016/j.jhydrol.2013.07.012

Tucci, C.E.., 2002. Impactos da variabilidade climática e do uso do solo nos recursos hídricos.

Câmara Temática sobre Recur. Hídricos 150.

Van Griensven, A., Ndomba, P., Yalew, S., Kilonzo, F., 2012. Critical review of SWAT applications in the upper Nile basin countries. Hydrol. Earth Syst. Sci. https://doi.org/10.5194/hess-16-3371-2012

Velasco, I., Fritsch, J.M., 1987. Mesoscale convective complexes in the Americas. J. Geophys. Res. 92, 9591–9613. https://doi.org/10.1029/JD092iD08p09591

Viola, M.R., Mello, C.R., Beskow, S., Norton, L.D., 2014. Impacts of Land-use Changes on the Hydrology of the Grande River Basin Headwaters, Southeastern Brazil. Water Resour. Manag. https://doi.org/10.1007/s11269-014-0749-1

Wang, G., Yang, H., Wang, L., Xu, Z., Xue, B., 2014. Using the SWAT model to assess impacts of land use changes on runoff generation in headwaters. Hydrol. Process. 28, 1032–1042. https://doi.org/10.1002/hyp.9645

Wu, K., Johnston, C.A., 2007. Hydrologic response to climatic variability in a Great Lakes Watershed: A case study with the SWAT model. J. Hydrol. https://doi.org/10.1016/j.jhydrol.2007.01.030

Supplement of

Hydrologic Response to Large-Scale Land Use and Cover Changes in the Upper Paraná River Basin between 1985 and 2015

Sameh A. Abou Rafee, Edmilson D. Freitas, Jorge A. Martins, Carolyne B. Machado, Cintia B. Uvo

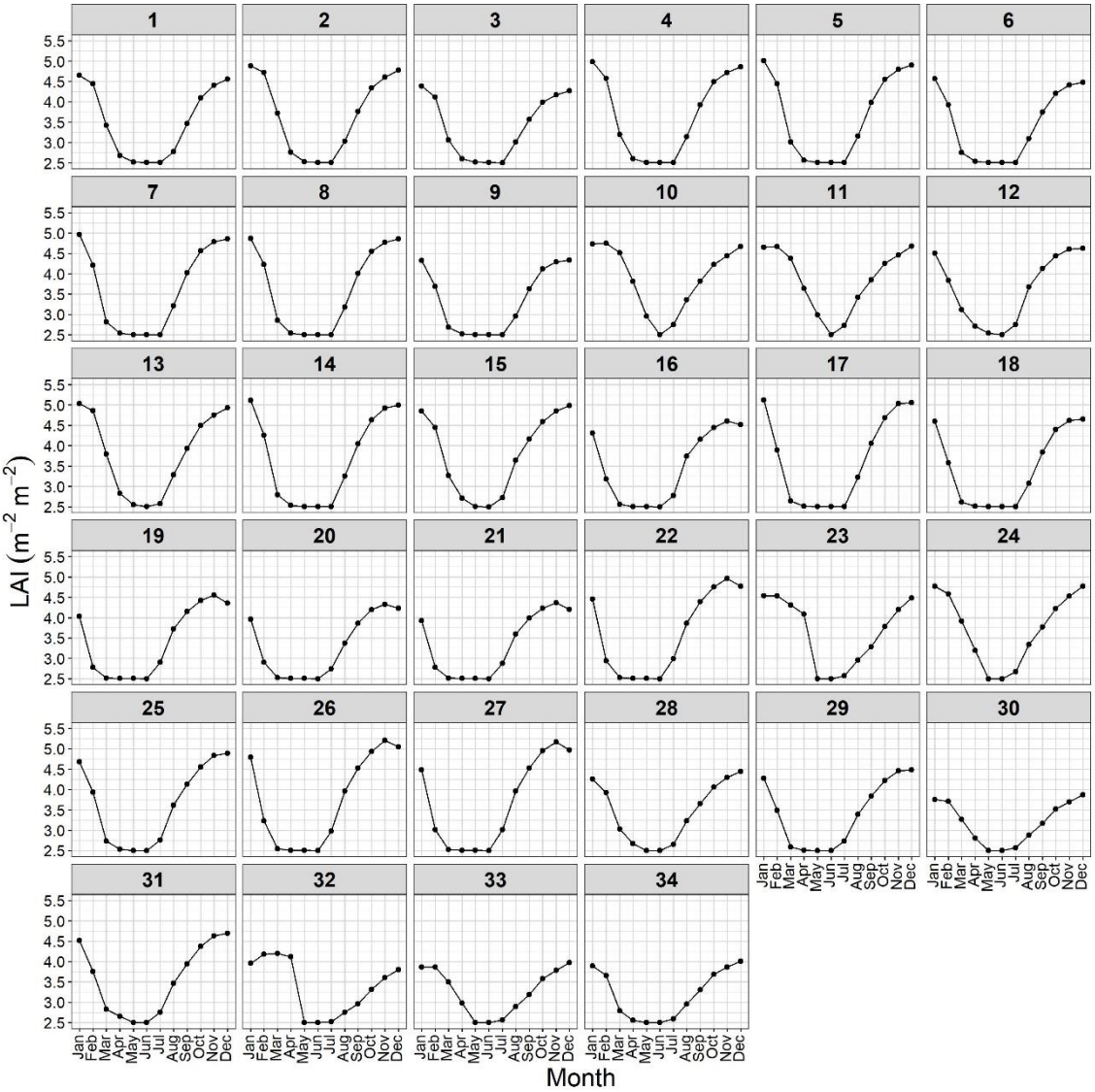

Figure S1. Average monthly simulated forest LAI values at each subbasin based on LUC 2015 scenario. **1.** Corumbá; **2.** Upper Paranaíba; **3.** Araguari; **4.** Meia Ponte-Middle Paranaíba; **5.** Dos Bois; **6.** Tijuco; **7.** Middle Paranaíba; **8.** Claro; **9.** Verde-Corrente-Aporé or Do Peixe; Lower Paranaíba; **10.** Upper Grande; **11.** Sapucaí; **12.** Pardo; **13.** Middle Grande; **14.** Lower Grande; **15.** Upper Tietê; **16.** Lower Tietê; **17.** São José dos Dourados-Upper Paraná; **18.** Sucuriú; **19.** Aguapei or Feio; **20.** Verde; **21.** Do Peixe-Middle Paraná; **22.** Anhanduí-Pardo; **23.** Tibagi; **24.** Upper Paranapanema; **25.** Lower Paranapanema; **26.** Middle Paraná; **27.** Brilhante-Invinheima; **28.** Ivaí; **29.** Middle Paraná; **30.** Piquiri; **31.** Iguatemi; Middle Paraná; **32.** Upper Iguaçu; **33.** Lower Iguaçu; **34.** Carapá- Guaçu-Lower Paraná..

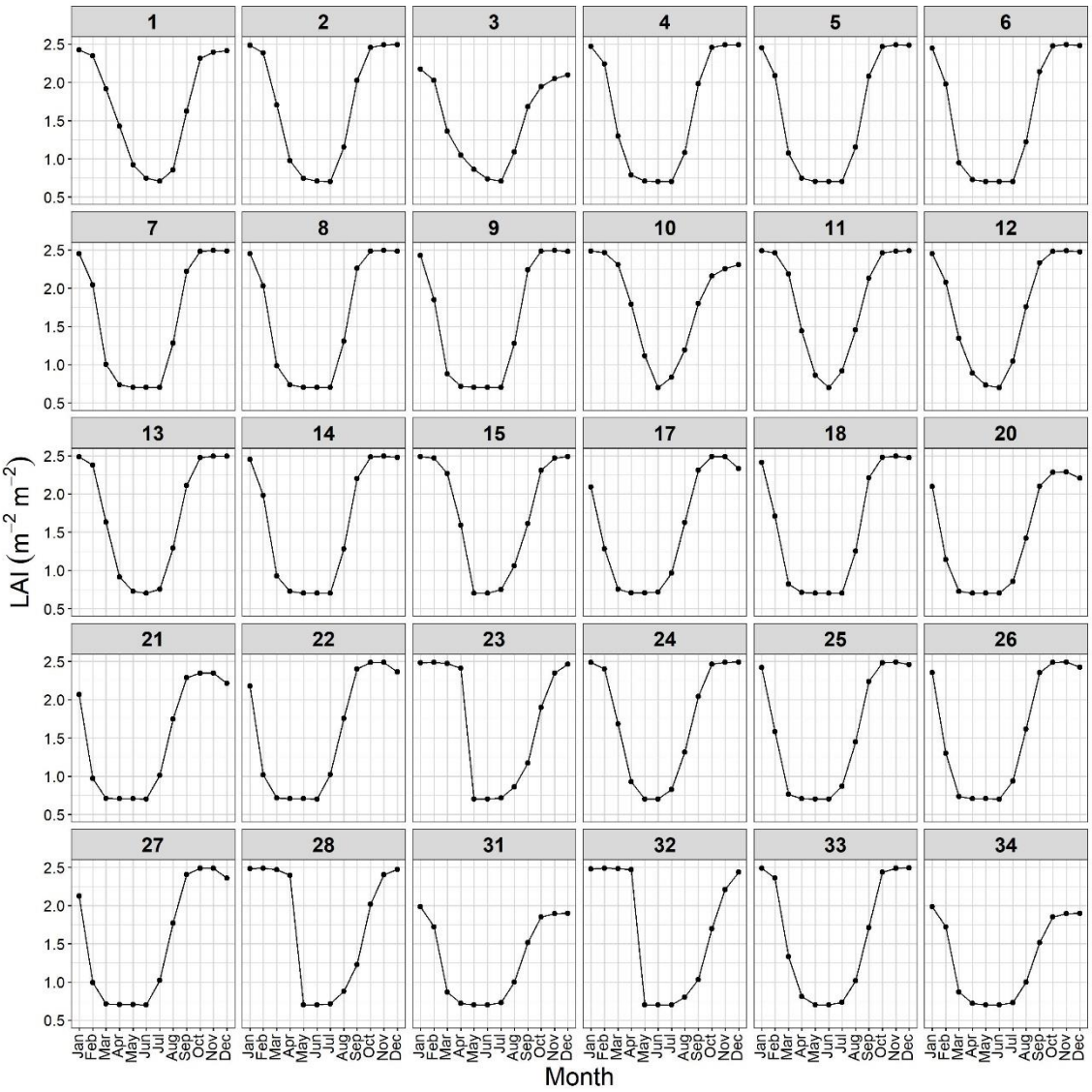

Figure S2. Average monthly simulated Cerrado LAI values at each subbasin based on LUC 2015 scenario. **1.** Corumbá; **2.** Upper Paranaíba; **3.** Araguari; **4.** Meia Ponte; Middle Paranaíba; **5.** Dos Bois; **6.** Tijuco; **7.** Middle Paranaíba; **8.** Claro; **9.** Verde-Corrente-Aporé or Do Peixe; Lower Paranaíba; **10.** Upper Grande; **11.** Sapucaí; **12.** Pardo; **13.** Middle Grande; **14.** Lower Grande; **15.** Upper Tietê; **17.** São José dos Dourados-Upper Paraná; **18.** Sucuriú; **20.** Verde; **21.** Do Peixe; Middle Paraná; **22.** Anhanduí; Pardo; **23.** Tibagi; **24.** Upper Paranapanema; **25.** Lower Paranapanema; **26.** Middle Paraná; **27.** Brilhante; Invinheima; **28.** Ivaí; **31.** Iguatemi; Middle Paraná; **32.** Upper Iguaçu; **33.** Lower Iguaçu; **34.** Carapá; Guaçu; Lower Paraná.

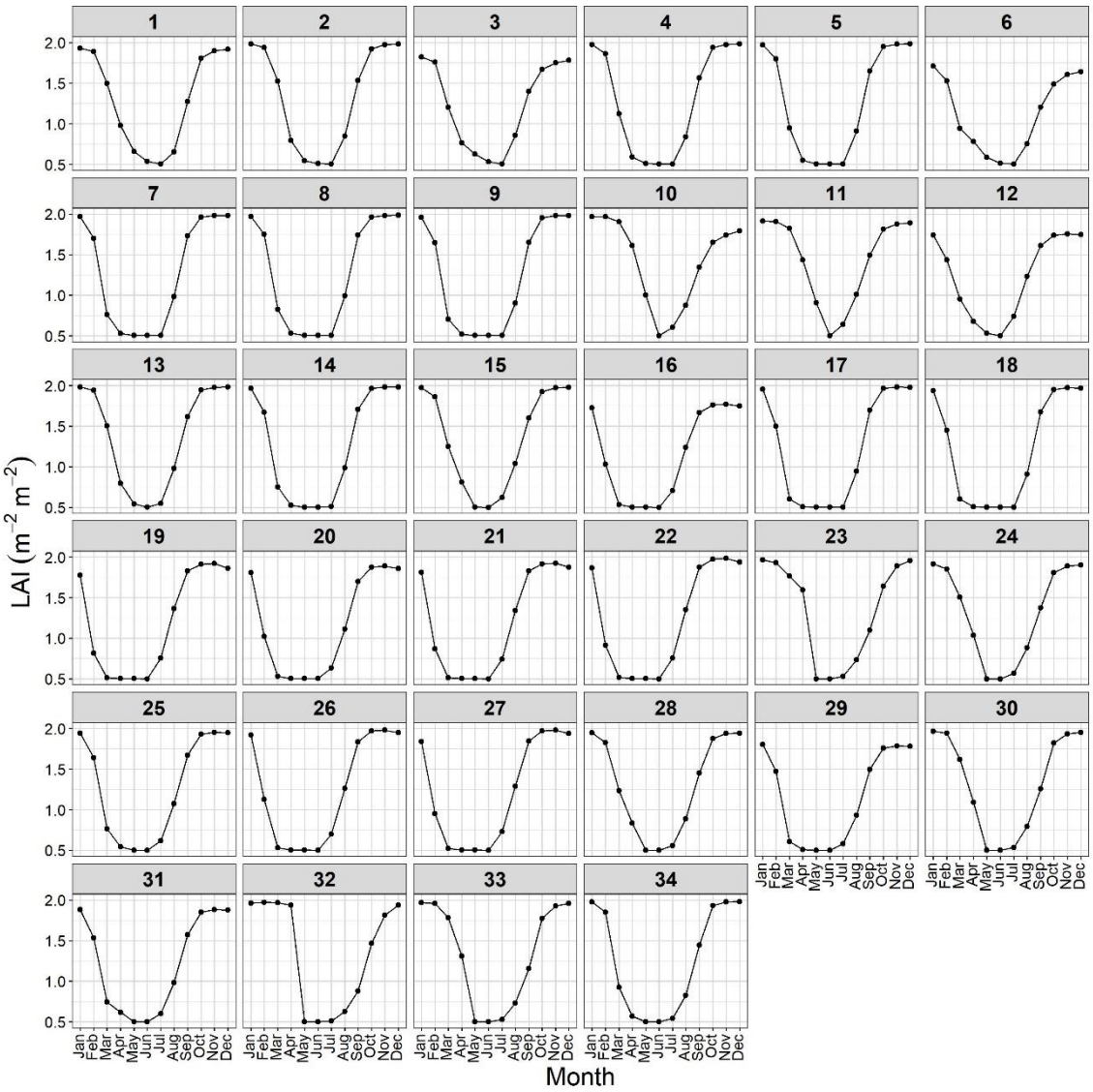

Figure S3. Average monthly simulated Grassland LAI values at each subbasin based on LUC 2015 scenario. **1.** Corumbá; **2.** Upper Paranaíba; **3.** Araguari; **4.** Meia Ponte-Middle Paranaíba; **5.** Dos Bois; **6.** Tijuco; **7.** Middle Paranaíba; **8.** Claro; **9.** Verde-Corrente-Aporé or Do Peixe; Lower Paranaíba; **10.** Upper Grande; **11.** Sapucaí; **12.** Pardo; **13.** Middle Grande; **14.** Lower Grande; **15.** Upper Tietê; **16.** Lower Tietê; **17.** São José dos Dourados-Upper Paraná; **18.** Sucuriú; **19.** Aguapei or Feio; **20.** Verde; **21.** Do Peixe-Middle Paraná; **22.** Anhanduí-Pardo; **23.** Tibagi; **24.** Upper Paranapanema; **25.** Lower Paranapanema; **26.** Middle Paraná; **27.** Brilhante-Invinheima; **28.** Ivaí; **29.** Middle Paraná; **30.** Piquiri; **31.** Iguatemi; Middle Paraná; **32.** Upper Iguaçu; **33.** Lower Iguaçu; **34.** Carapá- Guaçu-Lower Paraná.

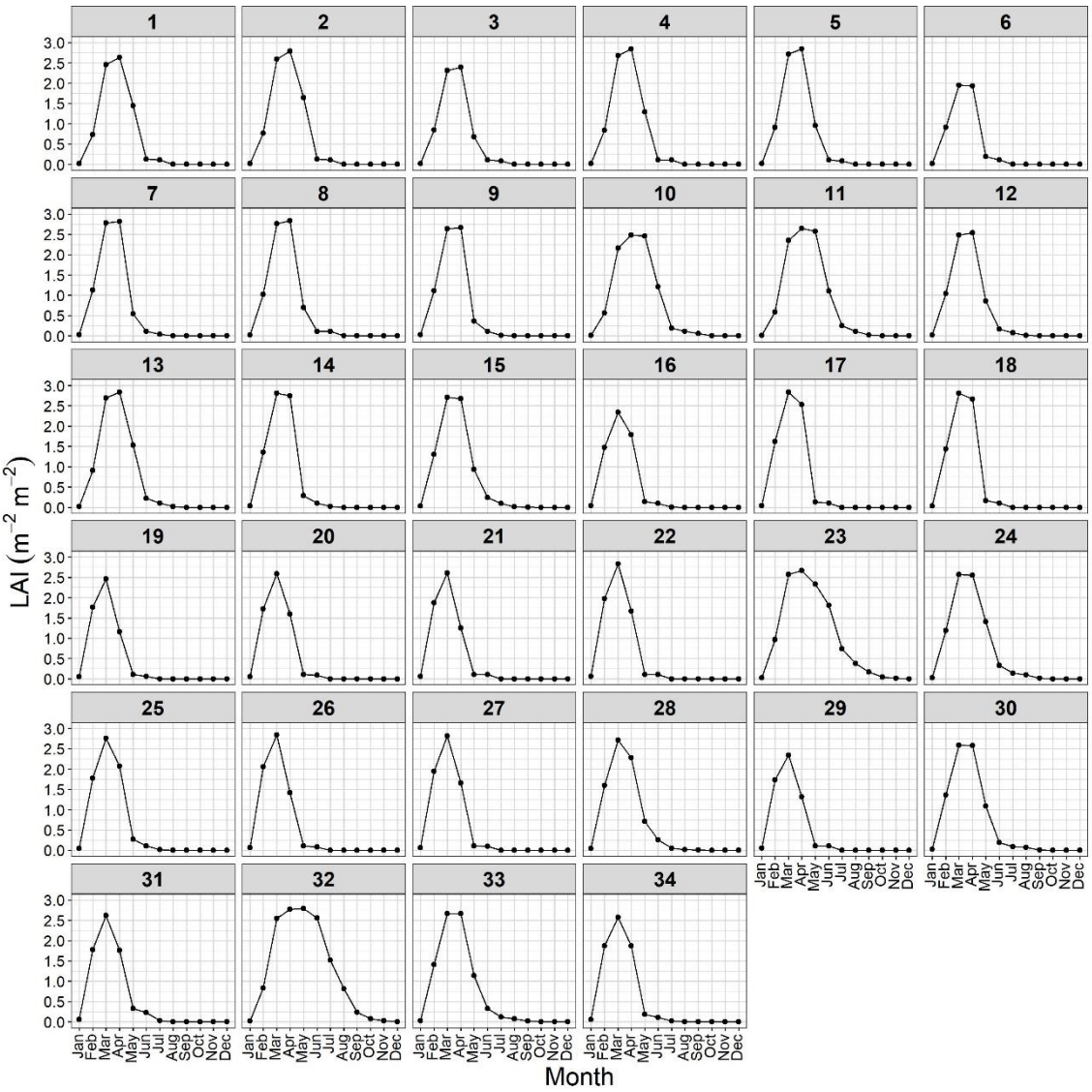

Figure S4. Average monthly simulated Cropland LAI values at each subbasin based on LUC 2015 scenario. **1.** Corumbá; **2.** Upper Paranaíba; **3.** Araguari; **4.** Meia Ponte-Middle Paranaíba; **5.** Dos Bois; **6.** Tijuco; **7.** Middle Paranaíba; **8.** Claro; **9.** Verde-Corrente-Aporé or Do Peixe; Lower Paranaíba; **10.** Upper Grande; **11.** Sapucaí; **12.** Pardo; **13.** Middle Grande; **14.** Lower Grande; **15.** Upper Tietê; **16.** Lower Tietê; **17.** São José dos Dourados-Upper Paraná; **18.** Sucuriú; **19.** Aguapei or Feio; **20.** Verde; **21.** Do Peixe-Middle Paraná; **22.** Anhanduí-Pardo; **23.** Tibagi; **24.** Upper Paranapanema; **25.** Lower Paranapanema; **26.** Middle Paraná; **27.** Brilhante-Invinheima; **28.** Ivaí; **29.** Middle Paraná; **30.** Piquiri; **31.** Iguatemi; Middle Paraná; **32.** Upper Iguaçu; **33.** Lower Iguaçu; **34.** Carapá- Guaçu-Lower Paraná.

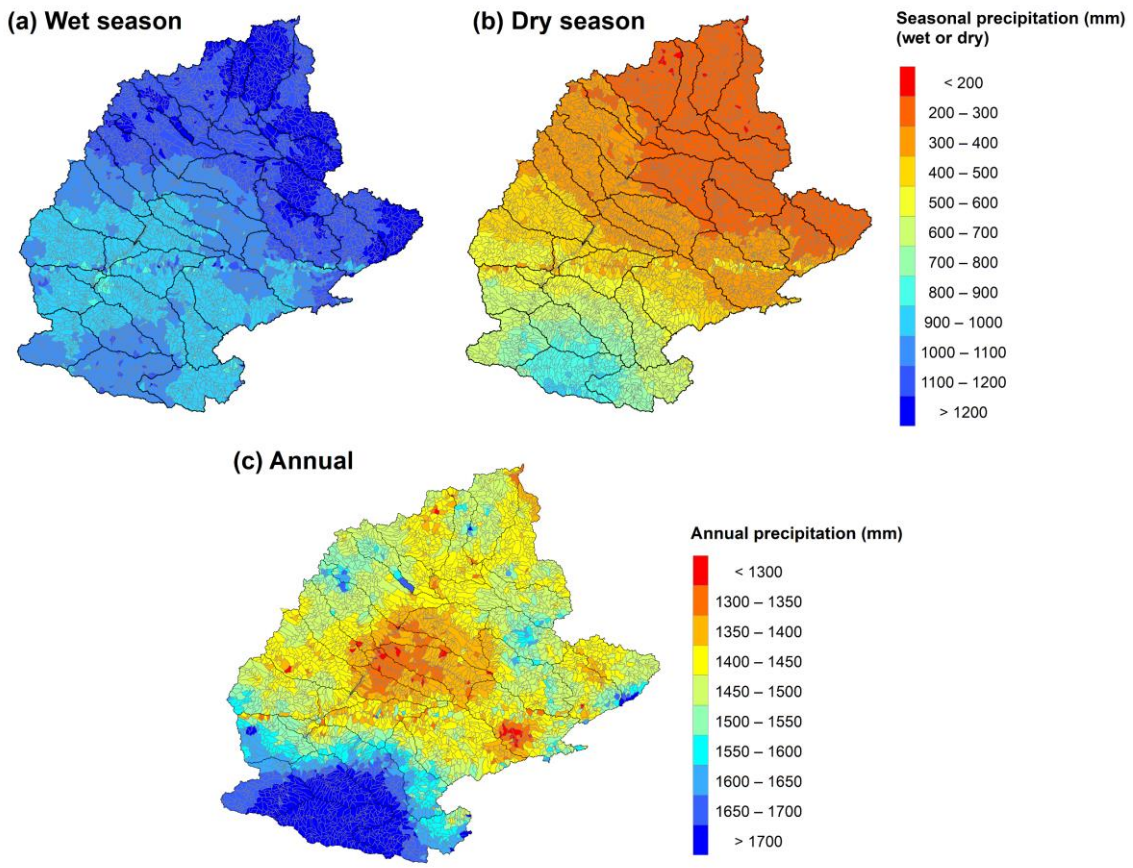

Figure S5. Annual (October to September), wet (October to March), and dry (April to September) season average precipitation totals (1984 – 2015) at the subbasins discretization level of the UPRB.

.

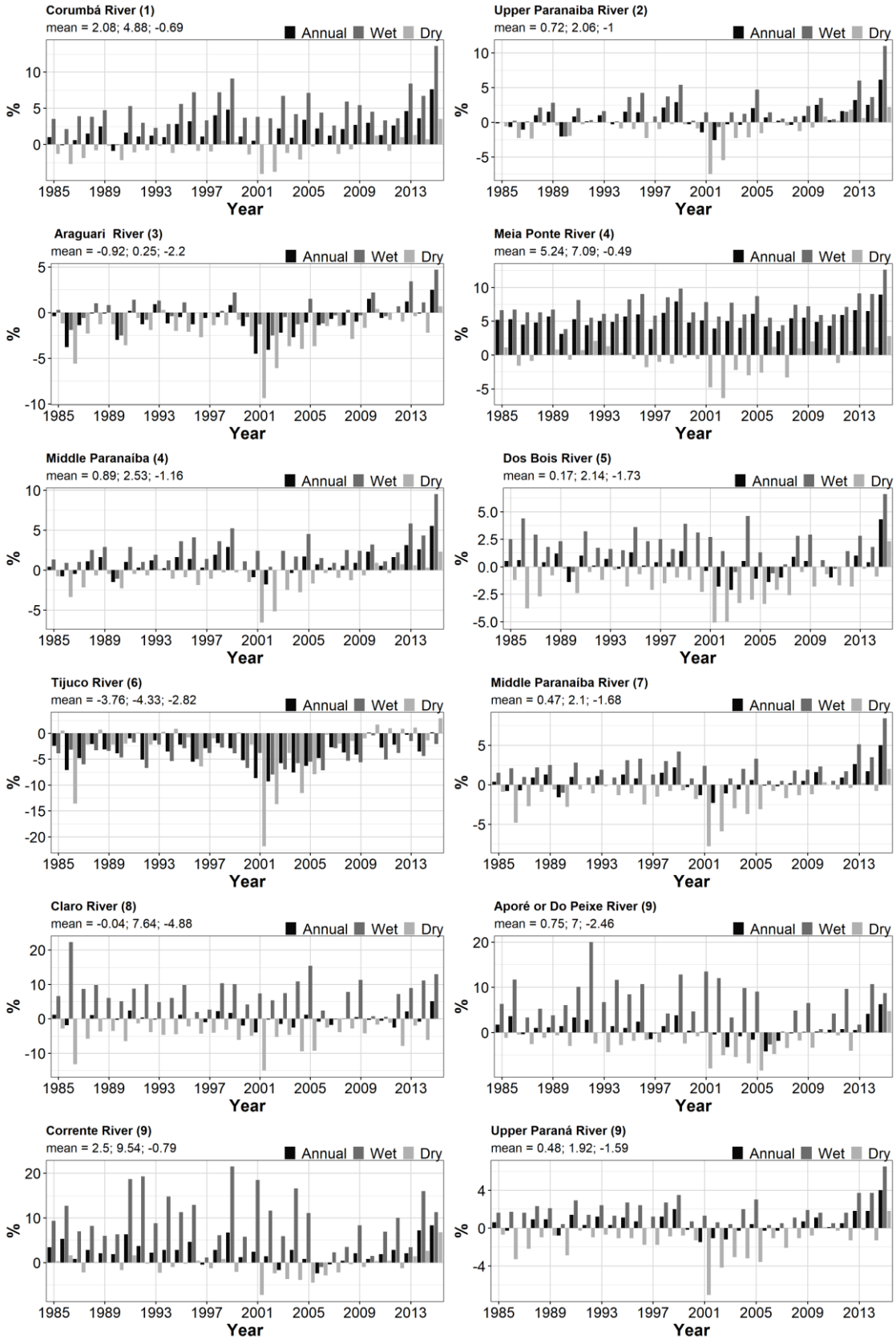

Figure S6. Cont.

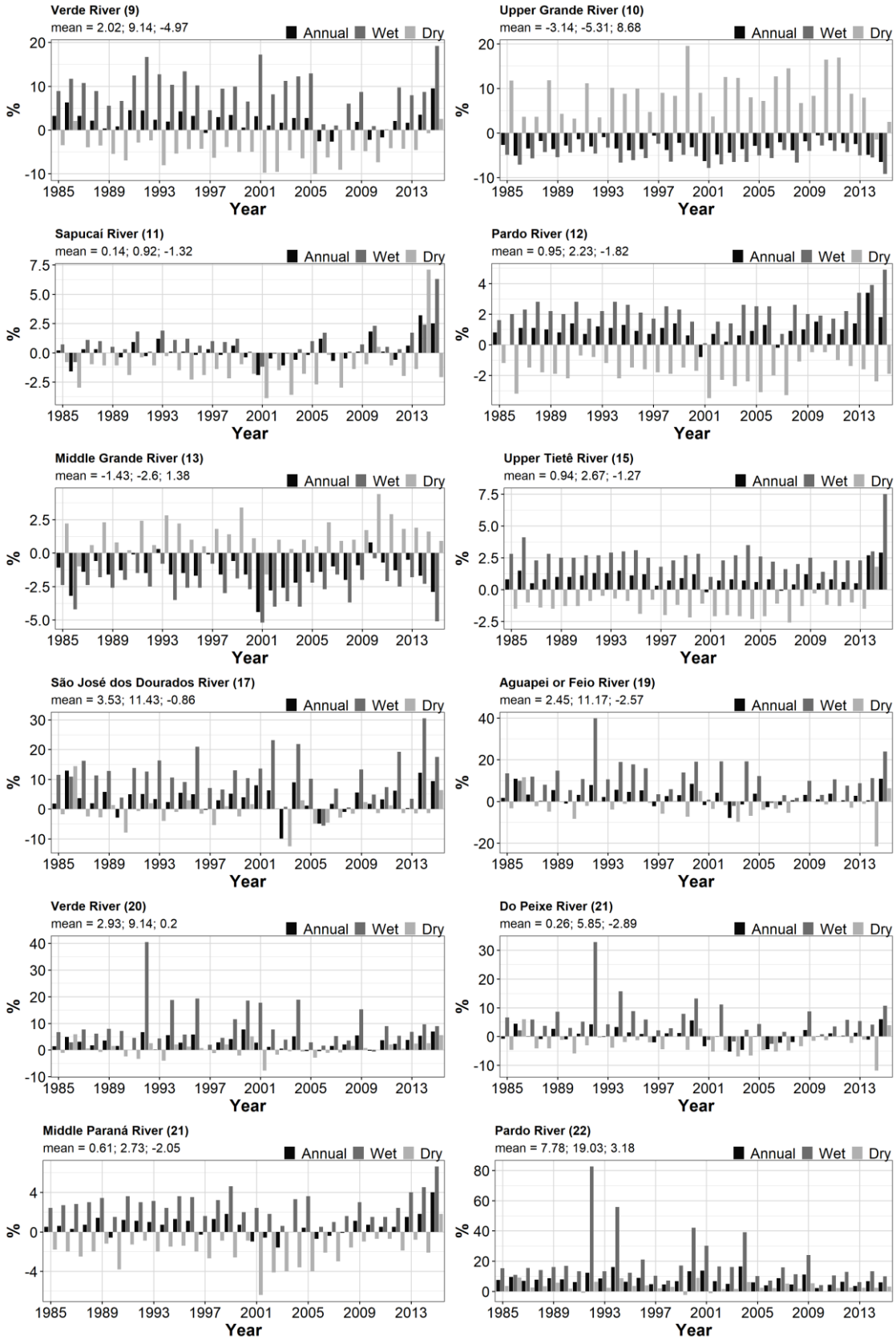

Figure S6. Cont.

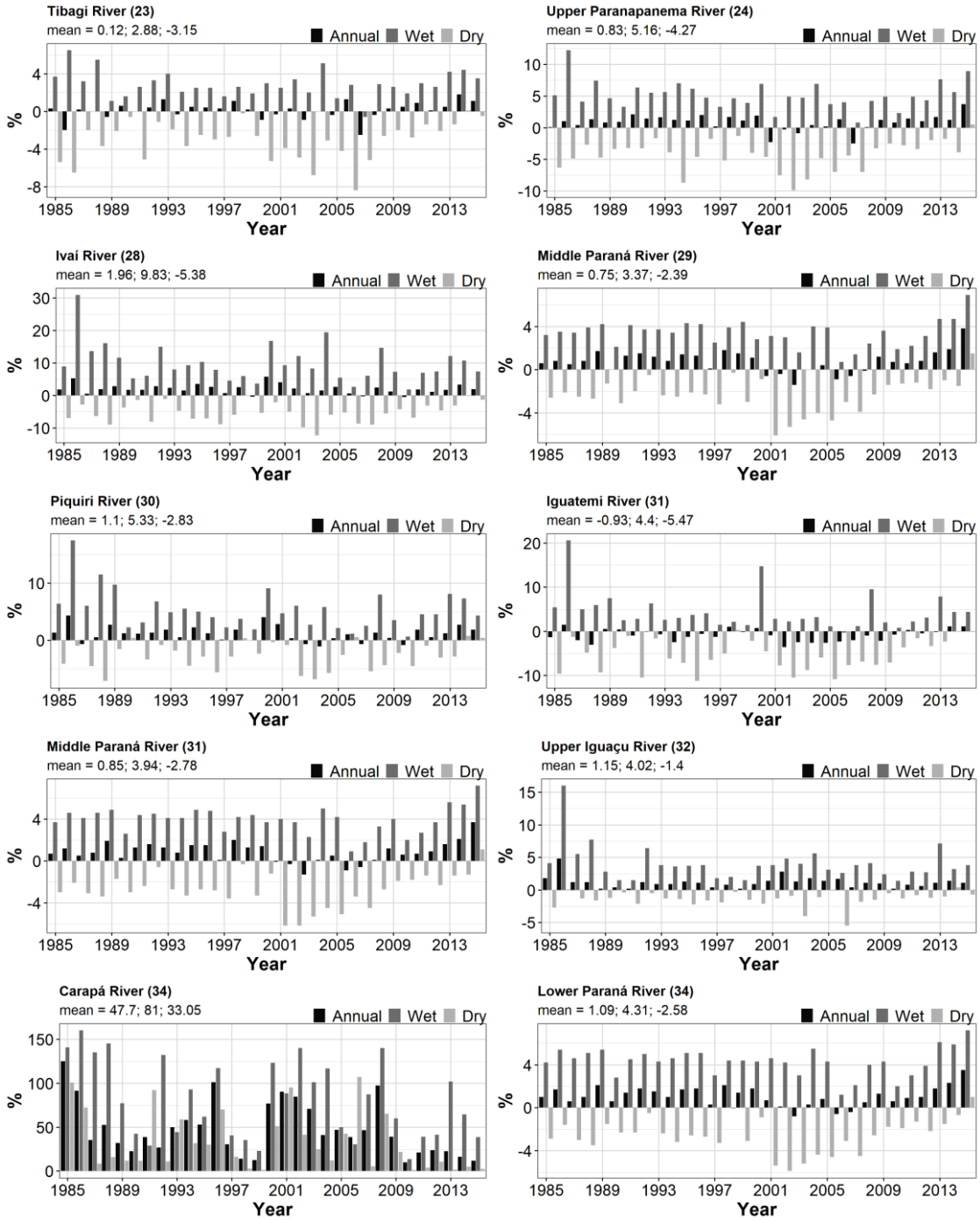

Figure S6. Temporal evolution of relative changes (%) in discharge for annual (October – September), wet (October – March) and dry (April – September) season under the scenarios for the year 2015 relative to 1985 at the last outlet of the rivers from the major subbasins of the UPRB. At the top left of the plots are shown the mean values and the name of the rivers with the respective number of the subbasin.

Paper IV

IV. **Abou Rafee, S.A.,** Uvo, C.B., Martins, J.A., Machado, C.B., Freitas, E.D., 2020. Land Use and Cover Changes versus Climate Shift: Who is the main player in river discharge? A case study in the Upper Paraná River Basin. *Science of the Total Environment* (Submitted 2020-06-06, Under review).

Land Use and Cover Changes versus Climate Shift: Who is the main player in river discharge? A case study in the Upper Paraná River Basin

Sameh A. Abou Rafee[1,2], Cintia B. Uvo[2], Jorge A. Martins[3], Carolyne B. Machado[1], Edmilson D. Freitas[1]

[1]Department of Atmospheric Sciences, University of São Paulo, São Paulo, Brazil
[2]Division of Water Resources Engineering, Lund University, Lund, Sweden
[3]Federal University of Technology – Parana, Londrina, Brazil
Correspondence to: S.A. Abou Rafee (sameh.adib@iag.usp.br)

Abstract

The Upper Paraná River Basin (UPRB) has undergone extensive Land Use and Cover Changes (LUCC) during the 20th century, in particularly during the early 1960s. During the 1970s the global climatic event known as "climate shift" took place that led to a shift in the precipitation patterns over the basin. Concurrently, an increase in the annual discharge at the Lower Paraná river was observed. This research assesses the impacts of the LUCC and the 1970s climate shift on this increase of discharge through hydrological modelling using the Soil and Water Assessment Tool (SWAT) model. The numerical simulations were based on three different land use and cover from a pristine period (around the Year 1500), 1960 and 1985. The results showed that both changes in land use and cover, as well as the climate shift had a significant impact on the annual discharge at the largest rivers of the UPRB, and that the impact of climate shift was larger. For instance, LUCC between 1960 and 1985 responds about 6% of the increase at the river mouth of the UPRB, whereas climate shift of about 32%. This result implies that the previous studies estimate overestimated the role of LUCC within the basin.

Keywords: SWAT model, precipitation change, large-scale modelling.

1. Introduction

The Upper Paraná River Basin (UPRB) is part of the second largest river basin in South America, the La Plata River Basin. The UPRB houses more than 65 million inhabitants (IBGE, 2019), and plays an important role in the economic activity of Brazil. According to the Brazilian National Water Agency (ANA), the UPRB has the highest demand for water resources in Brazil, mostly for agriculture and industrial activities. Besides, the basin has the highest hydroelectric power generation capacity in South America. As reported by the Brazilian Electricity Regulatory Agency (ANEEL, 2020), more than 62% of electricity in Brazil is generated by hydropower plants, which almost 30% are provided from the basin. Currently, the UPRB houses 156 large hydropower plants (with a capacity of more than 30 MW) that provide about 52,000 MW (Fig. 1). Also, the basin houses 595 small hydropower plants (capacity between 1.1 MW and 30 MW) and 214 micro hydropower plants (capacity up to 1 MW) which provide 7,074 MW and 193 MW, respectively.

The UPRB has undergone extensive Land Use and Cover Changes (LUCC) during the 20th century (Rudke, 2018; Rudke et al., 2019; Tucci, 2002). As reported by the Brazilian Ministry of the Environment, the basin had significant natural vegetation suppression (MMA, 2012, 2011). For instance, about 76% of the Atlantic forest biome and 49% of the cerrado (Brazilian savanna) were deforested and replaced mainly by grassland and cropland areas. This deforestation started mainly in the early 1960s when Brazil had a rapid population growth and economic development. As stated by several studies, these changes have affected the hydrological regime of the basin (Antico et al., 2016; Camilloni and Barros, 2003; Lee et al., 2018; Tucci, 2002; Tucci and Clarke, 1998).

In addition to the LUCC, the 1970s climate shift (Jacques-Coper and Garreaud, 2015) is pointed out as one of the main events that led to a variation in precipitation patterns over the UPRB that consequently could have affected the basin hydrology. The impacts of the climate shift on precipitation has been investigated over North American (Hartmann and Wendler, 2005; Litzow, 2006) and South American (Agosta and Compagnucci, 2008; Jacques-Coper and Garreaud, 2015) regions, and considered by the researchers as an unprecedented event. Climate shift is defined as the short period when several climate oscillations such as Pacific Decadal Oscillation (PDO) and El Niño–Southern Oscillation (ENSO) changed phases, out of which could lead the climate system to a new state (Jacques-Coper and Garreaud, 2015; Meehl et al., 2009; Tsonis et al., 2007; Wang et al., 2009; Yuan Zhang et al., 1997). During the 1970s climate shift, a cold to warm sea surface temperature shift in the tropical pacific was observed. Thereby, it induced an increase in annual mean precipitation in southernmost areas of South America (Jacques-Coper and Garreaud, 2015).

In the 1970s, a shift in annual discharge also was observed in the Lower Paraná river. As shown in Figure 2, the comparison of 37 years of annual discharge before and after the climate shift (considered as the period 1974 – 1977) shows an increase in the average annual median of about 26% at Guairá site (see Figure 1), which covers a drainage area of 804,000 km^2 within the UPRB. Therewith, hydropower plants were planned over the Paraná river due to the increased discharge and high demand for electricity (Tucci and Clarke, 1998). For example, ITAIPU Hydroelectric Dam, one of the largest installed capacity of electricity in the world with 14,000 MW was planned to build 18 generation units in 1974. However, the original design of the powerhouse provided space for two additional units, which were effectively incorporated into the

original design due to the increase in discharge observed in the following years (https://www.itaipu.gov.br/institucional/documentos-oficiais).

To date, no study in the literature addressed the integration of both LUCC and climate shift effects at a high spatial resolution on a large-scale basin. Besides, the causes that led to increased discharge at the Lower Paraná river have not yet been clearly explained. Hence, this work intends to use hydrological modelling to fill this gap and answer the following question: To which extent are changes associated with observed land use and cover, and climate shift responsible for the increase in the discharge of the Paraná River?

2. Material and Methods

2.1. Study Area

The study area is located in the central-southern region of Brazil, comprising the Upper Paraná River Basin (UPRB), between the coordinates 26° 51′ 23.35″ and 15° 27′ 25.54″ S latitude, and 56° 7′ 4.61″ and 43° 34′ 50.61″ W longitude. The basin has a drainage area of 900,480 km^2 and altitude varying from 78 up to 2778 meters above sea level. It covers six Brazilian states and a portion of Paraguay (Figure 1).

The area of the UPRB covers diverse climate classification as defined by Köppen and consequently, the precipitation regimes and its causes, varies spatially over the basin. In the northern part of the basin under the influence of the South American Monsoon System (SAMS) (Carvalho et al., 2011; Grimm et al., 2007; Marengo et al., 2012) has dry winters (< 30 mm), and wet summers (> 800 mm) (Abou Rafee et al., 2020). On the other hand, the precipitation over the southern part of the UPRB is spread over seasons ranging from 240 (winter) to 500 mm (summer) (Abou Rafee et al., 2020). The precipitation in the southern parts of UPRB is associated with different systems such as Mesoscale

Convective Systems (MCS), South American Low-Level Jet, the passage of cold fronts, and the South Atlantic Convergence Zone (Carvalho et al., 2004; Morales Rodriguez et al., 2010; Velasco and Fritsch, 1987).

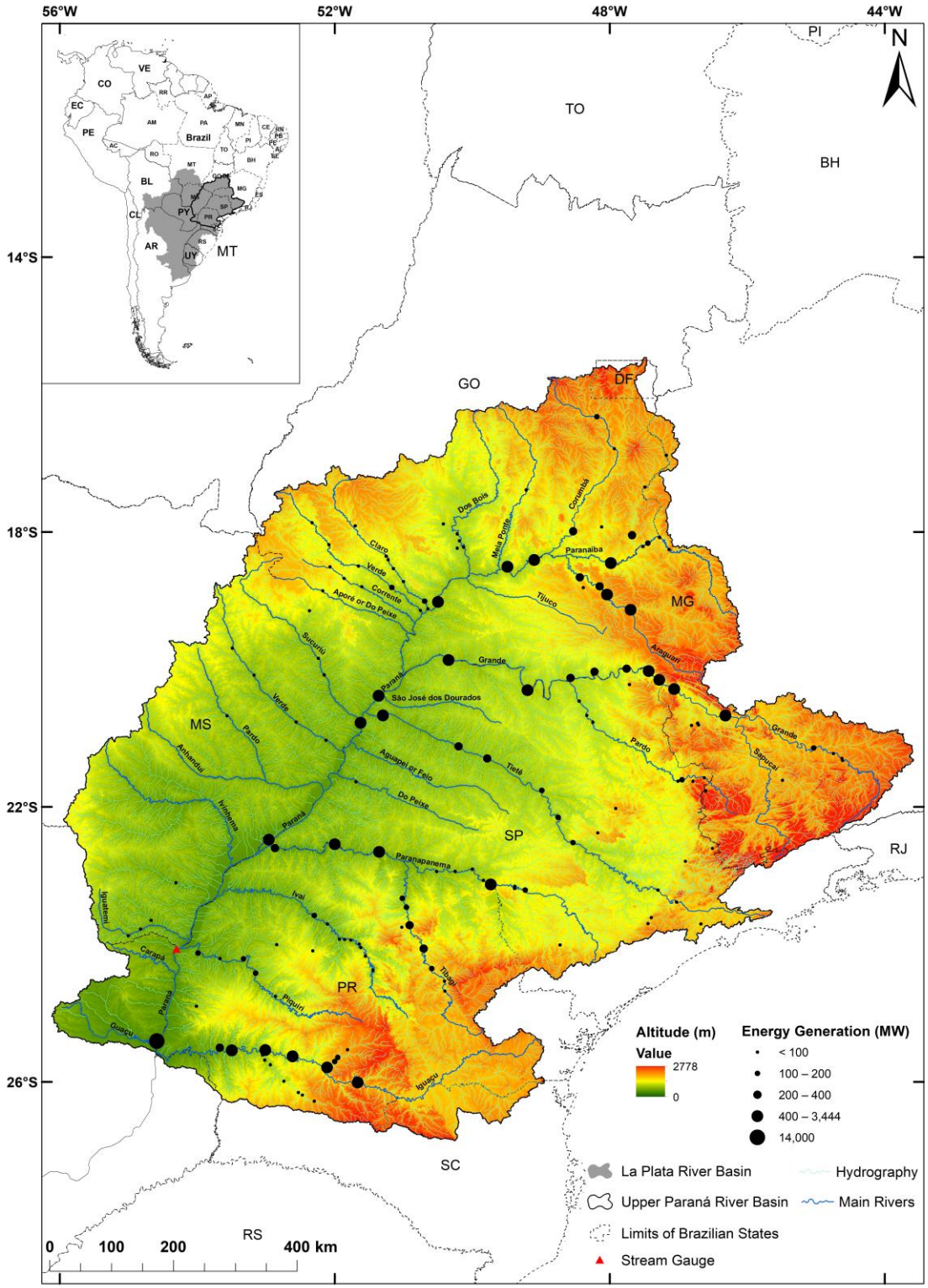

Figure 1. Location of the UPRB showing the topographic patterns, hydrography, and the spatial distribution of the largest hydropower plants (installed or planned with a capacity of more than 30 MW). The topography map was generated from Shuttle Radar Topography Mission (SRTM) data, the hydropower plants' database derived from the Brazilian Electricity Regulatory Agency (ANEEL, 2020), and the hydrography data were provided by the Brazilian National Water Agency (ANA).

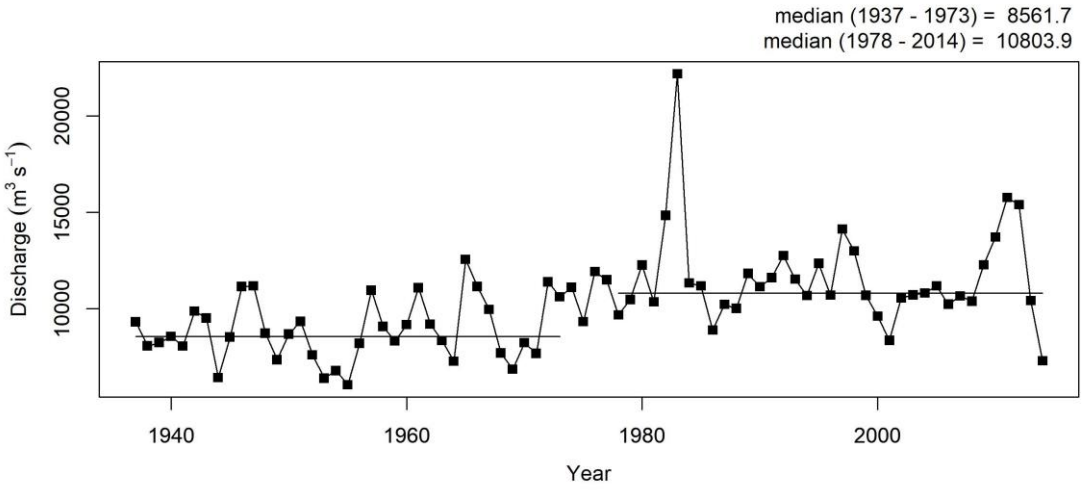

Figure 2. Annual discharge at Guairá stream gauge site (red triangle in Figure 1) from 1937 to 2014.

2.2. SWAT model

To evaluate the specific impacts of LUCC and of climate shift on the UPRB discharge, the Soil and Water Assessment Tool (SWAT) model with an ArcGIS interface (Arnold et al., 1998, https://swat.tamu.edu) was applied. SWAT is an open source, semi-distributed, and physically based model highly recommended for large-scale hydrological modelling (Abbaspour et al., 2015; Abou Rafee et al., 2019; Rouholahnejad et al., 2014). Climatic and physical data are required to build a hydrological project with the SWAT model.

Following previous studies (e.g. Jacques-Coper and Garreaud, 2015), this work, considers the period 1974 – 1977 as when the climate shift occurred and created a project to compare discharge before 1974 and after 1977 considering the LUCC and observed precipitation. As before the 1960s few measurements were made over the basin, the defined period for simulations was from 1961 to 1990, i.e., 13 years before climate shift and after climate shift are simulated and results compared. A brief description of the data used as well as the model set up are presented in the following sections.

2.2.1 Climatic Data

The daily climatic data were prepared for the simulation period from January 1956 to December 1990, being the first five years used to the warming up of the model (1956 – 1960). Daily maximum and minimum temperature, solar radiation, wind speed, and relative humidity were obtained from the European Centre for Medium-Range Weather Forecasts (ECMWF) reanalysis ERA-20C at the grid resolution of 0.25 degrees. Daily precipitation data from the Brazilian National Water Agency (ANA) were collected. A total of 2,739 rain gauge stations (2,292 within basin), out of which 38% have less than 20% of missing data (Figure 3) were provided. For detailed information about the precipitation data processing, the reader is referred to Abou Rafee et al. (2019). These data were interpolated to a spatial resolution of 0.1 degrees using the Inverse Distance Weighted (IDW) method.

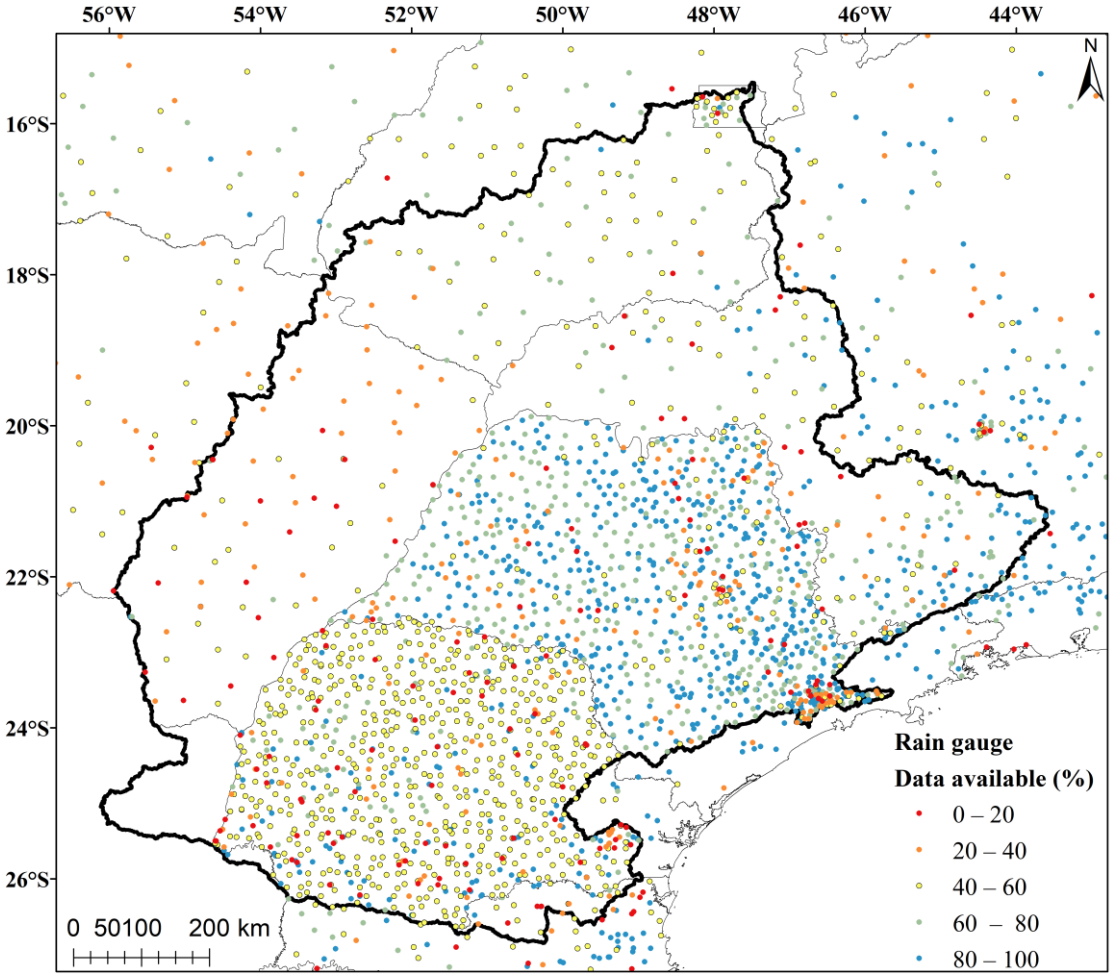

Figure 3. Spatial distribution of rain gauge stations in the UPRB showing its percentage data availability.

2.2.2. Physical data

Topographic data at a 90-meter resolution used was collected from the Shuttle Radar Topography Mission (SRTM) (available from http://srtm.csi.cgiar.org/srtmdata/). The soil data used in the work was built using information from the Brazilian Agriculture Research Corporation (EMBRAPA) and the Harmonized World Soil Database (HWSD). It is the same data used by Abou Rafee et al. (2019), to which the reader is referred for further details.

Three simulations of discharge were made and scenarios created. Similar to all simulations are the input data of climatic, soil, and topography. A different Land Use and

Cover (LUC) was used in each simulation. They are a pristine LUC of around 1500, a LUC for 1960 and one for 1985. The description of each LUC is presented as follows:

LUC – 1985

The LUC for 1985 was based on the classification made by Rudke (2018). The map was generated from pixel-based classifications, using 50 Landsat-8 scenes. Based on his classification, the UPRB were divided into six major categories: forest, cerrado (Brazilian savanna), cropland, grassland, water, and urban areas.

LUC – T0

A map of the original vegetation, representing the unchanged landscape from a pristine period (around the Year 1500) named in this work as T0 was constructed. The original vegetation vectors were based on the classification performed by the RADAMBRASIL project. This project generated mappings of the 70's and 80's decades, being the first national effort to know the physical and biotic conditions of the national territory using a large amount of material and human resources (IBGE, 2017). The categories of natural vegetation and savanna physiognomies from the T0 map were merged into forest and cerrado, respectively (see Figure S1). In addition, the water and natural vegetation categories (cerrado or forest) from the 1985 map were maintained. Hence, three classes were defined as forest, cerrado, and water areas.

LUC – 1960

The LUC for 1960 was created based on the previous described maps (T0 and 1985) and the mapping products of Dias et al. (2016) (available at www.biosfera.dea.ufv.br/en-US/bancos). Dias et al. (2016) made the first effort of a spatialized database of agriculture areas in Brazil between 1940 and 2012 that includes

the percentage, per pixel, of croplands and grasslands. The reconstruction was based on satellite images and census of agriculture data obtained by municipality. Dias et al. (2016) provide the cropland and grassland areas estimates (see Figure S2) with an annual temporal resolution and 1 km of spatial resolution. This work reconstructed LUC 1960 reconstruction by following the steps described below:

I. The methodology consisted in considering the estimates from Dias et al. (2016) to define areas of cropland and grassland, and the LUC from T0 to define areas of cerrado and forest. Urban areas of 1985 map were added to the 1960 map. It was assumed that urban categories maintained their areas between 1960 and 1985 since they represent less than 1% of the UPRB. The map from 1960 describing urban areas are not available on a large-scale, on just a few municipal topographic maps, that are not feasible to use in this study. Therefore, the conversion from cerrado and forest to urban areas were not evaluated from 1960 to 1985.

II. The map from Dias et al. (2016) with a spatial resolution of 1 km was resampled to match the 90 meters from the maps of T0 and 1985. In this case, the bilinear interpolation technique (Hilker et al., 2014) was applied.

III. Pixels with estimates of cropland and grassland lower than 15% were defined as natural vegetation areas. These areas followed the forest or cerrado categories from the T0 map.

IV. Pixels with estimates of cropland and grassland higher than 15% were divided into these two categories (cropland or grassland) according to the highest percentage.

V. Pixels classifieds as urban areas, water, forest and cerrado from the 1985 LUC map were maintained in the 1960 LUC map. Areas of natural vegetation in the 1985 are assumed to have been always natural and not a regeneration.

VI. To evaluate the level of agreement of the reconstruction, the aforementioned steps of estimation of cropland and grassland areas were applied to the LUC from 1985. The reconstruction of the 1985 map performed satisfactorily with 72% of similarity based on Global Accuracy test.

2.2.3. Model setup

The simulations for the three LUC described previously were built with the highest possible spatial discretization allowed by the model system. Five classes of slopes were created: 0– 3%, 3 – 8%, 8 – 20%, 20 – 45%, and > 45%. The basin was divided into 5,187 subbasins with an average drainage area of 173 km^2. These subbasins were further divided into 24,839 (LUC T0), 34,029 (LUC 1960) and 50,272 (LUC 1985) Hydrologic Response Units (HRUs) using a threshold of 5% for land use, 10% for soil, and 20% for slope. The best-fit calibration parameters and parametrizations adopted by Abou Rafee et al. (2019) were used. Abou Rafee et al. (2019) reported satisfactory results for most of 78 river outlets calibrated and validated, especially for large rivers of the UPRB. In addition, the simulations were performed with the modified plant growth module developed by Strauch and Volk (2013).

2.3. Numerical scenarios

The construction of specific scenarios to assess the impacts due to LUCC between 1960 and 1985 and due to climate shift on river discharge were defined based on the series of discharge as shown in Table 1.

Five scenarios were created, A to E as shown in Table 1. Scenario A was defined by the relative change in the average annual median discharge under the values of D3 relative to the values of D1 was calculated. Scenario B, the same but with the values of D4 relative to D2. Scenario C, with the values of D2 relative to D1. Scenario D with the values of D4 relative to D3. Scenario E with the values of D4 relative to D1. Scenario A and B indicate the impact of LUCC between 1960 and 1985 for two periods of precipitation patterns (1961 – 1973 and 1978 – 1990). Scenarios C and D show the effect of the changes in precipitation before (1961 – 1973) and after (1978 – 1990) climate shift over the annual discharge values. In these cases, the comparison is performed for the same simulation (i.e., same LUC). Finally, Scenario E estimates the effect of both LUCC and climate shift as the comparison is performed for different precipitation periods and LUC.

In addition, five scenarios were constructed with the simulation T0 as shown in Table 2. The same criteria of the aforementioned scenarios were used but the simulation with LUC 1960 was replaced by the simulation T0. On these conditions, the maximum impact of LUCC until the year 1985 on annual discharge was achieved. In this case, in order to distinguish from the previous ones, the scenarios are referred by Roman Numerals from I to V.

Table 1. Overview of the defined discharge series for the construction of the scenarios A to E.

Discharge	Description
D1	Discharge values between 1961 and 1973 from simulation with LUC 1960
D2	Discharge values between 1978 and 1990 from simulation with LUC 1960
D3	Discharge values between 1961 and 1973 from simulation with LUC 1985
D4	Discharge values between 1978 and 1990 from simulation with LUC 1985
Scenarios	**Description**
Scenario A	D3 minus D1
Scenario B	D4 minus D2
Scenario C	D2 minus D1
Scenario D	D4 minus D3
Scenario E	D4 minus D1

Table 2. Overview of the defined discharge series for the construction of the scenarios I to V.

Discharge	Description
D1’	Discharge values between 1961 and 1973 from simulation with LUC T0
D2’	Discharge values between 1978 and 1990 from simulation with LUC T0
D3’	Discharge values between 1961 and 1973 from simulation with LUC 1985
D4’	Discharge values between 1978 and 1990 from simulation with LUC 1985
Scenarios	**Description**
Scenario I	D3’ minus D1’
Scenario II	D4’ minus D2’
Scenario III	D2’ minus D1’
Scenario IV	D4’ minus D3’
Scenario V	D4’ minus D1’

For the analysis of the scenarios, ten outlets were selected. The selection was based on the largest rivers of the UPRB or those that had their upstream subbasins with

expressive suppression of natural vegetation (forest or cerrado) replaced mainly by cropland or grassland areas. The location of the selected outlets is shown in Figure 4. Four outlets of Paraná river were evaluated: Upper Paraná (4) after the confluence of Lower Tietê (3); Middle Paraná (6), before the confluence of Ivinhema (7), Lower Paraná (8), the closet outlet to the Guaira stream gauge site (for Location see Figure 1), and Lower Paraná (10), the river mouth of the UPRB.

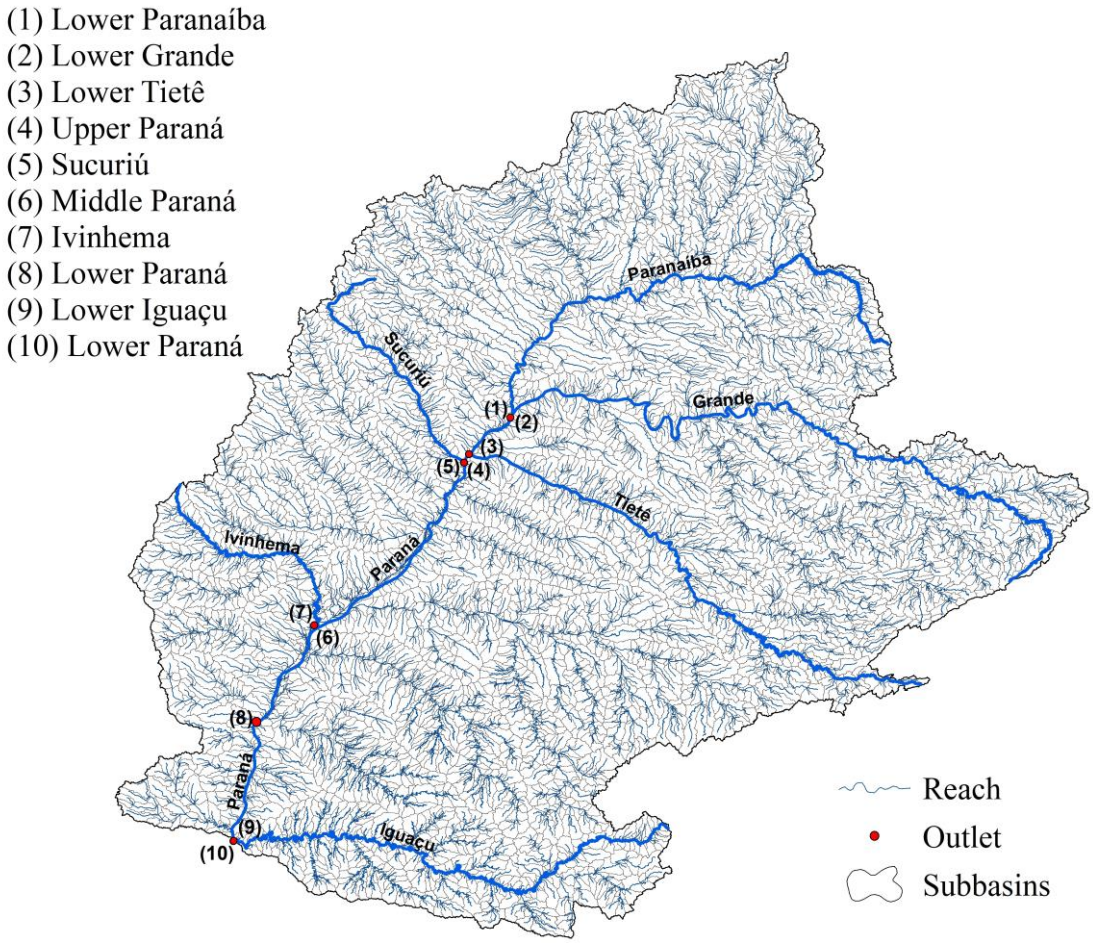

Figure 4. Location of the outlets selected with their respective number, and subbasins discretization.

3. Results and discussion

3.1. LUC T0, 1960 and 1985

Figure 5 shows the generated LUC map from T0, 1960 and 1985. Overall, the east part of the basin had the greatest natural vegetation suppression. Forested areas decreased from 57% in T0 to 35.9% in 1960, and to 17.6% in 1985. The area of cerrado decreased only 1.4% from T0 to the reconstruction for 1960, but it experienced an expressive reduction from 1960 to 1985 to almost half of the original area. The expressive natural vegetation suppression could be associated with the development of agri-business in Brazil since the early 1960s (Mueller and Mueller, 2016).

The original vegetation areas were replaced mainly by grassland and cropland, which represents, respectively, 9% and 12%, in 1960, and 27.7% and 31.1%, in 1985. Grassland and cropland areas are mostly located in the central-eastern part of the UPRB, close to the main socio-economically city of the basin, São Paulo. As stated in the methodology section, the water areas classified at the 1985 map were maintained in all LUC that represent 1.7% of the basin. Urban areas cover 0.9% of the UPRB in both 1985 and 1960 LUC. No urban areas are present at T0.

As noted in Figures 5a-c, the rate of LUCC from T0 to 1960 is much lower than from 1960 to 1985. This is due to the agricultural expansion at the beginning of the twentieth century, which resulted on an extensive transformation of the ecosystems (Salazar et al., 2015). The population growth of UPRB followed a similar development, presenting an exponential increase in the early 1960s (IBGE, 2010).

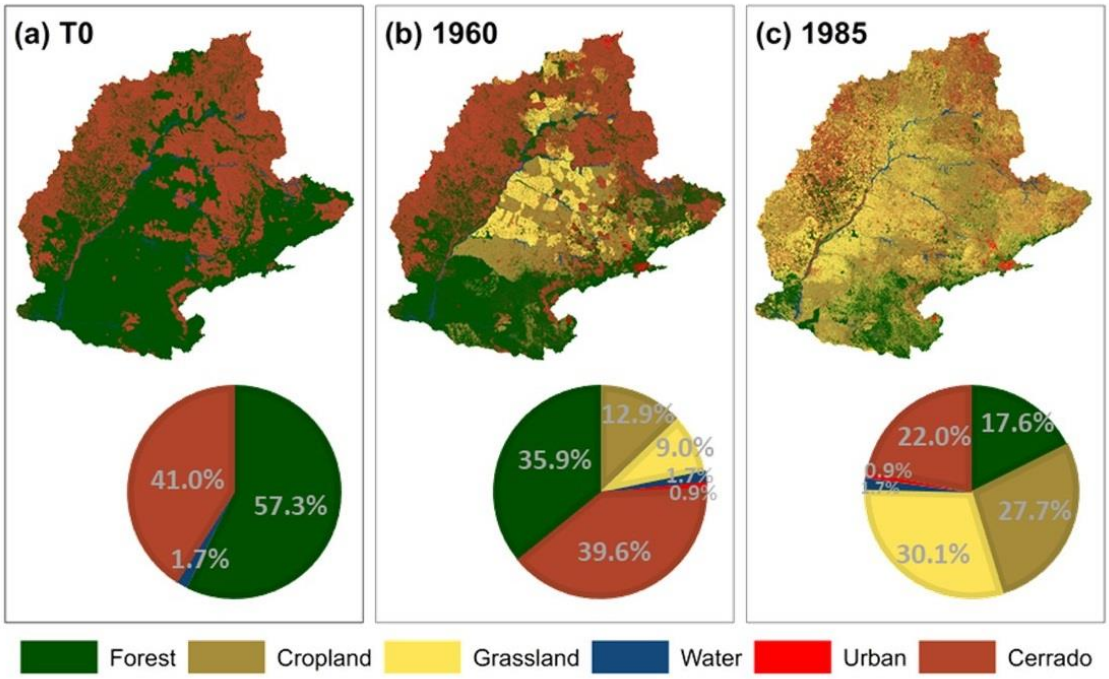

Figure 5. Land Use and Cover (LUC) for (a) T0; 1960 (b) and 1985 (c).

3.2. Precipitation change

Figure 6 shows the relative changes in the average annual median precipitation under the period 1978 – 1990 relative to 1961 – 1973. The data were interpolated using the IDW method at the grid resolution of 0.05 degrees. Overall, the changes in precipitation were mostly positive and occurred mainly in the southern parts of the basin. Only specific areas in the northern-eastern part of the UPRB showed decreased precipitation.

In the northern part of the basin, the increased precipitation values are mostly ranging between 0 – 10% and some areas up to 15%. This increase could be associated with the significant changes in the SAMS in early the 1970s as reported by Carvalho et al. (2011). According to the authors, the mean duration of SAMS increased from 170 days (1948–1972) to 195 days (1972–1982).

In the southern region of the UPRB, the annual median precipitation increased more than 20%. Our results are supported by the ones from Liebmann et al. (2004) that observed increase of precipitation in this region after the observed climate shift, observing increasing when comparing the 1948 – 1975 period to 1976 – 1999, i.e., before and after the climate shift. The precipitation increase in this southern region is related to the fact that this area is more affected by the low frequency oscillations such as ENSO and PDO if compared to other parts of the basin (e.g. Cavalcanti et al., 2015; da Silva et al., 2011; Grimm et al., 2000). Grimm et al. (1998) connects ENSO and PDO to the strengthened of the upper-tropospheric subtropical jet, that intensifies the MCS inducing more precipitation over the region.

It is important to recognize that many rain gauge stations have a high percentage of missing data, especially before the climate shift period, which may affect the results of the interpolation method. However, the basin has 629 stations with less than 5% missing data that are mainly located in the central-east and south-east of the basin, areas where the increase in precipitation before and after the climate shift can be seen (Figure 6).

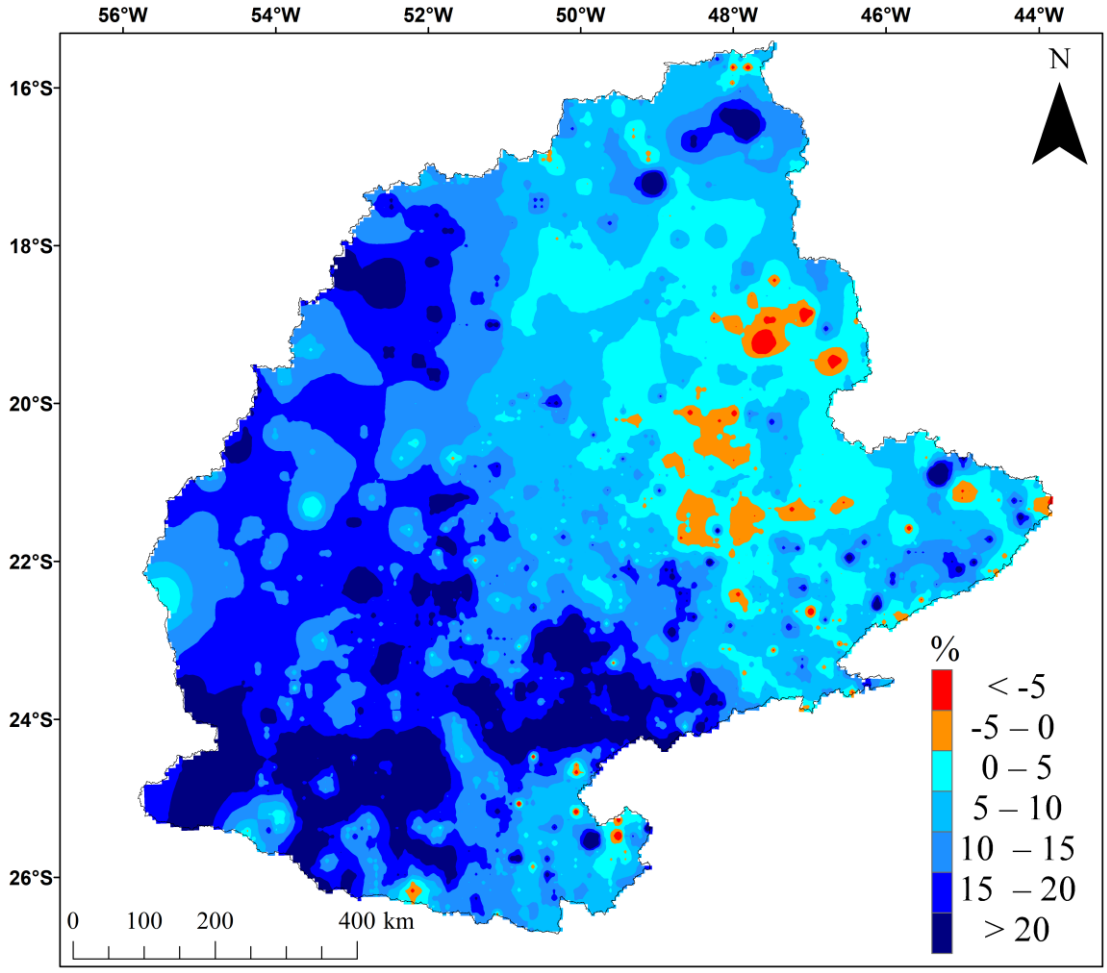

Figure 6. Spatial distribution of the relative change (%) in the average annual median precipitation under the period 1978 – 1990 relative to 1961 – 1973.

3.3. Scenarios analysis

3.3.1. LUCC 1960 – 1985 vs. Climate shift

Figure 7 illustrates the relative changes (%) in the average annual median discharge in the scenarios A to E. Overall, all scenarios and runs generated increased discharge. Also, the scenarios related to the climate shift (C and D) had higher increases compared to only LUCC scenarios (A and B).

Considering the precipitation from 1961 – 1973, scenario A showed that the LUCC between 1960 and 1985 lead to an increase in the discharge from 4% to 16.7% (at Ivinhema river) in all displayed rivers, except for the Lower Grande river where the changes were 1.8%. In scenario B, which considered the precipitation during the period 1978 – 1990, the LUCC lead an increased discharge of about 11% and 18% at the Lower Iguaçu and Ivinhema rivers, respectively. Both rivers had significant LUCC in their upstream subbasins as shown in Figure 5. Note that 1960 already registered enough changes in LUC to impact the discharge within the basin. For example, at the upstream to the Lower Tietê river has only a few fragments of its original LUC in 1960.

Scenarios C and D show the impacts in discharge due to the changes in precipitation (between 1961 – 1973 and 1978 – 1990) considering the LUC from 1960 and 1985, respectively. It was observed that the higher changes at discharge are located in the southern part of the basin. For instance, both scenarios showed that the Lower Iguaçu and Lower Paraná rivers had an increase of more than 30% in the average annual median discharge when comparing the precipitation for 1961 – 1973 and 1978 – 1990 periods. This increase is likely associated with the increase of precipitation amounts mainly concentrated close to rivers mouth (Figure 6).

Scenario E assesses the joint effect of LUCC and climate shift on discharge. The highest increases in discharge are observed at the Lower Ivinhema and Lower Iguaçu rivers outlets with about 67% and 52%, respectively. This scenario clarify that the Paraná river increased presents a discharge that amplifies from upstream to downstream with the confluence of the largest rivers of the basin that also presented a significant increase. The Upper, Middle and Lower Paraná (river mouth of the UPRB) rivers presented a discharge increase of about 14%, 15%, and 38%, respectively.

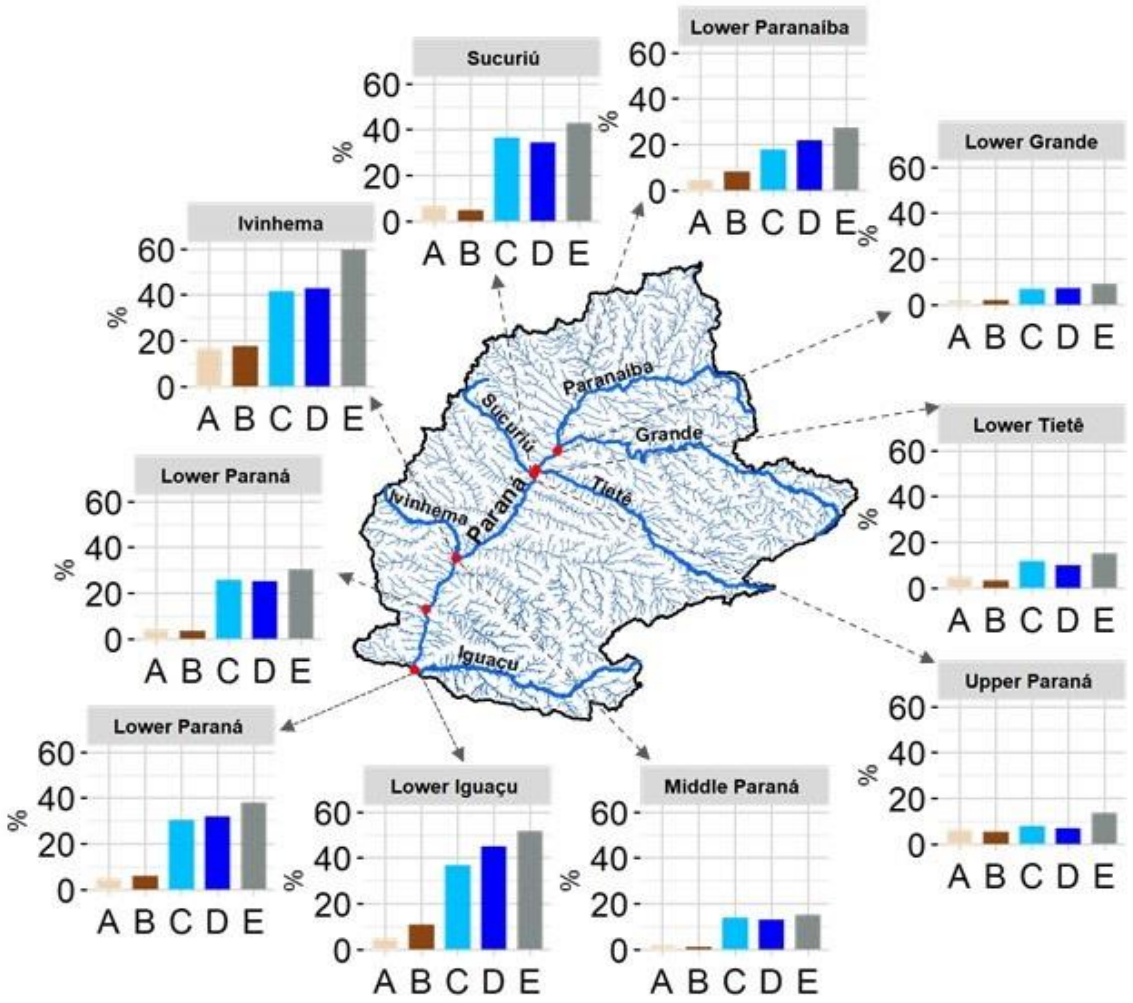

Figure 7. Relative changes (%) in the average annual median discharge at the largest rivers of the UPRB in scenarios A to E. The scenarios are defined in Table 1.

3.3.2. LUCC T0 – 1985 vs. Climate shift

The maximum impact of LUCC until 1985 on the discharge was assessed by the comparison between the simulation with the LUC from T0 (around the Year 1500) and from 1985. The scenarios that covered this issue are presented in Figure 8. Similar to the previously described scenarios A to E, it was observed increased discharge in scenarios I to IV.

The scenarios I and II related to the LUCC between T0 and 1985 had the increased discharge much higher compared to the scenarios A and B. The highest values are observed at the Lower Tietê river outlet as a consequence of the large LUCC in the upstream subbasins. In these subbasins, the natural vegetation areas, composed mostly by forests were replaced mainly by grassland and cropland (see Figure 5). This caused an increase in the average annual median discharge more than 55% under the scenarios.

Scenario III assess the effect of the precipitation change between 1961 – 1973 and 1978 – 1990 considering the T0 LUC. Similar relative changes discharges to scenario C (with LUC 1960) were achieved. The scenario IV has the same characteristics as scenario D.

Finally, scenario V assesses the consequence of changes in LUC up to 1985 and in precipitation due to the climate shift. Again, the highest changes in discharge were observed at the Lower Tietê that presented an increase of about 85% in the average annual median. The river mouth of the UPRB (Lower Paraná), the discharge increased more than 50%.

In all the rivers outlet analyzed, the scenarios I to IV revealed that the changes in precipitation had a higher impact in the annual discharge than the LUCC, except for the Lower Tietê and the Upper Paraná rivers. In these cases, changes in precipitation over the Tietê subbasin were not as high as in the southern part of the basin which were exceeded

20% (see Figure 6). In the southern part of the basin, despite the important observed LUCC, the changes in precipitation had a greater impact on discharge. This becomes clear when analyzing the changes in discharge at the Lower Paraná (river mouth of the UPRB), Scenario I and II, related to LUCC, indicate a discharge increase of about 15%, while the climate shift scenarios (III and IV) of about 30%.

Therefore, a possible explanation for the increased discharge is that the increased precipitation corresponds exactly close to areas mostly downstream of the basin and has nowhere to flow, which the scenario would be different if this increase occurred at the head of the basin. In this case, infiltration and evapotranspiration processes would have more time to occur within the basin until the discharge reaches the river mouth of the UPRB (Lower Paraná). Besides, the regions with the greatest increase in precipitation are also the regions that were recently anthropized, as they were covered by natural vegetation in 1960 (Figure 5). Therewith, the natural vegetation suppression led to an increase in the amount of surface runoff, which is one of the major contributors to discharge. Hence, around the 1970s both LUCC and climate shift occurred simultaneously within the basin. The combination of both in the same period may also have enhanced the increased discharge observed.

The numerical experiments indicate that the increase in annual discharge observed at the Lower Paraná (8, see Figure 4) locations is mostly associated to changes in precipitation due to the climate shift even when the large LUCC between T0 and 1985 was considered. Our results are in disagreement with previous ones such as Lee et al. (2018) that reported that LUCC as the main cause of changes in annual discharge of the Lower Paraná river. The discrepancies between the results presented in this work and Lee et al. (2018) may be due to the different spatial resolution. Lee et al. (2018) used grid-cell with approximately 50 km × 50 km, whereas our simulations used a spatial discretization

of 5,187 subbasins, in turn, divided into HRUs 24,839 (LUC T0), 34,029 (LUC 1960) and 50,272 (LUC 1985).

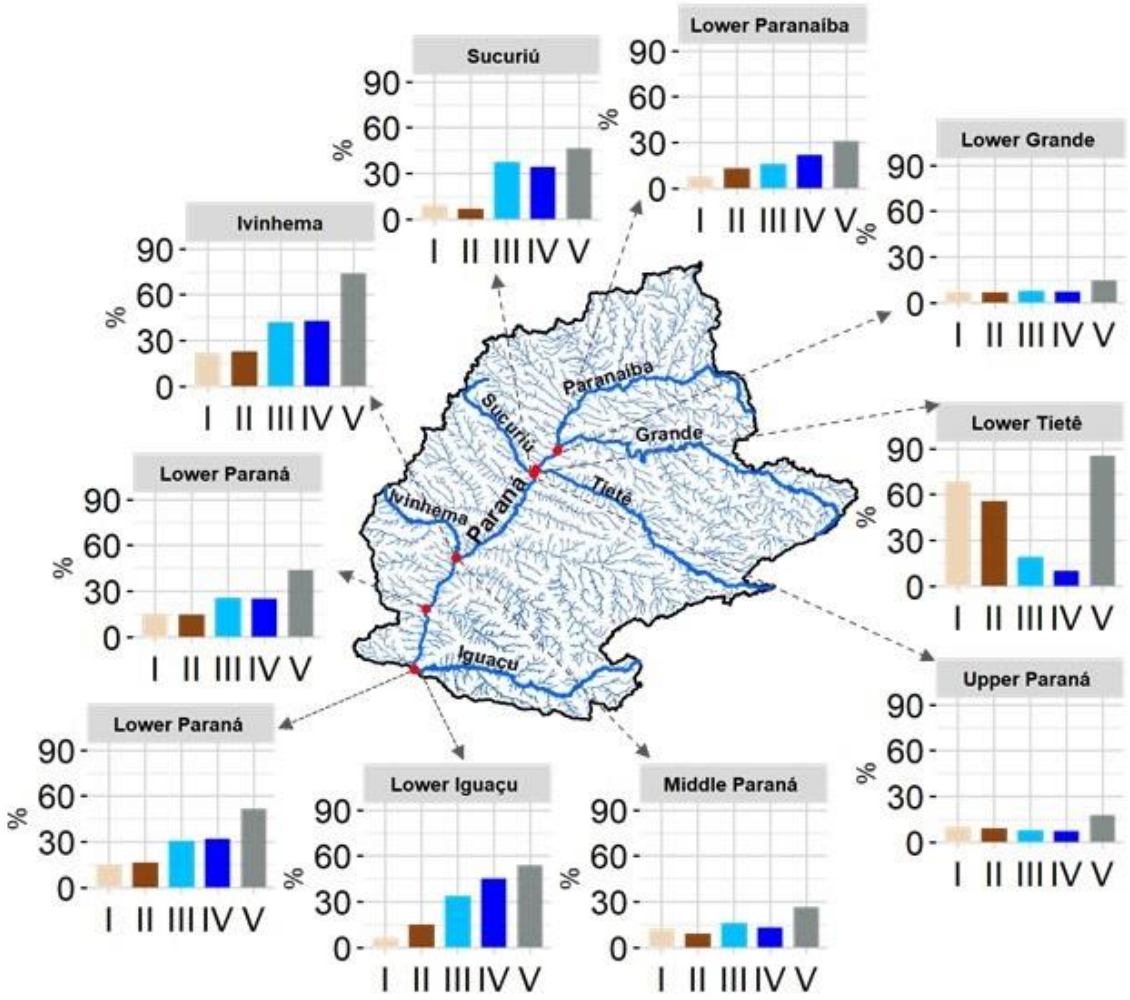

Figure 8. Relative changes (%) in the average annual median discharge at the largest river of the UPRB in scenarios I to V. The scenarios are defined in Table 2.

4. Conclusions

This paper analyzed the effect of LUCC and the 1970s climate shift in the UPRB. Numerical simulations to estimate discharge were performed by the SWAT model using three LUC from T0 (around the Year 1500), 1960 and 1985.

Analysis of precipitation showed that there was a significant change in precipitation after the observed 1970s climate shift, where more than 20% in the average

annual median was observed mainly in the southern parts of the basin. Also, the results from LUC estimations indicated that more than half of the natural vegetation was suppressed from T0 up to 1985. The simulations indicated that both LUCC and precipitation change due to climate shift have a significant impact on the annual discharge at the largest rivers of the UPRB. However, the main driver is the climate shift which affected mainly the southern region of the basin. For instance, LUCC from T0 up to 1985 responds about 16% of the increase at the river mouth of the UPRB, whereas climate shift causes an increase discharge of about 32%.

The provided results should be regarded with much attention by the policy makers and managers given the importance of the UPRB in various sectors of the economy and development of Brazil. Besides the possible future LUCC, climate shift may occur again in the next decades. Therefore, whether positive or negative phase it is, it will affect the water supply and energy generation, or increase the risk of floods in areas within the basin.

Acknowledgments. This study was financed in part by the "Coordenação de Aperfeiçoamento de Pessoal de Nível Superior – Brasil" (CAPES) - Finance Code 001 (Process # 88887.115875/2015- 01) and "Fundação de Amparo à Pesquisa do Estado de São Paulo" FAPESP (process #2015/03804-9). The authors would like to gratefully acknowledge "Agência Nacional de Águas" (ANA) by providing the precipitation and discharge data.

References

Abbaspour, K.C., Rouholahnejad, E., Vaghefi, S., Srinivasan, R., Yang, H., Kløve, B., 2015. A continental-scale hydrology and water quality model for Europe:

Calibration and uncertainty of a high-resolution large-scale SWAT model. J. Hydrol. 524, 733–752. https://doi.org/10.1016/j.jhydrol.2015.03.027

Abou Rafee, S.A., Freitas, E.D., Martins, J.A., Martins, L.D., Domingues, L.M., Nascimento, J.M.P., Machado, C.B., Santos, E.B., Rudke, A.P., Fujita, T., Souza, R.A.F., Hallak, R., Uvo, C.B., 2020. Spatial Trends of Extreme Precipitation Events in the Paraná River Basin. J. Appl. Meteorol. Climatol. 59, 443–454. https://doi.org/10.1175/JAMC-D-19-0181.1

Abou Rafee, S.A., Uvo, C.B., Martins, J.A., Domingues, L.M., Rudke, A.P., Fujita, T., Freitas, E.D., 2019. Large-scale hydrological modelling of the Upper Paraná River Basin. Water (Switzerland). https://doi.org/10.3390/w11050882

Agosta, E.A., Compagnucci, R.H., 2008. The 1976/77 austral summer climate transition effects on the atmospheric circulation and climate in Southern South America. J. Clim. 21, 4365–4383. https://doi.org/10.1175/2008JCLI2137.1

ANEEL, 2020. BIG - Banco de Informações de Geração - Capacidade de Geração do Brasil - Usinas hidrelétricas, BIG. Available online: https://www2.aneel.gov.br/aplicacoes/capacidadebrasil/Combustivel.cfm (accessed March 2020).

Antico, A., Torres, M.E., Diaz, H.F., 2016. Contributions of different time scales to extreme Paraná floods. Clim. Dyn. 46, 3785–3792. https://doi.org/10.1007/s00382-015-2804-x

Arnold, J.G., Srinivasan, R., Muttiah, R.S., Williams, J.R., 1998. Large Area Hydrologic Modelling and Assessment Part I : Model Development. Am. Water Resour. Assoc. https://doi.org/10.1111/j.1752-1688.1998.tb05961.x

Camilloni, I.A., Barros, V.R., 2003. Extreme discharge events in the Paraná River and

their climate forcing. J. Hydrol. https://doi.org/10.1016/S0022-1694(03)00133-1

Carvalho, L.M.V., Jones, C., Liebmann, B., 2004. The South Atlantic convergence zone: Intensity, form, persistence, and relationships with intraseasonal to interannual activity and extreme rainfall. J. Clim. https://doi.org/10.1175/1520-0442(2004)017<0088:TSACZI>2.0.CO;2

Carvalho, L.M.V., Jones, C., Silva, A.E., Liebmann, B., Silva Dias, P.L., 2011. The South American Monsoon System and the 1970s climate transition. Int. J. Climatol. 31, 1248–1256. https://doi.org/10.1002/joc.2147

Cavalcanti, I.F.A., Carril, A.F., Penalba, O.C., Grimm, A.M., Menéndez, C.G., Sanchez, E., Cherchi, A., Sörensson, A., Robledo, F., Rivera, J., Pántano, V., Bettolli, L.M., Zaninelli, P., Zamboni, L., Tedeschi, R.G., Dominguez, M., Ruscica, R., Flach, R., 2015. Precipitation extremes over La Plata Basin - Review and new results from observations and climate simulations. J. Hydrol. https://doi.org/10.1016/j.jhydrol.2015.01.028

da Silva, G.A.M., Drumond, A., Ambrizzi, T., 2011. The impact of El Niño on South American summer climate during different phases of the Pacific Decadal Oscillation. Theor. Appl. Climatol. https://doi.org/10.1007/s00704-011-0427-7

Dias, L.C.P., Pimenta, F.M., Santos, A.B., Costa, M.H., Ladle, R.J., 2016. Patterns of land use, extensification, and intensification of Brazilian agriculture. Glob. Chang. Biol. https://doi.org/10.1111/gcb.13314

Grimm, A.M., Barros, V.R., Doyle, M.E., 2000. Climate variability in southern South America associated with El Nino and La Nina events. J. Clim. https://doi.org/10.1175/1520-0442(2000)013<0035:CVISSA>2.0.CO;2

Grimm, A.M., Ferraz, S.E.T., Gomes, J., 1998. Precipitation anomalies in southern Brazil

associated with El Nino and La Nina events. J. Clim. https://doi.org/10.1175/1520-0442(1998)011<2863:PAISBA>2.0.CO;2

Grimm, A.M., Pal, J.S., Giorgi, F., 2007. Connection between spring conditions and peak summer monsoon rainfall in South America: Role of soil moisture, surface temperature, and topography in eastern Brazil. J. Clim. 20, 5929–5945. https://doi.org/10.1175/2007JCLI1684.1

Hartmann, B., Wendler, G., 2005. The significance of the 1976 Pacific climate shift in the climatology of Alaska. J. Clim. https://doi.org/10.1175/JCLI3532.1

Hilker, T., Lyapustin, A.I., Tucker, C.J., Hall, F.G., Myneni, R.B., Wang, Y., Bi, J., De Moura, Y.M., Sellers, P.J., 2014. Vegetation dynamics and rainfall sensitivity of the Amazon. Proc. Natl. Acad. Sci. U. S. A. https://doi.org/10.1073/pnas.1404870111

IBGE, 2019. População. Available online: http://www.ibge.gov.br/apps/populacao/projecao/ (accessed November 2019)

IBGE, 2017. Recuperação e compatibilização do projeto RADAMBRASIL, tema vegetação. Available online: http://www.metadados.geo.ibge.gov.br/geonetwork_ibge/srv/por/metadata.show?id=19626&currTab=simple (accessed January 2020)

IBGE, 2010. Evolução da população total. Available online: https://brasil500anos.ibge.gov.br/estatisticas-do-povoamento/evolucao-da-populacao-brasileira.html (accessed December 2019)

Jacques-Coper, M., Garreaud, R.D., 2015. Characterization of the 1970s climate shift in South America. Int. J. Climatol. https://doi.org/10.1002/joc.4120

Lee, E., Livino, A., Han, S.C., Zhang, K., Briscoe, J., Kelman, J., Moorcroft, P., 2018. Land cover change explains the increasing discharge of the Paraná River. Reg.

Environ. Chang. https://doi.org/10.1007/s10113-018-1321-y

Liebmann, B., Vera, C.S., Carvalho, L.M.V., Camilloni, I.A., Hoerling, M.P., Allured, D., Barros, V.R., Báez, J., Bidegain, M., 2004. An observed trend in central South American precipitation. J. Clim. https://doi.org/10.1175/3205.1

Litzow, M.A., 2006. Climate regime shifts and community reorganization in the Gulf of Alaska: how do recent shifts compare with 1976/1977? ICES J. Mar. Sci. https://doi.org/10.1016/j.icesjms.2006.06.003

Marengo, J.A., Liebmann, B., Grimm, A.M., Misra, V., Silva Dias, P.L., Cavalcanti, I.F.A., Carvalho, L.M.V., Berbery, E.H., Ambrizzi, T., Vera, C.S., Saulo, A.C., Nogues-Paegle, J., Zipser, E., Seth, A., Alves, L.M., 2012. Recent developments on the South American monsoon system. Int. J. Climatol. https://doi.org/10.1002/joc.2254

Meehl, G.A., Hu, A., Santer, B.D., 2009. The mid-1970s climate shift in the pacific and the relative roles of forced versus inherent decadal variability. J. Clim. https://doi.org/10.1175/2008JCLI2552.1

MMA, 2012. Monitoramento do desmatamento nos biomas brasileiros por satélite: monitoramento do bioma Mata Atlântica - 2008 a 2009. Ministério do Meio Ambient. Brasília, DF 101.

MMA, 2011. Monitoramento do desmatamento nos biomas brasileiros por satélite: monitoramento do bioma Cerrado - 2009 a 2010.

Morales Rodriguez, C.A., da Rocha, R.P., Bombardi, R., 2010. On the development of summer thunderstorms in the city of São Paulo: Mean meteorological characteristics and pollution effect. Atmos. Res. https://doi.org/10.1016/j.atmosres.2010.02.007

Mueller, C., Mueller, B., 2016. The evolution of agriculture and land reform in Brazil,

1960-2006, in: Economic Development in Latin America: Essay in Honor of Werner Baer. https://doi.org/10.1057/9780230297388_10

Rouholahnejad, E., K.C. Abbaspour, R. Srinivasan, V. Bacu, and A.L., 2014. Water resources of the Black Sea Basin at high spatial and temporal resolution. Water Resour. Res. 50, (7):5866-5885. https://doi.org/10.1002/2013WR014132.Received

Rudke, A.P., 2018. Dinâmica da cobertura do solo para a bacia hidrográfica do alto rio Paraná. Master´s Thesis, Federal University of Tecnology Parana, Londrina, Brazil.

Rudke, A.P., Fujita, T., Almeida, D.S. de, Eiras, M.M., Xavier, A.C.F., Rafee, S.A.A., Santos, E.B., Morais, M.V.B. de, Martins, L.D., Souza, R.V.A. de, Souza, R.A.F., Hallak, R., Freitas, E.D. de, Uvo, C.B., Martins, J.A., 2019. Land cover data of Upper Parana River Basin, South America, at high spatial resolution. Int. J. Appl. Earth Obs. Geoinf. https://doi.org/10.1016/j.jag.2019.101926

Salazar, A., Baldi, G., Hirota, M., Syktus, J., McAlpine, C., 2015. Land use and land cover change impacts on the regional climate of non-Amazonian South America: A review. Glob. Planet. Change. https://doi.org/10.1016/j.gloplacha.2015.02.009

Strauch, M., Volk, M., 2013. SWAT plant growth modification for improved modeling of perennial vegetation in the tropics. Ecol. Modell. https://doi.org/10.1016/j.ecolmodel.2013.08.013

Tsonis, A.A., Swanson, K., Kravtsov, S., 2007. A new dynamical mechanism for major climate shifts. Geophys. Res. Lett. https://doi.org/10.1029/2007GL030288

Tucci, C.E.., 2002. Impactos da variabilidade climática e do uso do solo nos recursos hídricos. Câmara Temática sobre Recur. Hídricos 150.

Tucci, C.E.M., Clarke, R.T., 1998. Environmental issues in the la Plata Basin. Int. J. Water Resour. Dev. https://doi.org/10.1080/07900629849376

Velasco, I., Fritsch, J.M., 1987. Mesoscale convective complexes in the Americas. J. Geophys. Res. 92, 9591–9613. https://doi.org/10.1029/JD092iD08p09591

Wang, G., Swanson, K.L., Tsonis, A.A., 2009. The pacemaker of major climate shifts. Geophys. Res. Lett. https://doi.org/10.1029/2008GL036874

Yuan Zhang, Wallace, J.M., Battisti, D.S., 1997. ENSO-like interdecadal variability: 1900-93. J. Clim. https://doi.org/10.1175/1520-0442(1997)010<1004:eliv>2.0.co;2

Supplement of

Land Use and Cover Changes versus Climate Shift: Who is the main player in river discharge? A case study in the Upper Paraná River Basin

Sameh A. Abou Rafee, Cintia B. Uvo, Jorge A. Martins, Carolyne B. Machado, Edmilson D. Freitas

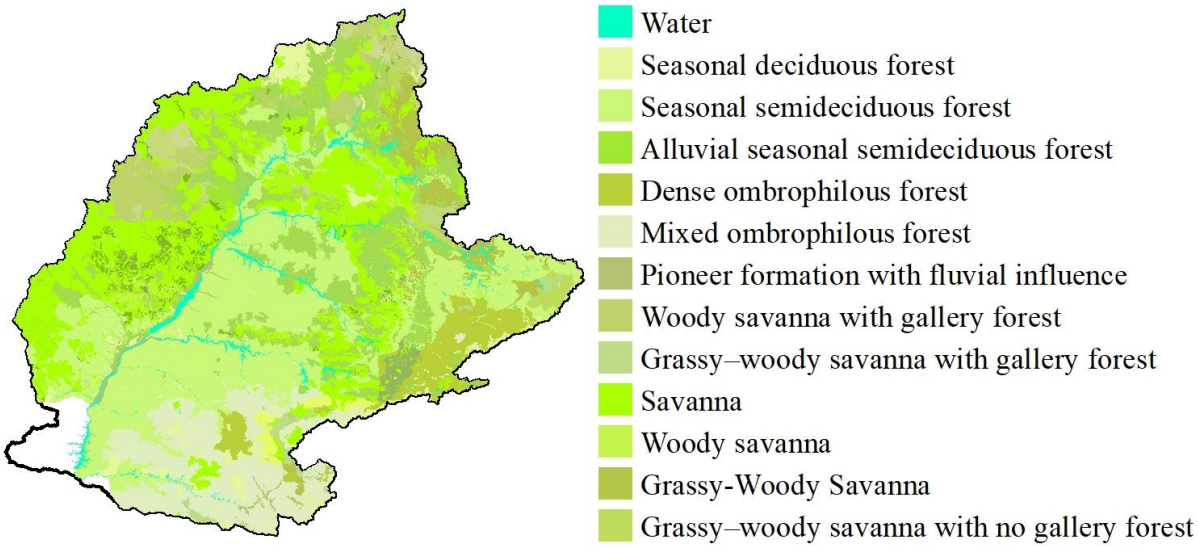

Figure S1. Major land use and cover categories classified by RADAMBRASIL project.

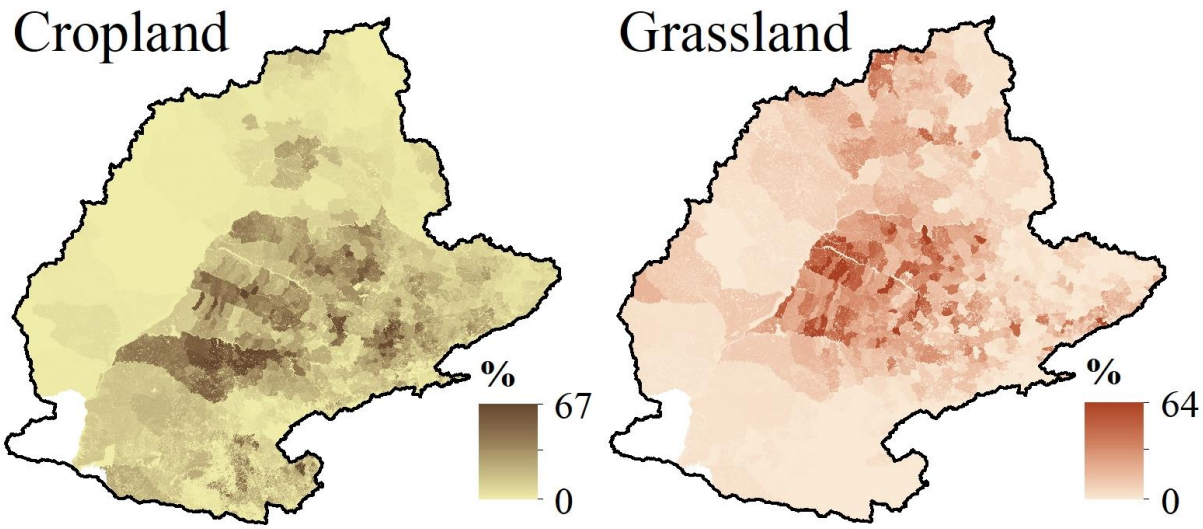

Figure S2. Percentage cropland and grassland areas for the year 1960 based on estimation from Dias et al. (2016).